



**UNIVERSIDADE ESTADUAL DE CAMPINAS**

**INSTITUTO DE BIOLOGIA**

**Felipe Calzado**

**Análise comparativa do mecanismo de secreção de proteínas  
heterólogas em *Aspergillus nidulans***

**Comparative analysis of the heterologous protein secretion in  
*Aspergillus nidulans***

**Campinas**

**2017**

**Felipe Calzado**

**Análise comparativa do mecanismo de secreção de proteínas heterólogas  
em *Aspergillus nidulans***

**Comparative analysis of the heterologous protein secretion in *Aspergillus  
nidulans***

*Dissertação apresentada ao Instituto de Biologia da  
Universidade Estadual de Campinas como parte dos  
requisitos exigidos para a obtenção do título de Mestre  
em Ciências, na área de concentração em Fármacos,  
Medicamentos e Insumos para Saúde.*

*Dissertation presented to the Institute of Biology of the  
University of Campinas in partial fulfillment of the  
requirements for the Master's degree of Sciences, in the  
field of concentration of Drugs, Medicines and Supplies  
for Health.*

*Orientador: Dr. André Ricardo de Lima Damásio*

*Coorientadora: Dra. Gabriela Felix Persinoti*

ESTE EXEMPLAR CORRESPONDE À  
VERSÃO FINAL DA DISSERTAÇÃO  
DEFENDIDA PELO ALUNO FELIPE  
CALZADO, E ORIENTADA PELO PROF. DR.  
ANDRÉ RICARDO DE LIMA DAMÁSIO.

Campinas

2017

**Agência(s) de fomento e nº(s) de processo(s):** FAPESP, 2014/23051-2

Ficha catalográfica  
Universidade Estadual de Campinas  
Biblioteca do Instituto de Biologia  
Mara Janaina de Oliveira - CRB 8/6972

C139a Calzado, Felipe, 1991-  
Análise comparativa do mecanismo de secreção de proteínas heterólogas em *Aspergillus nidulans* / Felipe Calzado. – Campinas, SP : [s.n.], 2017.

Orientador: André Ricardo de Lima Damásio.  
Coorientador: Gabriela Felix Persinoti.  
Dissertação (mestrado) – Universidade Estadual de Campinas, Instituto de Biologia.

1. *Aspergillus*. 2. RNA-seq. 3. Expressão heteróloga. I. Damásio, André Ricardo de Lima, 1983-. II. Persinoti, Gabriela Felix. III. Universidade Estadual de Campinas. Instituto de Biologia. IV. Título.

Informações para Biblioteca Digital

**Título em outro idioma:** Comparative analysis of the heterologous protein secretion in *Aspergillus nidulans*

**Palavras-chave em inglês:**

*Aspergillus*

RNA-seq

Heterologous expression

**Área de concentração:** Fármacos, Medicamentos e Insumos para Saúde

**Titulação:** Mestre em Ciências

**Banca examinadora:**

André Ricardo de Lima Damásio [Orientador]

Roberto do Nascimento Silva

Flavia Fisch Winck

**Data de defesa:** 13-03-2017

**Programa de Pós-Graduação:** Biociências e Tecnologia de Produtos Bioativos

## **BANCA EXAMINADORA**

Prof. Dr. André Ricardo de Lima Damásio (orientador)

Prof. Dr. Roberto do Nascimento Silva

Profa. Dra. Flavia Vischi Winck

*Os membros da Comissão Examinadora acima assinaram a Ata de Defesa, que se encontra no processo de vida acadêmica do aluno.*



## **AGRADECIMENTOS**

À Universidade Estadual de Campinas, através do Instituto de Biologia e ao Programa de Pós Graduação em Biociências e Tecnologia de Produtos Bioativos.

Ao Laboratório Nacional de Ciência e Tecnologia do Bioetanol - CTBE e ao Centro Nacional de Pesquisa em Energia e Materiais - CNPEM, por disponibilizar toda estrutura e suporte técnico e financeiro.

À Fundação de Amparo à Pesquisa do Estado de São Paulo – FAPESP pelo suporte financeiro para o desenvolvimento dessa pesquisa.

Ao meu orientador, professor e amigo Dr. André Ricardo de Lima Damásio por me guiar e ensinar durante minha trajetória de pesquisa, desde o início de meu estágio no CTBE até a conclusão deste mestrado. Obrigado pela confiança, paciência e tempo em mim depositados para juntos contribuirmos um pouco mais com a ciência e construção de conhecimento. Tenho orgulho de ter desenvolvido este estudo sob sua orientação e levo comigo todo aprendizado, amadurecimento científico e profissional adquiridos nesta jornada!

À minha coorientadora Dra. Gabriela Felix Persinoti, por ter me ajudado muito nas análises de bioinformática deste estudo. Sem você nada disto poderia ter sido concluído. Agradeço também pela indicação no curso de bioinformática que realizei em Cornélio Procópio/PR, foi de grande valia para minha formação e aprendizagem nesta área fascinante!

Aos pesquisadores que participaram do meu exame de qualificação, Dra. Thabata Alvarez, Dr. Renato Vicentini e ao Dr. Marcio Bajgelman. Obrigado pela colaboração e pelas dicas que ajudaram muito a guiar o andamento e finalização deste trabalho.

Aos meus companheiros e amigos Marcelo e Mariane por terem acompanhado meus primeiros passos nesta área de pesquisa, me ensinado desde pipetar direito até a construir este trabalho final. Foi muito bom ter vocês ao meu lado sempre incentivando, ensinado e divertindo. Sou muito sortudo de ter vocês ao meu lado.

Aos meus amigos de grupo de pesquisa. Fabiano, muito obrigado por todo apoio e estar sempre disposto a ajudar e a ensinar, aprendi muito com você e com nossas conversas filosóficas sobre ciência e sobre coisas da vida. A Jaqueline e ao César, mesmo recém-chegados já me ajudaram bastante, obrigado pela companhia e pela amizade, é muito bom ter vocês todos por perto!

A Rebeca e ao Thiago que me ajudaram muito, acompanhando meus primeiros passos no laboratório como “novato” meio perdido... Obrigado por sempre guiarem meu caminho e pela amizade, vocês fizeram tudo ficar mais fácil e divertido!

Aos amigos, pesquisadores e funcionários do CTBE, por sempre terem me ajudado de forma direta e indireta. O apoio de todos vocês foi essencial para minha formação pessoal e profissional. Dr. Fábio Squina, Dra. Juliana Velasco, Douglas, Fernanda M, João, Ricardo, Bruna, Marcelo L, Robson, Mariana, Cristiane A, Antônio, Eli, Beto, Fernandinha, Letícia, Aline, Lívia, Emerson, Borin, Roberta, Cames, Evandro, Vivi, e a todos os outros colaboradores.

Ao César Estevo, a Paula Pavan e a todos meus amigos de faculdade, vocês participaram da minha formação e contribuíram para que eu chegasse até aqui. Obrigado pela amizade e pelo apoio.

Especial agradecimento ao Carlos Pelaio e a Raquel Calzado, vocês sempre me ajudaram de todas as formas possíveis com a única finalidade de permitir que eu conquistasse meus sonhos. Serei eternamente grato por tudo. Obrigado pelo companheirismo e pela amizade.

À minha família, sem vocês nada do que tenho ou do que sou seria possível, obrigado por sempre acreditarem em mim e estarem tão presentes em todas as fases da minha vida!

*“Não sei o que possa parecer aos olhos do mundo, mas aos meus pareço apenas ter sido como um menino brincando à beira-mar, divertindo-me com o fato de encontrar de vez em quando um seixo mais liso ou uma concha mais bonita que o normal, enquanto o grande oceano da verdade permanece completamente por descobrir à minha frente”*

***Isaac Newton***

## RESUMO

Como forma de diminuir o uso de energias de origem fóssil e aumentar a utilização de energias renováveis, há um grande incentivo mundial recente no desenvolvimento de biorrefinarias, o que envolve processos de conversão integrada de biomassa vegetal e equipamentos para produção de energia, combustíveis e produtos químicos renováveis. Nesta perspectiva o etanol de segunda geração obtido a partir da conversão de biomassa vegetal lignocelulósica em açúcares fermentáveis tem sido foco de muitas pesquisas atualmente a fim de viabilizar seu uso. No entanto, devido à natureza recalcitrante da biomassa lignocelulósica, o custo de processamento corrente na produção de biocombustíveis se torna um importante gargalo a ser superado. Uma das formas de superar este problema é melhorar a produção de enzimas necessárias na etapa de hidrólise enzimática da biomassa vegetal, um processo ainda hoje considerado muito caro. Os fungos filamentosos se destacam na produção e secreção de enzimas lignocelulolíticas de forma homóloga e heteróloga, entretanto pouco se sabe sobre a regulação dos mecanismos de secreção de proteínas nestes microrganismos. Pensando nisso, a utilização do fungo filamentoso modelo *Aspergillus nidulans* se torna um importante recurso de estudos por ser geneticamente bem caracterizado. Nosso objetivo neste trabalho foi realizar a análise comparativa dos mecanismos de secreção de diferentes proteínas heterólogas em *A. nidulans* a partir de dados de transcriptoma gerados pela técnica de RNA-seq (*Next Generation RNA sequencing*). Para monitorar o processo de secreção, adotamos 3 genes alvo: alfa-arabinofuranosidase GH51 (AbfA) e beta-glucosidase GH3 (BglC) de *A. fumigatus*, e mananase GH5 termofílica (1542) de *Thermotoga petrophila*. Estes genes foram transformados em *A. nidulans*, sendo que para AbfA atingiu-se altos níveis de secreção, diferente de BglC e 1542, onde os níveis de secreção foram mínimos. Com isso foram definidos perfis transcriptômicos dos genes relacionados a secreção de proteínas em *A. nidulans*, representando a resposta da super expressão de três genes heterólogos em diferentes tempos de indução. Em geral houveram processos biológicos super-regulados relacionados principalmente ao metabolismo, proteínas com função ligante, transporte e defesa celulares. Além disso, foram identificados 17 genes diferencialmente expressos envolvidos diretamente com a via de secreção de *A. nidulans*, representando importantes alvos para manipulação genética deste organismo. Este foi o primeiro estudo que descreve a resposta transcriptômica da secreção de proteínas heterólogas em *A. nidulans*, gerando uma nova perspectiva ao comparar três diferentes proteínas heterólogas com níveis crescentes de secreção.

## ABSTRACT

As a way to reduce the use of fossil fuels and increase the use of renewable energies, there is a major recent worldwide incentive in the development of biorefineries, which involves integrated conversion processes of plant biomass and equipment for the production of energy, fuels and renewable chemicals. In this perspective, the second generation of ethanol obtained from the conversion of lignocellulosic biomass to fermentable sugars has been the focus of many currently researches in order to make its use feasible. However, due to the recalcitrant nature of lignocellulosic biomass, the current processing cost in the production of biofuels becomes an important bottleneck to be overcome. One of the ways to overcome this problem is to improve the production of enzymes required in the enzymatic hydrolysis of plant biomass, a process still considered very expensive nowadays. The filamentous fungi stand out in the production and secretion of lignocellulolytic enzymes in a homologous and heterologous way, however little is known about the regulation of the protein secretion mechanisms in these microorganisms. Considering this, the use of the filamentous fungus model *Aspergillus nidulans* becomes an important resource of studies to be well genetically characterized. Our objective in this work was to perform a comparative analysis of the mechanisms of secretion of different heterologous proteins in *A. nidulans* through transcriptome data analysis using RNA-seq technique (Next Generation RNA sequencing). To monitor the secretion process, we adopted 3 target genes: alfa-arabinofuranosidase GH51 (AbfA) and beta-glucosidase GH3 (BglC) from *A. fumigatus*, and thermophilic mannanase GH5 (1542) from *Thermotoga petrophila*. These genes were transformed into *A. nidulans*, and for AbfA high secretion levels were reached, different from BglC and 1542, where secretion levels were minimal. Thereby, transcriptomic profiles of the genes related to protein secretion were defined in *A. nidulans*, representing the super expression response of three heterologous genes at different induction times. In general there were overrepresented biological processes related mainly to metabolism, protein with binding function, cellular transport and defense. In addition, 17 differentially expressed genes directly involved with the *A. nidulans* secretion pathway were identified, representing important targets for the genetic manipulation of this organism. This was the first study to describe the transcriptomic response of heterologous protein secretion in *A. nidulans*, generating a new perspective when comparing three different heterologous proteins with increasing levels of secretion.

## SUMÁRIO

RESUMO .....	8
ABSTRACT .....	9
<b>1. INTRODUÇÃO .....</b>	<b>11</b>
<b>2. CAPÍTULO 1: REVISÃO BIBLIOGRÁFICA .....</b>	<b>15</b>
2.1. Etanol de segunda geração.....	15
2.2. Secreção de proteínas por fungos filamentosos.....	21
2.3. Produção de proteínas heterólogas em <i>Aspergillus</i> .....	25
2.4. Referências Bibliográficas.....	31
<b>3. CAPÍTULO 2: ARTIGO CIENTÍFICO.....</b>	<b>37</b>
3.1 ABSTRACT.....	38
3.2. BACKGROUND.....	39
3.3 RESULTS AND DISCUSSION.....	42
3.3.1. The recombinant target proteins are secreted in different levels.....	42
3.3.2. The heterologous genes are highly expressed in <i>A. nidulans</i> .....	44
3.3.3. Global transcriptional response to heterologous protein production.....	46
3.3.4. Recombinant strains adapts differently at early and late times of heterologous genes induction.....	51
3.3.5. Differential expression of genes related to the secretion pathway.....	58
3.4. CONCLUSIONS.....	64
3.5. MATERIALS AND METHODS.....	65
3.6 REFERENCES.....	69
3.7. SUPPLEMENTARY MATERIALS.....	74
<b>4. CAPÍTULO 3: CONSIDERAÇÕES FINAIS.....</b>	<b>136</b>
4.1 Referências Bibliográficas.....	136
<b>5. ANEXOS.....</b>	<b>140</b>
5.1. Artigos publicados.....	140
5.2. Capítulos de livros publicados.....	142
5.3. Aprovação do projeto na CIBio.....	144
5.4. Declaração de direitos autorais.....	145

## 1. INTRODUÇÃO

A queima dos combustíveis fósseis, utilizada como maior fonte de energia atualmente, é um dos maiores problemas que afetam o meio ambiente e também a economia global. A substituição de combustíveis fósseis por biocombustíveis se torna hoje uma solução de grande relevância por auxiliar na redução das emissões de dióxido de carbono, gás que é o principal impulsionador do efeito estufa [1]. Neste contexto, especialistas acreditam que as biorrefinarias possam vir a constituir uma indústria-chave do século XXI, responsável até mesmo por uma nova revolução industrial, em virtude da importância das tecnologias que empregam e dos efeitos sobre o paradigma industrial [2]. A biorrefinaria envolve processos de conversão integrada de biomassa e equipamentos para produção de energia, combustíveis e produtos químicos renováveis [3]. O desenvolvimento de tecnologias para o estabelecimento de novas biorrefinarias tem incentivado a substituição das atuais tecnologias petroquímicas baseadas em recursos fósseis pelas baseadas em recursos renováveis, como a biomassa vegetal [4].

A biomassa vegetal é o recurso mais abundante e mais renovável existente, produzida a partir da fotossíntese das plantas diretamente de luz, gás carbônico e água, e ainda será considerado dominante nos próximos anos. A lignocelulose é o principal constituinte da biomassa vegetal, sendo composta por uma mistura de celulose associada a hemicelulose, lignina, pectina e outras substâncias em menores quantidades [5]. Quando submetidos a hidrólise enzimática, os polissacarídeos de celulose e hemicelulose são convertidos em glicose e outros açúcares fermentáveis, que podem ser convertidos a combustíveis líquidos e muitos outros químicos de valor agregado [6].

O etanol produzido a partir da fermentação direta da sacarose da cana-de-açúcar ou obtido do amido de milho e outros cereais é conhecido como **primeira geração** de biocombustíveis. Atualmente o Brasil e os Estados Unidos produzem cerca de 80% da oferta mundial [7]. Muitas pesquisas têm sido realizadas desde 1970 voltadas para produção de bioetanol a partir da degradação da lignocelulose de bagaço de cana, processo conhecido como **segunda geração** de biocombustíveis [8]. Diversos fatores influenciam o custo final da produção do etanol de primeira e segunda geração. Para que a produção do etanol de segunda geração se torne economicamente viável, alguns esforços precisam ser colocados em prática: 1) diminuição do preço da energia utilizada no processo; 2) diminuição do custo e aumento da eficiência das enzimas utilizadas na hidrólise enzimática da biomassa vegetal ; 3) otimização das etapas de pré-tratamento; 4) melhoramento no processo de fermentação a partir de pentoses,

entre outros [9]. A melhoria nestes processos poderia reduzir cerca de 37% dos custos na produção do etanol de segunda geração [9].

Uma das maiores barreiras econômicas na produção dos biocombustíveis é a elevada recalcitrância das fibras de lignocelulose. As ligações  $\beta$ -(1,4)-glicosídicas dos polissacarídeos de celulose caracterizam a estrutura fibrosa e rígida das plantas e as tornam resistentes a químicos, microrganismos ou degradação enzimática [5]. A hidrólise enzimática da celulose, caracterizada pela sua conversão a glicose, é catalisada por celulases, sendo este o principal ponto na bioconversão como um todo. Por conta da elevada recalcitrância das fibras de celulose, grandes quantidades de enzimas são necessárias durante a hidrólise celulolítica.

Apesar de eficientes, as etapas de pré-tratamento e hidrólise enzimática representam custos muito elevados, reconhecidas como gargalos na produção e viabilização do etanol de segunda geração [10]. É estimado que, o uso de microrganismos que secretam enzimas que degradam a biomassa vegetal, reduzindo assim a etapa de pré-tratamento, poderia reduzir o custo do processo em cerca de 40% [11]. Embora estudos mostrem diversas melhorias na atividade de enzimas, na sua estabilidade e a redução de custos na sua produção, as enzimas estão disponíveis a cerca de US\$ 1.5-2.0 por Kg, valores ainda considerados elevados [12]. A fim de reduzir este custo, diversos estudos estão sendo realizados a fim de otimizar o processo de produção de enzimas, com foco especificamente na etapa de hidrólise enzimática.

Fungos filamentosos são notoriamente as maiores fontes de enzimas utilizadas para conversão de lignocelulose em açúcares fermentáveis para a produção de biocombustíveis. As estratégias utilizadas por esses organismos na degradação da lignocelulose são diversas, mas nosso conhecimento relacionado aos mecanismos de secreção e produção de proteínas nesse processo ainda é muito limitado. Dentre os fungos filamentosos, o ascomiceto *Aspergillus nidulans* tem sido um organismo modelo de estudos em genética e biologia celular por mais de 60 anos. *A. nidulans* é o representante do gênero melhor caracterizado e estudado, possuindo diversas aplicações em biotecnologia [13]. Manipulações genéticas com foco nos mecanismos de secreção de proteínas em *Aspergillus* estão sendo realizadas, na tentativa de aumentar a produção de enzimas lignocelulolíticas homólogas ou heterólogas, o que pode possibilitar o desenvolvimento de linhagens produtoras de enzimas de interesse comercial [14].

Aproximadamente 50% das enzimas industriais são produzidas por fungos filamentosos, com destaque para o gênero *Aspergillus* como grande contribuinte para o alcance destes níveis [15]. As enzimas comerciais produzidas por *Aspergillus* incluem amilases, celulases, glicose oxidases, catalases, lipases, pectinases, proteases e xilanases nas indústrias



de alimentos, detergentes, biocombustíveis, tecidos e papel [16]. Apesar dos fungos filamentosos possuírem um sistema de secreção de proteínas de alta capacidade, estes têm falhado na produção de grandes quantidades de proteínas heterólogas quando comparados com proteínas homólogas, e estes problemas parecem estar relacionados a múltiplos fatores [17]: (I) baixa eficiência de transformação; (II) altos níveis de proteases ou elementos tóxicos produzidos por algumas espécies; (III) alterações pós-traducionais promovidas por proteases. Fatores que influenciam negativamente a maturação das proteínas no retículo endoplasmático parecem ser a chave para obtenção do aumento nas taxas de secreção de proteínas homólogas e heterólogas [18].

Como forma de compreender os mecanismos utilizados pelos fungos filamentosos ao secretar proteínas recombinantes, muitos estudos tem utilizado a transcriptômica para investigar situações de estresse na via de secreção de espécies do gênero *Aspergillus* [1,19–21]. Combinando os dados dos transcriptômica com os dados de genômica e proteômica, é possível fazer avaliações mais específicas utilizando as novas técnicas disponíveis, para o entendimento aprofundado da base molecular da secreção de proteínas nesses fungos filamentosos [22].

Diante do exposto, o principal **objetivo** neste trabalho foi realizar a análise comparativa dos mecanismos de secreção de diferentes proteínas heterólogas em *A. nidulans*. Para isso, foram gerados dados de transcriptômica a partir da técnica de RNA-seq (*Next Generation RNA sequencing*), analisados com auxílio de ferramentas de bioinformática e com colaboração da pesquisadora Dra. Gabriela Felix Persinoti/CTBE. Para monitorar o processo de secreção, adotamos 3 genes alvo: alfa-arabinofuranosidase GH51 (AbfA) e beta-glucosidase GH3 (BglC), originadas de *Aspergillus fumigatus*, e mananase GH5 termofílica (1542) da bactéria hipertermofílica *Thermotoga petrophila*. Estes genes foram transformados em *A. nidulans*, sendo que para AbfA atingiu-se altos níveis de secreção, diferente de BglC e 1542, onde os níveis de secreção foram mínimos. A análise das linhagens recombinantes de *A. nidulans* por transcriptômica permitiu a identificação de 476 genes diferencialmente expressos, sendo destes apenas 30 em comum em todas as condições analisadas.

Com isso foram definidos perfis transcriptômicos dos genes regulados durante a secreção de proteínas heterólogas em *A. nidulans* em diferentes tempos de indução. Além disso foram identificados 17 genes diferencialmente expressos em todas as condições experimentais, envolvidos com a via de secreção de *A. nidulans*, representando importantes alvos para manipulação genética deste organismo. Este é o primeiro estudo que descreve a resposta transcriptômica da secreção de proteínas heterólogas em *A. nidulans*, gerando uma nova

perspectiva ao comparar três diferentes proteínas heterólogas com níveis crescentes de secreção. Nossos resultados fornecem novos conhecimentos no entendimento de como *A. nidulans* se adapta a superprodução e secreção de proteínas heterólogas, disponibilizando novos alvos para manipulação genética com possíveis chances de melhorias nos níveis de secreção proteica. Estudos futuros com este organismo podem elucidar ainda mais os mecanismos utilizados pelos fungos filamentosos ao secretar proteínas, e auxiliar a superar gargalos enfrentados atualmente pela indústria que utiliza sua complexa maquinaria na obtenção de enzimas.

## CAPÍTULO 1

### 2. REVISÃO BIBLIOGRÁFICA

#### 2.1. Etanol de segunda geração

A maior parte da energia consumida no mundo é proveniente de fontes não renováveis, como o petróleo e o carvão mineral. Esse dado é um fator agravante em grande parte dos países, pois cria uma situação de fragilidade econômica devido à possibilidade de esgotamento desses recursos, o que acarretará no aumento dos preços do petróleo nos mercados internacionais e de seus derivados [6]. A utilização do petróleo e seus derivados como fontes de energia é o principal impulsionador do aquecimento global devido aos gases de efeito estufa emitidos durante sua queima. Para contornar tal problema, diversas conferências mundiais têm debatido os efeitos ocasionados a partir do uso dessas fontes de energia não renováveis, como por exemplo, aumento do nível dos oceanos, aumento da incidência de doenças transmissíveis por mosquitos e outros vetores, alteração no regime pluvial, desertificação, perda de áreas agricultáveis, problemas relacionados ao abastecimento de água doce e aumento de fluxos migratórios de animais; chuvas ácidas; ilhas de calor e problemas respiratórios na população dos grandes centros urbanos [23].

Em virtude da problemática gerada pela queima de combustíveis fósseis, faz-se necessária a alteração da matriz energética mundial para uma mais limpa, renovável e sustentável. Para isto, é necessário o desenvolvimento de novos cultivares além de técnicas e tecnologias visando altos rendimentos e baixos custos [24]. Pensando nisso, o desenvolvimento de tecnologias para biorrefinaria se torna um importante atrativo. A biorrefinaria envolve processos de conversão integrada de biomassa e equipamentos para produção de energia, combustíveis e produtos químicos renováveis [3]. O desenvolvimento de tecnologias para o estabelecimento de novas biorrefinarias tem incentivado a substituição das atuais tecnologias petroquímicas baseadas em recursos fósseis por recursos renováveis como a biomassa [4].

Partindo do conceito de biorrefinaria, em 2004 o Departamento Norte-Americano de Energia elaborou uma lista de doze potenciais plataformas químicas obtidas a partir da análise de cerca de 300 substâncias baseadas em precursores de biomassa (carboidratos, ligninas, gorduras e proteínas), plataformas de processos, componentes básicos, e sua aplicação final [4,25]. Estas doze plataformas químicas (**Figura 1**) com grupos funcionais múltiplos, podem

ser produzidas biologicamente ou quimicamente a partir de açúcares e convertidos posteriormente em uma variedade de produtos químicos e materiais de elevado valor [3]. O fator mais importante na comercialização destes produtos é o processo de produção que deve ser mais economicamente competitivo que o processo de refinaria de petróleo já utilizado [4]. Desta forma fica evidente a abrangência que o conceito de biorrefinaria engloba, passando por todas as vertentes de uso da biomassa, seja para produção de biocombustíveis como para a produção de diversos químicos e energia [24].

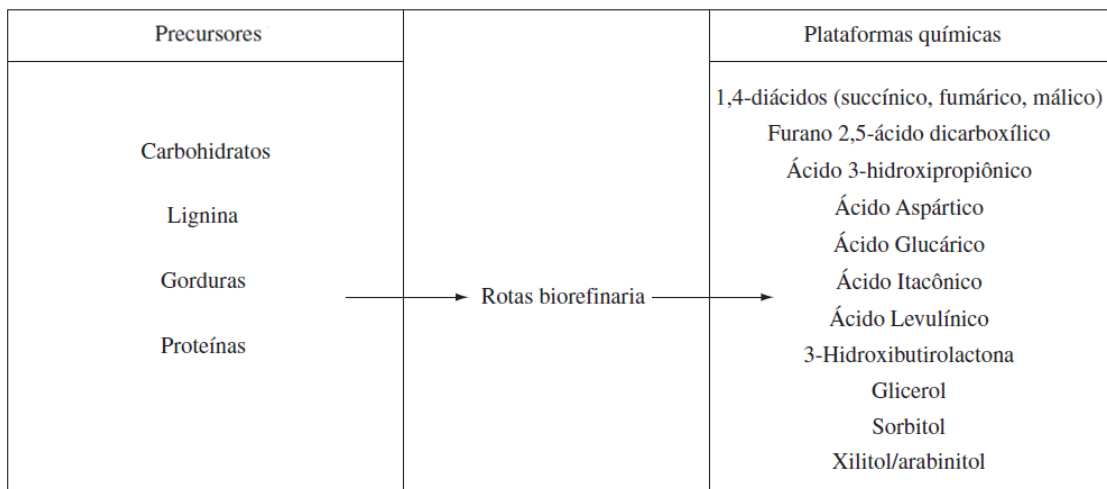


**Figura 1.** Principais plataformas químicas relacionadas pelo Departamento de Energia Norte-Americano [3,25] – Figura adaptada [3].

As previsões atuais indicam que até 2025, mais de 30% das matérias-primas para a indústria química serão produzidas a partir de fontes renováveis [3]. Para se atingir tais metas, é indispensável o desenvolvimento de novas tecnologias para plataformas de biorrefinarias, tais como conversão de matérias-primas a base de lignocelulósicos com ênfase na separação eficiente de lignina, celulose e hemicelulose [3]. A introdução do conceito de biorrefinarias nas usinas produtoras de biocombustíveis pode levar a uma redução de custos, aumento do lucro e independência [24]. No Brasil, diversos processos de biorrefinaria já estão sendo utilizados, um em especial destaque está relacionado ao etanol de segunda geração. Mas antes de se discutir os principais desafios de sua implementação no Brasil, é necessário o entendimento do cenário atual deste biocombustível.

Na década de 70, no cenário da crise mundial do petróleo, o governo brasileiro criou o Programa Nacional de Álcool Combustível (PRÓ-ÁLCOOL), com o principal objetivo de impulsionar o início da substituição de combustíveis de origem fóssil por etanol carburante

(álcool etílico hidratado). O Brasil é hoje considerado detentor de tecnologia de ponta na produção do etanol a partir de cana-de-açúcar, o qual é produzido por um custo médio de US\$ 0,22/L. Já nos Estados Unidos o etanol é produzido a partir do milho ao custo de US\$ 0,35/L [26]. Segundo dados divulgados pela Empresa de Pesquisa Energética (EPE), com o estudo “Análise de Conjuntura dos Biocombustíveis no Brasil 2015”, a produção brasileira de etanol bateu recorde em 2015 ao atingir 30 bilhões de litros, crescimento de 6% em relação a 2014. Apesar disto, segundo relatório da Universidade de Illinois (Chicago-EUA), o Brasil perdeu o posto de maior produtor de etanol do mundo para os Estados Unidos no ano de 2012. Porém não é o que indicam os dados da FAO (2014), mostrando que o Brasil foi ultrapassado já em 2006 em produção de etanol (**Figura 2**) [27].

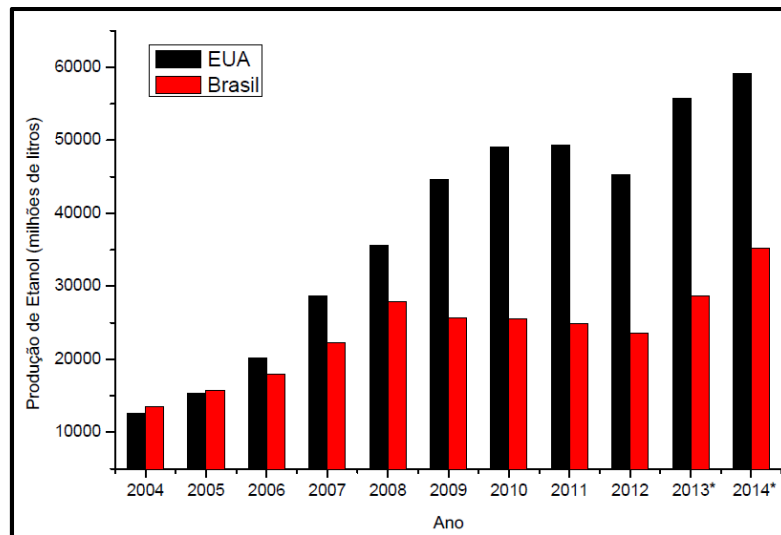


**Figura 2.** Comparação da produção de etanol no Brasil e EUA, segundo dados da FAO (2014), com projeção dos anos 2013/2014 [27].

Como forma de prever quais seriam as ações necessárias para garantir a alta produção de etanol no país, o governo brasileiro, por meio do Centro de Gestão e Estudos Estratégicos (CGEE), encomendou um estudo desenvolvido pelo NIPE/UNICAMP. Neste projeto o objetivo foi avaliar o potencial do país em substituir 5% da demanda mundial de gasolina por etanol de cana-de-açúcar até 2025 [28]. Algumas das conclusões deste projeto foram que existiam alguns gargalos tecnológicos que deveriam ser superados para que o Brasil se tornasse o maior produtor de etanol do mundo, e garantisse elevada exportação deste combustível. Neste cenário foi criado o CTBE (Laboratório Nacional de Ciência e Tecnologia do Bioetanol), um centro tecnológico em Campinas/SP determinado a criar um método economicamente viável para a produção do etanol de segunda geração, e com isso aumentar a produção de etanol no país.

O etanol de segunda geração (2G) apresenta grande potencial de crescimento, pois não depende da produção de alimentos para sua industrialização e nem da expansão da área plantada com cana-de-açúcar. A produção deste combustível depende do reaproveitamento dos co-produtos gerados da produção de etanol de primeira geração (1G) e açúcar, como o bagaço e a palha da cana que juntos representam dois terços do potencial energético da planta [23]. Perspectivas indicam que cerca de 300 litros de etanol/tonelada de bagaço de cana seco aumentariam o rendimento de produção de etanol/ha em até 100% [23]. No entanto, devido à natureza recalcitrante da biomassa celulósica, o custo de processamento corrente do etanol 2G ainda é muito mais elevado do que o etanol 1G [10].

Recentemente o Brasil conta com projetos fomentados pelo Plano Conjunto BNDES-Finep de Apoio à Inovação Tecnológica Industrial dos Setores Sucroenergético e Sucroquímico (PAISS), que viabilizaram a implementação das três primeiras Plantas produtoras de etanol 2G no Brasil, atingindo cerca de 140 milhões de litros por ano. Contudo, tal volume ainda é considerado pequeno quando comparado à demanda interna de combustíveis, hoje suprida com gasolina importada [29]. Um estudo publicado em 2015 denominado “De promessa a realidade: como o etanol celulósico pode revolucionar a indústria da cana-de-açúcar - uma avaliação do potencial competitivo e sugestões de política pública” realizado em conjunto entre CTBE e BNDES, concluiu que por conta de avanços nas etapas de produção, conversão de biomassa e da redução no custo de enzimas, o etanol 2G pode ser mais competitivo que o etanol convencional e próximo do patamar de preço de barril de petróleo a US\$ 44, no longo prazo [29].

Atualmente operam no Brasil cerca de 390 usinas geradoras de etanol 1G [30]. Diversos estudos exploram a capacidade da configuração de produção de etanol 1G e 2G integrados, porém algumas conclusões mostram que esta produção integrada ainda não é economicamente competitiva [30]. Tal dificuldade se deve principalmente a grande recalcitrância da biomassa lignocelulósica em questão, sendo que a desconstrução da biomassa com a utilização de enzimas é um dos grandes gargalos na produção de etanol 2G [31].

Para obtenção do etanol 2G, é necessário converter os materiais lignocelulósicos em açúcares fermentáveis. A lignocelulose representa cerca de 90% da biomassa vegetal, sendo composta basicamente por celulose, hemicelulose e lignina. Em geral, tal conversão de lignocelulose a açúcares fermentáveis envolve o pré-tratamento da matéria bruta para, então, submetê-la à hidrólise enzimática (**Figura 3**). O pré-tratamento (químico, físico e/ou biológico)

auxilia a hidrólise enzimática ao alterar ou remover a hemicelulose e/ou a lignina, aumentar a área superficial e diminuir o grau de polimerização e cristalinidade da celulose [32].

Durante a etapa de hidrólise enzimática, pelo menos três classes de enzimas constituem o complexo celulolítico: (I)  $\text{exo-}\beta\text{-1,4-D-glucanases}$ , que hidrolisam a cadeia celulósica a partir de suas extremidades liberando celobioses, (II)  $\text{endo-}\beta\text{-1,4-D-glucanases}$ , que hidrolisam as ligações internas da cadeia celulósica de maneira aleatória, e (III)  $\beta\text{-1,4-D-glucosidases}$ , que promovem a hidrólise da celobiose em glicose e podem também clivar unidades glicosídicas a partir de celo-oligossacarídeos. Essas enzimas atuam em sinergia para hidrolisar a celulose criando sítios acessíveis umas para as outras e aliviando problemas de inibição pelos produtos [32].

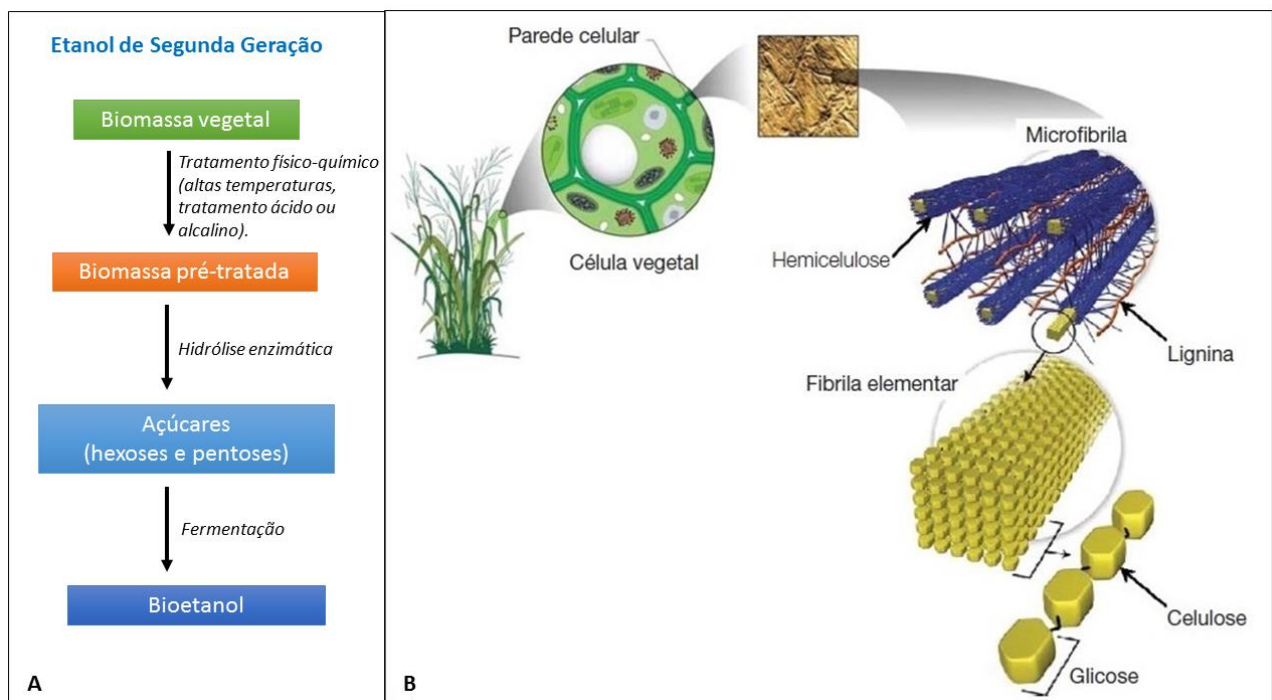


**Figura 3.** (A) Etapas para obtenção do etanol de segunda geração em que há pré-tratamento da biomassa vegetal, hidrólise enzimática da biomassa pré-tratada e fermentação a partir dos açúcares resultantes da hidrólise – adaptada [11]; (B) Arquitetura da parede celular vegetal constituída por lignocelulose - Figura adaptada [32].

As hemicelulases, um grupo de enzimas de caráter bem heterogêneo, também são necessárias durante a etapa de hidrólise enzimática da biomassa: (I)  $\text{endo-}\beta\text{-1,4-D-xilanases}$ , que hidrolisam ligações glicosídicas internas aleatoriamente na cadeia de xilano, (II)  $\beta\text{-1,4-D-xilosidases}$ , que “atacam” xilooligossacarídeos a partir das pontas não redutoras da cadeia de

xilano liberando xilose, (III) endo- $\beta$ -1,4-D-mananases, que clivam ligações internas na cadeia de manano, (IV)  $\beta$ -1,4-D-manosidases, que clivam manooligossacarídeos em manose, e (V) enzimas que removem os grupos substituintes laterais (ramificações), como  $\alpha$ -D-galactosidases,  $\alpha$ -L-arabinofuranosidases,  $\alpha$ -D-glucuronidases, acetil xilano esterases e feruloil esterases [32]. Apesar de eficientes, as etapas de pré-tratamento e hidrólise enzimática representam custos muito elevados, reconhecidas como gargalos na produção e viabilização do etanol 2G [10]. É estimado que, o uso de microrganismos que secretam enzimas que degradam a biomassa vegetal, reduzindo assim a dependência da etapa de pré-tratamento, poderia reduzir o custo do processo em cerca de 40% [11]. Embora estudos mostrem diversas melhorias na atividade de enzimas, na sua estabilidade e a redução de custos na sua produção, as enzimas estão disponíveis a cerca de US\$ 1.5-2.0 por Kg, valores ainda considerados elevados [12]. No entanto, o custo por litro de enzimas pode variar com o pré-tratamento aplicado, o grau de conversão de polímeros (celulose e hemicelulose) em açúcares, e a conversão de açúcares em etanol [10,12].

A contribuição dos custos de enzimas para a economia da produção de etanol 2G continua sendo um tema muito debatido. Klein-Marcuschamer et al. (2012) observaram que o custo da produção de enzimas é muito variável e controverso na literatura. Enquanto alguns autores argumentam que o custo da produção de enzimas é uma grande barreira para a produção de biocombustíveis, outros assumem implicitamente que não é, estimando um custo relativamente baixo ou assumindo que os altos custos diminuirão com os avanços tecnológicos e inovação [12].

A fim de reduzir este custo, muitas pesquisas estão sendo realizadas para otimizar os processos de produção de enzimas, com foco especificamente na etapa de hidrólise enzimática. Neste contexto, fungos filamentosos lignocelulolíticos são amplamente utilizados na indústria por sua alta capacidade de secretar um arsenal complexo de enzimas, desconstruindo sinergicamente polissacarídeos da parede celular vegetal [33,34]. Exemplos destes microrganismos são os fungos filamentosos dos gêneros *Trichoderma* e *Aspergillus*. Esses fungos são a maior fonte comercial de celulases, sendo também considerados com maior capacidade de produzir e secretar essas enzimas [8]. As estratégias destes microrganismos em degradar lignocelulose são diversas, mas o conhecimento científico relacionado aos mecanismos de secreção e regulação da produção enzimática ainda é muito limitado [35,36].

O desenvolvimento do etanol 2G no Brasil atualmente enfrenta diversos desafios e apresenta estudos crescentes que visam viabilizar seu uso. Para reduzir os custos na produção



de etanol a partir da conversão da biomassa, fungos filamentosos podem ser a chave neste processo. Estes organismos são capazes de secretar naturalmente uma grande variedade de enzimas ao meio externo e apresentam importantes alternativas para redução dos custos de produção de enzimas, necessárias principalmente na etapa de hidrólise enzimática da produção do etanol 2G. Dessa forma, os estudos relacionados ao metabolismo desses organismos podem ser direcionados para aumentar produção e secreção de enzimas de interesse.

## 2.2. Secreção de proteínas por fungos filamentosos

Os fungos são de grande importância em diversos campos da biotecnologia atualmente, como na produção de papel, na indústria têxtil, alimentícia, farmacêutica e ainda muitos outros setores que utilizam as enzimas produzidas por esses microrganismos. Além disso, diversas características do metabolismo dos fungos estão sendo exploradas para produção e obtenção de compostos bioativos e antibióticos [37].

Os fungos possuem um excelente sistema para expressão e secreção de proteínas homólogas e heterólogas que podem ser eficientemente expressas nestes organismos. Muitas proteínas possuem modificações pós-traducionais como glicosilações, sulfatações e fosforilações necessárias para sua correta funcionalidade, sendo esta característica uma grande vantagem na utilização dos fungos como modelo de expressão e secreção de proteínas, uma vez que os fungos são capazes de realizar tais modificações. Quando comparados com os sistemas de expressão em culturas de células de mamíferos, os fungos (em destaque os fungos filamentosos) possuem um crescimento bem mais rápido e em meios de cultivo baratos [38].

Os fungos filamentosos são caracterizados por possuírem estruturas filamentosas ramificadas ou hifas e esporos assexuais (conídios). Eles são em maior parte quimio-organotróficos e obtém energia e carbono a partir da oxidação de compostos orgânicos [18]. Alguns exemplos de relevância industrial desse grupo são os gêneros *Aspergillus*, *Penicillium* e *Trichoderma* [18]. Este grupo de fungos é ainda conhecido por sua capacidade de secretar grande quantidade de proteínas, característica relacionada a alta taxa de crescimento e pela capacidade de suportar elevada densidade de biomassa. *Aspergillus niger*, por exemplo, é capaz de produzir 25-30 g/L de glucoamilase e *Trichoderma reesei* também já foi descrito como produtor de cerca de 100 g/L de proteínas extracelulares [39].

A via de secreção de proteínas nos fungos filamentosos é relativamente complexa (**Figura 4**). No retículo endoplasmático (RE) as proteínas são enoveladas e podem sofrer

modificações pós-traducionais [22]. Caso as proteínas não sejam corretamente modificadas ou enoveladas elas permanecem no RE para serem ligadas a chaperonas (como BIP ou calnexina) para correto enovelamento. Ainda, algumas proteínas enoveladas incorretamente são transportadas de volta ao citosol para serem degradadas pelo proteassoma [40]. As proteínas corretamente modificadas são encaminhadas para as vesículas revestidas por “*coating protein II*” (COP II) para então serem direcionadas ao complexo de Golgi, onde podem sofrer outras modificações tardias, como glicosilações e processamento pelo peptídeo sinal. Quando as proteínas já estão “maduras” são finalmente encaminhadas para vesículas de secreção onde podem então ser transportadas por exocitose ao meio extracelular [22].

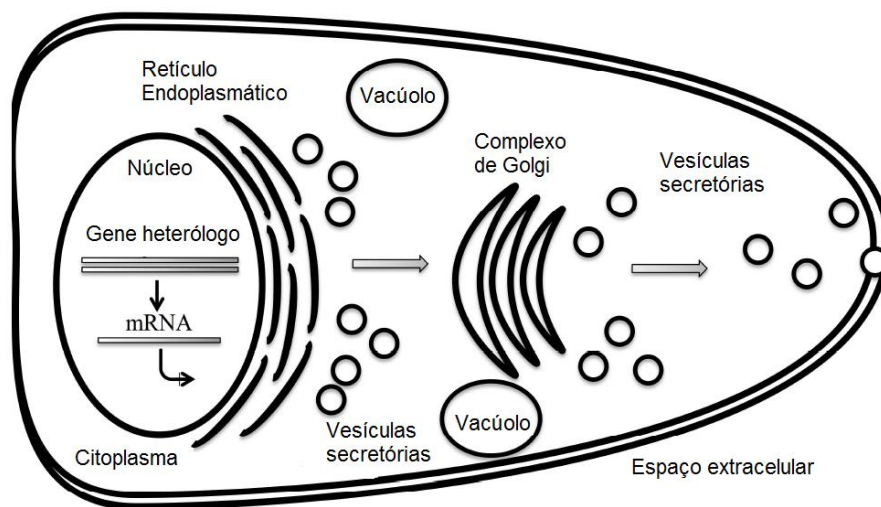


**Figura 4.** Visão geral da via de secreção de proteínas recombinantes em fungos filamentosos – Figura adaptada [41].

Apesar dos fungos filamentosos possuírem um sistema de secreção de proteínas de alta capacidade, estes têm falhado na produção de grandes quantidades de proteínas heterólogas quando comparados com proteínas homólogas, e estes problemas parecem estar relacionados a múltiplos fatores [17]: (I) baixa eficiência de transformação; (II) altos níveis de proteases ou elementos tóxicos produzidos por algumas espécies; (III) alterações pós-traducionais promovidas por proteases. Fatores que influenciam negativamente a maturação das proteínas no RE se configuram como a chave para obtenção do aumento nas taxas de secreção de proteínas homólogas e heterólogas [18].

Muitas estratégias têm sido testadas para contornar problemas em secreção de proteínas, sendo uma delas a manipulação de componentes da via de secreção, o que pode auxiliar na identificação de possíveis elementos reguladores que inibem esta via. A exemplo disso, em uma revisão bibliográfica, Ward et al. (2012) aponta diversas pesquisas que têm realizado a

superexpressão de proteínas auxiliares do enovelamento das proteínas presentes no lúmen do RE como foldases, chaperonas e enzimas relacionadas a glicosilação, obtendo sucesso [18]. Estão sendo também realizadas tentativas de aumentar o número de cópias do gene de interesse e conseqüentemente o número de proteínas sintetizadas, além do uso combinado de linhagens deficientes em proteases [18]. Apesar disso, alguns estudos têm demonstrado que o gargalo na produção de proteínas heterólogas não é causado pela baixa expressão do gene heterólogo, mas sim a processos pós-transcricionais na via de secreção [42].

Na via de secreção dos fungos filamentosos, o RE tem a função de enovelar corretamente as proteínas a serem secretadas e ainda auxiliar no encaminhamento das proteínas ao seu destino correto. Diversas variações fisiológicas ou ambientais podem causar distúrbios na homeostase do RE o que pode levar a um acúmulo de proteínas mal enoveladas em seu lúmen [22]. Este fato pode gerar o incorreto enovelamento e modificações pós-traducionais formando agregados e impossibilitando assim a secreção ao meio extracelular, gerando uma situação de estresse de RE. Para lidar com isso, a via de sinalização intracelular “*unfolded protein response*” (UPR) é ativada, o que causa uma resposta transcricional que aumenta a capacidade de enovelamento das proteínas do RE na tentativa de restauração de sua homeostase [16].

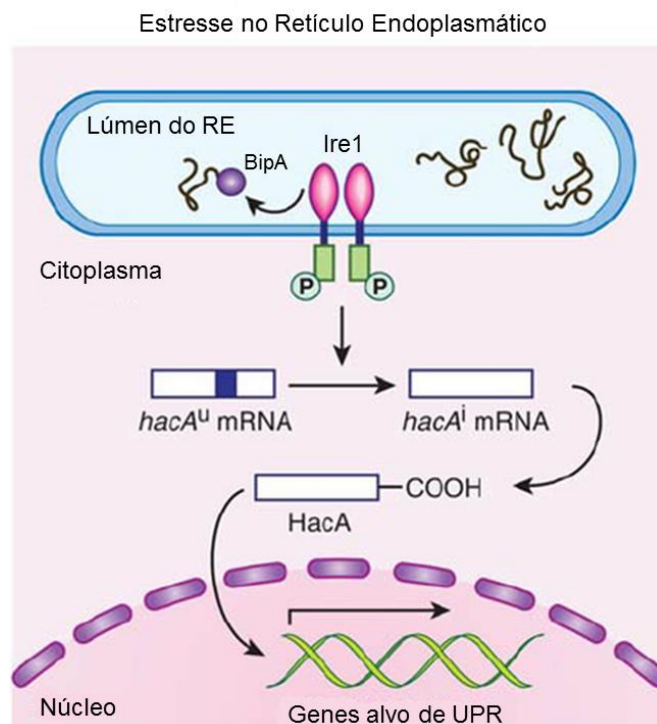


**Figura 5.** Representação da resposta a proteínas mal enoveladas no RE (UPR). Durante o estresse de RE proteínas mal enoveladas se ligam a Ire1 recrutando a chaperona BipA e promovendo sua oligomerização e autofosforilação. O domínio citoplasmático com atividade de RNase de Ire1 é ativado

e promove o splicing do RNAm de *hacA*. O fator de transcrição HacA se liga a regiões promotoras de genes alvo de UPR no núcleo, promovendo uma resposta celular a fim de contornar o estresse de RE. A resposta de UPR se caracteriza pelo aumento da capacidade de enovelamento no RE, expansão do RE e aumento de sua capacidade degradativa. Figura adaptada [43].

UPR representa uma via conservada de sinalização coordenada por dois componentes reguladores fundamentais (**Figura 5**): o fator de transcrição do tipo bZIP, Hac1/HacA, e a RNase/quinase localizada na membrana do RE, Ire-1 [44]. Ire-1 é ativada por proteínas mal enoveladas presentes no RE. Quando ativa, esta RNase promove o splicing alternativo de *hacA*, ativando este fator de transcrição [22]. Esta ativação de HacA permite que o RE se adapte promovendo a regulação do sistema de secreção, aumento da capacidade de enovelamento no RE, ampliação da superfície do RE, reestruturação dos processos de transporte celulares entre RE e Golgi, além de promover degradação de proteínas mal enoveladas através da via conhecida como degradação associada ao RE (“*ER-associated degradation*” - ERAD) [44].

UPR tem sido estudada nos fungos filamentosos como possível solução de superar obstáculos encontrados na produção e secreção de proteínas homólogas e heterólogas [44]. Em geral, estes microrganismos exibem a regulação Ire-1/HacA bastante conservada regulando as funções do RE de diversas formas durante situação de estresse de secreção proteica [45]. Os genes regulados durante UPR se encontram predominantemente divididos em categorias funcionais associados a via de secreção, incluindo chaperonas residentes do RE, genes envolvidos no metabolismo de fosfolipídios, síntese de ácidos graxos, translocação, glicosilação de proteínas, síntese e remodelagem da parede celular, transporte vesicular e degradação proteica [44,46,47]. Como forma de monitorar a regulação de UPR na célula e consequentemente suas categorias funcionais, diversos genes alvo já foram descritos diferencialmente expressos nesta situação de estresse de RE, como é o caso da chaperona BipA [22,48]. O gene *bipA* (AN2062) em *A. nidulans* codifica uma chaperona residente do RE da família HSP70, bastante estudada por ser um alvo de UPR com seus níveis aumentados durante o estresse de RE [49]. Outro alvo bastante conhecido é o gene *sec63* que codifica uma proteína de translocação de RE, subunidade do complexo Sec63 em *Saccharomyces pombe* [50]. O ortólogo de *sec63* em *A. nidulans* (AN0834) também já foi identificado e relacionado ao estresse de RE [46], sendo superexpresso após adição de ditionitrito (DTT), droga que atua como forte agente redutor desestabilizando o ambiente oxidativo do RE e prevenindo a formação de pontes dissulfeto [22].

Outra via bastante estudada como forma de melhorar a secreção de proteínas em fungos filamentosos é a ERAD. Esta via de degradação representa um processo no qual as proteínas mal enoveladas no RE são deslocadas para o citoplasma para degradação pelo proteassoma. Conservada entre células de leveduras, fungos filamentosos, plantas e mamíferos, ERAD é outra importante resposta causada por proteínas mal enoveladas na via de secreção [51]. Espécies de fungos filamentosos como *T. reesei* e *A. niger* são conhecidas por sua alta capacidade de secreção, mas elas significativamente diferem em suas respostas por ERAD. Geralmente, os componentes homólogos de ERAD em levedura podem ser facilmente identificados em *T. reesei* [52]. Em contraste, algumas proteínas homólogas, tais como Cue1p, Rad23p, Ubx2p, e Yos9p são difíceis de encontrar expressas em *A. niger* [51]. Em *A. nidulans*, Ubx2/Sel1 já foi identificada como indicador de ERAD, tornando-se um importante alvo de estudos nesta espécie [46].

A complexidade e a relativa falta de entendimento da fisiologia dos fungos filamentosos, em comparação com outros microrganismos como bactérias, têm impedido rápido desenvolvimento destes organismos como fábricas altamente eficientes para a produção de proteínas heterólogas [51]. Como forma de contornar esta situação, muitos estudos de transcriptômica investigando UPR e estresse de RE foram previamente realizados em espécies do gênero *Aspergillus* [1,19–21]. Combinando os dados de transcriptômica com os dados de genômica e proteômica, será possível fazer avaliações mais específicas utilizando as novas técnicas disponíveis, para o entendimento aprofundado da base molecular da secreção de proteínas nesses fungos filamentosos [22].

### **2.3. Produção de proteínas heterólogas em *Aspergillus***

A secreção de proteínas é um dos mais importantes e complexos processos realizados pelos Eucariotos. Os fungos filamentosos são bastante conhecidos por sua capacidade de secretar altos níveis proteicos, com níveis descritos chegando a marca de 100 g/L em algumas espécies [34]. Aproximadamente 50% das enzimas industriais são produzidas por fungos filamentosos, com destaque do gênero *Aspergillus* como grande contribuinte para o alcance destes níveis [15]. As enzimas comerciais produzidas por *Aspergillus* incluem amilases, celulases, glicose oxidases, catalases, lipases, pectinases, proteases e xilanases nas indústrias de alimentos, detergentes, tecidos e papel [16].

O gênero *Aspergillus* é constituído por mais de 180 espécies descritas e, em sua maioria, realizam a degradação de polissacarídeos vegetais [53]. São de grande importância industrial por produzirem enzimas recombinantes em larga escala e quando comparados com outros microrganismos como *Escherichia coli* e *Saccharomyces cerevisiae*, *Aspergilli* possui sistemas muito mais complexos de modificações pós-traducionais, fato que em grande parte das vezes é considerado a chave para a secreção proteica adequada [21]. A maior parte das proteínas homólogas e heterólogas produzidas industrialmente são provenientes de um número muito limitado de espécies de fungos, sendo principalmente obtidas a partir de *Aspergillus niger*, *Aspergillus oryzae* e *Trichoderma reesei*. No entanto, estas espécies de fungos podem não ser os hospedeiros apropriados no estudo de secreção de enzimas principalmente por estarem encobertos por patentes e direitos de propriedade intelectual [14].

Atualmente os estudos com a espécie *A. nidulans* são facilitados por este organismo possuir um ciclo sexual bem caracterizado, um sistema genético manipulável, tendo disponibilidade de muitos alelos mutantes de domínio amplo e ainda por ter muitos reguladores de vias específicas, fatos que possibilitam vantagens para o desenvolvimento e construção de linhagens mutantes [14]. A análise do genoma em combinação com estudos de proteoma mostram que este fungo possui um potencial de degradação de polissacarídeos muito similar aos outros fungos também utilizados industrialmente. Além disso, os mecanismos regulatórios envolvidos com o controle de expressão das atividades de degradação da parede celular vegetal são bastante conservados em *Aspergillus* [14]. Por estas características os fungos do gênero *Aspergillus* possuem uma grande variedade de enzimas lignocelulolíticas que facilitam a degradação e obtenção de nutrientes para seu crescimento em diferentes tipos de substratos relacionados a biomassa vegetal [54], conforme representado na **Figura 6**.

Os fungos filamentosos em geral possuem grande variedade de enzimas ativas em carboidratos (*Carbohydrate-Active Enzymes* – CAZymes), sendo a sacarificação da lignocelulose uma função natural desempenhada por muitas espécies fúngicas e muito explorada pela indústria na produção de enzimas comerciais [35]. Dentre as CAZymes que mais se destacam na secreção de *Aspergillus* são as glicosil hidrolases (GHs), grupo amplo de enzimas que hidrolisam a ligação glicosídica em poli-, oligo- e até dissacarídeos. As GHs têm sido bastante estudadas e produzidas por expressão heteróloga em espécies de *Aspergillus*, mas apesar disso, a eficiência na obtenção de grandes quantidades de enzimas geralmente é baixa quando comparados aos níveis de proteínas homólogas, podendo estar de 10 até 1000 vezes menos expressa [51,55]. Estudos relacionados ao mecanismo de secreção nestes fungos

filamentosos como regulação gênica, modificações pós-traducionais e referentes a síntese de proteases estão sendo realizados com o intuito de aumentar a produção destas enzimas [56].

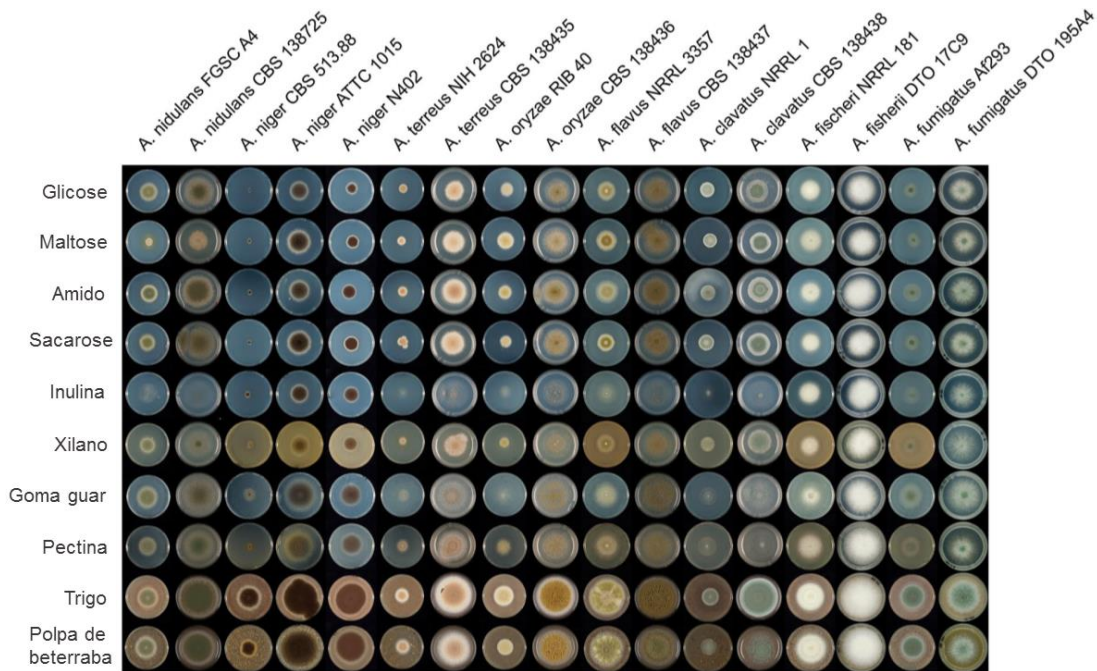


**Figura 6.** Perfil de crescimento de oito espécies de *Aspergillus* em diferentes fontes de carbono provenientes de biomassa vegetal. Figura adaptada [54].

Em busca de novas formas a fim de melhorar a produção de proteínas recombinantes em *Aspergillus*, diversos estudos mostraram desenvolvimento de vetores de expressão com grande potencial de produção e secreção de proteínas alvo [14,57]. A exemplo disso, recentemente Segato et al. (2012) desenvolveram um vetor de expressão que pode ser utilizado em diferentes espécies de *Aspergillus* (*A. nidulans* e *A. awamori*). Este vetor de expressão e secreção denominado pEXPYR (**Figura 7**), quando integrado no genoma de *Aspergillus*, dirige a superexpressão proteica por indução com maltose, permitindo a secreção de proteínas alvo ao meio extracelular [58]. Estudos utilizando este vetor têm mostrado resultados bastante promissores na produção de proteínas homólogas e heterólogas, particularmente GHs de origem fúngica ou bacteriana [58–62]. Apesar disso, os níveis finais de proteínas recombinantes obtidos com este vetor chegam até 50-100mg/L no meio extracelular [58]. Estes valores de proteínas alvo secretadas estão de acordo com o que é encontrado para outros vetores de expressão de proteínas recombinantes em *Aspergillus* (**Tabela 1**), como o exemplo de 70,3 mg/L de proteína heteróloga secretada por *A. oryzae* [42].

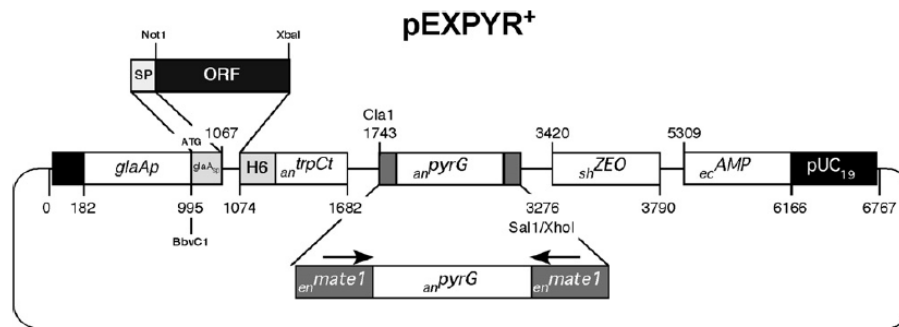


**Figura 7.** pEXPYR é um vetor de transformação em *Aspergillus* (*A. nidulans* e *A. awamori*) para super-expressão proteica e secreção. Este vetor é baseado em pUC19 de *E. coli*, com resistência a ampicilina (*ecAMP*) e ao marcador eucarioto seletivo fleomicina (*shZEO*). O vetor ainda possui o promotor glicoamilase (*glaAp*) de *A. niger* acompanhado com o peptídeo sinal na região N-terminal e o terminador triptofano (*antrpCt*). A sequência contendo DNA alvo pode ser inserida entre os sítios de restrição de NotI/XbaI ou entre BbvCI/XbaI para manter o peptídeo sinal nativo. Há ainda uma cauda de histidina (H6) para purificação proteica por cromatografia de afinidade presente na região C-terminal. O gene Orotidina-5'-Fosfato Carboxilase (*pyrG*) de *A. niger* é utilizado como complemento para *A. nidulans pyrG89* ou *A. awamori pyrGU3A*, nas suas linhagens engenheiradas. Os marcadores são flanqueados por repetição do *mate1* de 40 pares de bases em *A. nidulans* que facilita a excisão de *pyrG*, o que restaura o genótipo *pyrG*<sup>-</sup> para futuras transformações com pEXPYR – adaptado de [58].

**Tabela 1.** Níveis de secreção de proteínas heterólogas relatados na literatura para espécies do gênero *Aspergillus*.

Enzima	Organismo fonte	Organismo hospedeiro	Níveis de Expressão	Referência
endo-1,4-β-xylanase	<i>Penicillium funiculosum</i>	<i>Aspergillus awamori</i>	1.6 mg/mL	[58]
α-L-arabinofuranosidase	<i>Aspergillus niger</i>	<i>Aspergillus awamori</i>	3.2 mg/mL	[58]
α-galactosidase	<i>Cyamopsis tetragonoloba</i>	<i>Aspergillus awamori</i>	0.4 mg/L	[63]
thaumatin	<i>Thaumatococcus daniellii</i>	<i>Aspergillus awamori</i>	11 mg/L	[64]
α-L-arabinofuranosidase	<i>Aspergillus niveus</i>	<i>Aspergillus nidulans</i>	57.6 mg/L	[61]
endo-1,4-β-xylanase	<i>Aspergillus niveus</i>	<i>Aspergillus nidulans</i>	14 mg/L	[59]
endo-1,4-β-xylanase	<i>Penicillium funiculosum</i>	<i>Aspergillus nidulans</i>	0.6 mg/mL	[65]
α-L-arabinofuranosidase	<i>Aspergillus niger</i>	<i>Aspergillus nidulans</i>	1.6 mg/mL	[65]
endo-1,4-β-xylanase	<i>Penicillium funiculosum</i>	<i>Aspergillus nidulans</i>	2.8 mg/mL	[58]
interleukin-6	<i>Homo sapiens</i>	<i>Aspergillus nidulans</i>	5 mg/L	[66]
lysozyme	<i>Gallus gallus</i>	<i>Aspergillus niger</i>	12 mg/L	[67]
laccase	<i>Pycnoporus cinnabarinus</i>	<i>Aspergillus niger</i>	1.6 mg/mL	[68]
α1-proteinase	<i>Homo sapiens</i>	<i>Aspergillus niger</i>	12 mg/L	[69]
thaumatin	<i>Thaumatococcus daniellii</i>	<i>Aspergillus niger</i>	7 mg/L	[70]
β-mannosidase	<i>Aspergillus aculeatus</i>	<i>Aspergillus oryzae</i>	250 mg/L	[71]
lysozyme	<i>Homo sapiens</i>	<i>Aspergillus oryzae</i>	15.2 mg/L	[72]
chymosin	<i>Bos taurus</i>	<i>Aspergillus oryzae</i>	83.1 mg/L	[73]



Na **Tabela 1** foi realizada uma revisão dos valores de secreção de diferentes proteínas heterólogas expressas em espécies do gênero *Aspergillus*. Estes valores de secreção heteróloga ainda estão muito distantes de valores homólogos já relatados na literatura, chegando a 25 g/L em *A. niger* [18]. Esta grande disparidade de valores entre secreção de proteínas homólogas e heterólogas se torna um dos principais gargalos na produção de proteínas recombinantes a ser superado pela indústria [34]. Como forma de contornar tal problema, muitos pesquisadores estudam especificamente a maquinaria de secreção como solução futura [15,17].

Muitos estudos têm tentado esclarecer a extraordinária capacidade de secreção de *Aspergillus*, principalmente a nível de transcriptoma [15,20,21,46,48,74]. Estes estudos levaram à identificação de genes que desempenham papéis importantes nas diferentes fases da secreção proteica, tal como translocação, enovelamento, transporte de carga e exocitose [15]. A exemplo disso, Liu et al (2014) geraram uma lista de genes que representam componentes do sistema de secreção de *A. oryzae*, utilizando como modelo o sistema de secreção relatado para *S. cerevisiae* [21]. Outro exemplo relevante foi realizado por Kwon et al (2012). Estes pesquisadores definiram o grupo de genes de *A. niger* relacionados a elevada secreção de glicoamilase, caracterizando um conjunto de genes envolvidos de forma mais geral no tráfego intensificado de proteínas através da via secretora de *A. niger* [48]. Sims et al (2005), descreveram a influência da produção e secreção de proteínas heterólogas ao comparar o transcriptoma de *A. nidulans* obtido pela técnica de micro arranjos. Além disso, foi realizado um estudo comparativo dos efeitos desta produção com a adição de droga (DTT) que promove estresse de RE, induzindo UPR [46]. Estes pesquisadores observaram que a semelhança transcriptômica entre a linhagem recombinante com a linhagem nativa induzida com DTT foi de apenas 23%. Este fato pode ter ocorrido devido a adição de DTT perturbar mais drasticamente a via de secreção do que a produção de uma proteína recombinante [46]. É conhecido na literatura que secreção de diversas proteínas recombinantes podem induzir UPR [22], o que pode gerar tanto respostas gerais, quanto proteína-específicas dependendo da proteína alvo sendo superproduzida, algo que não pode ser mimetizado pela indução de bloqueadores de secreção, como DTT [46].

Atualmente com a disponibilidade pública de centenas de sequências de genomas fúngicos, bem como o advento de métodos de alto rendimento como transcriptômica e proteômica, é possível a aquisição de dados em larga escala e a caracterização de novos transcritos e proteínas ainda sem função designada [75]. Pensando nisso, com genoma sequenciado em 2005 e anotado desde então, *A. nidulans* se tornou um importante modelo de

estudos de genômica e transcriptômica [13,76]. Estudos de transcriptômica já realizados com este organismo buscaram identificação de novos promotores, identificação de hidrofobinas e a resposta à drogas [13,33,46]. Além disso, *A. nidulans* é conhecido por ser comumente utilizado em estudos de regulação gênica e secreção de enzimas lignocelulolíticas [58,77]. Dessa forma, *A. nidulans* se torna uma importante ferramenta no estudo do melhoramento de secreção de proteínas heterólogas, considerado o gargalo na produção de proteínas a níveis industriais, especialmente na indústria de biocombustíveis.

Diante do exposto, o principal **objetivo** neste trabalho foi comparar as adaptações celulares de *A. nidulans* no momento de secreção heteróloga de diferentes proteínas alvo. Para esta finalidade, selecionamos três enzimas lignocelulolíticas alvo que apresentam níveis decrescentes de secreção: alfa-arabinofuranosidase GH51 (AbfA) e beta-glucosidase GH3 (BglC) clonadas de *A. fumigatus*, e mananase GH5 termofílica (1542) clonada de *Thermotoga petrophila* (bactéria hipertermofílica). Estas três enzimas foram selecionadas pois a degradação dos carboidratos alvos representam passos chave em diversas aplicações industriais, incluindo produção de papel, processamentos alimentícios, processos relacionados a biorrefinaria e a produção de etanol 2G [78]. Além disso, foi selecionada uma enzima de característica termofílica. Enzimas termofílicas são muito exploradas pela indústria por variadas razões: menores riscos de contaminação, excelente cinética enzimática, maiores taxas de produtividade, entre outras, que em geral, reduzem os custos na produção industrial [79].

Os genes correspondentes a cada enzima heteróloga foram transformados em *A. nidulans*, gerando três linhagens recombinantes: *A. nidulans* AbfA, *A. nidulans* BglC e *A. nidulans* 1542. Através de dados de PCR em tempo real, avaliamos a expressão dos genes heterólogos e de genes chave envolvidos em UPR: *hacAi*, *bipA* e *sell* em função do tempo para as 3 cepas recombinantes. Sabe-se que os níveis de secreção para AbfA são muito maiores do que para BglC e 1542, portanto, a análise de seus genes diferencialmente expressos e também genes envolvidos em UPR sinalizaram em quanto tempo o stress celular se normaliza ou ainda se os níveis de stress de RE são constantes. Os dados de qPCR foram fundamentais para definir tempos específicos de indução de expressão heteróloga nas linhagens para análise de RNA-seq (*Next Generation RNA sequencing*). Com isso foram definidos perfis transcriptômicos dos genes relacionados a secreção em *A. nidulans*, representando a resposta a alta expressão de três genes heterólogos em diferentes tempos de indução. Além disso, foram identificados 17 genes diferencialmente expressos envolvidos com a via de secreção de *A. nidulans*, representando importantes alvos para manipulação genética deste organismo.

Este foi o primeiro estudo que descreve a resposta transcriptômica da secreção de proteínas heterólogas em *A. nidulans*, gerando uma nova perspectiva ao comparar três diferentes proteínas heterólogas com níveis crescentes de secreção. Nossos resultados fornecem novos conhecimentos no entendimento de como *A. nidulans* se adapta a superprodução e secreção de proteínas heterólogas, disponibilizando novos alvos para manipulação genética com possíveis chances de melhorias nos níveis de secreção proteica. Estudos futuros com este organismo podem elucidar ainda mais os mecanismos utilizados pelos fungos filamentosos ao secretar proteínas, e auxiliar a superar gargalos enfrentados atualmente pela indústria que utiliza sua complexa maquinaria na obtenção de enzimas.

#### 2.4. Referências Bibliográficas

1. Ries L, Pullan ST, Delmas S, Malla S, Blythe MJ, Archer DB. Genome-wide transcriptional response of *Trichoderma reesei* to lignocellulose using RNA sequencing and comparison with *Aspergillus niger*. *BMC Genomics*. 2013;14:541.
2. Bastos VD. Etanol, alcoolquímica e biorrefinarias. *Banco Nac. Desenvolv. Econômico e Soc.* 2007;1:1–35.
3. Pervaiz M, Correa CA. Biorefinaria: desenvolvimento de plataformas químicas através de tecnologias integradas de biomassa. *Polímeros Ciência e Tecnol.* 2009;19:E9–11.
4. Choi S, Song CW, Shin JH, Lee SY. Biorefineries for the production of top building block chemicals and their derivatives. *Metab. Eng. Elsevier*; 2015;28:223–39.
5. Seiboth B, Verena CI, Seiboth S-. *Trichoderma reesei*: A Fungal Enzyme Producer for Cellulosic Biofuels, *Biofuel Production-Recent Developments and Prospects*. *Biotechnol. Biofuels*. 2011;127.
6. Nunes R de M, Guarda EA, Carlos J, Serra V, Martins ÁA. Resíduos agroindustriais: potencial de produção do etanol de segunda geração no Brasil. *Liberato*. 2013;14:113–23.
7. Baeyens J, Kang Q, Appels L, Dewil R, Lv Y, Tan T. Challenges and opportunities in improving the production of bio-ethanol. *Prog. Energy Combust. Sci. Elsevier Ltd*; 2015;47:60–88.
8. Gusakov A V. Alternatives to *Trichoderma reesei* in biofuel production. *Trends Biotechnol. Elsevier Ltd*; 2011;29:419–25.
9. Macrelli S, Mogensen J, Zacchi G. Techno-economic evaluation of 2nd generation bioethanol production from sugar cane bagasse and leaves integrated with the sugar-based ethanol process. *Biotechnol. Biofuels*. 2012;5:22.
10. Kumar R, Tabatabaei M, Karimi K, Horváth IS. Recent updates on lignocellulosic biomass derived ethanol -A review. *Biofuel Res*. 2016;9:347–56.
11. Chung D, Cha M, Guss AM, Westpheling J. Direct conversion of plant biomass to ethanol by engineered *Caldicellulosiruptor bescii*. *Proc. Natl. Acad. Sci.* 2014;111:8931–6.

12. Klein-Marcuschamer D, Oleskowicz-Popiel P, Simmons BA, Blanch HW. The challenge of enzyme cost in the production of lignocellulosic biofuels. *Biotechnol. Bioeng.* Wiley Subscription Services, Inc., A Wiley Company; 2012;109:1083–7.
13. Sibthorp C, Wu H, Cowley G, Wong PWH, Palaima P, Morozov IY, et al. Transcriptome analysis of the filamentous fungus *Aspergillus nidulans* directed to the global identification of promoters. *BMC Genomics.* 2013;14:847.
14. Tamayo-Ramos J, Orejas M. Enhanced glycosyl hydrolase production in *Aspergillus nidulans* using transcription factor engineering approaches. *Biotechnol. Biofuels.* 2014;7:103.
15. Schalén M, Anyaogu DC, Hoof JB, Workman M. Effect of secretory pathway gene overexpression on secretion of a fluorescent reporter protein in *Aspergillus nidulans*. *Fungal Biol. Biotechnol.* BioMed Central; 2016;3:3.
16. Fleißner A, Dersch P. Expression and export: recombinant protein production systems for *Aspergillus*. *Appl. Microbiol. Biotechnol.* 2010;87:1255–70.
17. Gouka RJ, Punt PJ, van den Hondel CAMJJ. Efficient production of secreted proteins by *Aspergillus* : progress, limitations and prospects. *Appl. Microbiol. Biotechnol.* 1997;47:1–11.
18. Ward OP. Production of recombinant proteins by filamentous fungi. *Biotechnol. Adv.* Elsevier B.V.; 2012;30:1119–39.
19. Delmas S, Pullan ST, Gaddipati S, Kokolski M, Malla S, Blythe MJ, et al. Uncovering the Genome-Wide Transcriptional Responses of the Filamentous Fungus *Aspergillus niger* to Lignocellulose Using RNA Sequencing. Nielsen J, editor. *PLoS Genet.* 2012;8:e1002875.
20. Zhou B, Xie J, Liu X, Wang B, Pan L. Functional and transcriptomic analysis of the key unfolded protein response transcription factor HacA in *Aspergillus oryzae*. *Gene.* Elsevier B.V.; 2016;593:143–53.
21. Liu L, Feizi A, Österlund T, Hjort C, Nielsen J. Genome-scale analysis of the high-efficient protein secretion system of *Aspergillus oryzae*. *BMC Syst. Biol.* 2014;8:73.
22. Guillemette T, Ram AFJ, Carvalho NDSP, Joubert A, Simoneau P, Archer DB. Methods for Investigating the UPR in Filamentous Fungi. *Methods Enzymol.* 2011;1:1–29.
23. Araujo GF de GJFGF de, Navarro LFS, Santos BAS. O ETANOL DE SEGUNDA GERAÇÃO E SUA IMPORTÂNCIA ESTRATÉGICA ANTE O CENÁRIO ENERGETICO INTERNACIONAL CONTEMPORÂNEO. *Fórum Ambient. Alta Paul.* 2013;9:1–11.
24. Alvim JC, Alvim FALS, Sales VHG, Sales PVG, Oliveira EM de, Costa ACR da. Biorefineries: Concepts, classification, raw materials and products. *J. Bioenergy Food Sci.* 2014;1:61–77.
25. Werpy TA, Holladay JE, White JF. Top Value Added Chemicals From Biomass. U.S. Dep. energy. Richland, WA; 2004;Nov.
26. Alves JMB., Macri RCV. Etanol De Segunda Geração: Estudo De Materiais Lignocelulósicos E Aplicações Da Lignina. *Ciência Tecnol. Revista Ciência e Tecnologia;* 2013;5:1
27. Feroldi M, Urio M. Gestão e Controle de Qualidade da Produção de Bioetanol. *Rev. Monogr. Ambient. - REMOA.* 2014;13:3377–87.

28. Cerqueira Leite RC de, Verde Leal MRL, Barbosa Cortez LA, Griffin WM, Gaya Scandiffio MI. Can Brazil replace 5% of the 2025 gasoline world demand with ethanol? *Energy*. 2009 ;34:655–61.
29. Bonomi A, Dayan C, Jesus F De. De promessa a realidade : como o etanol celulósico pode revolucionar a indústria da cana-de-açúcar - uma avaliação do potencial competitivo e sugestões de política pública. *Biocombustíveis BNDES setorial*. 2015;41:237–94.
30. Losordo Z, McBride J, Rooyen J Van, Wenger K, Willies D, Froehlich A, et al. Cost competitive second-generation ethanol production from hemicellulose in a Brazilian sugarcane biorefinery. *Biofuels, Bioprod. Biorefining*. John Wiley & Sons, Ltd; 2016;10:589–602.
31. Navarro D, Rosso M-N, Haon M, Olivé C, Bonnin E, Lesage-Meessen L, et al. Fast solubilization of recalcitrant cellulosic biomass by the basidiomycete fungus *Laetisaria arvalis* involves successive secretion of oxidative and hydrolytic enzymes. *Biotechnol. Biofuels*. 2014;7:143.
32. Canilha L, Milagres AMF, Silva SS, Silva JBAE, Felipe MG a., Rocha GJM, et al. Sacarificação Da Biomassa Lignocelulósica Através De Pré-Hidrólise Ácida Seguida Por Hidrólise Enzimática: Uma Estratégia De “Desconstrução” Da Fibra Vegetal. *Rev. Anal*. 2009;48–54.
33. Brown NA, Ries LNA, Reis TF, Rajendran R, Corrêa dos Santos RA, Ramage G, et al. RNAseq reveals hydrophobins that are involved in the adaptation of *Aspergillus nidulans* to lignocellulose. *Biotechnol. Biofuels*. 2016;9:145.
34. Nevalainen H, Peterson R. Making recombinant proteins in filamentous fungi- are we expecting too much? *Front. Microbiol*. 2014;5:75.
35. Daly P, Munster JM van, Raulo R, Archer DB. Transcriptional regulation and responses in filamentous fungi exposed to lignocellulose. *Mycol. Curr. Futur. Dev*. 2016;46:82-127.
36. Zhao Z, Liu H, Wang C, Xu J. Comparative analysis of fungal genomes reveals different plant cell wall degrading capacity in fungi. *BMC Genomics*. *BMC Genomics*; 2014;15:6.
37. Magaña-Ortíz D, Coconi-Linares N, Ortiz-Vazquez E, Fernández F, Loske AM, Gómez-Lim M a. A novel and highly efficient method for genetic transformation of fungi employing shock waves. *Fungal Genet. Biol. Elsevier Inc.*; 2013;56:9–16.
38. Nielsen KH. Protein expression-yeast. *Methods Enzymol*. 2014;536:133–47.
39. Demain A, Vaishnav P. Production of recombinant proteins by microbes and higher organisms. *Biotechnol. Adv*. 2009;27:297–306.
40. Alberts B, Johnson A, Lewis J, Raff M, Roberts K, And Walter P. *Molecular Biology of the Cell*. *Angew. Chemie Int. Ed*. 2001;40:9823.
41. Rubio MV, Tramontina R, Gonçalves TA, Uchima CA, Segato F, Squina FM, et al. Heterologous Expression of Carbohydrate-Active Enzymes in Filamentous Fungi. *Mycol. Curr. Futur. Dev*. 2015;1:148–201.
42. Yoon J, Aishan T, Maruyama JI, Kitamoto K. Enhanced production and secretion of heterologous proteins by the filamentous fungus *Aspergillus oryzae* via disruption of vacuolar protein sorting receptor gene *AoVps10*. *Appl. Environ. Microbiol*. 2010;76:5718–27.

43. Heimel K. Unfolded protein response in filamentous fungi—implications in biotechnology. *Appl. Microbiol. Biotechnol.* 2015;99:121–32.
44. Richie DL, Feng X, Krishnan K, Askew DS. Secretion stress and antifungal resistance: An Achilles' heel of *Aspergillus fumigatus*? *Med. Mycol.* 2011;49:S101–6.
45. Montenegro-Montero A, Goity A, Larrondo LF. The bZIP transcription factor HAC-1 is involved in the unfolded protein response and is necessary for growth on cellulose in *Neurospora crassa*. *PLoS One.* 2015;10:e0131415.
46. Sims AH, Gent ME, Lanthaler K, Dunn-Coleman NS, Oliver SG, Robson GD. Transcriptome Analysis of Recombinant Protein Secretion by *Aspergillus nidulans* and the Unfolded-Protein Response In Vivo. *Appl. Environ. Microbiol.* 2005;71:2737–47.
47. Guillemette T, van Peij NN, Goosen T, Lanthaler K, Robson GD, van den Hondel CA, et al. Genomic analysis of the secretion stress response in the enzyme-producing cell factory *Aspergillus niger*. *BMC Genomics.* 2007;8:158.
48. Kwon MJ, Jørgensen TR, Nitsche BM, Arentshorst M, Park J, Ram AF, et al. The transcriptomic fingerprint of glucoamylase over-expression in *Aspergillus niger*. *BMC Genomics.* 2012;13:701.
49. Cerqueira GC, Arnaud MB, Inglis DO, Skrzypek MS, Binkley G, Simison M, et al. The *Aspergillus* Genome Database: Multispecies curation and incorporation of RNA-Seq data to improve structural gene annotations. *Nucleic Acids Res. Oxford University Press;* 2014;42:D705–10.
50. Wood V, Harris MA, McDowall MD, Rutherford K, Vaughan BW, Staines DM, et al. PomBase: a comprehensive online resource for fission yeast. *Nucleic Acids Res.* 2012;40:D695–9.
51. Su X, Schmitz G, Zhang M, Mackie RI, Cann IKO. Heterologous Gene Expression in Filamentous Fungi. *Adv. Appl. Microbiol. Elsevier;* 2012;81:1-61.
52. Martinez D, Berka RM, Henrissat B, Saloheimo M, Arvas M, Baker SE, et al. Genome sequencing and analysis of the biomass-degrading fungus *Trichoderma reesei* (syn. *Hypocrea jecorina*). *Nat. Biotechnol.* 2008;26:553–60.
53. de Vries RP. Regulation of *Aspergillus* genes encoding plant cell wall polysaccharide-degrading enzymes; relevance for industrial production. *Appl. Microbiol. Biotechnol.* 2003;61:10–20.
54. Benoit I, Culleton H, Zhou M, DiFalco M, Aguilar-Osorio G, Battaglia E, et al. Closely related fungi employ diverse enzymatic strategies to degrade plant biomass. *Biotechnol. Biofuels. BioMed Central;* 2015;8:107.
55. Lambertz C, Garvey M, Klinger J, Heesel D, Klose H, Fischer R, et al. Challenges and advances in the heterologous expression of cellulolytic enzymes: a review. *Biotechnol. Biofuels. BioMed Central;* 2014;7:1–15.
56. Bergquist PL, Te'o VSJ, Gibbs MD, Curach NC, Nevalainen KMH. Recombinant enzymes from thermophilic micro-organisms expressed in fungal hosts. *Biochem. Soc. Trans.* 2004;32:293–7.

57. Schoberle TJ, Nguyen-Coleman CK, May GS. Plasmids for increased efficiency of vector construction and genetic engineering in filamentous fungi. *Fungal Genet. Biol.* Elsevier Inc.; 2013;58–59:1–9.
58. Segato F, Damásio ARL, Gonçalves TA, de Lucas RC, Squina FM, Decker SR, et al. High-yield secretion of multiple client proteins in *Aspergillus*. *Enzyme Microb. Technol.* 2012;51:100–6.
59. Damásio ARDL, Silva TM, Almeida FBDR, Squina FM, Ribeiro D a., Leme AFP, et al. Heterologous expression of an *Aspergillus niveus* xylanase GH11 in *Aspergillus nidulans* and its characterization and application. *Process Biochem.* 2011;46:1236–42.
60. Rubio MV, Zubieta MP, Franco Cairo JPL, Calzado F, Paes Leme AF, Squina FM, et al. Mapping N-linked glycosylation of carbohydrate-active enzymes in the secretome of *Aspergillus nidulans* grown on lignocellulose. *Biotechnol. Biofuels.* 2016;9:168.
61. Damásio AR de L, Pessela BC, Segato F, Prade RA, Guisan JM, Polizeli M de LTM. Improvement of fungal arabinofuranosidase thermal stability by reversible immobilization. *Process Biochem.* 2012;47:2411–7.
62. Calzado F, Prates ET, Gonçalves TA, Rubio M V., Zubieta MP, Squina FM, et al. Molecular basis of substrate recognition and specificity revealed in family 12 glycoside hydrolases. *Biotechnol. Bioeng.* 2016;113:2577–86.
63. Gouka RJ, Punt PJ, Hessing JG. Analysis of heterologous protein production in defined recombinant *Aspergillus awamori* Analysis of Heterologous Protein Production in Defined Recombinant *Aspergillus awamori* Strains. 1996;62:1951–7.
64. Moralejo FJ, Cardoza RE, Gutierrez S, Martin JF. Thaumatin production in *Aspergillus awamori* by use of expression cassettes with strong fungal promoters and high gene dosage. *Appl. Environ. Microbiol. American Society for Microbiology (ASM)*; 1999;65:1168–74.
65. Gonçalves TA, Damásio ARL, Segato F, Alvarez TM, Bragatto J, Brenelli LB, et al. Functional characterization and synergic action of fungal xylanase and arabinofuranosidase for production of xylooligosaccharides. *Bioresour. Technol.* 2012;119:293–9.
66. Contreras R, Carrez D, Kinghorn JR, Vandenhondel CAMJJ, Fiers W. Efficient Kex2-Like Processing of a Glucoamylase-Interleukin-6 Fusion Protein by *Aspergillus-Nidulans* and Secretion of Mature Interleukin-6. *Bio-Technology.* 1991;9:378–81.
67. Archer DB, Jeenes DJ, Mackenzie DA, Brightwell G, Lambert N, Lowe G, et al. Hen Egg White Lysozyme expressed in, and secreted from, *Aspergillus niger* is correctly processed and folded. *Biotechnology.* 1990;8:741–5.
68. Record E, Punt PJ, Chamkha M, Labat M, van den Hondel CAMJJ, Asther M. Expression of the *Pycnoporus cinnabarinus* laccase gene in *Aspergillus niger* and characterization of the recombinant enzyme. *Eur. J. Biochem.* 2002;269:602–9.
69. Karnaukhova E, Ophir Y, Trinh L, Dalal N, Punt PJ, Golding B, et al. Expression of human  $\alpha$ 1-proteinase inhibitor in *Aspergillus niger*. *Microb. Cell Fact. BioMed Central*; 2007;6:34.
70. Faus I, del Moral C, Adroer N, del Río JL, Patiño C, Sisniega H, et al. Secretion of the sweet-tasting protein thaumatin by recombinant strains of *Aspergillus niger* var. *awamori*. *Appl. Microbiol. Biotechnol.* 1998;49:393–8.

71. Kanamasa S, Takada G, Kawaguchi T, Sumitani J, Arai M. Overexpression and purification of *Aspergillus aculeatus* beta-mannosidase and analysis of the integrated gene in *Aspergillus oryzae*. *J. Biosci. Bioeng.* 2001;92:131–7.
72. Jin F-J, Katayama T, Maruyama J, Kitamoto K. Comparative genomic analysis identified a mutation related to enhanced heterologous protein production in the filamentous fungus *Aspergillus oryzae*. *Appl. Microbiol. Biotechnol. Applied Microbiology and Biotechnology*; 2016;100:9163–74.
73. Yoon J, Aishan T, Maruyama J -i., Kitamoto K. Enhanced Production and Secretion of Heterologous Proteins by the Filamentous Fungus *Aspergillus oryzae* via Disruption of Vacuolar Protein Sorting Receptor Gene *Aovps10*. *Appl. Environ. Microbiol.* 2010;76:5718–27.
74. Andersen MR, Vongsangnak W, Panagiotou G, Salazar MP, Lehmann L, Nielsen J. A trispecies *Aspergillus* microarray: comparative transcriptomics of three *Aspergillus* species. *Pnas.* 2008;105:4387–92.
75. Garzia A, Etxebeste O, Rodríguez-Romero J, Fischer R, Espeso E a., Ugalde U. Transcriptional changes in the transition from vegetative cells to asexual development in the model fungus *Aspergillus nidulans*. *Eukaryot. Cell.* 2013;12:311–21.
76. Galagan JE, Calvo SE, Cuomo C, Ma L-J, Wortman JR, Batzoglou S, et al. Sequencing of *Aspergillus nidulans* and comparative analysis with *A. fumigatus* and *A. oryzae*. *Nature.* 2005;438:1105–15.
77. de Assis LJ, Ries LNA, Savoldi M, dos Reis TF, Brown NA, Goldman GH. *Aspergillus nidulans* protein kinase A plays an important role in cellulase production. *Biotechnol. Biofuels. BioMed Central*; 2015;8:213.
78. Gilbert HJ, Stålbrand H, Brumer H. How the walls come crumbling down: recent structural biochemistry of plant polysaccharide degradation. *Curr. Opin. Plant Biol.* 2008;11:338–48.
79. Gladden JM. Production of Extremophilic Bacterial Cellulase Enzymes in *Aspergillus Niger*. *Sandia Natl. Lab.* 2013;SAND2013:7889.



## CAPÍTULO 2

### 3. ARTIGO CIENTÍFICO:

Manuscrito a ser submetido para a revista *SCIENTIFIC REPORTS*.

#### **Transcriptomic profile of heterologous protein production by *Aspergillus nidulans***

Felipe Calzado<sup>1,2</sup>, Gabriela F Persinoti<sup>1</sup>, Mariane P. Zubieta<sup>1,2</sup>, Marcelo V. Rubio<sup>1,2</sup>, Fabiano J. Contesini<sup>1</sup>, Fabio M. Squina<sup>1</sup>, André R. L. Damásio<sup>2\*</sup>

<sup>1</sup>Brazilian Bioethanol Science and Technology Laboratory (CTBE), Brazilian National Center for Research in Energy and Materials (CNPEN), Campinas-SP, Brazil

<sup>2</sup> Department of Biochemistry and Tissue Biology, Institute of Biology, State University of Campinas (UNICAMP), Campinas-SP, Brazil

**\*To whom correspondence should be addressed:**

André R. L. Damasio; Department of Biochemistry and Tissue Biology, Institute of Biology, University of Campinas (UNICAMP), Campinas-SP, Brazil Email: adamasio@unicamp.br

### 3.1. ABSTRACT

Filamentous fungi are important players in the production and secretion of homologous and heterologous lignocellulolytic enzymes, however, the regulation of protein secretion in these organisms need to be further explored. In order to investigate this regulation, the filamentous fungi *Aspergillus nidulans*, a model and genetically well-characterized organism, was subjected to a comparative transcriptomic analysis of three different recombinant strains producing the following heterologous proteins: 1) GH51 alpha-arabinofuranosidase (*A. nidulans*<sub>ABFA</sub>); 2) GH3 beta-glucosidase (*A. nidulans*<sub>BglC</sub>) and 3) GH5 thermophilic mannanase (*A. nidulans*<sub>1542</sub>). The three heterologous genes were highly expressed when compared with the endogenous reference gene. We observed that the levels of secretion depend on the protein sequence context and the overexpression of the heterologous genes did not affect the strains physiology. Furthermore, we identified 17 differentially expressed genes strictly related to recombinant protein secretion. This is the first study that describes the transcriptomic response to heterologous protein secretion in *A. nidulans*, giving a new perspective by comparing three different heterologous proteins with crescent secretion levels. Our results provided insights to understand how *A. nidulans* adapts to the overproduction of heterologous proteins and showed new potential targets of genetic manipulation for the improvement of the yields of protein secretion in this microbial system.

**Keywords:** *Aspergillus*; RNA-seq; Heterologous expression; Secretion of client proteins;

### 3.2. BACKGROUND

*Aspergilli* have a high capacity for producing large amounts of extracellular enzymes that provide nutrient sources from complex organic materials, featuring its saprophytic lifestyles<sup>1</sup>. The inherent ability of efficient protein secretion has led to their biotechnological exploitation as cell factories for the production of industrially important enzymes. A broad range of homologous and heterologous enzymes such as amylases, xylanases, and cellulases can be produced by *Aspergillus* species and contribute significantly to the expansion and growth of the enzyme market<sup>2</sup>. A recent report published by BBC Research states that the global market for industrial enzymes was worth nearly \$4.5 billion in 2012 and nearly \$4.8 billion in 2013. The market is expected to reach around \$7.1 billion by 2018, an annual growth rate of 8.2% over the 5-year forecast period<sup>3</sup>. *Aspergillus* is one of the largest group of enzymes producing microorganisms, corresponding to 30% of commercial enzymes produced according to the Association of Manufacturers and Formulators of Enzyme Products list<sup>4</sup>. Despite the above-mentioned *Aspergillus* advantages, there are many challenges to overcome regarding the expression of enzymes in fungal systems.

It has been shown that the main bottleneck in the production of heterologous proteins is not related low mRNA expression<sup>5</sup>. Instead, experimental evidence suggests that most target proteins produced in filamentous fungi are lost or stuck in the secretory pathway due to errors in processing, modification or misfolding that result in their elimination by endoplasmic reticulum (ER) quality control<sup>6,7</sup>. Misfolded proteins alter the cell homeostasis and proper ER functioning resulting in a state known as ER stress. ER stress activates a conserved signaling pathway called *unfolded protein response* (UPR) and *ER-associated protein degradation* (ERAD), which upregulates genes responsible for restoring protein folding homeostasis in the cell and degrades misfolded protein in the cytosol by the ubiquitin-proteasome system, respectively<sup>8</sup>.

In fungi, the UPR sensor is the inositol-requiring protein 1 (IRE1), which is an ER-resident transmembrane protein that contains a luminal domain that functions as a sensor of the folded state of proteins and has a site-specific endoribonuclease (RNase) domain at the cytoplasmic C-terminus<sup>9</sup>. In the presence of unfolded proteins, Kar2/BiP dissociates from IRE1, which subsequently oligomerizes for activation<sup>10</sup>. The IRE1 oligomer is activated by autophosphorylation and the RNase domain becomes responsible for the unconventional splicing of the *hacA<sup>u</sup>* (*hacA* uninduced form, non-spliced) mRNA<sup>9</sup>. The presence of an unconventional intron in the mRNA of the bZIP transcription factor *hacA<sup>u</sup>* causes

translational attenuation in the absence of ER stress<sup>11</sup>. The length of the intron is variable along species. *Aspergillus* and *Trichoderma* have an unconventional intron of 20-nucleotides (nt) in length, while the unconventional intron in *Saccharomyces cerevisiae* is 252 nt, 26 nt in mice and 23 nt in *Caenorhabditis elegans*<sup>12,13</sup>. In addition to the unconventional splicing, *hacA<sup>i</sup>* (*hacA* induced form, spliced) of *Trichoderma* and *Aspergillus* are truncated at the 5' flanking region upon UPR induction by removal of an upstream ORF<sup>14,15</sup>. *HacA<sup>i</sup>* then moves to the nucleus where it recognizes and binds to unfolded protein response elements (UPREs) in the promoter region of regulated genes. UPR-responsive genes provide an elevated protein folding capacity, secretion, ER expansion, and degradation of irreversibly misfolded proteins by the proteasome<sup>16</sup>.

Manipulation of the UPR pathway and its components has been a common attempt to improve the production of heterologous proteins in filamentous fungi<sup>17-19</sup>. Many ER stress-induced UPR genes, including protein folding-related genes such as chaperones and foldases, were co-expressed with heterologous gene. However, the overexpression of chaperones usually does not increase the production of heterologous proteins. In *S. cerevisiae*, the overexpression of *bipA* increased the amount of extracellular prochymosin over 20-fold, but the secretion of thaumatin was not significantly improved<sup>20</sup>.

Genomic and transcriptomic approaches have been used to understand the overexpression and production of heterologous enzymes and its capacity to induce the UPR, providing valuable information on *Aspergillus* genes involved with secretion and the coordination between UPR and ERAD. The induction of UPR in *A. niger* was investigated by transcriptome analysis comparing the UPR induced by chemicals and by overexpression of the tissue plasminogen activator (t-PA)<sup>16</sup>. Approximately 94 genes were commonly induced, mostly related to the functional categories protein folding, translocation/signal peptidase complex, glycosylation, vesicle trafficking, and lipid metabolism<sup>16</sup>. In addition, another study has shown that UPR resulted in activation of approximately 400 genes in *S. cerevisiae* (7-8% of the genome)<sup>21</sup>. This reflects the complex network of interactions between the UPR and other signaling pathways in cell, mainly in the secretory pathway. Transcriptome profile can be particularly important to provide an overview of all genes and pathways regulated by UPR in the cell.

Previous works have shown that UPR is activated in recombinant strains and its scope is mainly focused on the secretion pathway<sup>6,22,23</sup>. We performed a comparative transcriptome analysis of *A. nidulans* by designing three recombinant strains producing the following

heterologous proteins: 1) GH51 alpha-arabinofuranosidase (*A. nidulans*<sub>AbfA</sub>); 2) GH3 beta-glucosidase (*A. nidulans*<sub>BglC</sub>) and 3) GH5 thermophilic mannanase (*A. nidulans*<sub>1542</sub>). These three proteins were produced and secreted at different levels (AbfA > BglC > 1542). *A. nidulans* transcriptional profile in response to different heterologous genes at early and late times of induction was determined. Furthermore, 17 differential expressed (DE) genes were common to all the conditions analyzed and these genes were related to the secretory pathway. This is the first study that describes the transcriptomic response to heterologous protein secretion in *A. nidulans*, giving a new perspective by comparing three different heterologous proteins with variable secretion levels. Our results provided insights to understand how *A. nidulans* adapts to the overproduction of heterologous proteins and highlighted new potential targets to genetic manipulation and improvement of the protein secretion yields in this microbial system.

### 3.3. RESULTS AND DISCUSSION

#### 3.3.1. The recombinant proteins are secreted in different levels

In order to understand *A. nidulans* mechanisms for heterologous protein production, three different proteins were monitored: GH51 alpha-arabinofuranosidase (AbfA) and GH3 beta-glucosidase (BglC) both cloned from *Aspergillus fumigatus*, and a GH5 thermophilic mannanase (1542) cloned from the hyperthermophilic bacterium *Thermotoga petrophila*. The target sequences were cloned into pEXPYR vector and transformed in *A. nidulans*<sub>A773</sub><sup>24</sup>. The recombinant strains were carefully selected due to the crescent level of the target proteins secretion, AbfA > BglC > 1542. The transformed strains were named *A. nidulans*<sub>AbfA</sub>, *A. nidulans*<sub>BglC</sub> and *A. nidulans*<sub>1542</sub>.

To evaluate the time course of the enzymes secretion, the recombinant strains were grown in maltose to induce the *glaAp* promoter<sup>24</sup> and activate expression of the heterologous genes (**Figure 1**). Despite the differences in the secretion of the target proteins, the three strains showed a similar profile of mycelium dry weight, total proteins and pH, with *A. nidulans*<sub>1542</sub> showing higher levels of dry weight at 36h of induction. The similar growth profiles show that the overexpression of heterologous genes not resulted in major physiological changes of the strains.

AbfA was the highest secreted protein with a peak of activity at 48h, but from 6h it was already possible to detect activity (**Figure 1A**). BglC was less secreted than AbfA and the peak of activity was early at 24h (**Figure 1B**). In general, after 48h of cultivation, we observed a clear profile of protein degradation (**Figure 1**; SDS-PAGE) for the three recombinant strains evidenced by the decrease of relative enzymatic activity. At this time of cultivation, the cells were probably disrupted due to the absence of nutrients. Peaks of beta-glucosidase activity were detected from 72 to 120h by using pNPG (**Figure 1B**), but these activities are due to a native intracellular beta-glucosidase (AN2828; strong band between 75 and 85 kDa) confirmed by LC-MS/MS (data not shown). In contrast to AbfA and BglC, it was not possible to detect the 1542 in the gel, however, a residual activity was evident with similar amounts from 18 to 120h, suggesting that this thermophilic enzyme was resistant to *A. nidulans* mechanisms of protease degradation (**Figure 1C**). It is important to emphasize that the enzymatic activity of this mannanase was measured at high temperatures (87°C), avoiding the possibility of false positive results. Secretion of proteins into the medium driven by strong promoters (such as *glaAp*) are

often subjected to proteolysis in the extracellular space. This is very common in filamentous fungi systems that secrete native proteases, or in response to glucose starvation or increases in pH<sup>24</sup>.

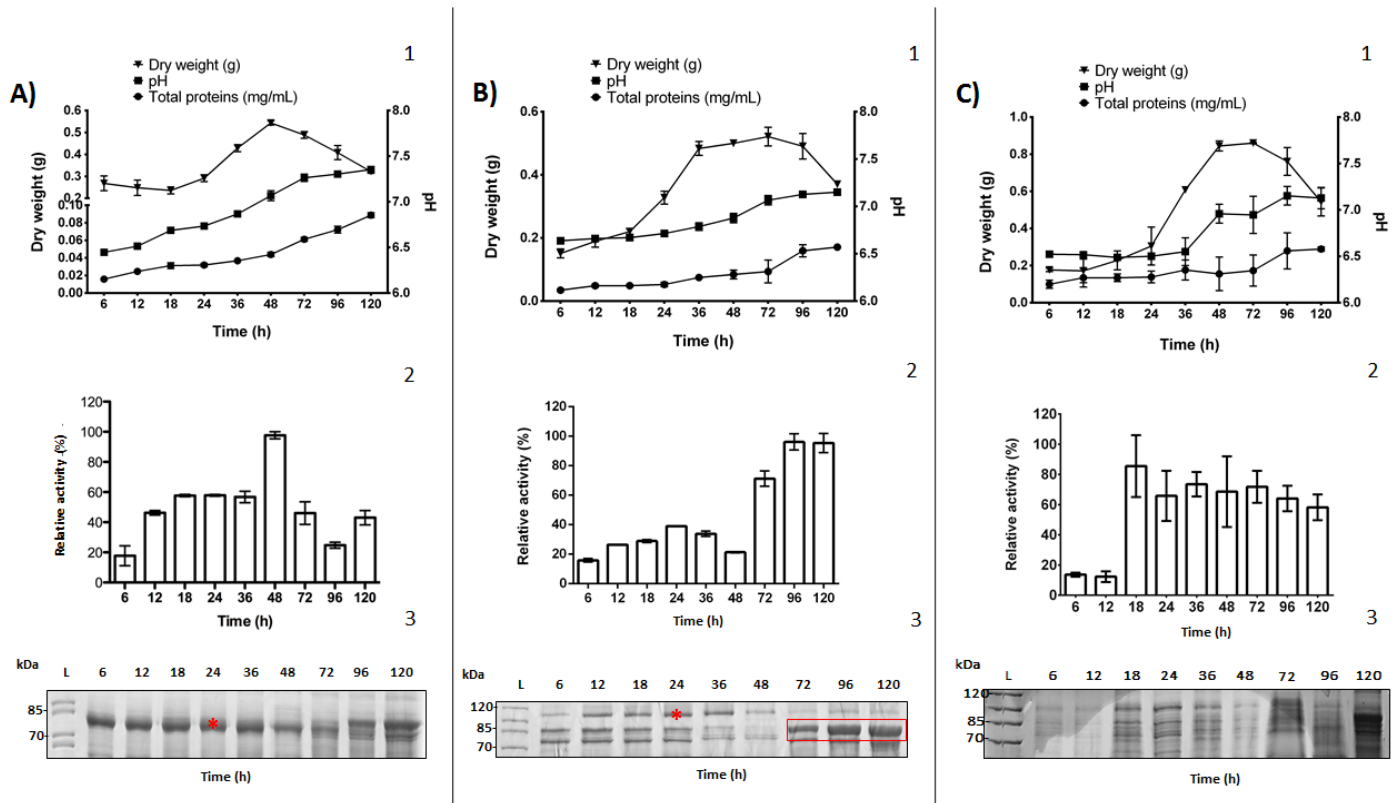


**Figure 1. Time course of heterologous protein production by recombinant *A. nidulans* strains.** 1- Dry weight (g) of the mycelium from *A. nidulans* strains, final pH of the cultivation medium, total proteins secreted in the extracellular medium by the *A. nidulans* strains in different cultivation periods. 2 – Relative enzymatic activity of the *A. nidulans* strains in different cultivation periods. The highest enzymatic activity was considered 100%. 3 – 12% SDS-PAGE of the heterologous proteins secreted by the *A. nidulans* strains in different cultivation periods. 10 µg of proteins were applied. The target proteins are indicated by an asterisk. The red box indicates *A. nidulans* native and intracellular beta-glucosidases detected after 48h of cultivation. **A)** *A. nidulans*<sub>AbFA</sub>; **B)** *A. nidulans*<sub>BglC</sub>; **C)** *A. nidulans*<sub>1542</sub>; the band corresponding to 1542 protein was not detected in the SDS-PAGE. The error bars indicate the standard deviation of three replicates.

In order to investigate whether the low BglC and 1542 secretion were caused by problems during protein folding, the same approaches of SDS-PAGE and enzymes activity were carried out in the intracellular fraction (**Figure S1**). The overexpression of heterologous

proteins might causes their intracellular accumulation, suggesting a breakdown or overloading of the secretory pathway <sup>25</sup>. Bands related to recombinant proteins were not evidenced in the intracellular fraction (**Figure S1**). This result leads us to infer that most of the target proteins are immediately secreted, with low levels of unfolded/misfolded proteins trapped inside the cell.

In general, we observed that the secretion levels depend on the protein sequence context and the overexpression does not affect the overall strains physiology. The levels of target proteins secretion were crescent from 1542 to AbfA and intermediate levels for BglC. We sought to understand at the transcriptome level whether or not these differences in secretion levels of heterologous enzymes were due to differences in mRNA expression.

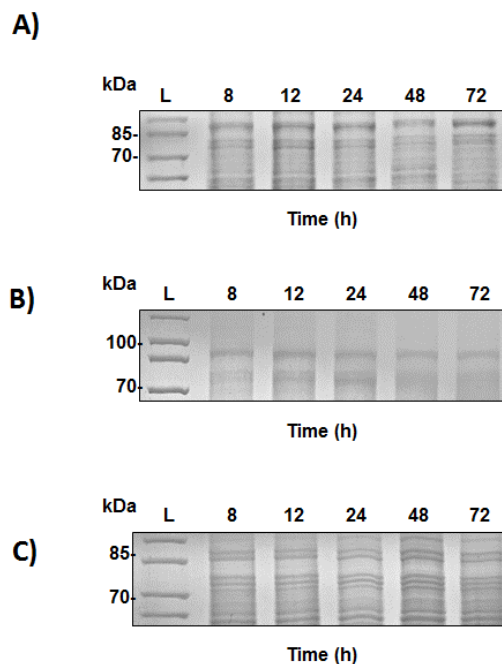


**Figure S1. Profile of intracellular heterologous proteins produced over time.** 12% SDS-PAGE analysis of the heterologous proteins extracted from the lysed mycelium of recombinant *A. nidulans* strains after different cultivation periods. 10 µg of proteins were applied. **A)** *A. nidulans*<sub>AbfA</sub>; **B)** *A. nidulans*<sub>BglC</sub>; **C)** *A. nidulans*<sub>1542</sub>. Lanes from left to right (for all *A. nidulans* strains): L- Molecular weight marker, 8 – 8h cultivation, 12 – 12h cultivation, 24 – 24h cultivation, 48 – 48h cultivation, 72 – 72h cultivation. The *A. nidulans* strains were cultivated with maltose as described in the Material and Methods section.

### 3.3.2. The heterologous genes are highly expressed in *A. nidulans*

The production of recombinant proteins in filamentous fungi by using strong promoters activates some regulatory genes in pathways related to protein quality control and UPR <sup>26–28</sup>. The UPR represents an adaptive response that aims to restore cellular homeostasis triggered by an ER stress <sup>29</sup>. In order to investigate if the overexpression of recombinant genes in *A. nidulans* triggers UPR, the expression of the target genes *abfA*, *bglC* and *1542* were measured by qPCR. The *abfA* and *bglC* were highly expressed when compared with the endogenous reference gene



(*tubC*), while the *1542* mRNA levels were similar to *tubC*. The genes were even detected after 72h of maltose induction (**Figure 2A**).

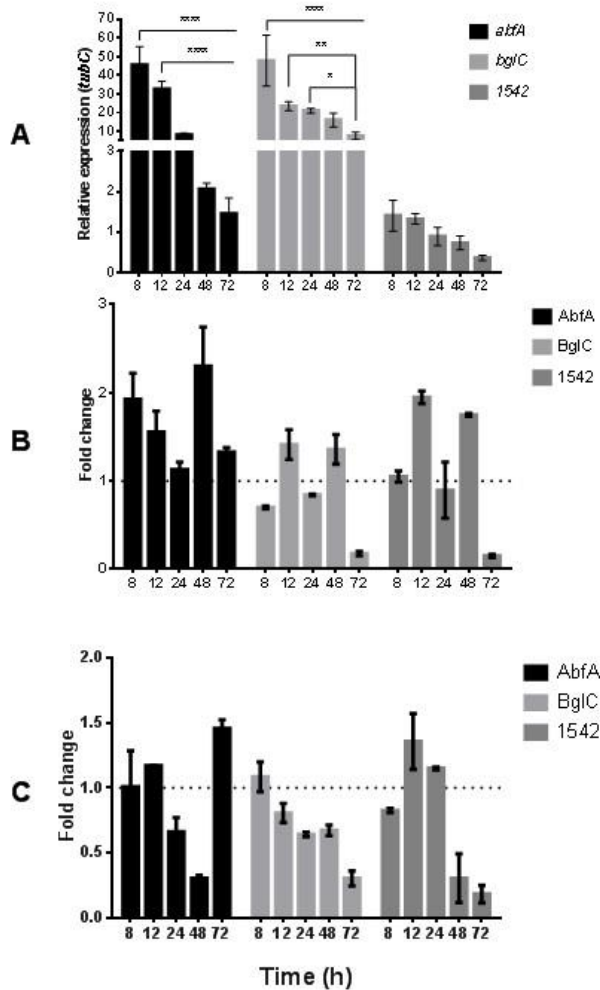


**Figure 2. Gene expression profile of recombinant *A. nidulans* strains over time obtained by qPCR.** Gene expression levels were determined by qPCR in different cultivation periods expressed in logarithmic scale as Fold Change. **A)** Gene expression profile of the heterologous genes *abfA*, *bglC* and *1542*. **B)** Expression levels of *bipA* on *A. nidulans*<sub>AbfA</sub>, *A. nidulans*<sub>BglC</sub> and *A. nidulans*<sub>1542</sub>. **C)** Expression levels of *sec63* on *A. nidulans*<sub>AbfA</sub>, *A. nidulans*<sub>BglC</sub> and *A. nidulans*<sub>1542</sub>. *tubC* was used as a reference gene and the strain *A. nidulans*<sub>A773</sub> as the experimental control.  $\Delta\Delta Ct$  method was used for gene expression calculation. Asterisks indicate statistically different results (two-way ANOVA and Bonferroni post-test  $p$ -value  $<0.05$ ). The strains were cultivated as described in Material and Methods section. The means of three biological replicates was showed and the error

bars indicate the standard deviation.

UPR target genes such as *bipA* and *sec63* were quantified in function of time (**Figures 2B and C**)<sup>22,25,30,31</sup>. The *bipA* was overexpressed in all recombinant strains at 12h and in *A. nidulans*<sub>AbfA</sub> at 8h (**Figure 2**), probably due to the higher production of AbfA compared to the other recombinant proteins. The *sec63* was overexpressed in *A. nidulans*<sub>AbfA</sub> and *A. nidulans*<sub>1542</sub> at 12h and only in *A. nidulans*<sub>1542</sub> at 24h. Late overexpression (48 and 72h) of *bipA* and *sec63* were assumed to be related to the absence of carbon source since the maltose was totally consumed (**Figure S2**), causing starvation, UPR and cell death<sup>32</sup>. In *Trichoderma reesei*, protein overproduction induced the overexpression of UPR target genes only at early cultivation stages (from 1 to 12h)<sup>33</sup>. After 12h the amount of UPR target genes returned to the basal levels. The heterologous expression of a bacterial xylanase B (*xynB*) in *A. niger* also not showed high

mRNA levels of UPR target genes (*gla*, *bip*, and *hac1*)<sup>34</sup>. Here we observed overexpression of *bipA* and *sec63* primarily at 12h after induction of the heterologous genes expression. Based on the time course of recombinant proteins production, the fast maltose consumption and qPCR data, we defined 2 and 8h of heterologous genes expression as standards to understand how *A. nidulans* strains adapt to the production of heterologous proteins.

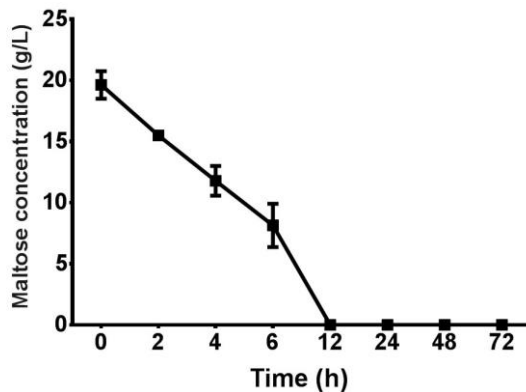


**Figure S2. Maltose consumption in culture medium over time.** Consumption of maltose in the cultivation medium by the recombinant strain *A. nidulans*<sub>AbfA</sub> in different cultivation periods. Maltose concentration was analyzed by HPLC.  $10^8$  spores were used as inoculum. The media were maintained static at 37°C. The error bars indicate the standard deviation of three replicates.

A discrepancy between high mRNA levels (**Figure 2A**) and low secreted proteins (**Figure 1B and C**) was also reported for the heterologous expression of two cellobiohydrolases (CBHs) from *A. terreus* and *T. reesei* expressed in *A. carbonarius*<sup>35</sup>. They speculated that proteolytic degradation could be one of the reasons for this result, possibly together with other factors such as incorrect folding, post-translational processing, and impairment of intracellular transport<sup>35</sup>. The indirect relationship between mRNA and protein levels is frequently reported suggesting that transcription is not a bottleneck in these systems. In an attempt to establish a list of cellular processes altered during the adaptation of *A. nidulans* to the overexpression of recombinant genes, we analyzed the three recombinant strains by RNA-seq at 2 and 8h.

### 3.3.3. Global transcriptional response to heterologous protein production

Differential expression analysis by RNA-seq data was performed by pairwise comparisons of each recombinant strain compared with the control strain *A. nidulans*<sub>A773</sub>. In general, by applying the pipeline and filters described in Methods, we obtained 476 differentially expressed (DE) genes (**Figure 3**). Except for the conditions BglC and 1542 8h, there was a predominant up-regulation response during the overexpression of recombinant genes in *A. nidulans*. Thirty out 476 DE genes were common for the three recombinant strains. The strains *A. nidulans*<sub>AbfA</sub> and *A. nidulans*<sub>1542</sub> additionally showed 74 DE genes in common. This observation can be supported by the Venn diagrams and the PCA analysis (**Figure 3 and**

**Figure S3).** This relative similarity between *A. nidulans*<sub>AbfA</sub> and *A. nidulans*<sub>1542</sub> surely cannot be explained by the titer of mRNA that is not similar for all the strains (**Figure 3**), and probably the protein features such as amino acids composition, the complexity of folding and post-translational modifications are determinant to the success of production and secretion. Optimal expression levels of recombinant proteins are known to be variable for different proteins, as protein folding rates vary according to the protein size and structure<sup>36</sup>.

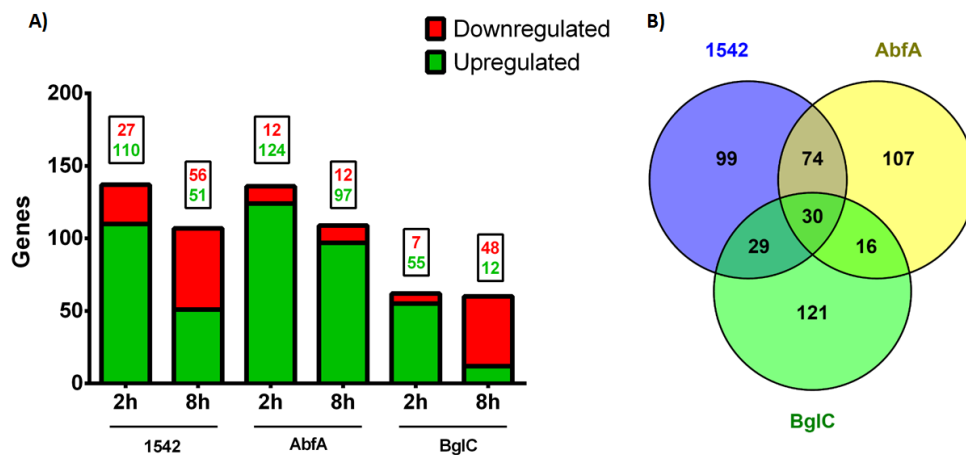


**Figure 3. Global analysis of differentially expressed genes obtained with RNA-seq.** **A)** Bar chart representing differentially expressed genes by recombinant *A. nidulans* strains from transcriptomic data in different cultivation periods. The rectangles above the bars represent the number of up and downregulated genes by the recombinant strains. Transcriptomic data from recombinant strains were generated under heterologous protein production induction. RNA-seq data of the each recombinant strains were compared to the control strain *A. nidulans*<sub>Δ773</sub> and  $(\log_2)$  Fold Change  $\leq -2.0$  or  $\geq 2.0$  and adjusted p-value  $\leq 0.01$  were used as thresholds. In general, 476 differentially expressed genes were identified in all strains and time points analyzed. **B)** Venn Diagram representing differentially expressed genes analyzed by the RNA-seq in 2h and 8h cultivation of the three recombinant *A. nidulans* strains. Venn diagram was created using the online tool Venny 2.1.

To better understand the general cellular processes regulated during the production of recombinant proteins in *A. nidulans*, the annotation of DE genes was performed with FunCat<sup>37</sup>. The most significant functional category was "metabolism", followed by "protein with binding function or cofactor", "cellular transport" and "cell defense". These four categories were overrepresented in all the strains and time points analyzed. In a more detailed analysis of functional subcategories depicted in **Figure 4**, we found several altered processes related to cellular stress, such as the subcategories of metabolism, transport routes and cellular defense.

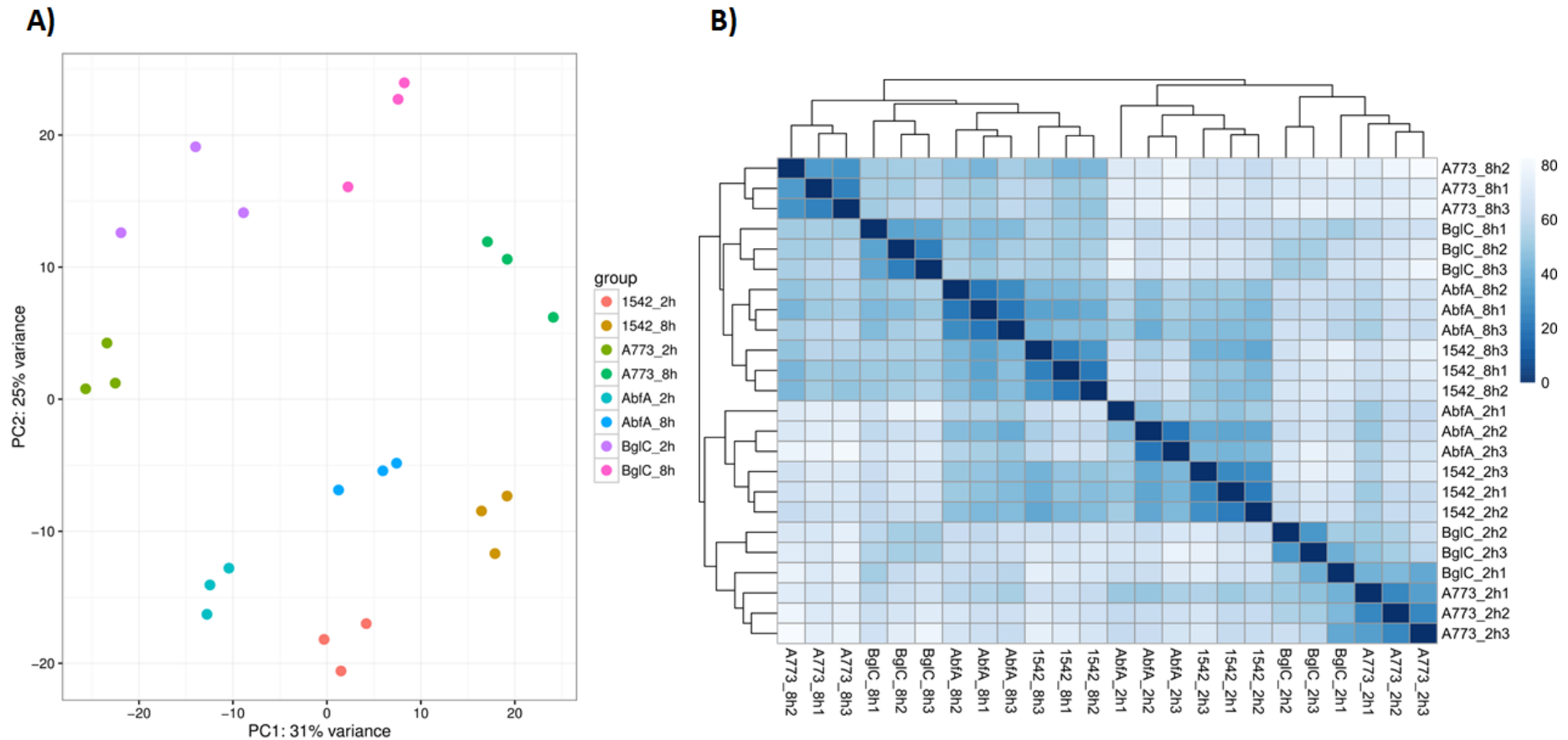


**Figure S3. Principal component analysis (PCA) and Hierarchical clustering of the samples analyzed.** **A)** PCA analysis of *A. nidulans* recombinant strains represented by the first two principal components. The percentage of the variance explained by each PC is shown on the axis. **B)** Hierarchical clustering of sample-to-sample distances. Two distinct groups can be observed, representing the two time points analyzed in the RNA-seq. Within each time point, more similarity is observed between *A. nidulans*<sub>AbfA</sub> and *A. nidulans*<sub>1542</sub> strains. PCA analysis and heatmap of sample distances were calculated from the regularized log transformation of the count data as implemented in DESeq2 package.

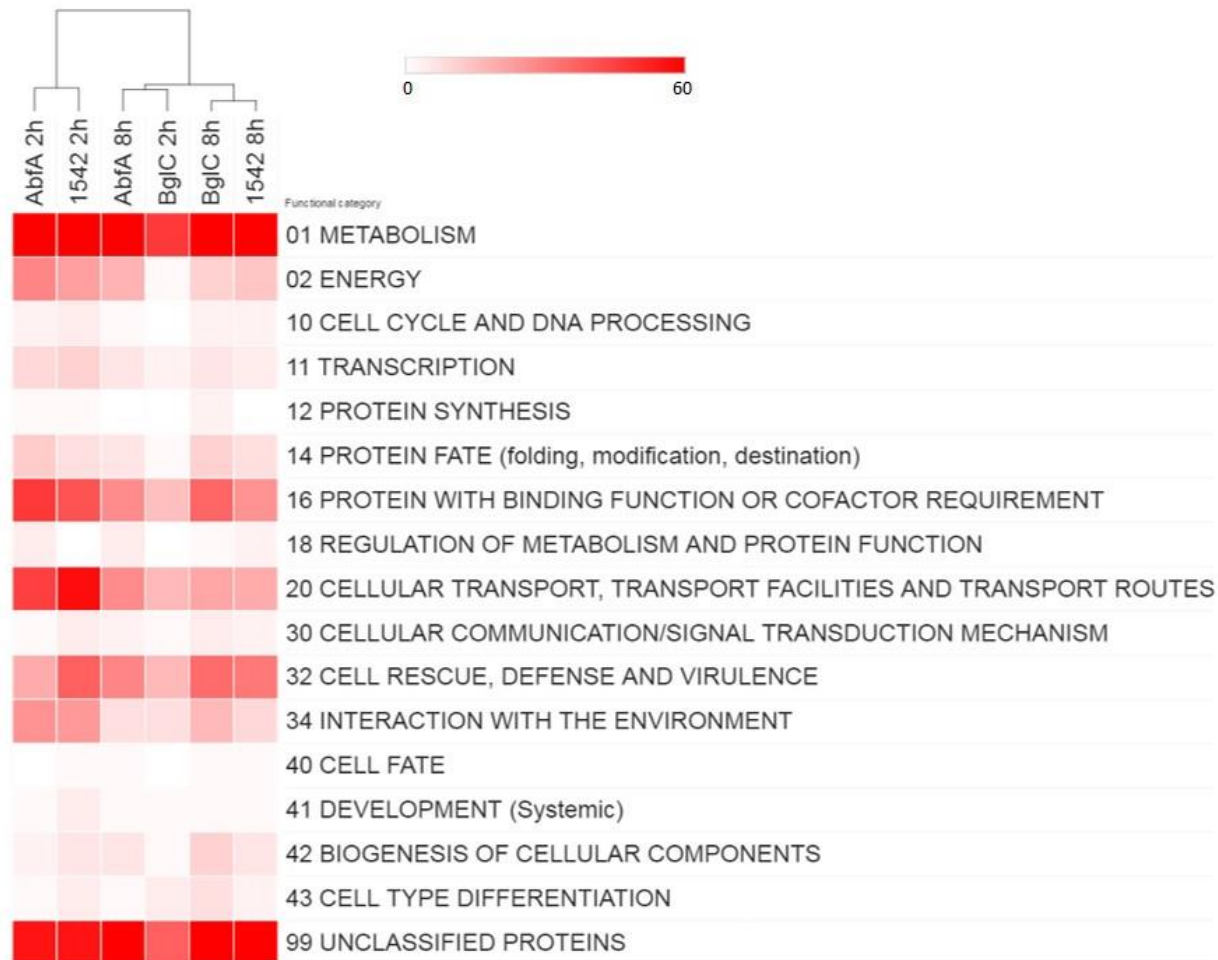


**Figure 4. Functional annotation heatmap of the transcriptomic data generated by RNA-seq analysis of recombinant *A. nidulans* strains.** MIPS FunCat terms annotations of *A. nidulans*<sub>1542</sub>, *A. nidulans*<sub>AbfA</sub> and *A. nidulans*<sub>BglC</sub> show a broad variety of biological process associated with the differentially expressed genes of the recombinant *A. nidulans* strains in different cultivation periods. The analysis of functional categories of the global transcriptomic data were performed with FunCat (The Functional Catalogue). Functional categories heatmap represent the number differentially genes found in the transcriptomic data based on the reference genome annotation in FunCat. Heatmap was created with online software from Broad Institute – Morpheus.

These subcategories were also found representative of other *Aspergillus* species under protein overproduction<sup>27,38,39</sup>. The overexpression of glucoamylase (GlaA) in *A. niger* resulted in the activation of “translocation”, “protein glycosylation”, “vesicle transport” and “ion homeostasis” processes<sup>38</sup>. The functional categories “cellular transport”, “amino acid metabolism”, “aminoacyl-tRNA biosynthesis” and “metabolism” were overrepresented in *A. oryzae* strain expressing a constitutively active form of HacA, suggesting the importance of HacA for UPR, fungal growth, and physiology<sup>39</sup>. As already mentioned, in our data we found several altered processes related to cellular stress, such as metabolism, transport routes and cellular defense. This conclusion is supported by qPCR data that showed an upregulation of *bipA* in all the strains and *sec63* in the strain *A. nidulans*<sub>1542</sub> (**Figure 2**). In spite of this, the specific FunCat functional subcategory "stress response" (32.01) was not representative in any strain and we can conclude that ER stress during heterologous proteins production by *A. nidulans* remains low and constant.

The basic sensing pathway to detect ER stress or an increase in the folding load is highly conserved from yeast to human. The increase of misfolded proteins stimulates the Ire1 autophosphorylation and dimerization triggering the unconventional splicing of an intron in the *hacA*<sup>u</sup>, creating the transcriptionally active form *hacA*<sup>i</sup><sup>29</sup>. HacA is a conserved bZIP transcription factor in eukaryotic cells, which regulates gene expression in response to various forms of secretion stress and as part of secretory cell differentiation<sup>16</sup>. In order to evaluate the canonical pathway of UPR, we analyzed the ratio of *hacA* splicing in the *A. nidulans* recombinant strains based on the RNAseq data (**Figure S4**). The levels of *hacA* splicing were higher for AbfA and 1542 than for BglC at 2h, and after 8h the levels of *hacA* splicing for all the recombinant strains were lower than the control strain, showing a normalization of the UPR canonical pathway. This result suggests that there is no accumulation of BglC misfolded form at 2 or 8h after induction of recombinant protein production or the presence of an alternative pathway of ER stress and UPR. In the other hand, for AbfA and 1542 is possible to infer there is some misfolded proteins accumulation at 2h. Wang et al (2014) observed the *hac1* levels in *T. reesei* Rut C30 and QM9414 strains. The transcript level of total *hac1* increased earlier in Rut C30 (1h of induction) and the response maintained longer than that in QM9414<sup>33</sup>. Comparing with our data, during the expression of recombinant genes the *hacA* expression appears up-regulated at earlier times, with a similar response with *T. reesei*<sup>33</sup>.

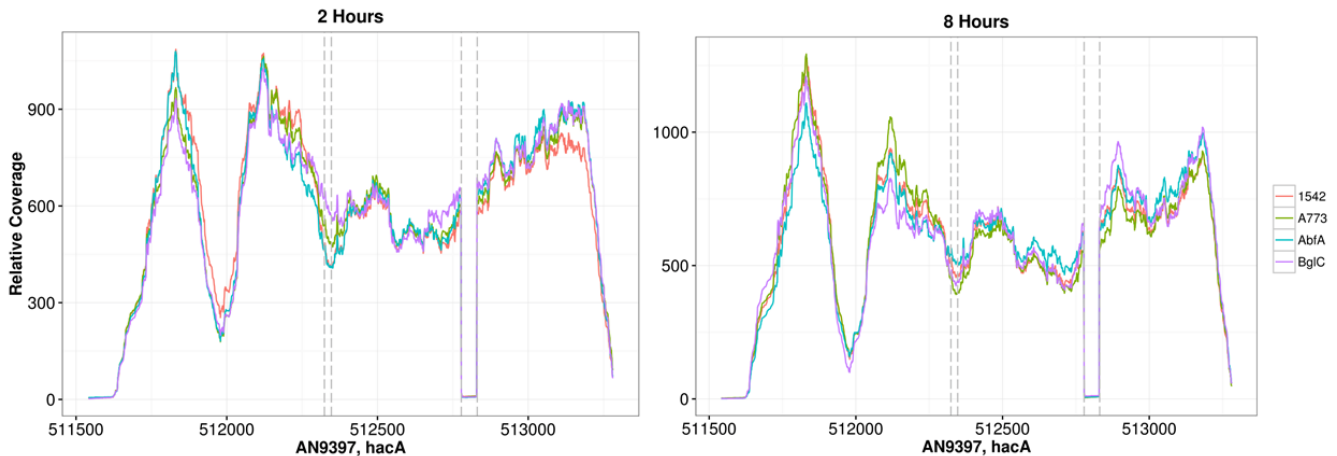


**Figure S4. RNA-seq coverage plots for the *hacA* mRNA.** The number of sequence reads on the y-axis (relative to total counts) is shown along the length of *hacA* gene. Colored lines represent the recombinant strains studied. Vertical dashed lines demarcate predicted intron boundaries. The coverage plot for 2h shows more unconventional splicing for the strains *A. nidulans*<sub>AbfA</sub> and *A. nidulans*<sub>1542</sub>.

Based on the general analysis of RNA-seq of the recombinant strains, it was possible to observe a predominant up-regulation response. Moreover, biological processes related to metabolism, protein with binding function and cellular transport were overrepresented. Although there are not many processes related to cell stress, we observed the unconventional splicing of *hacA* for the recombinant strains *A. nidulans*<sub>AbfA</sub> and *A. nidulans*<sub>1542</sub>, indicating some level of UPR. The global analysis showed a mild stress at 2h of induction of heterologous protein production, which was normalized after 8h.

### 3.3.4. Recombinant strains adapts differently at early and late times of heterologous genes induction

To further evaluate how the recombinant strains adapt to heterologous protein production, a strain-specific expression profile was established. The DE genes previously identified were classified as being involved in early, continuous or late response, according to the expression profile at the time points analyzed. Early response corresponds to DE genes exclusively at 2h; continuous response, DE genes at both 2h and 8h; and late response, DE genes exclusively at 8h. The strain-specific profiles (**Figure S5**) show a clear transcriptional difference between the early and late responsive genes, and also a higher number of common genes between the strains *A. nidulans*<sub>AbfA</sub> and *A. nidulans*<sub>1542</sub>. These two strains presented a more evident early response, while *A. nidulans*<sub>BglC</sub> presented a predominant late response.

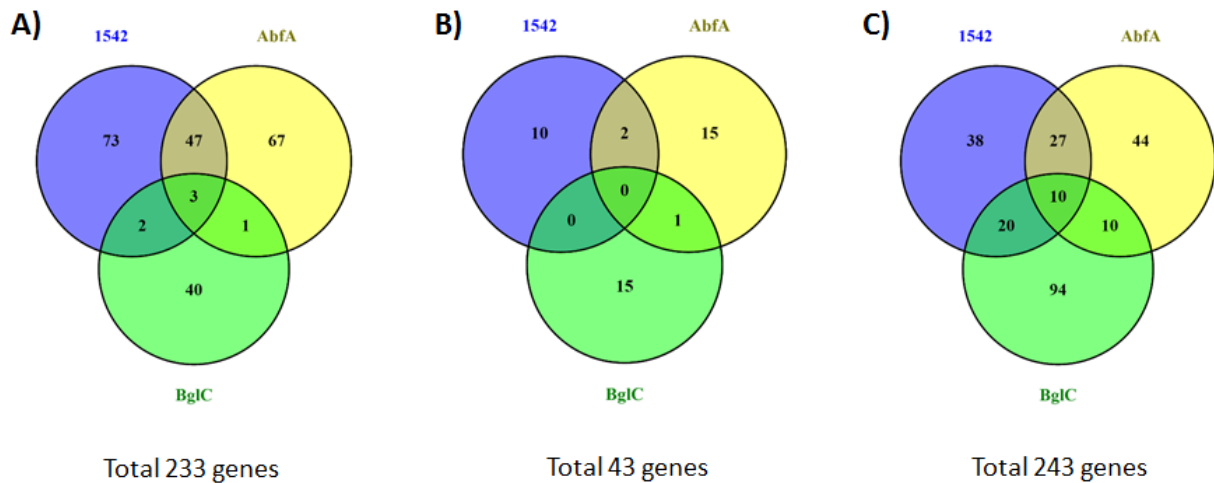


**Figure S5. Differentially expressed genes profile of early, late and continuous responses.** Venn diagrams representing differentially expressed (DE) genes in the recombinant *A. nidulans* strains. **A)** Early response corresponds to DE genes only at 2h; **B)** continuous response, DE genes at both 2h and 8h; **C)** and late response, DE genes only at 8h. Venn diagrams were created with the Venny 2.1 online tool.

It is interesting to notice that there are fewer genes associated with the continuous response, reinforcing that there are distinct responses between 2 and 8h of heterologous protein induction. The strains *A. nidulans*<sub>AbfA</sub> and *A. nidulans*<sub>1542</sub> presented a more evident early response, with 52% and 54% of the DE genes respectively classified as early responsive genes. The opposite was observed for *A. nidulans*<sub>BglC</sub>, which presented 68% of the DE genes as late responsive genes (**Figure S5**). Functional annotation indicated that in general DE genes were mainly involved in metabolism and transport (**Figure 5**). The early responsive genes were also associated with transmembrane transport and amino acids metabolism, while the late responsive genes were predominantly related to C-compound and carbohydrate metabolism. Only *A. nidulans*<sub>AbfA</sub> presented a continuous response in this analysis with the predominance of fatty acid metabolism and C-compound subcategories.

Besides processes related to metabolism, by analyzing the specific time responsive genes of each recombinant strain, it is clear that *A. nidulans*<sub>1542</sub> and *A. nidulans*<sub>BglC</sub> presented more functional categories associated with “32 Cell Rescue, Defense and Virulence” than *A. nidulans*<sub>AbfA</sub>, which, on the other hand, predominantly presented processes related do “02 Energy” (**Figure 5**). *A. nidulans*<sub>AbfA</sub> is the strain with higher levels of secreted proteins, it is expected to require more energy to correctly fold and secret overproduced proteins<sup>40</sup>. *A. nidulans*<sub>1542</sub> and *A. nidulans*<sub>BglC</sub> had both categories related to cell defense; this might be one



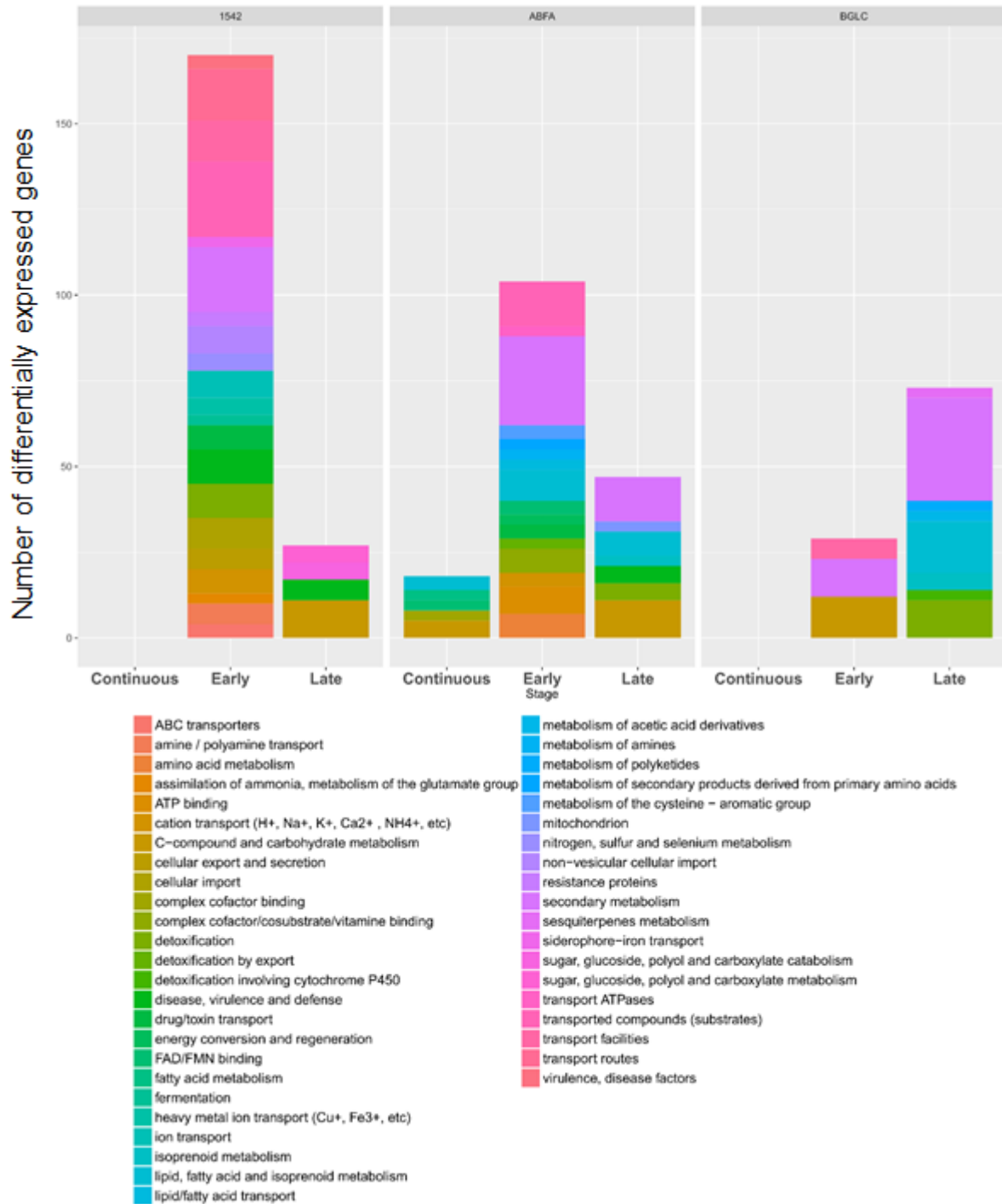


**Figure 5. Functional annotation of differentially expressed genes of early, late and continuous responses.** Functional annotations of differentially expressed (DE) genes in the recombinant *A. nidulans* strains. The Early response corresponds to DE genes only at 2h; continuous response, DE genes at both 2h and 8h; and late response, DE genes only at 8h. The analysis of functional categories was performed with FunCat (The Functional Catalogue). The functional categories graph values represent the number altered genes found (abs set) in the transcriptome data based on the reference genome annotation.

of the explanations for their lower levels of secreted proteins. Filamentous fungi have multiple defense systems to maintain genome stability and to prevent the propagation of selfish DNA such as those of transposable elements and viruses. These defenses can also be deployed against transformed exogenous DNA intended for transgene expression<sup>5</sup>. In this perspectives, defenses against foreign genes may pose significant barriers to the use of filamentous fungi as hosts for heterologous gene expression, which involves the transformation of foreign DNA<sup>5</sup>.

These early, late and continuous specific responses enabled us to observe that each *A. nidulans* recombinant strain had a specific adaptation during the secretion of heterologous proteins. In order to determine a specific profile for each recombinant strain over time, we analyzed three functional subcategories specifically related to proteins production and secretion, “32.01.07 unfolded protein response (e.g. ER quality control)”, “14.13 protein/peptide degradation” and “14.07.02.02 N-directed glycosylation, deglycosylation” (**Figure S6/Additional file 1**). These three functional subcategories are specifically related to UPR, ERAD and glycosylation, respectively, important processes to monitor cellular stress caused by recombinant protein production. During the overexpression of recombinant genes, large amounts of transcripts go to ER to be translated and later folded into fully functional proteins. If the heterologous protein does not fold well, it will accumulate in the ER and generate a condition termed ER stress or protein secretion stress<sup>5</sup>. The cell counteracts ER stress by different stress response mechanisms, including UPR and ERAD<sup>41</sup>.

First, by observing 75 genes related to “32.01.07 Unfolded protein response (e.g. ER quality control)” (**Additional file 1: Table S1**), 15 genes were DE (**Figure S6A; Additional file 1: Table S2**), and only one gene were common in all strains (AN1163). This gene encodes a chaperone with orthologue in *S. cerevisiae* (Hsp78p), described in this yeast as able to prevent the aggregation of misfolded proteins as well as resolubilize protein aggregates<sup>42</sup>. The strain *A. nidulans*<sub>BglC</sub> showed more specific DE genes related to UPR, and almost all of them were described as chaperones (AN2432, AN6010, AN8269, AN9124 and AN2646). The unique exception was the late up-regulated gene AN1296 described as an RNA ligase (TRL1, orthologue in *S. cerevisiae*), required for tRNA splicing and for both splicing and translation of HAC1 mRNA in the UPR<sup>42</sup>. The canonical biological marker of UPR in *A. nidulans*, the *hacA*, were down-regulated in the strains *A. nidulans*<sub>1542</sub> and *A. nidulans*<sub>SA6A</sub> at 2h. In spite of the down-regulation of *hacA*, which is contrary to what is described in the literature for other *Aspergillus* species for recombinant protein production<sup>5</sup>, this result corroborates to our *hacA* coverage data (**Figure S4**) showing discrete unconventional splicing in all the strains.

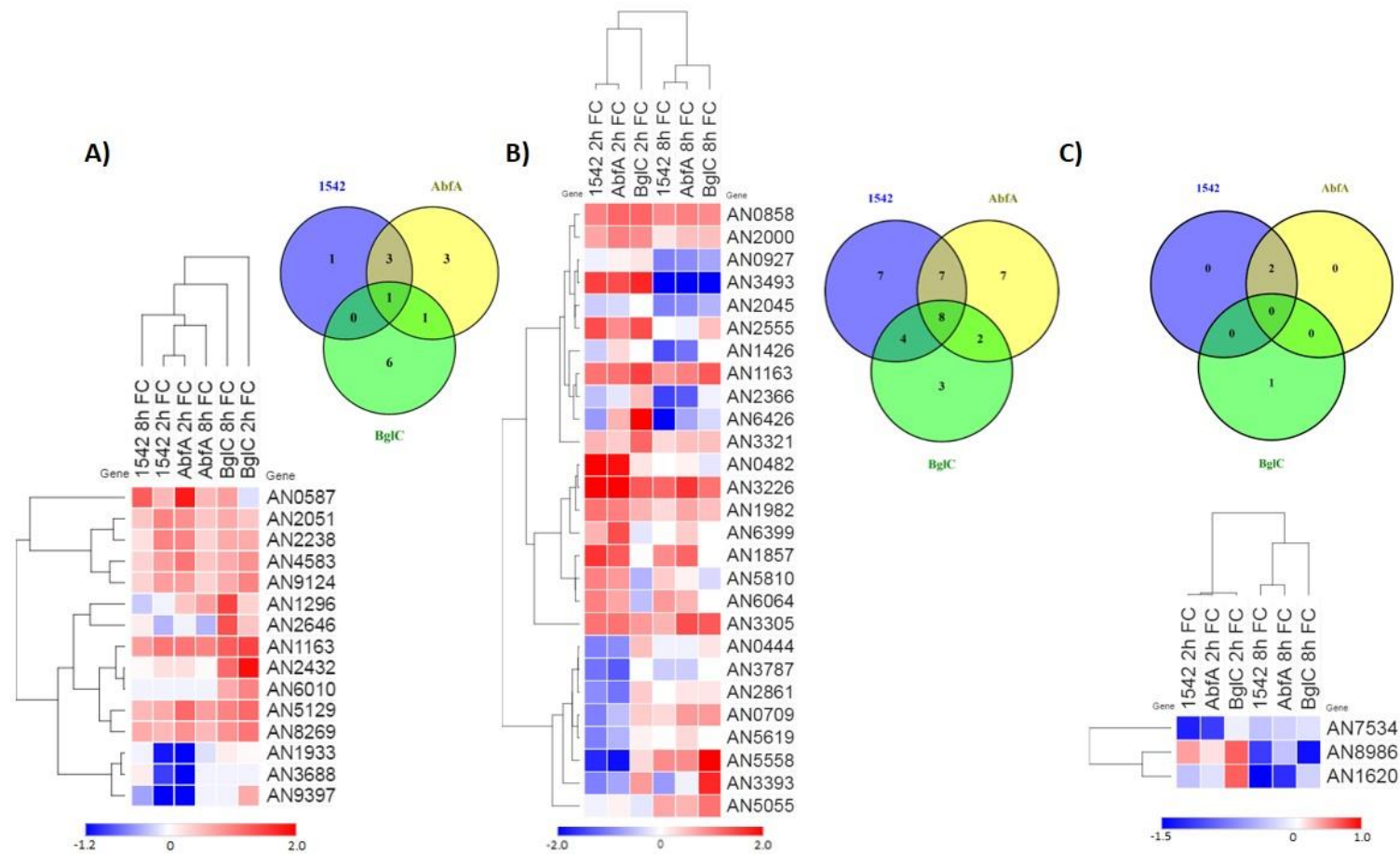


**Figure S6. Differentially expressed genes profile of proteins production pathways.** Heatmaps and venn diagrams of FunCat annotated proteins in *A. nidulans* were compared to RNAseq data of the three recombinant strains for the functional subcategories: **A)** 32.01.07 Unfolded protein response (e.g. ER quality Control). **B)** 14.13 Protein/peptide degradation. **C)** N-directed glycosylation, deglycosylation. Each generated group were functional annotated with FunCat (The Functional Catalogue). Venn diagrams were created with online tool Venny 2.1. Heatmaps were created with online software from Broad Institute – Morpheus.

The other functional subcategory analyzed were “14.13 Protein/peptide degradation” with 354 genes (**Additional file 1: Table S3**). From that, 38 genes were found DE in the recombinant strains (**Figure S6B and Additional file 1: Table S4**). Eight genes were common in all recombinant strains and two of them are chaperones (AN0858 and AN1163), with the orthologues in *S. cerevisiae*, HSP104 and HSP78<sup>42</sup>. The other six genes were *pkfC* (AN3226) and AN6931, which both encodes a protein (ENV9) proposed to be involved in vacuolar functions in *S. cerevisiae*; the predicted threonine-type endopeptidase (AN3493) and the *prtA* (AN5558), which encodes a broad-specificity thermostable alkaline protease; the extracellular deuterolysin-type metalloproteinase (AN7962) and the gene AN11028 predicted as a nucleotide binding protein with oxidoreductase activity<sup>31</sup>. Another interesting observation was that the strain with the lower level of protein production, *A. nidulans*<sub>1542</sub> showed more DE genes in this functional subcategory indicating that the degradation of proteins could interfere in this strain. This observation is supported by the differential expression of ubiquitin-ligase genes (AN0444 and AN0927) and peptidases (AN5619 and AN5810) only in *A. nidulans*<sub>1542</sub>. The strain *A. nidulans*<sub>AbfA</sub> had also a great number of specific DE genes related to protein/peptide degradation, probably related to its higher amounts of heterologous proteins production, evidenced by ubiquitin-related genes (AN7491 and AN2000) and proteolysis genes (AN7201 and AN10900). It is well established that the high production of heterologous proteins is connected with different stress responses<sup>40</sup>, ERAD is one of the conserved mechanisms that filamentous fungi use to overcome ER stress caused by the accumulation of heterologous misfolded proteins<sup>43</sup>.

Finally, 43 genes related to the functional subcategory “14.07.02.02 N-directed glycosylation, deglycosylation” were analyzed (**Additional file 1: Table S5**). From that, only 3 genes were found DE in the recombinant strains (**Figure S6C and Additional file 1: Table S6**). These three genes were down-regulated and predicted as alpha-1,6-mannosyltransferases (AN8986, AN7534, and AN1620) with orthologues in *S. cerevisiae*, OCH1 and HOC1<sup>42</sup>. The enzyme OCH1 is involved in the transfer of mannose from GDP-Man onto the  $\alpha$ -1,3 branch of the tri-mannose core leading to a  $\alpha$ -1,6 extension, that is the substrate for additional mannosyltransferases throughout the yeast secretory pathway<sup>44</sup>. These alpha-1,6-mannosyltransferases are interesting targets for genetic manipulation in order to understand if glycosylation pattern involved with these enzymes might affect recombinant protein production levels in *A. nidulans*.

Two additional categories important to overcome cellular stress caused by overproduction of heterologous proteins were analyzed, autophagy and cell wall pathways. In order to analyze both pathways, Kimura et al. (2011) defined lists of genes involved in the *A. oryzae* autophagy pathway<sup>45</sup> and cell wall pathways were defined by Groot et al. (2009)<sup>46</sup>. Based on these lists we defined the homologous genes in *A. nidulans* by using the AspGD data, generating the set of 26 genes for autophagy and 95 for cell wall (which contemplates chitin synthesis, 1,3-alpha-glucan synthesis, 1,3-beta-glucan synthesis and cell wall integrity<sup>46</sup>).

For autophagy pathway, from 26 genes only 2 were DE in our RNA-seq data. The gene AN10728, up-regulated only in the strain *A. nidulans*<sub>1542</sub>, has an ortholog *S. cerevisiae* (*atg22*) that encodes a vacuolar integral membrane protein required for efflux of amino acids during autophagic body breakdown<sup>42</sup>. The other gene, AN2876 (uncharacterized) were up-regulated in the strains *A. nidulans*<sub>AbfA</sub> and *A. nidulans*<sub>BglC</sub>. It is known in the literature that autophagy is an important process that delivers misfolded secretory proteins accumulated in ER to vacuoles, mechanism already described for *A. oryzae*<sup>45</sup>. In another perspective, autophagy was also described to be dispensable to overcome ER stress in *A. niger*<sup>47</sup>. Despite this controversy, *A. nidulans* recombinant strains showed only 2 DE genes, which is a limited data to come to a specific conclusion of this pathway.

For the cell wall pathway, 31 related genes were DE in our RNA-seq data. The transcriptomic response of cell wall genes was primarily of down-regulation, and 6 genes were common for all recombinant strains. Two interesting genes, AN1604 (*agnE*) and AN5885 (*agsA*), were down-regulated at 2h and up-regulated at 8h. The first is predicted as a putative glycosylphosphatidylinositol (GPI)-anchored alpha-1,3-glucanase. The second encodes the catalytic subunit of alpha-1,3 glucan synthase complex; plays a minor role in alpha-1,3 glucan synthesis<sup>31</sup>. In general, *A. nidulans*<sub>1542</sub> and *A. nidulans*<sub>AbfA</sub> showed a very similar response, specifically at 2h, as previously observed for UPR and ERAD related genes. *A. nidulans*<sub>AbfA</sub> showed more DE genes in cell wall pathway, which might indicate that this strain is more exposed to secretion stress which also influences the cell wall homeostasis<sup>48</sup>. Fiedler et al. (2014) showed that *A. niger* senses and respond to cell wall stress with at least three transcription factors, RlmA, MsnA and CrzA<sup>49</sup>. Our transcriptomic data of *A. nidulans* recombinant strains showed the *A. nidulans*<sub>1542</sub> and *A. nidulans*<sub>AbfA</sub> down-regulation of *rlmA* (orthologous), which indicates that these recombinant strains were regulated by cell wall stress caused by heterologous protein production<sup>49</sup>.

The classification of early, continuous and late responses allowed us to observe that there is a great transcriptomic difference between the time points analyzed (2 and 8h) and a great transcriptomic similarity between the strains *A. nidulans*<sub>AbfA</sub> and *A. nidulans*<sub>1542</sub>. These similarities and differences lead us to determine specific profiles of the three recombinant strains over time. Five functional subcategories were used to understand the specific profile of heterologous protein secretion stress in *A. nidulans*, with UPR, glycosylation, ERAD, autophagy and cell wall synthesis/integrity. After analyzing protein secretion stress, we sought to deeper analyze the secretion pathway genes.

### 3.3.5. Differential expression of genes related to the secretion pathway

It has been shown that the bottleneck in the production of heterologous proteins is not only caused by low expression of heterologous genes, but it is due to posttranscriptional processes in the secretory pathway<sup>50</sup>. Many studies have attempted to comprehend the superior secretion capacity of *Aspergillus*, primarily at the transcriptomic level<sup>6,16,25,27,38</sup>. These studies identified genes that play major roles in different stages of protein production such as translocation, folding, cargo transport and exocytosis<sup>51</sup>. Liu et al. (2014) defined a list of genes involved in the secretion pathway of *A. oryzae* using the secretory model of *S. cerevisiae* as a scaffold. Based on this list we defined the homologous or best hits genes in *A. nidulans* by using the AspGD data, generating a set of 374 genes (**Additional file 2: Table S7**).

Seventeen genes were DE in the recombinant strains (**Additional file 2: Table S8**) and each recombinant strain presented a singular response. The *A. nidulans*<sub>1542</sub> strain showed a predominant down-regulation response while *A. nidulans*<sub>BglC</sub> had an up-regulation response (**Figure 6A**). *A. nidulans*<sub>AbfA</sub> also provides more genes in common with *A. nidulans*<sub>1542</sub> than *A. nidulans*<sub>BglC</sub> (**Figure 6B**), reinforcing the idea that the cellular response of these two recombinant strains was very similar. When we classified these 17 secretion pathway genes into early, continuous and late response genes, we found 12, 2 and 4 genes, respectively, strengthen that the early response becomes basal overtime, which was already observed in the global analysis (**Figure 6**).

In order to understand the functional categories represented by the 17 DE genes of the secretion pathway, it was performed a functional category analysis with FunCat. The most represented functional categories were "stress response", "protein folding and stabilization" and "unfolded protein response", with 10, 8 and 8 genes respectively (**Figure 6C**). The absence of representative categories directly related to the ER stress in the global annotation of the

transcriptome (**Figure 5**), shows that the overexpression of heterologous genes does not influence only the secretion pathway, but other biological processes such as transport facilities/routes, homeostasis of ions and fatty acids metabolism. The overproduction of  $\alpha$ -amylase in *A. oryzae* altered some biological processes such as “protein N-linked glycosylation”, “ER translocation and folding”, “signal peptide processing”, “ER to Golgi” and others<sup>27</sup>.

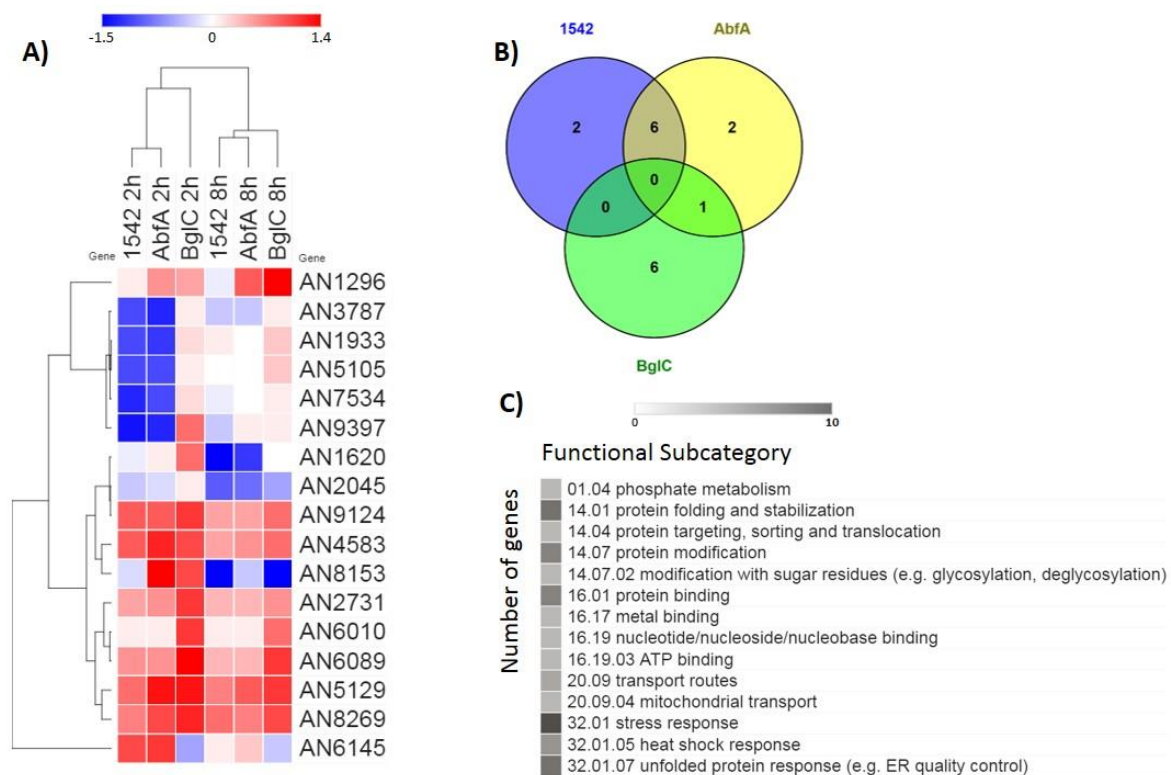


**Figure 6. Secretory pathway analysis of the differentially expressed genes obtained from the RNA-seq data.** **A)** Bar chart representing the differentially expressed genes related to the secretion pathway in *A. nidulans*. The rectangles above the bars represent the number of specific up and downregulated genes by the recombinant *A. nidulans* strains. Data from recombinant strains were compared to the control strain *A. nidulans*<sub>A773</sub> and  $(\log_2)$  Fold Change  $\leq -1.0$  or  $\geq 1.0$  and adjusted p-value  $\leq 0.01$  were used as thresholds. **B)** Venn Diagram representing the 17 differentially expressed genes related to the secretion pathway. No gene was found in common to all the recombinant strains. Venn diagram was created using the online tool Venny 2.1. **C)** Functional annotations of differentially expressed genes related to the secretory pathway of recombinant *A. nidulans*<sub>AbfA</sub>, *A. nidulans*<sub>BglC</sub> and *A. nidulans*<sub>1542</sub>. The analysis of functional categories was performed with FunCat (The Functional Catalogue). The functional categories graph values represent the number altered genes found (abs set) in the transcriptome data based on the values of the reference genome annotation. All functional subcategories that had 5 or more differentially expressed genes are represented. *A. nidulans* strains were cultivated as described in the

Material and Methods section. Heatmaps were created with online software from Broad Institute – Morpheus.

Based on the secretion pathway genes (Liu et al. 2014) we created a secretory machinery profile for the three recombinant strains highlighting some process such as protein folding, glycosylation, sugar transporters, stress response and others (**Figure 7**). The similar pattern between the strains *A. nidulans*<sub>AbfA</sub> and *A. nidulans*<sub>1542</sub> is evident as already observed in the general transcriptomic response (**Figures 3, S3 and 5**). This conclusion was corroborated by the biological processes overrepresented: “protein folding and stabilization”, “protein modification” and “stress response”. We consider some explanations for this observation, first, the enzyme BglC is a very complex protein with 797 amino acids and according to NetNGlyc 1.0 it is predicted to have 5 N-glycosylation sites, while AbfA and 1542 are smaller proteins (656 and 667 amino acids, respectively) with 3 and 1 predicted N-glycosylation sites, respectively. *A. nidulans*<sub>BglC</sub> showed 6 exclusive up-regulated genes related to the secretion pathway (**Figure 6**), with 5 chaperones genes (AN2731, AN6010, AN6089, AN8269 and AN9124) involved in protein folding, stabilization, targeting, sorting and translocation (**Additional file 2: Table S8**). This observation also indicates the hypothesis that *A. nidulans*<sub>BglC</sub> needs to overcome the properly folding being a complex protein. The sixth DE gene in this strain was AN1296, found up-regulated at 2h and 8h and moderately up-regulated in *A. nidulans*<sub>AbfA</sub>. The orthologous of this gene in *S. cerevisiae* (TRL1) is required for tRNA splicing and for both splicing and translation of *hac1* mRNA in the UPR<sup>42</sup>. This result converges with our relative coverage data (**Figure S4**) that shows the unconventional splicing of *hacA* suggesting the induction of UPR for the heterologous protein production, as previously reported<sup>15,22,29,39,52,53</sup>. In the other hand, *hacA* was down-regulated in *A. nidulans*<sub>1542</sub> and *A. nidulans*<sub>AbfA</sub> at early induction times (**Additional file 2: Table S8**), demonstrating that the unconventional splicing of *hacA* is required for UPR activation, but not necessarily the *hacA* overexpression<sup>22</sup>. Liu et al. (2014) also observed that the mRNA levels of the *hacA* were not increased in the *A. oryzae* recombinant strains, indicating that *hacA* splicing is not the only mechanism for activating UPR in this organism<sup>27</sup>.

The recombinant strain *A. nidulans*<sub>AbfA</sub> also had two exclusives up-regulated genes, the AN4583 and AN6145. Both genes are predicted as peptidyl-prolyl cis-trans isomerases (PPIases)<sup>31</sup>. These proteins accelerate the folding of proteins, and these two PPIases may be interesting targets for genetic manipulation in order to improve protein secretion<sup>54</sup>.





The strain *A. nidulans*<sub>1542</sub> showed only two exclusive DE genes. The first one is a predicted 1,2- $\alpha$ -mannosidase (AN2045) with an orthologous (gh47-3) in *N. crassa* described to be an ER-associated ubiquitin-dependent protein with catabolic process and N-glycan processing (according to UniProt). The second was the AN8153 down-regulated at 2h and 8h, which was not observed for other strains that showed an up-regulation response at 2h. This gene is predicted as an ATP binding, with nucleoside-triphosphatase activity and nucleotide binding activity<sup>31</sup>. In *S. cerevisiae* the best hit is CDC48, an ATPase; subunit of a polyubiquitin-selective segregase complex involved in ERAD, with a role in mobilizing membrane-bound transcription factors by regulated ubiquitin/proteasome-dependent processing in macroautophagy<sup>42</sup>. Both down-regulated genes (AN2045 and AN8153) were related to ERAD, and *A. nidulans*<sub>1542</sub> strain had several DE genes in this pathway as already observed with the FunCat subcategory “Protein/peptide degradation” (**Figure S6**). Moreover, DE genes related to ERAD identified in this strain could partially explain the low levels of 1542 secretion. In *A. niger*, a knock-out of one ERAD factor improved the production of a heterologous beta-glucuronidase<sup>55</sup>. DE genes related to ERAD evidenced by *A. nidulans* recombinant strains studied in this work seems to be potential targets for genetic manipulation in an attempt to improve heterologous protein secretion.

Heterologous production of non-fungal proteins is often disappointingly low in *Aspergilli*. The reasons for this phenomenon are relatively poorly understood, but it seems that the limitations are at the post-translational level with bottlenecks occurring in the processing of the protein and secretion<sup>51</sup>. The protein 1542 is a bacterial thermophilic enzyme and thermozymes are naturally difficult to be well secreted by mesophilic fungi<sup>28,56,57</sup>. A recombinant thermophilic xylanase B produced in *T. reesei* featured multiple forms of the enzyme, decorated with various *N*- and *O*-glycans, which has not been described previously in the glycosylation patterns of *T. reesei*<sup>28</sup>. Such thermophilic enzymes might require differential posttranslational modifications or specific chaperones to reach their fully functional and stable folded state<sup>56</sup>. The 1542 has 55% of similarity with an endogenous mannanase of *A. nidulans* (ManC; AN6427). ManC has 4 predicted N-glycosylation sites (N34, N62, N90, and N238) and only the N62 is in a region of low similarity with the 1542. The other 3 predicted N-glyc sites of ManC have high similarity with 1542 and these sites are probably not glycosylated due to the absence of serine or threonine to complete the sequon (N-X-S/T) (**Figure S7**)<sup>58</sup>. Site-directed mutagenesis to match the ManC N-glyc sites could alleviate the folding pathway of 1542, decreasing the proportion of misfolded proteins and consequently improving the secretion yield.

Tyo et al. (2012) identified biological mechanisms which alter the secretory pathway in response to secretion of recombinant proteins with different sizes, a small protein (human insulin precursor) and a comparatively larger protein ( $\alpha$ -amylase) in *Saccharomyces cerevisiae*<sup>36</sup>. By

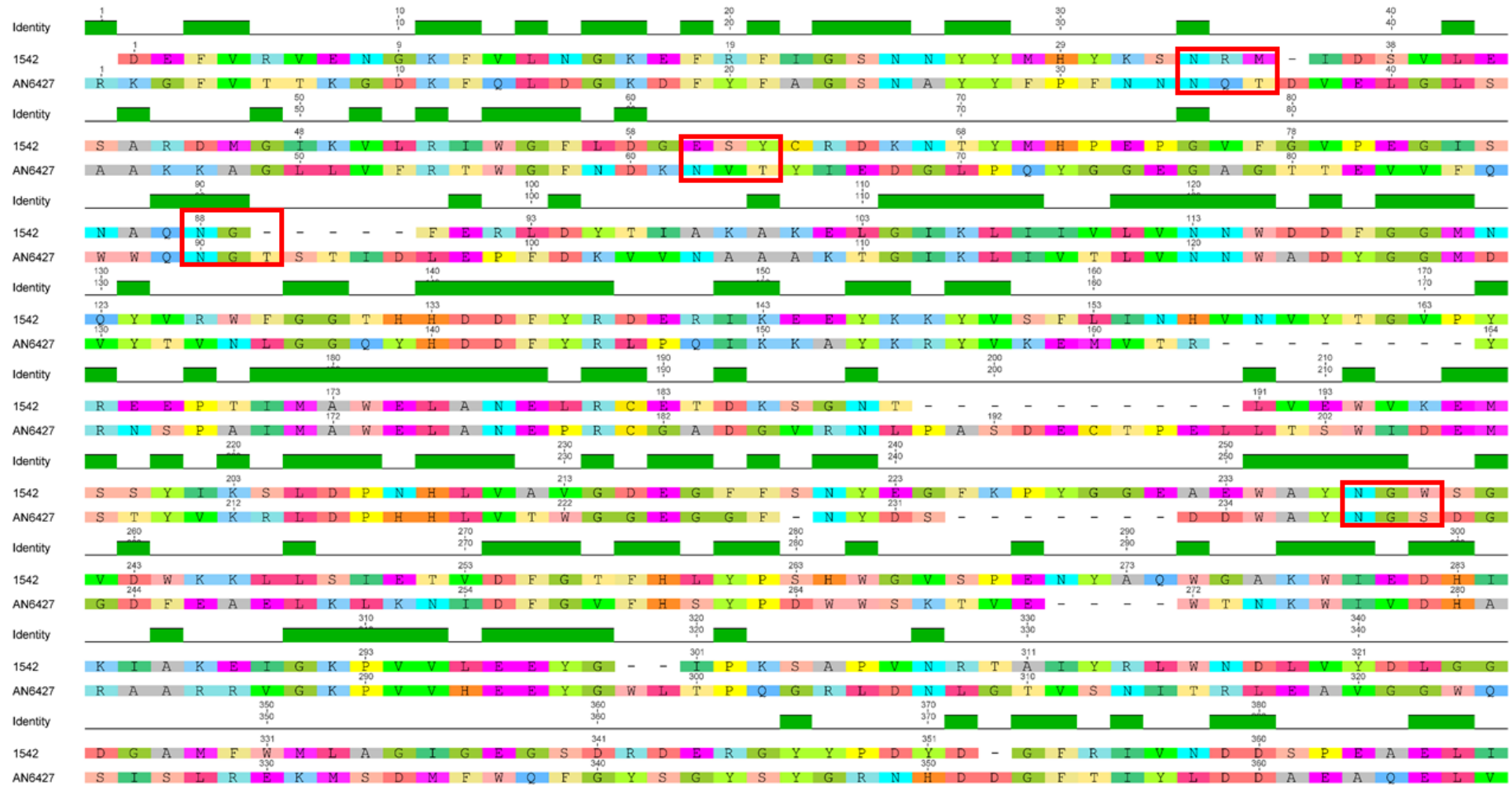


**Figure S7. Sequence alignment of the proteins 1542 and the endo-beta-(1,4)-mannanase AN5427 from *A. nidulans*.** The two sequences were aligned using Geneious software. The dark green triangles show the identical regions in the two sequences. The red triangles show the N-glycosylation sequons predicted by NetNGlyc software. The 1542 has 55% of similarity with the endogenous mannanase of *A. nidulans* (ManC; AN6427). ManC has 4 predicted N-glycosylation sites (N34, N62, N90, and N238) and only the site N62 is in a region of low similarity with the 1542. The other 3 predicted N-glyc sites of ManC have high similarity with 1542 and these sites are not glycosylated due to the absence of serine or threonine to complete the sequon (N-X-S/T).

perturbing the yeast secretory pathway with these proteins, they conclude that to maintain an optimal ratio of secretion, either protein folding rates must increase and oxidation rates decrease (by repressing ERAD and UPR). In this scenario, recombinant proteins would be slowly folded, albeit without high cellular stresses. This would result in longer overall process times but may be required due to the difficult to fold proteins<sup>36</sup>.

Additionally several studies [<sup>26,28,37,47</sup> including the present one], evidence that different recombinant proteins have different secretion levels in fungi. By observing the secretory pathway profile (**Figure 7**) is clear that *A. nidulans* does not respond equally for all overexpressed proteins, instead, it regulates different processes to correctly fold and secrete each recombinant protein.

### 3.4. CONCLUSIONS

Despite the importance of *Aspergilli* as microbial cell factory with many industrial applications, only a limited number of genetic tools are currently available for efficient overproduction and subsequent secretion of heterologous proteins<sup>41</sup>. In our study, *A. nidulans* mechanisms for secretion of heterologous proteins were investigated. We performed a comparative analysis through the expression profile of genes regulated by the production of recombinant hydrolytic enzymes in *A. nidulans* from transcriptomic data generated by RNA-seq.

The general response to heterologous protein production was primarily an up-regulation response. The transcriptomic data were classified at early, continuous and late responses, and it was possible to observe a different profile at 2 and 8h of induction of protein production. At 2h, we observed the unconventional splicing of *hacA*, which was normalized at 8h. A transcriptomic profile for each strain was established based on the functional categorization of DE genes. With this analysis, several proteins including many chaperones were DE and appear to be interesting candidates for genetic manipulation and better understand their effects on heterologous protein secretion in *A. nidulans*.

Finally, by observing the secretion pathway, we found 17 DE genes distributed into the three recombinant strains. The most representative functional categories represented by these genes were used to build a secretory pathway profile of the transcriptional response. This was the first study to address the transcriptomic response to heterologous protein production in *A. nidulans*, additionally monitoring three different recombinant proteins with different secretion levels. In this way, we could provide insights to better understand how *A. nidulans* adapts to

the overproduction of heterologous proteins and highlight potential targets for genetic manipulation for superior yields of protein secretion.

### 3.5. MATERIALS AND METHODS

*A. nidulans*<sub>Δ773</sub> (pyrG89;wA3;pyroA4) was purchased from the Fungal Genetics Stock Center (FGSC, St Louis, MO). The *A. nidulans*<sub>AbfA</sub>, *A. nidulans*<sub>BglC</sub> and *A. nidulans*<sub>1542</sub> were previously transformed and tested by our research group as described by Segato 2012<sup>24</sup>. 5-Fluorotic acid (5-FOA) was purchased from Oakwood Products Inc (NC9639762), and all other chemicals from Sigma–Aldrich, Megazyme and Fisher Scientific.

#### Media, cultivation, and solutions

Vegetative cultures and spore production were prepared by inoculation of conidia in minimal medium as described by Clutterbuck<sup>59</sup> and Pontecorvo<sup>60</sup>. *A. nidulans* strains were cultivated in the minimal medium contained 5 % of 20× Clutterbuck salts, 0.1 % of 1000× vitamins, 0.1 % of 1000× trace elements, pH 6.5 and supplemented with pyridoxine (1 mg/L), uracil/uridine (2.5 mg/L each) or as needed. Minimal medium was supplemented with 1% of glucose for mycelium growth (growth medium) or with 2 % of maltose and 250 mM of HEPES (Sigma–Aldrich) for promoter activation and protein production (induction medium). Incubation temperature was always at 37 °C.

#### Production and secretion of client proteins

Pre-cultures were prepared by inoculating fresh 10<sup>8</sup> spores/ml in 30 mL of minimal medium supplemented with 1% of glucose for the mycelium growth for 48 hours and shaking at 150 rpm at 37 °C. Strains cultivation were performed in biological triplicates. The mycelium was washed with autoclaved distilled water with a spatula, Miracloth, filter and then transferred to the induction medium. After defined times of protein induction, the mycelium was collected with a spatula, Miracloth and filter, dried, frozen in liquid nitrogen and stored at -80 °C. The rest of medium were collected by filtration, centrifuged at 10,000 × g for 10 min prior to concentration by ultrafiltration (10,000 Da cutoff Amicon), quantified by the Bradford method<sup>61</sup>, validated for purity by SDS-PAGE<sup>62</sup> and used for biochemical studies.

#### Standard enzyme activity assays

Enzymatic activity for beta-glucosidase GH3 (BglC) was conducted on 4-Nitrophenyl- $\beta$ -D-glucopyranoside (Sigma–Aldrich) and for alpha-arabinofuranosidase GH51 (AbfA) were conducted on 4-Nitrophenyl- $\alpha$ -L-arabinofuranoside (Sigma–Aldrich). The enzymatic activity assays were performed by adding 50  $\mu$ L of mycelium induction medium to 40  $\mu$ L of one of the 1 % (w/v) substrates in 10  $\mu$ L of 50 mM ammonium acetate buffer, pH 5.5 and incubating at 50 °C, for 45 min. The enzymatic reactions were stopped with sodium carbonate. The reactions were then spectrophotometrically quantified at 400 nm with a Multimode Infinite M200 Reader (Tecan, SC) compared with pNP standard curve.

Enzymatic activity of mannanase GH5 thermophilic (1542) was conducted on Locust bean gum (Sigma–Aldrich) substrate. The reaction was determined by adding 1 $\mu$ g of proteins in concentrated mycelium induction medium to 50  $\mu$ L of 1 % (w/v) substrate in 50 mM ammonium acetate buffer, pH 5.5 and incubating at 87 °C, for 600 min. The enzymatic release of reducing sugars, which react with DNS <sup>63</sup>, was spectrophotometrically quantified at 575 nm with a Multimode Infinite M200 Reader (Tecan, SC) and compared with glucose standard curve. This method was partially based on the DNS method described by Miller <sup>63</sup>. All incubations were carried out in a Thermal Cycler (MJ Research). Relative enzymatic activities were calculated based on U/mg values of each reaction. Statistics calculation and plotting were carried out with GraphPad Prism v 5.0 Software (California, US).

### **Intracellular protein analysis**

Total intracellular proteins were extracted from frozen mycelium. Biomass was ground in liquid nitrogen to a fine powder using the mortar and pestle. Powdered biomass was gently suspended in 5 mL of extraction buffer (20 mM Tris HCL pH8; 0.05 % (w/v) Triton™ X-100 (Sigma-Aldrich), 150 mM NaCl), containing protease inhibitors (2 mM PMSF and Protease Inhibitor Cocktail N221-1mL (Amresco), and centrifuged twice at 8000 rpm for 15 min at 4 °C; then, supernatant was collected for SDS-PAGE <sup>62</sup> profile analysis (**Figure S2**).

### **RNA extraction**

Total RNA were extracted from frozen mycelium using the Quick-RNA™ MiniPrep kit (Zymo Research) according to manufacturer's instructions. The integrity of extracted RNA was evaluated (RIN  $\geq$  8) on the Agilent Bioanalyzer 2100 and quantified using an ND-1000 NanoDrop (Thermo Scientific) spectrophotometer. Total purified RNA was stored at -80 °C until further processing.

### RNA-seq data analysis

For RNA-seq sample preparation, the total RNA from four *A. nidulans* strains (three recombinant strains and the parental strain) cultivated in 2 and 8 hours in biological triplicates, resulted in twenty-four samples for library preparation, using TruSeq Stranded mRNA Library Prep Kit v2 (Illumina) according to manufacturer's instructions. Sequencing libraries were prepared and sequenced using Illumina HiSeq 2500 at CTBE NGS sequencing facility. Approximately 148 million 100 bp paired-end reads were obtained for *A. nidulans*<sub>A773</sub>, *A. nidulans*<sub>AbfA</sub>, *A. nidulans*<sub>BglC</sub> strains and, 130 million reads were obtained for *A. nidulans*<sub>S1542</sub> strain, representing 115 GB. Reads were quality checked and filtered using FASTQC and Trimmomatic<sup>64</sup>, respectively, and rRNA contamination was assessed and removed using sortmeRNA<sup>65</sup>. The rate of rRNA contamination was low, lower than 16% in all samples, excepting one replicate of AbfA 8h (**Table S9**). QC reads were aligned to *Aspergillus nidulans* genome available at AspGD (<http://www.aspgd.org/>) using Tophat2<sup>66</sup>, and concordant pair alignment rate varied between 84 and 93%. A good replicate agreement was obtained for all conditions, as showed by PCA analysis and clustering of the samples data (**Figure S3**).

For differential expression analysis, pairwise comparisons between each strain and the control strain *A. nidulans*<sub>A773</sub> were performed using DESeq2 R/Bioconductor package<sup>67</sup>, applying a log<sub>2</sub> fold change  $\geq 2$  or  $\leq -2$  and an adjusted p-value  $\leq 0.01$  as thresholds. For the secretion pathway analysis, it was used a log<sub>2</sub> fold change  $\geq 1$  or  $\leq -1$  and an adjusted p-value  $\leq 0.01$  as thresholds. Graph constructions were performed using GraphPad Prism v 5.0 Software (California, US) and the online tool for Venn diagrams - Venny 2.1 (<http://bioinfogp.cnb.csic.es/tools/venny/>).

### Functional annotation

For the Functional annotation of DE genes identified by RNA-seq analysis, lists of genes were generated by filtering the results with log<sub>2</sub> FC  $\leq -1.0$  or  $\geq 1.0$  and adjusted p-value  $\leq 0.01$ . The gene expression values of recombinant strains compared to the control strain *A. nidulans*<sub>A773</sub> were used. The gene lists obtained were then used for functional annotation using FunCat (Functional Catalogue)<sup>37</sup>.

The selected genes for annotation with FunCat were faced with the database of the reference genome of *A. nidulans* and applied statistical Fisher test with p-value  $\leq 0.05$  as threshold. The enriched functional categories and subcategories were used for comparisons and

graphics generation. Data analysis was performed using GraphPad Prism v 5.0 Software (California, US).

### Secretion pathway analysis

A list of 374 genes of the secretory pathway was generated based on the work of Liu et al. (2014). This work defined a functional protein secretory component list of *A. oryzae* using the secretory model of *S. cerevisiae* as a scaffold<sup>27</sup>. This list was further adapted to filamentous fungi by adding *A. oryzae* orthologous of the secretory components reported in other *Aspergillus* species, such as *A. nidulans* and *A. niger*. The homologous genes in *A. nidulans* reported in AspGD resources were then used to generate a list of 374 genes (**Table S1**). Among those, 17 DE genes were found distributed into the three recombinant strains. For this result, it was used a less selective filter of  $\log_2 \text{FC} \leq -1.0$  or  $\geq 1.0$ , and an adjusted p-value  $\leq 0.01$ .

DE genes of the secretory pathway were functionally annotated with FunCat, and the most representative functional categories were used to build a secretory pathway profile of three recombinant strains (**Figure 8**). To generate this profile, the FC values of the DE genes involved with secretion pathway were used to create heatmaps using R.

### Real-Time PCR (qPCR) analysis

To quantify the expression of selected genes, quantitative real-time PCR (qRT-PCR) were performed. For this analysis, 2  $\mu\text{g}$  of pure RNA was used for cDNA synthesis using the First Strand cDNA kit Maxima<sup>TM</sup> Synthesis (Thermo Scientific) according to manufacturer's instructions. The cDNA was diluted 1/50 and used for real-time PCR analysis in the ViiA<sup>TM</sup> 7 Real-Time PCR System, using Maxima SYBR<sup>TM</sup> Green (Thermo Scientific) for signal detection in accordance with the manufacturer's instructions. The gene encoding  $\beta$ -tubulin (AN6838) was used as endogenous control for being a well stable gene in filamentous fungi<sup>68</sup>.

The thermal profile conditions for all PCRs were: 95 °C for 30 s; followed by 40 cycles of 95 °C for 10 s and 60 °C for 60 s. The melting curve was analyzed with ViiA<sup>TM</sup> 7 Software (Thermo Scientific) to confirm the presence of only one amplicon according to the  $T_m$  expected for each gene amplification. Gene expression values were calculated according to the  $2^{-\Delta\Delta\text{CT}}$  method<sup>69</sup>. Primers used in the qPCR experiments are described in Additional file 4 (**Table S10**). Data analysis was performed using GraphPad Prism v 5.0 Software (California, US).



### 3.6. REFERENCES

1. Lowe, R. G. T. & Howlett, B. J. Indifferent, affectionate, or deceitful: Lifestyles and secretomes of fungi. *PLoS Pathog.* **8**, 1–3 (2012).
2. Lubertozzi, D. & Keasling, J. D. Developing *Aspergillus* as a host for heterologous expression. *Biotechnol. Adv.* **27**, 53–75 (2009).
3. Reseach, B. Global Markets for Enzymes in Industrial Applications. *Focus Catal.* **1**, 2 (2014).
4. AMFEP. List of commercially available enzymes. *Assoc. Manuf. Formul. Enzym. Prod.* Amfep/15/0, <http://www.amfep.org/content/list-enzymes> (2015).
5. Su, X., Schmitz, G., Zhang, M., Mackie, R. I. & Cann, I. K. O. *Heterologous Gene Expression in Filamentous Fungi. Advances in Applied Microbiology* **81**, 1-61 (2012).
6. Guillemette, T. *et al.* Genomic analysis of the secretion stress response in the enzyme-producing cell factory *Aspergillus niger*. *BMC Genomics* **8**, 158 (2007).
7. Pakula, T. M. *et al.* Genome wide analysis of protein production load in *Trichoderma reesei*. *Biotechnol. Biofuels* **9**, 132 (2016).
8. Heimel, K. Unfolded protein response in filamentous fungi—implications in biotechnology. *Appl. Microbiol. Biotechnol.* **99**, 121–132 (2014).
9. Sidrauski, C. & Walter, P. The transmembrane kinase Ire1p is a site-specific endonuclease that initiates mRNA splicing in the unfolded protein response. *Cell* **90**, 1031–1039 (1997).
10. Perrone, C. A. A Novel Dynein Light Intermediate Chain Colocalizes with the Retrograde Motor for Intraflagellar Transport at Sites of Axoneme Assembly in *Chlamydomonas* and Mammalian Cells. *Mol. Biol. Cell* **14**, 2041–2056 (2003).
11. Ruegsegger, U., Leber, J. H., Walter, P. & Francisco, S. Block of HAC1 mRNA translation by long-range base pairing is released by cytoplasmic splicing upon induction of the unfolded protein response. *Cell* **107**, 103–114 (2001).
12. Calfon, M. *et al.* IRE1 couples endoplasmic reticulum load to secretory capacity by processing the XBP-1 mRNA. *Nature* **415**, 92–96 (2002).
13. Iwawaki, T., Akai, R., Kohno, K. & Miura, M. A transgenic mouse model for monitoring endoplasmic reticulum stress. *Nat. Med.* **10**, 98–102 (2004).
14. Mulder, H. J., Saloheimo, M., Penttilä, M. & Madrid, S. M. The transcription factor HACA mediates the unfolded protein response in *Aspergillus niger*, and up-regulates its own transcription. *Mol. Genet. Genomics* **271**, 130–140 (2004).
15. Saloheimo, M., Valkonen, M. & Penttilä, M. Activation mechanisms of the HAC1-mediated unfolded protein response in filamentous fungi. *Mol. Microbiol.* **47**, 1149–1161 (2003).
16. Carvalho, N. D. *et al.* Genome-wide expression analysis upon constitutive activation of the HacA bZIP transcription factor in *Aspergillus niger* reveals a coordinated cellular response to counteract ER stress. *BMC Genomics* **13**, 2–17 (2012).

17. Hayano, T., Hirose, M. & Kikuchi, M. Protein disulfide isomerase mutant lacking its isomerase activity accelerates protein folding in the cell. *FEBS Lett.* **377**, 505–511 (1995).
18. Valkonen, M., Penttilä, M. & Saloheimo, M. The *ire1* and *ptc2* genes involved in the unfolded protein response pathway in the filamentous fungus *Trichoderma reesei*. *Mol. Genet. Genomics* **272**, 443–51 (2004).
19. Xu, P., Raden, D., Doyle, F. J. & Robinson, A. S. Analysis of unfolded protein response during single-chain antibody expression in *Saccharomyces cerevisiae* reveals different roles for BiP and PDI in folding. *Metab. Eng.* **7**, 269–279 (2005).
20. Harmsen, M. M., Bruyne, M. I., Raué, H. A. & Maat, J. Overexpression of binding protein and disruption of the *PMR1* gene synergistically stimulate secretion of bovine prochymosin but not plant Thaumatin in yeast. *Appl. Microbiol. Biotechnol.* **46**, 365–370 (1996).
21. Travers, K. J. *et al.* Functional and genomic analyses reveal an essential coordination between the unfolded protein response and ER-associated degradation. *Cell* **101**, 249–258 (2000).
22. Heimel, K. Unfolded protein response in filamentous fungi—implications in biotechnology. *Appl. Microbiol. Biotechnol.* **99**, 121–132 (2015).
23. Nevalainen, K. M. H., Te'o, V. S. J. & Bergquist, P. L. Heterologous protein expression in filamentous fungi. *Trends Biotechnol.* **23**, 468–474 (2005).
24. Segato, F. *et al.* High-yield secretion of multiple client proteins in *Aspergillus*. *Enzyme Microb. Technol.* **51**, 100–106 (2012).
25. Sims, A. H. *et al.* Transcriptome Analysis of Recombinant Protein Secretion by *Aspergillus nidulans* and the Unfolded-Protein Response In Vivo. *Appl. Environ. Microbiol.* **71**, 2737–2747 (2005).
26. Pakula, T. M. *et al.* The Effects of Drugs Inhibiting Protein Secretion in the Filamentous Fungus *Trichoderma reesei*. *J. Biol. Chem.* **278**, 45011–45020 (2003).
27. Liu, L., Feizi, A., Österlund, T., Hjort, C. & Nielsen, J. Genome-scale analysis of the high-efficient protein secretion system of *Aspergillus oryzae*. *BMC Syst. Biol.* **8**, 73 (2014).
28. Nevalainen, H. & Peterson, R. Making recombinant proteins in filamentous fungi- are we expecting too much? *Front. Microbiol.* **5**, 75 (2014).
29. Guillemette, T. *et al.* in *Methods in enzymology* **490**, 1–29 (2011).
30. Wood, V. *et al.* PomBase: a comprehensive online resource for fission yeast. *Nucleic Acids Res.* **40**, D695–D699 (2012).
31. Cerqueira, G. C. *et al.* The *Aspergillus* Genome Database: Multispecies curation and incorporation of RNA-Seq data to improve structural gene annotations. *Nucleic Acids Res.* **42**, D705–D710 (2014).
32. Szilagyi, M. *et al.* Transcriptome changes initiated by carbon starvation in *Aspergillus nidulans*. *Microbiology* **159**, 176–190 (2013).

33. Wang, G., Zhang, D. & Chen, S. Effect of earlier unfolded protein response and efficient protein disposal system on cellulase production in Rut C30. *World J. Microbiol. Biotechnol.* **30**, 2587–2595 (2014).
34. Zhang, J. *et al.* Expression and high-yield production of extremely thermostable bacterial xylanaseB in *Aspergillus niger*. *Enzyme Microb. Technol.* **43**, 513–516 (2008).
35. Zoglowek, M., Lübeck, P. S., Ahring, B. K. & Lübeck, M. Heterologous expression of cellobiohydrolases in filamentous fungi - An update on the current challenges, achievements and perspectives. *Process Biochem.* **50**, 211–220 (2015).
36. Tyo, K. E., Liu, Z., Petranovic, D. & Nielsen, J. Imbalance of heterologous protein folding and disulfide bond formation rates yields runaway oxidative stress. *BMC Biol.* **10**, 16 (2012).
37. Ruepp, A. The FunCat, a functional annotation scheme for systematic classification of proteins from whole genomes. *Nucleic Acids Res.* **32**, 5539–5545 (2004).
38. Kwon, M. J. *et al.* The transcriptomic fingerprint of glucoamylase over-expression in *Aspergillus niger*. *BMC Genomics* **13**, 701 (2012).
39. Zhou, B., Xie, J., Liu, X., Wang, B. & Pan, L. Functional and transcriptomic analysis of the key unfolded protein response transcription factor HacA in *Aspergillus oryzae*. *Gene* **593**, 143–153 (2016).
40. Mattanovich, D., Gasser, B., Hohenblum, H. & Sauer, M. Stress in recombinant protein producing yeasts. *J. Biotechnol.* **113**, 121–135 (2004).
41. Fleißner, A. & Dersch, P. Expression and export: recombinant protein production systems for *Aspergillus*. *Appl. Microbiol. Biotechnol.* **87**, 1255–1270 (2010).
42. Cherry, J. M. *et al.* Saccharomyces Genome Database: the genomics resource of budding yeast. *Nucleic Acids Res.* **40**, D700–D705 (2012).
43. Hampton, R. Y. ER-associated degradation in protein quality control and cellular regulation. *Curr. Opin. Cell Biol.* **14**, 476–482 (2002).
44. Hamilton, S. R. & Gerngross, T. U. Glycosylation engineering in yeast: the advent of fully humanized yeast. *Current Opinion in Biotechnology* **18**, 387–392 (2007).
45. Kimura, S., Maruyama, J. ichi, Kikuma, T., Arioka, M. & Kitamoto, K. Autophagy delivers misfolded secretory proteins accumulated in endoplasmic reticulum to vacuoles in the filamentous fungus *Aspergillus oryzae*. *Biochem. Biophys. Res. Commun.* **406**, 464–470 (2011).
46. de Groot, P. W. J. *et al.* Comprehensive genomic analysis of cell wall genes in *Aspergillus nidulans*. *Fungal Genet. Biol.* **46**, S72–S81 (2009).
47. Burggraaf, A.-M. M. & Ram, A. F. J. Autophagy is dispensable to overcome ER stress in the filamentous fungus *Aspergillus niger*. *Microbiologyopen* **5**, 647–658 (2016).
48. Malavazi, I., Goldman, G. H. & Brown, N. A. The importance of connections between the cell wall integrity pathway and the unfolded protein response in filamentous fungi. *Brief. Funct.*

- Genomics* **13**, 456–470 (2014).
49. Fiedler, M. R. *et al.* The capacity of *Aspergillus niger* to sense and respond to cell wall stress requires at least three transcription factors: RlmA, MsnA and CrzA. *Fungal Biol. Biotechnol.* **1**, 5 (2014).
  50. Yoon, J., Aishan, T., Maruyama, J. I. & Kitamoto, K. Enhanced production and secretion of heterologous proteins by the filamentous fungus *Aspergillus oryzae* via disruption of vacuolar protein sorting receptor gene AoVps10. *Appl. Environ. Microbiol.* **76**, 5718–5727 (2010).
  51. Schalén, M., Anyaogu, D. C., Hoof, J. B. & Workman, M. Effect of secretory pathway gene overexpression on secretion of a fluorescent reporter protein in *Aspergillus nidulans*. *Fungal Biol. Biotechnol.* **3**, 3 (2016).
  52. Al-Sheikh, H. *et al.* Endoplasmic reticulum stress leads to the selective transcriptional downregulation of the glucoamylase gene in *Aspergillus niger*. *Mol. Microbiol.* **53**, 1731–1742 (2004).
  53. Krishnan, K. *et al.* Polysome profiling reveals broad translome remodeling during endoplasmic reticulum (ER) stress in the pathogenic fungus *Aspergillus fumigatus*. *BMC Genomics* **15**, 159 (2014).
  54. Pemberton, T. J. Identification and comparative analysis of sixteen fungal peptidyl-prolyl *cis/trans* isomerase repertoires. *BMC Genomics* **7**, 244 (2006).
  55. Jacobs, D. I. *et al.* Effective lead selection for improved protein production in *Aspergillus niger* based on integrated genomics. *Fungal Genet. Biol.* **46**, 141–152 (2009).
  56. Vieille, C. & Zeikus, G. J. Hyperthermophilic Enzymes: Sources, Uses, and Molecular Mechanisms for Thermostability. *Microbiol. Mol. Biol. Rev.* **65**, 1–43 (2001).
  57. Bergquist, P. L. *et al.* in *Progress in Biotechnology* **21**, 239–246 (2002).
  58. Deshpande, N., Wilkins, M. R., Packer, N. & Nevalainen, H. Protein glycosylation pathways in filamentous fungi. *Glycobiology* **18**, 626–637 (2008).
  59. Clutterbuck, A. J. Sexual and parasexual genetics of *Aspergillus* species. *Biotechnology* **23**, 3–18 (1992).
  60. Pontecorvo, G., Roper, J. A., Chemmons, L. M., Macdonald, K. D. & Bufton, A. W. J. in *Advances in Genetics* **5**, 141–238 (1953).
  61. Bradford, M. M. A rapid and sensitive method for the quantitation of microgram quantities of protein utilizing the principle of protein-dye binding. *Anal. Biochem.* **72**, 248–254 (1976).
  62. Shapiro, a L. & Maizel, J. V. Molecular weight estimation of polypeptides by SDS-polyacrylamide gel electrophoresis: further data concerning resolving power and general considerations. *Anal. Biochem.* **29**, 505–514 (1969).
  63. Miller, G. L. Use of Dinitrosalicylic Acid Reagent for Determination of Reducing Sugar. *Anal. Chem.* **31**, 426–428 (1959).

64. Bolger, A. M., Lohse, M. & Usadel, B. Trimmomatic: a flexible trimmer for Illumina sequence data. *Bioinformatics* **30**, 2114–2120 (2014).
65. Kopylova, E., Noé, L. & Touzet, H. SortMeRNA: Fast and accurate filtering of ribosomal RNAs in metatranscriptomic data. *Bioinformatics* **28**, 3211–3217 (2012).
66. Kim, D. *et al.* TopHat2: accurate alignment of transcriptomes in the presence of insertions, deletions and gene fusions. *Genome Biol.* **14**, R36 (2013).
67. Love, M. I., Huber, W. & Anders, S. Moderated estimation of fold change and dispersion for RNA-seq data with DESeq2. *Genome Biol.* **15**, 550 (2014).
68. Llanos, A., François, J. M. & Parrou, J. Tracking the best reference genes for RT-qPCR data normalization in filamentous fungi. *BMC Genomics* **16**, 71 (2015).
69. Livak, K. J. & Schmittgen, T. D. Analysis of Relative Gene Expression Data Using Real-Time Quantitative PCR and the  $2^{-\Delta\Delta CT}$  Method. *Methods* **25**, 402–408 (2001).

### 3.7. SUPPLEMENTARY MATERIALS

**Additional file 1: Functional subcategories analysis specifically related to proteins production and secretion.** *A. nidulans* genes described to be related to UPR, ERAD and glycosylation were analyzed with functional catalogue FunCat. Lists of genes generated were compared to *A. nidulans* RNA-seq data of the recombinant strains. **Table S1.** 75 genes related to the functional subcategory “32.01.07 Unfolded protein response (e.g. ER quality control)”. **Table S2.** 15 differentially expressed genes in the functional subcategory “32.01.07 Unfolded protein response (e.g. ER quality control)”. **Table S3.** 354 genes related to “14.13 Protein/peptide degradation”. **Table S4.** 38 differentially expressed genes in the functional subcategory “14.13 Protein/peptide degradation”. **Table S5.** 43 genes related to the functional subcategory “14.07.02.02 N-directed glycosylation, deglycosylation”. **Table S6.** 3 differentially expressed genes in the functional subcategory “14.07.02.02 N-directed glycosylation, deglycosylation”. **Tables S1, S3 and S5** contains Fold Change (FC) values of all three *A. nidulans* heterologous protein (1542, AbfA and BglC) secretor strains with 2 and 8 hours of induction. For each FC value there is a statistic p-value (padj) from t test. **Tables S2, S4 and S6** contains the differentially expressed genes related to each functional subcategories and its transcriptional responses characterization. Differentially expressed genes were obtained using the FC filters  $(\log 2) \leq -1.0$  or  $\geq 1.0$  and p-value  $\leq 0.01$ .

**Table S1.** 75 genes related to the functional subcategory “32.01.07 Unfolded protein response (e.g. ER quality control)”

Gene	1542 2h FC	padj	1542 8h FC	padj	AbfA 2h FC	padj	AbfA 8h FC	padj	BglC 2h FC	padj	BglC 8h FC	padj	Description
AN0235	-0,02	0,93	0,29	0,12	0,06	0,75	0,17	0,36	-0,09	0,67	0,24	0,20	Putative serine-threonine kinase with a predicted role in the endoplasmic reticulum (ER) unfolded protein response (UPR); ortholog of <i>S. cerevisiae</i> Ire1p; mutants are inviable and produce swollen hyphae
AN0349	0,29	0,03	0,15	0,38	-0,03	0,85	-0,25	0,08	-0,14	0,41	0,11	0,49	Ortholog(s) have role in protein refolding and mitochondrial matrix localization
AN0381	-0,01	0,96	0,01	0,98	-0,07	0,68	-0,17	0,29	-0,43	0,00	-0,18	0,27	Ortholog(s) have unfolded protein binding activity, role in protein folding and chaperonin-containing T-complex, nucleus localization
AN0429	-0,23	0,09	-0,18	0,30	-0,14	0,34	-0,21	0,17	0,17	0,31	0,11	0,53	Ortholog(s) have protein transporter activity, unfolded protein binding activity and role in protein import into mitochondrial inner membrane, protein import into mitochondrial outer membrane
AN0587	0,63	0,32	1,34	0,05	1,87	0,00	0,64	0,37	-0,12	0,89	0,81	0,25	Putative Hsp70 family chaperone; transcript is induced by nitrate
AN0847	-0,25	0,03	0,08	0,61	-0,01	0,93	0,10	0,47	-0,39	0,00	-0,11	0,43	Putative chaperone of the endoplasmic reticulum (ER) lumen
AN0866	-0,77	0,00	-0,32	0,15	-0,32	0,10	0,03	0,91	0,60	0,00	-0,25	0,25	Ortholog of <i>A. nidulans</i> FGSC A4 : AN3519, AN2646, AN0587, AN7370 and <i>A. fumigatus</i> Af293 : Afu1g15200, Afu3g03790, Afu4g14040, Afu5g06900, Afu7g08575
AN10365	0,90	0,00	0,36	0,12	0,60	0,00	0,00	1,00	-0,80	0,00	-0,28	0,21	Ortholog(s) have role in hyphal growth
AN1047	0,60	0,03	0,44	0,18	0,87	0,00	0,67	0,02	0,78	0,01	0,63	0,03	Putative heat shock protein
AN10706	0,30	0,15	0,17	0,55	0,47	0,02	0,33	0,13	0,41	0,07	0,53	0,01	Ortholog(s) have endoplasmic reticulum localization
AN10778	0,51	0,03	0,22	0,49	0,52	0,03	0,30	0,27	0,88	0,00	0,60	0,02	Ortholog(s) have mitochondrion localization
AN10994	0,27	0,17	0,17	0,48	-0,01	0,97	0,02	0,93	-0,41	0,04	-0,09	0,71	Ortholog(s) have ubiquitin-protein transferase activity, role in protein autoubiquitination, protein import into peroxisome matrix, receptor recycling, protein monoubiquitination and cytosol, nucleus, peroxisome localization
AN11163	-0,01	0,94	0,03	0,85	-0,07	0,53	-0,18	0,09	-0,24	0,02	-0,22	0,04	Has domain(s) with predicted calcium ion binding, mannosyl-oligosaccharide 1,2-alpha-mannosidase activity and membrane localization
AN1163	1,15	0,01	0,87	0,07	1,20	0,00	1,07	0,02	1,51	0,00	1,32	0,00	Putative chaperone; ortholog of <i>S. cerevisiae</i> Hsp78p; expression upregulated after exposure to farnesol
AN1282	-0,25	0,01	-0,21	0,04	0,01	0,96	-0,09	0,43	0,05	0,70	-0,07	0,55	Ortholog(s) have protein complex scaffold activity, role in posttranslational protein targeting to membrane, response to heat and TRC complex, nucleus localization
AN1296	0,09	0,75	-0,20	0,52	0,53	0,02	0,89	0,00	0,42	0,11	1,54	0,00	Ortholog(s) have 2',3'-cyclic-nucleotide 3'-phosphodiesterase activity, GTP-dependent polyribonucleotide 5'-hydroxyl-kinase activity, RNA ligase (ATP) activity
AN1358	0,03	0,79	0,28	0,01	-0,01	0,93	0,18	0,09	-0,36	0,00	0,18	0,11	Ortholog(s) have protein serine/threonine phosphatase activity and role in cellular response to osmotic stress, inactivation of MAPK activity involved in osmosensory signaling pathway, protein dephosphorylation

AN1488	0,03	0,79	0,19	0,05	-0,13	0,15	-0,04	0,71	-0,17	0,09	0,01	0,96	Putative zinc-finger protein with a predicted role in ER unfolded protein degradation
AN1510	0,55	0,06	0,08	0,86	0,46	0,13	0,12	0,76	0,36	0,29	0,06	0,88	Ortholog(s) have protein disulfide isomerase activity, protein disulfide oxidoreductase activity, thiol oxidase activity, role in oxidation-reduction process, protein folding and endoplasmic reticulum membrane localization
AN1761	0,29	0,08	0,27	0,17	0,39	0,02	0,61	0,00	0,17	0,38	0,57	0,00	Ortholog(s) have ubiquitin-protein transferase activity
AN1845	0,22	0,15	0,05	0,84	-0,02	0,93	-0,13	0,45	-0,34	0,03	-0,12	0,49	Endoplasmic reticulum packaging chaperone, required for incorporation of amino acid permeases (aspartate and proline transporters) into COPII coated vesicles for transport to the cell surface
AN1851	0,12	0,43	0,05	0,83	0,05	0,76	-0,16	0,32	-0,32	0,03	-0,24	0,12	Ortholog(s) have unfolded protein binding activity
AN1904	-0,51	0,00	-0,24	0,16	-0,36	0,01	-0,28	0,07	-0,42	0,01	-0,30	0,05	Ortholog(s) have chaperonin-containing T-complex localization
AN1933	-1,17	0,00	-0,08	0,78	-1,20	0,00	-0,18	0,44	0,16	0,52	0,21	0,36	Has domain(s) with predicted endoplasmic reticulum membrane, integral component of membrane localization
AN2051	1,08	0,00	0,59	0,11	0,98	0,00	0,53	0,13	0,52	0,16	0,72	0,04	Putative Hsp90p co-chaperone linked to a regulatory pathway that controls autophagy; protein repressed by and starvation- and rapamycin-induced autophagy
AN2062	-0,88	0,00	0,18	0,56	-0,40	0,08	0,38	0,11	-0,08	0,78	0,64	0,00	Putative ER-resident chaperone of the HSP70 family; unfolded-protein response (UPR) target gene; transcript levels increase during the UPR
AN2149	-0,25	0,06	-0,13	0,47	-0,08	0,59	-0,21	0,14	-0,34	0,02	-0,17	0,27	Putative chaperonin complex component, TCP-1 alpha subunit; ortholog of <i>S. cerevisiae</i> Tcp1p; expression reduced after exposure to farnesol
AN2238	1,03	0,00	0,34	0,44	1,03	0,00	0,49	0,20	0,74	0,04	0,70	0,06	Ortholog(s) have cytosol, nucleus localization
AN2246	-0,07	0,53	0,14	0,22	-0,04	0,75	-0,09	0,43	-0,19	0,07	0,09	0,45	Ortholog(s) have eukaryotic translation initiation factor 2alpha kinase activity, protein homodimerization activity
AN2432	0,31	0,20	0,11	0,76	0,38	0,11	0,12	0,67	1,93	0,00	1,23	0,00	Ortholog(s) have chaperone binding, unfolded protein binding activity, role in protein refolding and mitochondrial matrix localization
AN2472	-0,48	0,48	-0,69	0,37	1,18	0,06	1,11	0,08	-0,18	0,83	-0,92	0,18	Has domain(s) with predicted catalytic activity
AN2646	-0,36	0,45	0,24	0,70	-0,09	0,87	-0,31	0,54	0,58	0,23	1,40	0,00	Ortholog of <i>A. nidulans</i> FGSC A4 : AN3519, AN0587, AN0866, AN7370 and <i>A. fumigatus</i> Af293 : Afu1g15200, Afu3g03790, Afu4g14040, Afu5g06900, Afu7g08575
AN2761	0,20	0,13	0,19	0,21	0,26	0,05	0,24	0,08	-0,34	0,01	0,04	0,84	Putative ubiquitin-conjugating enzyme E2; transcript upregulated in response to camptothecin
AN2918	-0,14	0,34	-0,22	0,16	-0,19	0,20	-0,30	0,04	-0,37	0,01	-0,42	0,00	Putative chaperonin complex component, TCP-1 delta subunit; ortholog of <i>S. cerevisiae</i> Cct4p; expression reduced after exposure to farnesol
AN3070	0,00	0,99	0,01	0,97	-0,07	0,67	-0,05	0,76	-0,41	0,00	-0,16	0,30	Ortholog(s) have chaperonin-containing T-complex, nucleus localization
AN3134	-0,04	0,81	-0,12	0,50	0,03	0,87	-0,08	0,60	-0,39	0,00	-0,18	0,20	Ortholog(s) have role in cellular response to drug and chaperonin-containing T-complex, nucleus localization
AN3463	-0,39	0,00	0,08	0,57	-0,33	0,00	0,03	0,85	-0,09	0,48	0,17	0,12	Ortholog(s) have chaperone binding, sequence-specific DNA binding, unfolded protein binding activity
AN3592	-0,44	0,03	0,58	0,01	-0,24	0,29	0,28	0,22	-0,11	0,68	0,65	0,00	Putative calnexin with a predicted role in protein folding and protein quality control on the endoplasmic reticulum (ER) membrane



AN3688	-0,92	0,00	0,23	0,41	-1,31	0,00	0,07	0,81	0,03	0,92	0,10	0,74	Response regulator, part of a two-component signal transduction system involved in control of stress response and conidiation; transcript induced by hydrogen peroxide
AN3758	0,05	0,85	-0,38	0,11	-0,13	0,60	-0,45	0,04	0,13	0,63	-0,05	0,87	Ortholog(s) have unfolded protein binding activity, role in mitochondrial proton-transporting ATP synthase complex assembly and mitochondrion localization
AN4192	0,49	0,10	0,31	0,41	0,67	0,02	0,30	0,38	0,70	0,03	0,39	0,25	Ortholog(s) have cytosol localization
AN4235	-0,38	0,03	0,18	0,41	-0,67	0,00	-0,26	0,17	0,00	0,99	0,32	0,08	Ortholog(s) have Golgi apparatus, fungal-type vacuole membrane localization
AN4559	-0,38	0,04	0,04	0,89	-0,23	0,23	0,04	0,87	0,13	0,59	0,31	0,12	Ortholog(s) have mitochondrion localization
AN4583	0,87	0,01	0,42	0,29	1,11	0,00	0,54	0,12	0,92	0,01	0,71	0,04	Putative peptidyl-prolyl cis-trans isomerase D (PPIase); cyclophilin family member; protein abundance decreased by menadione stress; transcript levels increase during the unfolded-protein response (UPR) and in response to camptothecin
AN4616	-0,67	0,00	-0,35	0,13	-0,40	0,05	-0,22	0,34	-0,29	0,21	-0,27	0,24	Putative 70 kilodalton heat shock protein; protein induced by farnesol
AN4731	0,27	0,00	-0,25	0,01	-0,12	0,21	-0,55	0,00	0,03	0,82	-0,27	0,00	Ortholog(s) have role in cellular response to DNA damage stimulus, proteasome assembly, ubiquitin-dependent protein catabolic process and cytoplasm, nucleus localization
AN4753	-0,26	0,08	-0,13	0,52	-0,36	0,01	-0,35	0,02	0,50	0,00	0,23	0,15	Ortholog(s) have unfolded protein binding activity, role in aerobic respiration, mitochondrial respiratory chain complex IV assembly and integral component of membrane, mitochondrial inner membrane, plasma membrane localization
AN5129	0,79	0,01	0,64	0,05	1,24	0,00	0,88	0,00	1,29	0,00	1,04	0,00	70 kilodalton heat shock protein; protein abundance decreased by menadione stress; physically associates with importin-alpha, KapA; palA-dependent expression independent of pH; protein induced by farnesol
AN5438	0,00	0,99	0,04	0,91	0,13	0,62	0,09	0,76	-0,32	0,23	-0,03	0,93	Ortholog(s) have Hsp70 protein binding, Hsp90 protein binding activity, role in cellular response to drug, protein folding and cytosol, nucleus localization
AN5602	0,71	0,03	0,30	0,49	0,81	0,01	0,54	0,12	0,96	0,00	0,50	0,17	Ortholog(s) have ATPase activator activity, chaperone binding activity, role in protein folding, response to stress and cytosol localization
AN5713	0,03	0,82	0,06	0,75	0,09	0,49	0,10	0,46	-0,44	0,00	-0,06	0,72	Putative chaperonin complex component, TCP-1 eta subunit; ortholog of <i>S. cerevisiae</i> Cct7p; expression reduced after exposure to farnesol
AN5785	-0,70	0,00	-0,04	0,88	-0,48	0,00	0,01	0,95	-0,27	0,10	0,10	0,63	Ortholog(s) have unfolded protein binding activity
AN5954	-0,51	0,00	-0,08	0,66	-0,23	0,07	0,01	0,97	-0,40	0,00	-0,08	0,63	Protein with reduced expression after exposure to farnesol
AN6010	-0,02	0,92	0,05	0,88	0,03	0,91	-0,07	0,80	1,01	0,00	0,79	0,00	Hsp70-family protein; required for conidial germination; protein expressed at increased levels during osmoadaptation
AN6099	-0,53	0,06	-0,30	0,37	-0,45	0,11	-0,84	0,00	-0,17	0,62	0,19	0,57	Protein of unknown function
AN6170	-0,04	0,81	0,02	0,94	0,12	0,37	-0,06	0,68	-0,16	0,25	-0,02	0,90	Ortholog(s) have chaperone binding activity, role in ER-associated ubiquitin-dependent protein catabolic process, protein folding in endoplasmic reticulum, response to unfolded protein and endoplasmic reticulum lumen localization

AN6248	-0,57	0,00	-0,22	0,35	-0,31	0,10	-0,19	0,37	0,55	0,00	0,61	0,00	Ortholog(s) have adenylyl-nucleotide exchange factor activity, role in protein import into mitochondrial matrix, protein refolding and mitochondrial matrix, presequence translocase-associated import motor localization
AN6531	-0,07	0,70	0,06	0,80	-0,21	0,17	-0,11	0,52	-0,37	0,02	-0,10	0,58	Putative Sec1p-like protein with a predicted role in vacuolar protein sorting
AN6593	0,22	0,22	0,03	0,91	-0,19	0,31	-0,42	0,02	0,60	0,00	-0,01	0,97	Ortholog(s) have unfolded protein binding activity, role in aerobic respiration, mitochondrial respiratory chain complex IV assembly and integral component of mitochondrial inner membrane, plasma membrane localization
AN6630	-0,28	0,16	0,26	0,27	-0,05	0,82	0,21	0,32	-0,29	0,17	0,23	0,31	Putative nascent polypeptide-associated complex subunit alpha; induced by rapamycin-induced autophagy
AN6796	0,36	0,44	-0,38	0,49	0,13	0,80	-0,32	0,52	0,01	0,98	0,19	0,75	Ortholog(s) have intracellular localization
AN7143	-0,56	0,01	-0,27	0,30	-0,20	0,39	-0,06	0,82	-0,27	0,27	-0,34	0,15	Ortholog(s) have cytosol localization
AN7254	0,32	0,02	0,20	0,23	0,55	0,00	0,43	0,00	0,47	0,00	0,35	0,02	Protein with a conserved CDC48, cell division protein N-terminal domain and two ATPase domains of the AAA-superfamily; protein expressed at increased levels during osmoadaptation; protein induced by farnesol
AN7321	0,41	0,11	0,32	0,31	0,65	0,01	0,60	0,02	0,33	0,26	0,15	0,65	Ortholog(s) have eukaryotic translation initiation factor 2alpha kinase activity, role in negative regulation of translational initiation in response to osmotic stress, protein phosphorylation and cytosol localization
AN7370	-0,48	0,27	0,24	0,69	-0,24	0,61	-0,05	0,94	-0,24	0,65	0,67	0,14	Ortholog of <i>A. nidulans</i> FGSC A4 : AN3519, AN2646, AN0587, AN0866 and <i>A. fumigatus</i> Af293 : Afu1g15200, Afu3g03790, Afu4g14040, Afu5g06900, Afu7g08575
AN7649	-0,31	0,05	-0,35	0,04	-0,30	0,06	-0,35	0,03	0,31	0,06	0,06	0,78	Ortholog(s) have protein transporter activity, unfolded protein binding activity and role in protein import into mitochondrial inner membrane, protein import into mitochondrial outer membrane, regulation of growth rate
AN8035	0,40	0,00	0,02	0,91	0,30	0,01	-0,12	0,37	-0,02	0,92	-0,20	0,11	Putative transcription factor; hsf1 mRNA expression increased in the presence of farnesol
AN8253	-0,87	0,00	0,00	1,00	-0,70	0,00	0,11	0,67	-0,42	0,04	-0,05	0,87	Ortholog(s) have cytosol, nucleus localization
AN8269	0,66	0,03	0,71	0,03	0,96	0,00	0,68	0,03	1,14	0,00	0,95	0,00	90 kilodalton heat shock protein; physically associates with importin-alpha, KapA; palA-dependent expression independent of pH
AN8702	0,02	0,91	-0,10	0,66	0,00	0,99	-0,14	0,45	-0,22	0,22	-0,13	0,49	Ortholog(s) have protein homodimerization activity, ubiquitin-protein transferase activity and role in UV-damage excision repair, free ubiquitin chain polymerization, postreplication repair, protein K63-linked ubiquitination
AN9062	-0,07	0,74	-0,17	0,42	-0,30	0,08	-0,07	0,74	0,30	0,10	0,03	0,91	Ortholog(s) have protein domain specific binding activity, role in mitochondrial proton-transporting ATP synthase complex assembly and mitochondrion localization
AN9124	0,85	0,00	0,42	0,24	0,84	0,00	0,46	0,16	1,06	0,00	0,74	0,02	Ortholog(s) have ATPase inhibitor activity, Hsp70 protein binding, Hsp90 protein binding, mRNA binding activity, role in protein folding and cytosol, nucleus localization
AN9397	-1,45	0,00	-0,46	0,18	-1,37	0,00	0,00	1,00	0,70	0,02	0,09	0,83	Putative basic leucine zipper (bZIP) transcription factor that regulates the unfolded protein response; hacA mRNA expression increased in the presence of farnesol

**Table S2.** 15 differentially expressed genes in the functional subcategory “32.01.07 Unfolded protein response (e.g. ER quality control)”

AspGD	Strain	Regulation	Response	Name	Description in AspGD	Orthologs and best hit in <i>S. cerevisiae</i>	Description Saccharomyces Genome Database
AN0587	AbfA 2h	up	early (AbfA)		Putative Hsp70 family chaperone; transcript is induced by nitrate		
AN1163	1542 and AbfA 2h; BglC 2 and 8h	up	early (AbfA and 1542); continuous (BglC)		Putative chaperone; ortholog of <i>S. cerevisiae</i> Hsp78p; expression upregulated after exposure to farnesol	HSP78	Oligomeric mitochondrial matrix chaperone; cooperates with Ssc1p in mitochondrial thermotolerance after heat shock; able to prevent the aggregation of misfolded proteins as well as resolubilize protein aggregates
AN1296	BglC 8h	up	late (BglC)		Ortholog(s) have 2',3'-cyclic-nucleotide 3'-phosphodiesterase activity, GTP-dependent polyribonucleotide 5'-hydroxyl-kinase activity, RNA ligase (ATP) activity	TRL1	tRNA ligase; required for tRNA splicing and for both splicing and translation of HAC1 mRNA in the UPR; has phosphodiesterase, polynucleotide kinase, and ligase activities; localized at the inner nuclear envelope and partially to polysomes
AN1933	1542 and AbfA 2h	down	early (AbfA and 1542)		Has domain(s) with predicted endoplasmic reticulum membrane, integral component of membrane localization	ORM1	Protein that mediates sphingolipid homeostasis; evolutionarily conserved, required for resistance to agents that induce unfolded protein response; Orm1p and Orm2p together control membrane biogenesis by coordinating lipid homeostasis with protein quality control; ORM1 has a paralog, ORM2, that arose from the whole genome duplication
AN2051	1542 2h	up	early (1542)	cdc37	Putative Hsp90p co-chaperone linked to a regulatory pathway that controls autophagy; protein repressed by and starvation- and rapamycin-induced autophagy	CDC37	Essential Hsp90p co-chaperone; necessary for passage through the START phase of the cell cycle; stabilizes protein kinase nascent chains and participates along with Hsp90p in their folding
AN2238	1542 and AbfA 2h	up	early (AbfA and 1542)		Ortholog(s) have cytosol, nucleus localization	SIS1	Type II HSP40 co-chaperone that interacts with the HSP70 protein Ssa1p; shuttles between cytosol and nucleus; mediates delivery of misfolded proteins into the nucleus for degradation; involved in proteasomal degradation of misfolded cytosolic proteins; protein abundance increases in response to DNA replication stress; polyQ aggregates sequester Sis1p and interfere with clearance of misfolded proteins; similar to bacterial DnaJ proteins and mammalian DnaJB1

<b>AN2432</b>	BglC 2 and 8h	up	continuous (BglC)		Ortholog(s) have chaperone binding, unfolded protein binding activity, role in chaperone-mediated protein complex assembly, protein import into mitochondrial intermembrane space, protein refolding and mitochondrial matrix localization	HSP10	Mitochondrial matrix co-chaperonin; inhibits the ATPase activity of Hsp60p, a mitochondrial chaperonin; involved in protein folding and sorting in the mitochondria; 10 kD heat shock protein with similarity to <i>E. coli</i> groES
<b>AN2646</b>	BglC 8h	up	late (BglC)		Ortholog of <i>A. nidulans</i> FGSC A4 : AN3519, AN0587, AN0866, AN7370 and <i>A. fumigatus</i> Af293 : Afu1g15200, Afu3g03790, Afu4g14040, Afu5g06900, Afu7g08575	SSB1	Cytoplasmic ATPase that is a ribosome-associated molecular chaperone; functions with J-protein partner Zuo1p; may be involved in folding of newly-made polypeptide chains; member of the HSP70 family; interacts with phosphatase subunit Reg1p; SSB1 has a paralog, SSB2, that arose from the whole genome duplication
<b>AN3688</b>	AbfA 2h	down	early (AbfA)	srrA	Response regulator, part of a two-component signal transduction system involved in control of stress response and conidiation; transcript induced by hydrogen peroxide	SKN7	Nuclear response regulator and transcription factor; physically interacts with the Tup1-Cyc8 complex and recruits Tup1p to its targets; part of a branched two-component signaling system; required for optimal induction of heat-shock genes in response to oxidative stress; involved in osmoregulation; relocates to the cytosol in response to hypoxia; SKN7 has a paralog, HMS2, that arose from the whole genome duplication
<b>AN4583</b>	AbfA 2h	up	early (AbfA)	cyp7	Putative peptidyl-prolyl cis-trans isomerase D (PPIase); cyclophilin family member; protein abundance decreased by menadione stress; transcript levels increase during the unfolded-protein response (UPR) and in response to camptothecin	CPR6	Peptidyl-prolyl cis-trans isomerase (cyclophilin); catalyzes the cis-trans isomerization of peptide bonds N-terminal to proline residues; plays a role in determining prion variants; binds to Hsp82p and contributes to chaperone activity; protein abundance increases in response to DNA replication stress
<b>AN5129</b>	AbfA 2h, BglC 2 and 8h	up	early (AbfA); continuous (BglC)	hsp70	70 kilodalton heat shock protein; protein abundance decreased by menadione stress; physically associates with importin-alpha, KapA; palA-dependent expression independent of pH; protein induced by farnesol	SSA1	ATPase involved in protein folding and NLS-directed nuclear transport; member of HSP70 family; required for ubiquitin-dependent degradation of short-lived proteins; forms chaperone complex with Ydj1p; localized to nucleus, cytoplasm, cell wall; 98% identical to paralog Ssa2p with different functional specificity in propagation of yeast [URE3] prions, vacuolar-mediated degradations of gluconeogenesis enzymes; general targeting factor of Hsp104p to prion fibrils
<b>AN6010</b>	BglC 2h	up	early (BglC)	sgdE	Hsp70-family protein; required for conidial germination; protein expressed at increased levels during osmoadaptation	SSC1	Hsp70 family ATPase; constituent of the import motor component of the Translocase of the Inner Mitochondrial membrane (TIM23 complex); involved in protein translocation and folding; subunit of SceI endonuclease; SSC1 has a paralog, ECM10, that arose from the whole genome duplication

<b>AN8269</b>	BglC 2h	up	early (BglC)	hsp90	90 kilodalton heat shock protein; physically associates with importin-alpha, KapA; palA-dependent expression independent of pH	HSC82	Cytoplasmic chaperone of the Hsp90 family; plays a role in determining prion variants; redundant in function and nearly identical with Hsp82p, and together they are essential; expressed constitutively at 10-fold higher basal levels than HSP82 and induced 2-3 fold by heat shock; contains two acid-rich unstructured regions that promote the solubility of chaperone-substrate complexes; HSC82 has a paralog, HSP82, that arose from the whole genome duplication
<b>AN9124</b>	BglC 2h	up	early (BglC)		Ortholog(s) have ATPase inhibitor activity, Hsp70 protein binding, Hsp90 protein binding, mRNA binding activity, role in protein folding, protein localization and cytosol, nucleus localization	STI1	Hsp90 cochaperone; regulates spatial organization of amyloid-like proteins in the cytosol, thereby buffering the proteotoxicity caused by amyloid-like proteins; interacts with the Ssa group of the cytosolic Hsp70 chaperones and activates Ssa1p ATPase activity; interacts with Hsp90 chaperones and inhibits their ATPase activity; homolog of mammalian Hop
<b>AN9397</b>	1542 and AbfA 2h	down	early (AbfA and 1542)	hacA	Putative basic leucine zipper (bZIP) transcription factor that regulates the unfolded protein response; hacA mRNA expression increased in the presence of farnesol	HAC1	Basic leucine zipper (bZIP) transcription factor (ATF/CREB1 homolog); regulates the unfolded protein response, via UPRE binding, and membrane biogenesis; ER stress-induced splicing pathway facilitates efficient Hac1p synthesis; two functional forms of Hac1p are produced; translation initiation is repressed under non-stress conditions; protein abundance increases in response to DNA replication stress

**Table S3.** 354 genes related to “14.13 Protein/peptide degradation”.

Gene	1542 2h FC	padj	1542 8h FC	padj	AbfA 2h FC	padj	AbfA 8h FC	padj	BglC 2h FC	padj	BglC 8h FC	padj	Description
AN0030	0,36	0,52	0,32	0,64	0,13	0,82	0,28	0,65	0,26	0,69	-0,09	0,90	Has domain(s) with predicted hydrolase activity
AN0084	0,36	0,00	-0,04	0,84	0,19	0,13	-0,05	0,77	-0,33	0,01	-0,17	0,20	Ortholog(s) have Ran GTPase binding activity and role in G1/S transition of mitotic cell cycle, RNA export from nucleus, Ran protein signal transduction, protein import into nucleus, ubiquitin-dependent protein catabolic process
AN0122	0,18	0,53	0,35	0,26	0,15	0,62	0,35	0,22	-0,53	0,05	0,21	0,50	Has domain(s) with predicted ATP binding, ATP-dependent peptidase activity, nucleoside-triphosphatase activity, nucleotide binding, serine-type endopeptidase activity and role in protein catabolic process, proteolysis
AN0139	-0,40	0,29	-0,27	0,59	-0,34	0,38	-0,13	0,79	0,11	0,83	0,27	0,55	Putative asparaginase with a predicted role in asparagine metabolism
AN0224	0,51	0,00	0,01	0,97	0,00	0,99	-0,66	0,00	-0,56	0,00	-0,70	0,00	Ortholog(s) have Golgi apparatus, cytosol, nucleus localization
AN0226	-0,24	0,33	0,37	0,16	-0,31	0,20	0,75	0,00	0,35	0,18	0,98	0,00	Ortholog(s) have protein homodimerization activity, ubiquitin-protein transferase activity
AN0256	0,46	0,02	0,12	0,69	0,29	0,16	0,04	0,90	-0,65	0,00	-0,56	0,01	Predicted calpain-like cysteine protease involved in a signaling pathway that activates PacC transcription factor in response to alkaline ambient pH
AN0261	-0,25	0,01	-0,01	0,93	-0,25	0,01	-0,21	0,05	-0,30	0,00	-0,04	0,76	COPII coat component; considered a prototypic marker of transitional ER (endoplasmic reticulum); localizes to a cytosolic haze and to numerous small foci that predominate near the hyphal tips
AN0295	-0,22	0,10	-0,40	0,00	0,10	0,49	-0,26	0,06	0,28	0,05	-0,06	0,75	Ortholog(s) have role in ER-associated misfolded protein catabolic process and cytoplasm-associated proteasomal ubiquitin-dependent protein catabolic process, more
AN0329	-0,02	0,89	-0,22	0,15	0,26	0,05	-0,07	0,69	0,11	0,49	0,01	0,96	Ortholog(s) have polyubiquitin binding activity
AN0349	0,29	0,03	0,15	0,38	-0,03	0,85	-0,25	0,08	-0,14	0,41	0,11	0,49	Ortholog(s) have role in protein refolding and mitochondrial matrix localization
AN0369	0,81	0,00	0,34	0,20	0,83	0,00	0,33	0,18	0,23	0,41	0,06	0,86	Has domain(s) with predicted aminopeptidase activity, metalloexopeptidase activity and role in cellular process, proteolysis
AN0444	-1,01	0,00	-0,16	0,52	-0,96	0,00	-0,20	0,37	0,52	0,01	0,26	0,22	Putative HECT ubiquitin ligase
AN0482	2,07	0,00	-0,08	0,90	1,98	0,00	0,14	0,80	0,28	0,62	-0,27	0,63	Putative ubiquitin-conjugating enzyme; transcript repressed by nitrate
AN0551	0,02	0,95	0,71	0,01	-0,17	0,56	0,01	0,97	-0,54	0,05	0,41	0,15	Putative mannosyl-oligosaccharide 1,2-alpha-mannosidase with a predicted role in mannose polymer metabolism
AN0573	0,30	0,13	0,26	0,27	0,45	0,02	0,65	0,00	0,57	0,00	0,76	0,00	Has domain(s) with predicted Rab GTPase activator activity, role in regulation of Rab GTPase activity and intracellular localization
AN0686	-0,08	0,51	-0,11	0,47	-0,11	0,36	-0,14	0,28	0,41	0,00	0,25	0,04	Ortholog(s) have role in inner mitochondrial membrane organization, mitochondrion inheritance, mitochondrion morphogenesis, negative regulation of proteolysis, protein folding, replicative cell aging
AN0709	-1,05	0,00	0,37	0,23	-0,54	0,04	0,89	0,00	0,47	0,09	0,88	0,00	Putative zinc-finger protein; expression upregulated after exposure to farnesol
AN0770	0,29	0,01	-0,41	0,00	0,11	0,39	-0,51	0,00	-0,01	0,94	-0,33	0,00	Ortholog(s) have Dsc E3 ubiquitin ligase complex, endoplasmic reticulum localization

AN0788	0,25	0,24	0,14	0,63	0,06	0,80	0,11	0,66	-0,14	0,59	-0,11	0,69	Ortholog of <i>A. niger</i> CBS 513.88 : An09g02430, An03g05960, An09g00710, An09g00820, An09g01710 and <i>A. oryzae</i> RIB40 : AO090005000954, AO090003000250, AO090012000369, AO090010000570, AO090023000882, AO090120000022, AO090012000900
AN0810	-0,02	0,86	0,12	0,20	-0,01	0,95	-0,12	0,19	-0,12	0,20	0,08	0,36	Protein with a predicted role in ER-associated protein degradation
AN0814	0,50	0,00	-0,27	0,16	0,67	0,00	-0,76	0,00	0,17	0,41	-0,30	0,09	Activator of anaphase-promoting complex involved in mitotic spindle assembly checkpoint and regulation of mitotic metaphase/anaphase transition
AN0832	-0,26	0,07	-0,33	0,03	-0,05	0,79	-0,28	0,06	0,13	0,45	-0,08	0,65	Has domain(s) with predicted aminopeptidase activity, manganese ion binding activity and role in cellular process
AN0848	0,22	0,14	0,14	0,44	0,13	0,43	-0,10	0,56	-0,33	0,03	0,02	0,93	Ortholog(s) have role in mitochondrial genome maintenance, plasmid maintenance and cytosol, mitochondrion localization
AN0858	1,07	0,00	0,97	0,01	1,26	0,00	1,10	0,00	1,22	0,00	0,96	0,01	Putative chaperone
AN0871	0,22	0,29	-0,28	0,22	0,31	0,11	-0,08	0,76	-0,30	0,16	-0,18	0,46	Ortholog(s) have GPI-anchor transamidase activity, role in attachment of GPI anchor to protein and GPI-anchor transamidase complex localization
AN0911	0,09	0,63	0,09	0,70	-0,15	0,39	-0,12	0,55	-0,49	0,00	-0,17	0,36	Ortholog of <i>A. fumigatus</i> Af293 : Afu1g15770, <i>A. niger</i> CBS 513.88 : An01g14120, <i>A. oryzae</i> RIB40 : AO090005001123, <i>Aspergillus wentii</i> : Aspwe1_0039951 and <i>Aspergillus sydowii</i> : Aspsy1_0267314
AN0927	-0,17	0,37	-1,00	0,00	0,15	0,44	-0,97	0,00	0,21	0,32	-0,80	0,00	Ortholog(s) have ubiquitin-specific protease activity, role in cellular response to drug, protein deubiquitination and nuclear periphery, proteasome complex localization
AN1019	-0,02	0,93	-0,04	0,89	0,12	0,52	0,16	0,39	-0,01	0,97	0,03	0,89	Putative Scf complex protein; NeddH-associated protein; transcript upregulated in response to camptothecin
AN1058	0,28	0,27	-0,45	0,10	0,22	0,40	-0,97	0,00	0,31	0,26	-0,10	0,77	Ortholog of <i>A. fumigatus</i> Af293 : Afu1g12350, <i>A. oryzae</i> RIB40 : AO090001000294, <i>Aspergillus wentii</i> : Aspwe1_0172072, <i>Aspergillus sydowii</i> : Aspsy1_0053315 and <i>Aspergillus terreus</i> NIH2624 : ATET_00433
AN1159	-0,28	0,08	-0,25	0,14	-0,17	0,30	-0,43	0,00	0,61	0,00	-0,20	0,24	Has domain(s) with predicted acid-amino acid ligase activity
AN1163	1,15	0,01	0,87	0,07	1,20	0,00	1,07	0,02	1,51	0,00	1,32	0,00	Putative chaperone; ortholog of <i>S. cerevisiae</i> Hsp78p; expression upregulated after exposure to farnesol
AN1179	-0,01	0,97	0,28	0,20	-0,08	0,71	0,55	0,00	0,39	0,05	0,66	0,00	Protein with a predicted role in negative regulation of gluconeogenesis and protein targeting to vacuole; protein is translationally repressed by the conserved upstream open reading frame (uORF) AN1179-uORF
AN1184	-0,06	0,89	0,83	0,03	0,35	0,36	0,74	0,06	-0,26	0,58	0,24	0,62	Ortholog(s) have ribosome localization
AN1209	0,37	0,01	0,27	0,08	0,20	0,15	0,15	0,33	-0,03	0,89	0,10	0,55	Ortholog(s) have role in proteasome regulatory particle assembly, proteolysis and cytosol, nucleus, proteasome regulatory particle localization
AN1339	-0,53	0,00	-0,05	0,83	-0,41	0,00	0,15	0,37	0,29	0,06	0,21	0,20	Putative HECT ubiquitin ligase
AN1372	-0,33	0,03	-0,22	0,22	-0,35	0,02	-0,40	0,01	0,28	0,08	0,40	0,01	Has domain(s) with predicted serine-type endopeptidase activity, role in proteolysis and integral component of membrane localization
AN1426	-0,42	0,32	-1,48	0,00	0,33	0,45	-1,18	0,00	-0,06	0,92	0,00	1,00	Ortholog(s) have serine-type carboxypeptidase activity
AN1488	0,03	0,79	0,19	0,05	-0,13	0,15	-0,04	0,71	-0,17	0,09	0,01	0,96	Putative zinc-finger protein with a predicted role in ER unfolded protein degradation
AN1491	0,30	0,07	-0,16	0,42	0,16	0,38	-0,28	0,11	-0,28	0,13	-0,34	0,04	Subunit 1 of the COP9 signalosome; metalloprotease that binds zinc ions by its conserved JAMM motif; required for formation of cleistothecia; mutants produce aberrant red color within distinct hyphae; NeddH-associated protein

AN1539	0,53	0,00	0,05	0,87	0,37	0,05	-0,16	0,46	-0,40	0,05	-0,37	0,06	Subunit 4 of the COP9 signalosome; required for light-dependent asexual and sexual development and cleistothecia production; regulates secondary metabolite production, mutant hyphae are aberrant with abnormal red pigmentation
AN1573	-0,01	0,98	0,15	0,57	0,15	0,51	0,24	0,29	0,09	0,73	0,24	0,30	Putative aspartic-type protease; predicted glycosylphosphatidylinositol (GPI)-anchored protein
AN1632	0,45	0,06	0,24	0,45	0,57	0,02	0,79	0,00	0,21	0,49	0,51	0,05	Ortholog(s) have protein serine/threonine kinase activity
AN1638	0,59	0,00	-0,08	0,75	0,49	0,01	-0,12	0,58	-0,20	0,35	-0,07	0,76	Ortholog(s) have metalloaminopeptidase activity, serine-type peptidase activity, role in peptide catabolic process, proteolysis and cell wall-bounded periplasmic space, cytosol, fungal-type cell wall, glyoxysome, mitochondrion localization
AN1658	-0,10	0,74	0,35	0,29	-0,75	0,00	-0,10	0,78	-0,32	0,32	-0,01	0,99	Has domain(s) with predicted zinc ion binding activity
AN1700	-0,08	0,28	0,00	1,00	-0,05	0,49	-0,14	0,05	0,06	0,51	0,03	0,74	Putative 26S proteasome regulatory subunit; transcript upregulated in response to camptothecin
AN1706	-0,21	0,09	-0,26	0,06	-0,24	0,06	-0,34	0,01	0,20	0,16	-0,07	0,65	Has domain(s) with predicted peptidase activity and role in proteolysis
AN1742	0,84	0,00	0,83	0,00	0,59	0,02	0,74	0,00	0,05	0,90	0,22	0,47	Putative beta-1,4-mannosidase with a predicted role in polysaccharide degradation
AN1746	-0,33	0,00	0,30	0,00	-0,28	0,00	0,35	0,00	-0,22	0,01	0,24	0,00	Putative HECT ubiquitin ligase
AN1757	0,15	0,33	-0,26	0,13	0,07	0,69	-0,36	0,02	-0,08	0,69	-0,29	0,07	Predicted alpha 3 subunit of the 20S core proteasome; involved in N-myristoylation and cell morphogenesis
AN1760	-0,03	0,92	-0,09	0,75	0,07	0,76	0,18	0,43	0,18	0,45	0,23	0,33	Ortholog(s) have role in ascospore formation, autophagy, cellular response to nitrogen starvation and cytosol, nucleus localization
AN1761	0,29	0,08	0,27	0,17	0,39	0,02	0,61	0,00	0,17	0,38	0,57	0,00	Ortholog(s) have ubiquitin-protein transferase activity
AN1780	-0,25	0,08	-0,22	0,19	-0,54	0,00	-0,53	0,00	0,20	0,23	-0,28	0,06	Ortholog(s) have aminopeptidase activity, role in protein processing, protein stabilization and extrinsic component of mitochondrial inner membrane, nucleus localization
AN1850	0,23	0,07	-0,12	0,45	0,01	0,95	-0,30	0,02	0,79	0,00	0,44	0,00	Ortholog(s) have metalloendopeptidase activity, role in misfolded or incompletely synthesized protein catabolic process and mitochondrial inner membrane localization
AN1857	1,63	0,00	0,93	0,03	1,35	0,00	1,21	0,00	0,02	0,97	-0,05	0,94	Putative kynureninase with a predicted role in aromatic amino acid biosynthesis
AN1874	-0,02	0,93	0,01	0,98	-0,17	0,26	0,04	0,82	0,04	0,84	0,03	0,89	Putative HECT ubiquitin ligase
AN1875	-0,21	0,18	-0,24	0,17	-0,10	0,56	0,15	0,40	-0,19	0,27	-0,20	0,24	Ortholog(s) have sequence-specific DNA binding activity and role in budding cell bud growth, mitotic cell cycle, nucleocytoplasmic transport, ribosomal large subunit biogenesis
AN1879	0,04	0,82	0,12	0,48	-0,20	0,14	0,19	0,18	0,24	0,08	0,33	0,01	Ortholog(s) have gamma-glutamyltransferase activity, omega peptidase activity, role in glutathione catabolic process and cytoplasm, nucleus localization
AN1904	-0,51	0,00	-0,24	0,16	-0,36	0,01	-0,28	0,07	-0,42	0,01	-0,30	0,05	Ortholog(s) have chaperonin-containing T-complex localization
AN1922	0,04	0,79	-0,12	0,36	0,08	0,51	-0,21	0,06	-0,09	0,52	-0,23	0,04	Ortholog(s) have structural molecule activity
AN1966	-0,11	0,38	0,58	0,00	-0,02	0,87	0,59	0,00	0,05	0,75	0,59	0,00	Putative HECT ubiquitin ligase
AN1982	1,19	0,00	0,37	0,27	1,09	0,00	0,74	0,01	0,63	0,03	0,53	0,07	Ortholog of <i>A. nidulans</i> FGSC A4 : AN0814, <i>A. fumigatus</i> Af293 : Afu1g14730, Afu4g10570, <i>A. niger</i> CBS 513.88 : An04g06100, An01g12750 and <i>A. oryzae</i> RIB40 : AO090003001154, AO090003000500
AN2000	0,76	0,01	0,26	0,49	1,03	0,00	0,54	0,07	0,93	0,00	0,59	0,05	Polyubiquitin, contains four head to tail repeats of ubiquitin; transcript upregulated in response to camptothecin



AN2045	-0,41	0,04	-1,06	0,00	-0,40	0,05	-0,93	0,00	-0,03	0,93	-0,61	0,00	Has domain(s) with predicted calcium ion binding, mannosyl-oligosaccharide 1,2-alpha-mannosidase activity and membrane localization
AN2065	0,11	0,29	0,18	0,10	-0,10	0,34	-0,10	0,38	-0,32	0,00	-0,23	0,02	Putative deadenylase with a predicted role in RNA processing
AN2072	-0,08	0,65	-0,10	0,66	-0,21	0,20	-0,23	0,18	-0,05	0,84	-0,17	0,34	Putative ubiquitin-specific protease; ortholog of <i>S. cerevisiae</i> Doa4p
AN2073	0,11	0,54	0,04	0,89	-0,14	0,46	-0,07	0,76	-0,11	0,59	-0,13	0,53	Ortholog(s) have Cul3-RING ubiquitin ligase complex localization
AN2082	0,34	0,02	0,07	0,74	0,22	0,16	-0,09	0,63	-0,12	0,55	-0,07	0,72	Ortholog of <i>A. fumigatus</i> Af293 : Afu2g04840, <i>A. niger</i> CBS 513.88 : An11g04530, <i>A. oryzae</i> RIB40 : AO090003000287, <i>Aspergillus wentii</i> : Aspwe1_0120888 and <i>Aspergillus sydowii</i> : Aspsy1_0127836
AN2085	0,31	0,02	-0,20	0,19	0,29	0,03	-0,25	0,07	-0,17	0,29	-0,33	0,01	Ortholog(s) have endopeptidase activity and role in proteasomal ubiquitin-independent protein catabolic process, proteasome-mediated ubiquitin-dependent protein catabolic process
AN2092	0,13	0,36	-0,25	0,08	0,13	0,37	-0,27	0,04	-0,29	0,03	-0,38	0,00	Putative prolyl aminopeptidase, an enzyme known to remove N-terminal proline and hydroxyproline residues from peptides
AN2129	0,58	0,00	-0,11	0,68	0,52	0,01	-0,14	0,54	-0,41	0,06	-0,28	0,20	Subunit 5 of the COP9 signalosome (CSN) responsible for cleaving the ubiquitin-like protein Nedd8 from cullin-RING E3 ubiquitin ligases; required for normal cleistothecia development; mutants impaired in secondary metabolism
AN2149	-0,25	0,06	-0,13	0,47	-0,08	0,59	-0,21	0,14	-0,34	0,02	-0,17	0,27	Putative chaperonin complex component, TCP-1 alpha subunit; ortholog of <i>S. cerevisiae</i> Tcp1p; expression reduced after exposure to farnesol
AN2157	-0,71	0,00	0,13	0,48	-0,60	0,00	-0,34	0,02	-0,42	0,00	0,52	0,00	Putative aspartic endopeptidase
AN2194	-0,99	0,00	-0,36	0,25	-0,21	0,46	-0,72	0,01	0,20	0,53	0,21	0,50	Has domain(s) with predicted serine-type endopeptidase activity and role in proteolysis
AN2212	0,32	0,04	0,13	0,55	0,38	0,01	0,27	0,10	-0,04	0,86	-0,03	0,91	Putative ubiquitin-conjugating enzyme; transcript upregulated in response to camptothecin
AN2213	0,12	0,32	-0,10	0,49	0,10	0,40	-0,15	0,24	0,20	0,11	-0,04	0,79	Ortholog(s) have ATPase activity and role in peptide catabolic process, positive regulation of protein catabolic process, proteasome regulatory particle assembly, proteasome-mediated ubiquitin-dependent protein catabolic process
AN2233	0,57	0,00	-0,16	0,50	0,37	0,05	-0,34	0,07	-0,48	0,01	-0,46	0,01	Subunit 6 of the COP9 signalosome; required for formation of cleistothecia
AN2237	0,07	0,85	-0,68	0,04	-0,06	0,88	-0,83	0,01	0,25	0,51	0,41	0,24	Putative carboxypeptidase C; induced by carbon starvation-induced autophagy
AN2246	-0,07	0,53	0,14	0,22	-0,04	0,75	-0,09	0,43	-0,19	0,07	0,09	0,45	Ortholog(s) have eukaryotic translation initiation factor 2alpha kinase activity, protein homodimerization activity
AN2298	0,11	0,46	0,07	0,71	-0,02	0,89	-0,18	0,22	-0,49	0,00	-0,21	0,14	SumO activating (E1) enzyme
AN2302	-0,26	0,04	-0,05	0,78	-0,32	0,01	-0,19	0,17	0,00	0,98	0,04	0,84	Skp1-related protein with a predicted role in sulfur metabolism; regulated by sulfur metabolite repression; NeddH-associated protein
AN2304	0,39	0,01	0,03	0,91	0,46	0,00	-0,02	0,95	-0,28	0,11	0,03	0,90	Ortholog(s) have ubiquitin binding activity, role in negative regulation of protein catabolic process, nucleotide-excision repair, protein ubiquitination and cytosol, nuclear envelope localization
AN2366	-0,58	0,07	-1,58	0,00	-0,25	0,48	-1,40	0,00	0,55	0,12	-0,19	0,64	Putative trypsin-like protease with a role in the proteolytic cleavage of NmrA
AN2413	-0,24	0,34	0,15	0,64	-0,27	0,26	0,34	0,18	0,08	0,80	0,43	0,08	Has domain(s) with predicted acid-amino acid ligase activity
AN2416	0,00	0,99	0,07	0,75	-0,02	0,89	-0,17	0,30	-0,15	0,38	-0,11	0,53	Putative ubiquitin-activating enzyme; NeddH-associated protein; transcript upregulated in response to camptothecin

AN2421	0,34	0,27	0,06	0,89	-0,24	0,46	-0,26	0,44	0,24	0,50	0,35	0,29	Putative C2H2 zinc finger transcription factor; involved in regulation of conidiophore development; required for light-dependent activation of brlA transcription
AN2441	0,54	0,00	-0,31	0,07	0,49	0,00	-0,28	0,09	-0,23	0,20	-0,50	0,00	Putative E1 Neddh/Nedd8-activating enzyme
AN2442	0,01	0,94	0,25	0,11	-0,21	0,13	0,06	0,72	-0,28	0,06	0,09	0,62	Ortholog of <i>A. fumigatus</i> Af293 : Afu6g10590, <i>A. niger</i> CBS 513.88 : An11g00690, <i>A. oryzae</i> RIB40 : AO090023000215, <i>Aspergillus wentii</i> : Aspwe1_0039416 and <i>Aspergillus sydowii</i> : Aspsy1_0141765
AN2450	-0,12	0,35	-0,08	0,65	0,02	0,88	-0,25	0,05	-0,03	0,85	-0,01	0,96	SumO activating (E1) enzyme
AN2503	0,60	0,00	-0,06	0,86	0,47	0,03	-0,18	0,48	-0,43	0,07	-0,95	0,00	Ortholog(s) have role in response to endoplasmic reticulum stress
AN2513	0,80	0,00	0,29	0,17	0,64	0,00	0,29	0,14	-0,90	0,00	-0,08	0,76	Putative component of the EKC/KEOPS complex; interacts with PtkA, cyclin-dependent kinase, in metulae, phialides and conidia; essential; involved in hyphal growth and asexual development
AN2521	0,41	0,04	0,11	0,68	0,10	0,65	-0,05	0,85	-0,44	0,04	-0,23	0,30	ESCRT I complex required for trafficking from the membrane to the vacuoles targeting to vacuole; essential for pH signaling; mutants exhibit fragmented vacuoles
AN2555	1,43	0,00	-0,09	0,88	0,99	0,01	-0,16	0,75	1,44	0,00	0,51	0,27	Ortholog(s) have serine-type carboxypeptidase activity
AN2572	-0,08	0,86	-0,49	0,28	0,50	0,20	-0,40	0,35	0,85	0,03	0,39	0,39	Putative dipeptidyl-peptidase; transcript upregulated by nitrate limitation
AN2689	0,48	0,01	0,06	0,79	0,29	0,11	-0,25	0,18	-0,04	0,88	-0,38	0,03	SUMO-specific isopeptidase
AN2761	0,20	0,13	0,19	0,21	0,26	0,05	0,24	0,08	-0,34	0,01	0,04	0,84	Putative ubiquitin-conjugating enzyme E2; transcript upregulated in response to camptothecin
AN2772	-0,36	0,02	-0,11	0,59	-0,18	0,27	-0,19	0,29	-0,19	0,30	-0,11	0,59	Component of the Anaphase-Promoting Complex/Cyclosome (APC/C), which is a ubiquitin ligase required for cell cycle progression; negative regulator of mitosis
AN2810	0,37	0,07	-0,13	0,65	0,47	0,02	-0,30	0,19	-0,66	0,00	-0,77	0,00	Ortholog(s) have metallopeptidase activity
AN2861	-0,96	0,00	-0,01	0,99	-1,11	0,00	0,25	0,47	0,46	0,17	0,29	0,42	Putative F-box protein
AN2874	-0,53	0,19	-0,08	0,90	0,00	0,99	-0,33	0,48	0,15	0,78	-0,34	0,48	Protein of unknown function
AN2903	0,29	0,05	-0,05	0,82	0,20	0,20	-0,06	0,76	0,06	0,77	-0,06	0,78	Aspartic protease; protein expressed at decreased levels in a hapX mutant versus wild-type
AN2904	0,19	0,02	-0,22	0,02	0,09	0,35	-0,25	0,00	0,06	0,57	-0,27	0,00	Putative 26S proteasome regulatory subunit; ortholog of <i>S. cerevisiae</i> Rpt3p
AN2907	-0,47	0,00	0,16	0,39	-0,45	0,00	-0,01	0,96	-0,43	0,00	0,12	0,48	Ortholog(s) have role in ascospore formation, cellular protein localization, cellular response to caffeine and eukaryotic translation initiation factor 3 complex assembly, more
AN2917	0,38	0,00	-0,08	0,62	0,35	0,00	-0,08	0,54	0,03	0,83	-0,21	0,08	Ortholog(s) have role in positive regulation of RNA polymerase II transcriptional preinitiation complex assembly, positive regulation of protein catabolic process and proteasome regulatory particle assembly, more
AN2918	-0,14	0,34	-0,22	0,16	-0,19	0,20	-0,30	0,04	-0,37	0,01	-0,42	0,00	Putative chaperonin complex component, TCP-1 delta subunit; ortholog of <i>S. cerevisiae</i> Cct4p; expression reduced after exposure to farnesol
AN2946	0,18	0,21	-0,03	0,89	0,11	0,49	0,20	0,20	0,01	0,97	-0,21	0,18	Protein predicted to have a role in pheromone precursor processing
AN2965	-0,17	0,05	-0,04	0,78	-0,39	0,00	-0,27	0,00	-0,19	0,04	-0,21	0,02	Cell cycle regulator, binds to the anaphase-promoting complex/cyclosome (APC/C), targets cyclin B for destruction in G1 phase preventing transition to S phase
AN2972	0,04	0,85	-0,22	0,30	-0,18	0,33	-0,45	0,01	0,05	0,85	-0,16	0,43	Ortholog(s) have mitochondrion localization
AN2986	0,29	0,05	-0,20	0,26	0,05	0,79	-0,27	0,08	0,10	0,63	-0,31	0,04	Ortholog(s) have role in asexual sporulation

AN3003	0,42	0,01	-0,11	0,61	0,27	0,10	-0,34	0,04	0,20	0,29	-0,11	0,59	Ortholog(s) have ubiquitin-specific protease activity
AN3019	0,29	0,00	-0,10	0,36	0,11	0,27	-0,16	0,10	0,21	0,03	-0,15	0,14	Ortholog(s) have role in ubiquitin-dependent protein catabolic process and nucleus, proteasome regulatory particle, lid subcomplex, proteasome storage granule localization
AN3057	0,26	0,18	0,06	0,84	-0,10	0,64	-0,41	0,03	-0,47	0,02	-0,39	0,04	Has domain(s) with predicted oxidoreductase activity, acting on a sulfur group of donors, oxygen as acceptor activity and role in oxidation-reduction process, prenylcysteine catabolic process
AN3091	-0,14	0,22	-0,36	0,00	-0,14	0,24	-0,49	0,00	0,03	0,84	-0,19	0,10	Has domain(s) with predicted metalloendopeptidase activity, metallopeptidase activity and role in proteolysis
AN3098	-0,12	0,23	-0,06	0,66	-0,02	0,83	0,08	0,49	-0,06	0,59	-0,03	0,83	Putative secretory component; ortholog of <i>S. cerevisiae</i> Sec18p
AN3134	-0,04	0,81	-0,12	0,50	0,03	0,87	-0,08	0,60	-0,39	0,00	-0,18	0,20	Ortholog(s) have role in cellular response to drug and chaperonin-containing T-complex, nucleus localization
AN3136	0,25	0,18	0,42	0,03	0,04	0,85	0,18	0,38	0,27	0,18	0,39	0,04	Has domain(s) with predicted acid-amino acid ligase activity
AN3226	2,22	0,00	1,21	0,01	2,34	0,00	1,66	0,00	1,39	0,00	1,12	0,02	Has domain protein; aspermidine A secondary metabolism gene cluster member; protein levels decrease in response to farnesol
AN3305	1,13	0,01	0,63	0,26	1,15	0,01	1,43	0,00	0,80	0,12	1,38	0,00	Has domain(s) with predicted oxidoreductase activity and role in metabolic process
AN3321	0,65	0,09	0,37	0,39	0,44	0,27	0,50	0,18	1,24	0,00	0,52	0,17	Has domain(s) with predicted aspartic-type endopeptidase activity and role in proteolysis
AN3368	0,55	0,00	0,22	0,10	0,38	0,00	-0,07	0,66	0,00	0,98	0,11	0,46	Protein with beta-mannosidase activity, involved in degradation of mannans; transcriptionally induced by growth on xylose
AN3377	-0,45	0,51	0,06	0,95	0,22	0,77	1,32	0,03	0,26	0,75	1,08	0,10	Ortholog(s) have endopeptidase activity, role in proteolysis, zymogen activation and extracellular region localization
AN3393	-1,08	0,03	-0,82	0,12	-0,75	0,14	-0,14	0,83	0,87	0,09	1,78	0,00	Protein with similarity to neutral metalloprotease II
AN3449	0,48	0,01	-0,11	0,67	0,67	0,00	-0,16	0,47	-0,22	0,33	-0,21	0,35	Ortholog(s) have ubiquitin-specific protease activity, role in protein deubiquitination, regulation of transcription, DNA-templated and cytosol, nucleus localization
AN3453	-0,33	0,03	-0,38	0,02	-0,24	0,12	-0,28	0,09	0,20	0,27	-0,11	0,55	Has domain(s) with predicted ubiquitin-specific protease activity, role in ubiquitin-dependent protein catabolic process and intracellular localization
AN3459	0,54	0,00	0,37	0,02	0,48	0,00	0,29	0,06	-0,47	0,00	-0,17	0,32	Ortholog(s) have metallodipeptidase activity, omega peptidase activity, role in cellular response to cadmium ion, detoxification of cadmium ion, glutathione catabolic process and cytosol, mitochondrion, nucleus, ribosome localization
AN3464	0,21	0,17	-0,40	0,01	0,14	0,41	-0,37	0,01	0,13	0,49	-0,30	0,06	Ortholog(s) have cytosol, nucleus localization
AN3470	0,15	0,19	0,31	0,01	0,16	0,19	0,35	0,00	0,01	0,97	0,16	0,20	Ortholog(s) have cysteine-type endopeptidase activity
AN3493	1,55	0,00	-2,75	0,00	1,42	0,00	-2,10	0,00	1,71	0,00	-2,64	0,00	Predicted threonine-type endopeptidase; inp secondary metabolite gene cluster member
AN3583	-0,38	0,01	0,05	0,85	-0,30	0,06	0,14	0,45	0,18	0,32	0,31	0,06	Protein with homology to subtilisin serine proteases; enhanced specificity for cleavage of dibasic peptide sequences
AN3584	-0,05	0,72	-0,18	0,23	0,01	0,95	-0,06	0,69	0,17	0,24	-0,10	0,54	Ortholog(s) have phosphatidylinositol-3-phosphate binding activity and role in CVT pathway, early endosome to Golgi transport, mitochondrion degradation, piecemeal microautophagy of nucleus
AN3623	0,65	0,00	0,03	0,92	0,43	0,01	-0,04	0,87	-0,21	0,27	-0,01	0,97	Subunit 7 of the COP9 signalosome; required for formation of cleistothecia; putative pre-induction sporulation protein

AN3644	0,26	0,06	0,00	0,98	0,12	0,45	0,15	0,34	-0,39	0,01	-0,27	0,07	Ortholog(s) have protein homodimerization activity, ubiquitin-protein transferase activity and role in free ubiquitin chain polymerization, postreplication repair, protein K63-linked ubiquitination
AN3646	0,34	0,04	-0,14	0,52	0,21	0,22	-0,16	0,41	-0,55	0,00	-0,42	0,01	Ortholog(s) have role in cellular response to biotic stimulus, cellular response to starvation and cytoplasmic translation, more
AN3689	-0,42	0,01	-0,10	0,69	-0,18	0,31	0,27	0,13	0,06	0,78	0,07	0,76	Ortholog(s) have role in ascospore formation and cytosol, nucleus localization
AN3691	-0,58	0,00	-0,04	0,82	-0,50	0,00	0,07	0,64	-0,07	0,67	0,09	0,58	Ortholog(s) have role in endocytic recycling, filamentous growth and hyphal tip localization
AN3711	-0,25	0,02	-0,13	0,31	-0,48	0,00	-0,29	0,01	0,10	0,42	-0,01	0,96	Ortholog(s) have protein complex scaffold, ubiquitin-specific protease activity, role in histone H3-K4 methylation, histone H3-K79 methylation, histone deubiquitination and DUBm complex, SAGA complex, SLIK (SAGA-like) complex localization
AN3716	0,20	0,05	-0,15	0,20	0,28	0,01	-0,21	0,04	-0,03	0,85	-0,11	0,33	Ortholog of <i>A. fumigatus</i> Af293 : Afu6g12770, <i>A. niger</i> CBS 513.88 : An08g10710, <i>A. oryzae</i> RIB40 : AO090003000397, <i>Aspergillus wentii</i> : Aspwe1_0102826 and <i>Aspergillus sydowii</i> : Aspsy1_0032599
AN3756	0,39	0,01	-0,29	0,10	0,23	0,17	-0,33	0,04	-0,29	0,09	-0,63	0,00	Ortholog(s) have endopeptidase activity and role in proteasomal ubiquitin-independent protein catabolic process, proteasome-mediated ubiquitin-dependent protein catabolic process
AN3757	-0,17	0,40	0,02	0,95	-0,38	0,04	-0,31	0,12	-0,24	0,26	-0,01	0,96	Ortholog(s) have role in establishment of cell polarity, mycelium development, spore germination and endoplasmic reticulum, hyphal tip, plasma membrane localization
AN3787	-1,10	0,00	-0,47	0,12	-1,33	0,00	-0,44	0,12	0,07	0,85	-0,03	0,93	Ortholog(s) have glycoprotein binding, metal ion binding, misfolded protein binding, peptide-N4-(N-acetyl-beta-glucosaminy)asparagine amidase activity, structural constituent of cell wall activity
AN3853	-0,32	0,05	-0,47	0,01	-0,24	0,17	-0,53	0,00	0,85	0,00	0,65	0,00	Pitrilysin family metalloprotease; protein induced by farnesol
AN3918	0,37	0,00	-0,07	0,63	0,26	0,01	-0,07	0,59	0,03	0,84	-0,13	0,28	Ortholog(s) have aminopeptidase activity, role in protein catabolic process in the vacuole and fungal-type vacuole localization
AN3923	-0,08	0,41	0,12	0,27	-0,17	0,07	-0,02	0,89	-0,23	0,02	-0,04	0,75	Ortholog(s) have ubiquitin-protein transferase activity
AN3932	0,27	0,00	-0,27	0,00	0,06	0,55	-0,45	0,00	0,04	0,75	-0,21	0,03	Putative proteasome beta-5 subunit
AN3939	-0,01	0,95	0,01	0,97	-0,15	0,34	-0,07	0,71	-0,01	0,96	-0,04	0,85	Predicted ubiquitin protein ligase; role in ubiquitin-dependent protein catabolism and cullin-RING ubiquitin ligase complex localization; NeddH-associated protein
AN3943	0,26	0,18	0,22	0,35	0,04	0,84	-0,08	0,75	-0,17	0,45	-0,16	0,47	Has domain(s) with predicted pyroglutamyl-peptidase activity, role in proteolysis and cytosol localization
AN3959	-0,42	0,03	-0,24	0,32	-0,36	0,07	-0,24	0,29	-0,02	0,96	0,67	0,00	Has domain(s) with predicted metalloendopeptidase activity, metallopeptidase activity and role in proteolysis
AN3999	0,34	0,01	0,19	0,24	0,26	0,05	0,25	0,07	0,41	0,00	0,26	0,06	Putative HECT ubiquitin ligase
AN4018	0,46	0,00	-0,07	0,67	0,37	0,00	-0,11	0,42	-0,20	0,15	-0,28	0,02	Ortholog(s) have role in protein targeting to vacuole
AN4046	-0,35	0,06	0,08	0,76	-0,27	0,16	0,10	0,66	-0,19	0,40	-0,32	0,11	Ortholog(s) have Golgi apparatus, endoplasmic reticulum localization
AN4236	0,21	0,01	-0,15	0,14	0,25	0,00	-0,12	0,20	0,14	0,14	-0,10	0,31	Probable 26S proteasome subunit and member of the CDC48/PAS1/SEC18 family of ATPases; transcript upregulated in response to camptothecin
AN4282	0,22	0,10	0,31	0,03	0,26	0,05	0,12	0,46	-0,57	0,00	0,08	0,62	Ortholog(s) have metalloaminopeptidase activity, role in peptide catabolic process and intracellular localization
AN4317	-0,52	0,00	-0,18	0,16	-0,42	0,00	-0,21	0,07	-0,28	0,02	-0,07	0,63	Putative nuclear pore complex protein with homology to <i>Saccharomyces cerevisiae</i> Sec13p

AN4351	0,32	0,03	-0,05	0,83	0,25	0,08	-0,07	0,69	0,07	0,71	-0,04	0,83	Protein involved in a signaling pathway that activates PacC transcription factor in response to alkaline ambient pH
AN4399	-0,09	0,53	0,00	0,98	-0,25	0,04	-0,15	0,29	-0,25	0,05	-0,07	0,68	SumO conjugation (E2) enzyme
AN4404	0,27	0,01	0,14	0,24	0,36	0,00	0,20	0,06	-0,45	0,00	-0,09	0,49	Ortholog(s) have cytosol localization
AN4411	-0,15	0,21	0,03	0,85	-0,06	0,67	0,06	0,71	-0,42	0,00	0,00	0,98	Ortholog(s) have polyubiquitin binding, sterol binding activity
AN4422	-0,38	0,02	0,35	0,05	-0,53	0,00	0,05	0,83	-0,18	0,36	0,36	0,04	Putative aspartic-type endopeptidase; predicted glycosylphosphatidylinositol (GPI)-anchored protein
AN4449	0,29	0,03	-0,20	0,20	0,25	0,06	-0,31	0,02	0,03	0,90	-0,37	0,01	Ortholog(s) have endopeptidase activator activity and role in proteasomal ubiquitin-independent protein catabolic process, proteasome-mediated ubiquitin-dependent protein catabolic process
AN4457	0,13	0,45	-0,29	0,09	0,15	0,37	-0,31	0,05	-0,26	0,12	-0,40	0,01	Ortholog(s) have endopeptidase activator activity and role in proteasomal ubiquitin-independent protein catabolic process, proteasome-mediated ubiquitin-dependent protein catabolic process
AN4458	-0,20	0,23	-0,28	0,10	0,02	0,92	-0,28	0,08	0,13	0,49	-0,15	0,41	Ortholog(s) have nucleus localization
AN4492	0,06	0,73	-0,07	0,72	0,01	0,97	-0,23	0,12	-0,10	0,56	-0,21	0,17	Ortholog(s) have ubiquitin-specific protease activity and role in cellular response to drug, mitochondrial fission, peroxisome fission, proteasome-mediated ubiquitin-dependent protein catabolic process, protein deubiquitination
AN4510	-0,37	0,05	0,08	0,76	-0,47	0,01	-0,05	0,86	-0,31	0,14	0,07	0,80	F-box protein; mutant shows increased resistance to 2-deoxyglucose; BLAST indicates no apparent homologs in higher eukaryotes
AN4535	-0,31	0,09	0,14	0,59	-0,31	0,10	0,14	0,52	-0,60	0,00	0,04	0,87	Putative F-box protein
AN4548	-0,44	0,01	0,02	0,94	-0,31	0,07	-0,02	0,93	0,22	0,25	0,68	0,00	Ortholog(s) have mitochondrion localization
AN4557	-0,33	0,02	-0,32	0,03	-0,29	0,04	-0,42	0,00	0,47	0,00	0,36	0,01	Ortholog(s) have ATP binding, ATPase activity, metallopeptidase activity, role in protein complex assembly, proteolysis, signal peptide processing and m-AAA complex, mitochondrial inner boundary membrane localization
AN4599	0,21	0,50	0,19	0,64	0,29	0,35	0,72	0,01	-0,23	0,52	-0,10	0,81	Ortholog(s) have polynucleotide 5'-hydroxyl-kinase activity and role in cleavage in ITS2 between 5.8S rRNA and LSU-rRNA of tricistronic rRNA transcript (SSU-rRNA, 5.8S rRNA, LSU-rRNA), termination of RNA polymerase I transcription
AN4726	-0,45	0,01	-0,12	0,64	-0,45	0,01	-0,10	0,65	0,56	0,00	0,20	0,34	Ortholog(s) have endoplasmic reticulum, nuclear envelope localization
AN4731	0,27	0,00	-0,25	0,01	-0,12	0,21	-0,55	0,00	0,03	0,82	-0,27	0,00	Ortholog(s) have role in cellular response to DNA damage stimulus, proteasome assembly, ubiquitin-dependent protein catabolic process and cytoplasm, nucleus localization
AN4775	0,34	0,00	-0,19	0,16	0,31	0,01	-0,20	0,11	-0,08	0,61	-0,22	0,08	Ortholog(s) have role in cullin deneddylation, positive regulation of mitotic metaphase/anaphase transition, proteasome assembly, proteasome localization, proteasome-mediated ubiquitin-dependent protein catabolic process
AN4783	0,44	0,02	0,07	0,83	0,40	0,04	0,07	0,78	-0,65	0,00	-0,29	0,19	Subunit 2 of the COP9 signalosome; required for formation of cleistothecia; mutants produce aberrant red color within distinct hyphae
AN4784	-0,13	0,60	0,18	0,54	-0,15	0,54	0,16	0,56	-0,79	0,00	0,16	0,58	Ortholog of <i>A. fumigatus</i> Af293 : Afu3g06710, <i>A. oryzae</i> RIB40 : AO090020000326, <i>Aspergillus wentii</i> : Aspwe1_0173594, <i>Aspergillus sydowii</i> : Aspsy1_0056625 and <i>Aspergillus terreus</i> NIH2624 : ATET_08749
AN4810	-0,15	0,55	0,18	0,54	-0,10	0,70	-0,09	0,75	-0,04	0,91	-0,18	0,51	Has domain(s) with predicted hydrolase activity and role in metabolic process

AN4869	0,18	0,08	-0,38	0,00	0,17	0,10	-0,40	0,00	-0,02	0,90	-0,46	0,00	Putative 20S proteasome component; protein expressed at decreased levels in a hapX mutant versus wild-type; transcript upregulated in response to camptothecin
AN4872	0,01	0,97	0,39	0,09	0,18	0,43	0,45	0,04	-0,56	0,01	0,34	0,13	Fusion protein consisting of N-terminal ubiquitin and C-terminal extension protein (CEP) of the small ribosomal subunit; transcript upregulated in response to camptothecin
AN4925	-0,48	0,00	-0,13	0,48	-0,38	0,00	-0,14	0,39	0,01	0,98	-0,09	0,60	Ortholog(s) have endoplasmic reticulum localization
AN5055	-0,14	0,50	0,78	0,00	0,16	0,45	0,65	0,00	-0,21	0,35	1,18	0,00	Has domain(s) with predicted aminopeptidase activity, metalloexopeptidase activity and role in cellular process, proteolysis
AN5101	-0,51	0,26	-0,36	0,53	-0,27	0,58	1,12	0,01	-0,35	0,51	-0,11	0,87	Has domain(s) with predicted metallopeptidase activity
AN5102	-0,65	0,00	-0,06	0,79	-0,46	0,00	-0,14	0,47	-0,12	0,55	0,09	0,68	Ortholog(s) have FACT complex, mitotic spindle pole body localization
AN5121	0,22	0,06	-0,29	0,02	0,19	0,10	-0,43	0,00	0,17	0,20	-0,22	0,07	Protein similar to proteasome regulatory subunit 8; menadione stress-induced protein
AN5125	0,29	0,15	0,01	0,97	0,09	0,69	0,08	0,76	-0,02	0,95	-0,21	0,36	Has domain(s) with predicted identical protein binding, serine-type endopeptidase activity and role in negative regulation of catalytic activity
AN5131	0,11	0,49	0,34	0,02	0,19	0,19	0,63	0,00	-0,15	0,37	0,18	0,26	Ortholog(s) have protein tag activity
AN5174	0,40	0,01	0,36	0,04	0,16	0,37	0,03	0,89	0,08	0,74	0,25	0,14	Ortholog(s) have Atg8 ligase activity and role in C-terminal protein lipidation, CVT pathway, ascospore formation, cellular response to nitrogen starvation, macroautophagy, mitochondrion degradation, piecemeal microautophagy of nucleus
AN5186	-0,40	0,00	-0,10	0,51	-0,41	0,00	-0,07	0,62	-0,26	0,03	-0,05	0,74	Ortholog(s) have ubiquitin-specific protease activity, role in protein deubiquitination and cytosol, nucleus localization
AN5199	-0,02	0,93	-0,15	0,51	0,37	0,03	0,22	0,26	-0,09	0,69	-0,24	0,21	Ortholog(s) have cytosol, nucleolus localization
AN5351	0,38	0,06	0,38	0,09	0,14	0,54	0,45	0,03	0,37	0,10	0,49	0,02	Putative ubiquitin-conjugating enzyme
AN5368	1,09	0,04	-0,36	0,61	0,91	0,10	-0,54	0,36	0,68	0,28	-0,45	0,46	Has domain(s) with predicted oxidoreductase activity and role in metabolic process
AN5442	0,37	0,01	0,16	0,37	0,37	0,01	0,26	0,08	0,16	0,35	0,10	0,55	Putative carboxypeptidase Y
AN5466	1,51	0,01	-0,03	0,98	0,30	0,68	0,00	1,00	1,02	0,14	0,88	0,18	Protein of unknown function
AN5495	-0,40	0,04	0,12	0,66	-0,38	0,05	-0,16	0,47	0,04	0,88	0,23	0,29	Ortholog(s) have role in mitotic sister chromatid segregation, negative regulation of cyclin-dependent protein serine/threonine kinase by cyclin degradation, regulation of mitotic metaphase/anaphase transition
AN5517	-0,38	0,03	0,14	0,54	-0,53	0,00	0,28	0,13	0,12	0,58	0,26	0,18	Putative F-box protein
AN5558	-1,75	0,00	0,91	0,06	-1,95	0,00	0,91	0,05	0,36	0,52	2,38	0,00	Broad specificity thermostable alkaline protease; extracellular; regulated by nitrogen, carbon and sulfur metabolite repression; transcript repressed by light in developmentally competent mycelia
AN5588	0,07	0,63	-0,04	0,84	-0,03	0,81	-0,10	0,49	0,37	0,00	0,10	0,49	Ortholog(s) have ATP-dependent peptidase activity
AN5593	-0,30	0,01	-0,18	0,17	-0,21	0,08	-0,12	0,35	-0,31	0,01	-0,26	0,03	Putative F-box protein; NeddH-associated protein; required for control of sexual development in response to light; required for ascospore maturation development of fully grown sexual fruit bodies
AN5607	-0,23	0,07	0,05	0,80	-0,05	0,76	0,33	0,01	0,25	0,06	0,26	0,05	Ortholog(s) have peptidase activator activity, proteasome binding activity, role in proteasome assembly, regulation of proteasomal protein catabolic process and nucleus, proteasome core complex localization
AN5619	-1,01	0,00	0,03	0,91	-0,67	0,00	0,31	0,10	0,15	0,51	0,02	0,93	Ortholog(s) have metallopeptidase activity, role in ascospore wall assembly and ascospore wall, endoplasmic reticulum membrane localization

AN5653	-0,39	0,40	-0,45	0,41	-0,10	0,85	0,18	0,75	0,11	0,85	0,12	0,85	Has domain(s) with predicted oxidoreductase activity and role in metabolic process
AN5675	0,21	0,14	-0,10	0,60	0,34	0,01	0,05	0,78	0,10	0,56	0,01	0,95	Ortholog(s) have ubiquitin binding activity, role in proteasome-mediated ubiquitin-dependent protein catabolic process and cytoplasm, nucleus localization
AN5708	0,49	0,04	0,24	0,44	0,33	0,19	0,18	0,54	-0,54	0,04	-0,01	0,99	Ortholog(s) have protein serine/threonine phosphatase inhibitor activity
AN5747	0,06	0,67	-0,05	0,78	0,07	0,61	0,04	0,78	-0,32	0,01	-0,21	0,10	Ortholog(s) have protein domain specific binding activity
AN5748	-0,34	0,02	-0,10	0,63	-0,46	0,00	-0,42	0,01	-0,08	0,70	-0,08	0,69	Putative mannosyl-oligosaccharide 1,2-alpha-mannosidase with a predicted role in mannose polymer metabolism
AN5774	0,47	0,00	0,13	0,55	0,23	0,17	0,00	0,99	-0,08	0,70	-0,24	0,19	Ortholog(s) have protein complex scaffold activity
AN5784	0,16	0,22	0,01	0,97	0,15	0,26	0,01	0,97	-0,31	0,02	-0,10	0,54	Ortholog(s) have role in proteasomal ubiquitin-independent protein catabolic process, proteasome-mediated ubiquitin-dependent protein catabolic process and cytosol, nucleus, proteasome core complex, beta-subunit complex localization
AN5793	0,32	0,00	-0,11	0,45	0,37	0,00	-0,04	0,77	-0,19	0,14	-0,19	0,13	Putative 20S proteasome beta-type subunit; transcript upregulated in response to camptothecin
AN5798	0,02	0,92	0,21	0,16	0,11	0,44	0,17	0,25	0,03	0,88	0,14	0,36	Subunit 3 of the COP9 signalosome; required for formation of cleistothecia
AN5810	1,08	0,00	0,41	0,13	0,86	0,00	0,18	0,53	-0,69	0,01	-0,34	0,21	Prolidase specific for cleavage of X-Pro dipeptides
AN5812	0,18	0,08	-0,18	0,11	0,10	0,40	-0,34	0,00	-0,05	0,74	-0,19	0,09	Ortholog(s) have aminopeptidase activity, epoxide hydrolase activity, role in cellular lipid metabolic process, protein catabolic process and cytosol, nucleus localization
AN5872	0,16	0,21	-0,35	0,01	0,30	0,01	-0,32	0,01	-0,13	0,39	-0,34	0,01	Ortholog(s) have role in proteasomal ubiquitin-independent protein catabolic process, proteasome-mediated ubiquitin-dependent protein catabolic process
AN5893	0,07	0,81	0,18	0,57	0,04	0,88	0,18	0,49	-0,28	0,30	0,38	0,13	RGS (regulator of G-protein signaling) family member; negative regulator of G-protein signaling promoting conidiophore development; required for light-dependent activation of brlA transcription
AN5906	0,89	0,00	0,17	0,71	0,91	0,00	0,34	0,35	0,74	0,03	0,27	0,49	Has domain(s) with predicted ubiquitin-protein transferase activity, role in protein ubiquitination and ubiquitin ligase complex localization
AN5952	0,59	0,00	0,10	0,70	0,44	0,02	-0,27	0,19	-0,09	0,71	-0,31	0,13	Putative kynureninase with a predicted role in aromatic amino acid biosynthesis
AN5961	-0,05	0,72	0,23	0,09	-0,12	0,37	0,21	0,11	0,04	0,83	0,29	0,02	Has domain(s) with predicted ATP-dependent peptidase activity, zinc ion binding activity and role in proteolysis
AN6064	1,01	0,00	0,89	0,00	0,80	0,00	0,61	0,00	-0,59	0,00	-0,04	0,87	Ortholog(s) have hydrolase activity, acting on ester bonds activity
AN6073	-0,05	0,65	0,06	0,69	-0,04	0,75	-0,01	0,92	0,38	0,00	0,36	0,00	Putative prohibitin with a predicted role in mitochondrial maintenance; transcript upregulated in response to camptothecin
AN6086	0,47	0,00	0,03	0,91	0,52	0,00	0,14	0,42	0,32	0,05	0,08	0,68	Putative F-box protein; ortholog(s) have role in SCF-dependent proteasomal ubiquitin-dependent protein catabolism, cellular response to methylmercury and SCF ubiquitin ligase complex localization; NeddH-associated protein
AN6119	-0,16	0,29	-0,12	0,50	-0,16	0,28	-0,24	0,11	-0,16	0,32	-0,22	0,14	Ortholog(s) have endoplasmic reticulum, fungal-type vacuole localization
AN6136	-0,27	0,02	-0,19	0,19	-0,31	0,01	-0,22	0,08	0,06	0,71	-0,01	0,95	Ortholog(s) have endoplasmic reticulum localization

AN6138	-0,53	0,00	-0,07	0,76	-0,41	0,01	0,01	0,97	-0,14	0,46	0,13	0,49	Component of the Anaphase-Promoting Complex/Cyclosome (APC/C), which is a ubiquitin ligase required for cell cycle progression; mutations lead to DNA damage and block cytokinesis; tetratricopeptide repeat (TPR) gene family member
AN6164	-0,57	0,00	0,26	0,10	-0,53	0,00	0,24	0,12	-0,08	0,68	0,38	0,01	Has domain(s) with predicted ubiquitinyl hydrolase activity and role in ubiquitin-dependent protein catabolic process
AN6179	0,89	0,00	0,48	0,01	0,76	0,00	0,22	0,26	-0,41	0,03	0,02	0,93	Protein neddylation factor NEDD8
AN6193	0,07	0,71	0,09	0,71	0,21	0,25	0,20	0,30	0,53	0,00	0,37	0,04	Ortholog(s) have ATP-dependent peptidase activity, role in chaperone-mediated protein complex assembly, misfolded or incompletely synthesized protein catabolic process and mitochondrial matrix localization
AN6217	0,04	0,76	0,04	0,82	-0,08	0,47	0,02	0,90	-0,17	0,14	-0,05	0,74	Putative F-box protein
AN6250	0,70	0,01	0,45	0,16	0,82	0,00	0,48	0,10	0,45	0,14	0,30	0,35	Ortholog(s) have cytosol, nucleus localization
AN6263	-0,53	0,00	-0,15	0,56	-0,18	0,37	-0,14	0,54	-0,02	0,96	-0,20	0,36	Has domain(s) with predicted ATP binding, nucleoside-triphosphatase activity, nucleotide binding activity
AN6337	0,80	0,00	0,09	0,83	0,65	0,01	-0,16	0,61	0,31	0,30	-0,05	0,89	Ortholog(s) have intracellular localization
AN6354	-0,24	0,02	-0,09	0,51	-0,10	0,38	0,01	0,96	-0,12	0,31	0,00	1,00	Putative ubiquitin C-terminal hydrolase; ortholog of <i>S. cerevisiae</i> Ubp12p; expression reduced after exposure to farnesol; transcript upregulated in response to camptothecin
AN6359	-0,20	0,23	0,32	0,07	-0,42	0,01	0,36	0,03	0,23	0,21	0,34	0,04	Protein involved in sulfur metabolite repression; contains an F-box and seven WD repeats
AN6360	0,14	0,32	-0,31	0,02	0,29	0,02	0,00	0,99	0,35	0,01	-0,48	0,00	Has domain(s) with predicted role in autophagy
AN6399	0,66	0,07	-0,01	0,98	1,40	0,00	0,46	0,26	-0,24	0,62	0,07	0,89	Putative bleomycin hydrolase
AN6426	-0,82	0,03	-2,79	0,00	0,62	0,12	-0,73	0,07	2,34	0,00	-0,33	0,47	Has domain(s) with predicted metallopeptidase activity
AN6438	0,28	0,40	0,38	0,33	0,53	0,10	0,54	0,10	-0,06	0,89	0,68	0,04	Ortholog(s) have dipeptidyl-peptidase activity and role in proteolysis involved in cellular protein catabolic process
AN6487	-0,02	0,96	-0,71	0,00	0,05	0,85	-0,50	0,04	-0,06	0,86	-0,19	0,51	Putative aspartyl protease; ortholog of <i>S. cerevisiae</i> BAR1; expression reduced after exposure to farnesol
AN6528	-0,20	0,20	-0,09	0,67	-0,51	0,00	-0,36	0,02	0,18	0,31	-0,06	0,77	Protein predicted to have a role in pheromone precursor processing
AN6547	0,44	0,00	-0,18	0,19	0,30	0,01	-0,05	0,74	-0,18	0,20	-0,38	0,00	Ortholog(s) have role in proteasomal ubiquitin-independent protein catabolic process, proteasome-mediated ubiquitin-dependent protein catabolic process
AN6569	0,56	0,00	0,10	0,69	0,26	0,13	0,03	0,91	-0,71	0,00	-0,28	0,13	Putative component of the EKC/KEOPS complex, involved in regulation of arginine metabolism
AN6574	-0,44	0,00	-0,09	0,68	-0,37	0,01	-0,13	0,45	-0,16	0,36	-0,16	0,34	Ortholog(s) have ubiquitin-protein transferase activity
AN6609	0,10	0,68	-0,16	0,57	-0,02	0,95	0,33	0,13	0,28	0,23	0,38	0,08	Ortholog(s) have cytosol, nucleus localization
AN6640	0,41	0,05	0,49	0,03	0,38	0,08	0,14	0,60	-0,03	0,92	-0,11	0,70	Has domain(s) with predicted hydrolase activity and role in metabolic process
AN6641	-0,32	0,16	0,40	0,13	-0,20	0,40	0,35	0,18	-0,65	0,01	0,17	0,56	Has domain(s) with predicted role in cellular process
AN6686	0,07	0,83	-0,12	0,76	-0,31	0,22	0,13	0,68	-0,18	0,55	-0,17	0,59	Has domain(s) with predicted aspartic-type endopeptidase activity and role in proteolysis
AN6702	-0,48	0,00	-0,13	0,59	-0,58	0,00	-0,32	0,08	0,02	0,94	-0,08	0,73	Ortholog(s) have Golgi apparatus, endoplasmic reticulum localization
AN6726	0,08	0,46	-0,34	0,00	-0,04	0,78	-0,45	0,00	-0,23	0,04	-0,39	0,00	Ortholog(s) have role in proteasomal ubiquitin-independent protein catabolic process, proteasome-mediated ubiquitin-dependent protein catabolic process



AN6741	0,66	0,00	-0,30	0,05	0,36	0,01	-0,28	0,05	0,17	0,30	-0,29	0,05	Ortholog(s) have polyubiquitin binding activity
AN6888	-0,43	0,01	-0,33	0,08	-0,49	0,00	-0,55	0,00	-0,31	0,10	-0,10	0,63	Putative extracellular aspartic protease (aspergillopepsin)
AN6894	-0,22	0,09	-0,19	0,18	-0,09	0,52	-0,27	0,04	0,09	0,57	-0,03	0,88	Putative peptidyl-prolyl cis-trans isomerase (PPIase)
AN6906	-0,17	0,21	-0,10	0,59	-0,10	0,50	-0,07	0,69	-0,02	0,93	-0,17	0,25	Ortholog(s) have Prp19 complex, cytosol, nuclear envelope localization
AN6913	0,01	0,98	-0,12	0,63	-0,18	0,36	-0,16	0,44	0,42	0,03	-0,19	0,38	Ortholog(s) have ubiquitin-specific protease activity, role in protein deubiquitination and endoplasmic reticulum localization
AN6931	-0,08	0,86	-1,80	0,00	0,03	0,95	-1,39	0,00	0,34	0,42	-1,88	0,00	Has domain(s) with predicted oxidoreductase activity and role in metabolic process
AN6978	-0,31	0,08	-0,07	0,79	-0,59	0,00	-0,16	0,46	0,13	0,55	0,06	0,80	Putative nucleotide exchange factor involved in nucleocytoplasmic trafficking of macromolecules
AN6988	-0,02	0,88	-0,07	0,61	0,07	0,53	-0,06	0,61	-0,08	0,53	0,02	0,91	Ortholog(s) have protein domain specific binding activity
AN7035	-0,70	0,01	-0,32	0,34	-0,70	0,01	-0,02	0,96	0,91	0,00	0,28	0,38	Has domain(s) with predicted peptidase activity and role in proteolysis
AN7159	0,18	0,66	-0,65	0,09	0,24	0,54	-0,69	0,05	0,59	0,12	0,19	0,68	Ortholog(s) have tripeptidyl-peptidase activity
AN7201	-0,02	0,98	0,63	0,40	0,41	0,52	1,86	0,00	0,44	0,53	1,39	0,02	Ortholog(s) have role in proteolysis
AN7231	-0,22	0,41	-0,84	0,00	0,05	0,88	-0,79	0,00	0,40	0,15	0,44	0,10	Ortholog(s) have serine-type endopeptidase activity and role in proteolysis
AN7254	0,32	0,02	0,20	0,23	0,55	0,00	0,43	0,00	0,47	0,00	0,35	0,02	Protein with a conserved CDC48, cell division protein N-terminal domain and two ATPase domains of the AAA-superfamily; protein expressed at increased levels during osmoadaptation; protein induced by farnesol
AN7299	0,25	0,09	0,27	0,11	0,26	0,09	0,10	0,56	-0,62	0,00	0,08	0,67	Ortholog(s) have DNA binding activity and cytosol, nucleus localization
AN7309	-0,38	0,02	-0,17	0,43	-0,35	0,03	-0,30	0,09	-0,13	0,54	-0,24	0,19	Protein involved in DNA repair; mutants are sensitive to UV and show increased frequency of asexual recombination; transcript upregulated in response to camptothecin
AN7321	0,41	0,11	0,32	0,31	0,65	0,01	0,60	0,02	0,33	0,26	0,15	0,65	Ortholog(s) have eukaryotic translation initiation factor 2alpha kinase activity, role in negative regulation of translational initiation in response to osmotic stress, protein phosphorylation and cytosol localization
AN7338	-0,20	0,13	-0,28	0,05	-0,25	0,05	-0,11	0,46	-0,44	0,00	-0,35	0,01	Has domain(s) with predicted acid-amino acid ligase activity
AN7339	0,11	0,66	0,83	0,00	-0,29	0,17	0,47	0,04	-0,51	0,03	0,39	0,09	Has domain(s) with predicted oxidoreductase activity and role in metabolic process
AN7422	0,41	0,00	0,07	0,71	0,37	0,00	0,13	0,36	-0,04	0,84	-0,02	0,90	Putative ubiquitin carboxyl-terminal hydrolase; transcript upregulated in response to camptothecin
AN7428	0,43	0,00	0,33	0,02	0,41	0,00	0,46	0,00	0,01	0,96	0,32	0,02	Ortholog(s) have role in autophagy, cellular response to nitrogen starvation and cytosol, nucleus localization
AN7491	0,96	0,00	-0,28	0,28	1,07	0,00	-0,30	0,20	-0,59	0,01	-0,66	0,00	Putative ubiquitin C-terminal hydrolase; ortholog of <i>S. cerevisiae</i> Yuh1p which has role in protein deubiquitination; expression upregulated after exposure to farnesol
AN7529	0,49	0,25	-0,04	0,96	0,78	0,05	0,01	0,98	-0,67	0,16	-0,13	0,81	Putative metal-dependent amidase
AN7577	0,37	0,30	-1,04	0,00	0,50	0,15	-0,86	0,01	-0,39	0,32	-1,35	0,00	Has domain(s) with predicted acid-amino acid ligase activity
AN7579	0,26	0,00	-0,04	0,73	0,24	0,00	-0,04	0,69	0,18	0,03	-0,03	0,79	Ortholog(s) have polyubiquitin binding, structural molecule activity and role in negative regulation of protein catabolic process, ubiquitin-dependent protein catabolic process
AN7704	0,78	0,00	0,15	0,60	0,91	0,00	0,33	0,14	0,24	0,33	0,04	0,90	Ortholog(s) have role in proteasome-mediated ubiquitin-dependent protein catabolic process and cytoplasm, nucleus localization

AN7733	0,14	0,35	-0,12	0,48	0,24	0,08	-0,11	0,48	-0,24	0,14	-0,32	0,02	Ortholog(s) have protein-N-terminal asparagine amidohydrolase activity, protein-N-terminal glutamine amidohydrolase activity and role in cellular protein modification process, protein catabolic process
AN7926	-0,17	0,78	-0,26	0,71	-0,33	0,55	0,28	0,65	0,43	0,46	0,63	0,24	Has domain(s) with predicted oxidoreductase activity and role in metabolic process
AN7962	-3,35	0,00	0,91	0,17	-3,08	0,00	1,90	0,00	-0,06	0,94	3,12	0,00	Extracellular deuterolysin-type metallo-proteinase
AN8002	0,29	0,03	0,13	0,45	0,00	1,00	0,03	0,87	0,15	0,35	-0,05	0,76	Ortholog(s) have role in regulation of DNA-dependent DNA replication, regulation of mitotic metaphase/anaphase transition and anaphase-promoting complex, cytosol localization
AN8013	-0,06	0,67	0,00	0,98	-0,08	0,55	-0,36	0,00	-0,24	0,08	-0,26	0,04	Ortholog(s) have role in regulation of mitotic metaphase/anaphase transition and mitotic spindle pole body, nucleus localization
AN8017	-0,24	0,02	0,21	0,08	-0,27	0,01	0,22	0,05	-0,02	0,92	0,20	0,07	Ortholog(s) have cytosol, mitotic spindle pole body, nucleus localization
AN8044	-0,44	0,04	-0,04	0,91	-0,58	0,01	-0,18	0,49	-0,06	0,86	0,13	0,65	Ortholog(s) have metalloendopeptidase activity
AN8054	0,29	0,03	-0,20	0,23	0,26	0,07	-0,21	0,15	-0,03	0,89	-0,32	0,03	Predicted alpha 4 subunit of the 20S core proteasome; involved in N-myristoylation and cell morphogenesis; menadione stress-induced protein
AN8074	0,87	0,00	0,29	0,46	1,09	0,00	0,78	0,01	-0,09	0,82	-0,17	0,67	Has domain(s) with predicted ubiquitinyl hydrolase activity, zinc ion binding activity and role in ubiquitin-dependent protein catabolic process
AN8102	-0,03	0,94	-0,67	0,03	0,10	0,76	-0,31	0,33	0,98	0,00	-0,64	0,03	Putative pepsin-like aspartic protease; predicted glycosyl phosphatidylinositol (GPI)-anchor
AN8173	0,59	0,00	-0,14	0,45	0,41	0,01	-0,12	0,52	-0,33	0,06	-0,28	0,08	Ortholog(s) have actin monomer binding, protein kinase inhibitor activity, ribosome binding activity, role in negative regulation of protein phosphorylation and cytoplasm, nucleus, polysome, ribosome localization
AN8192	-0,39	0,01	0,22	0,25	-0,31	0,05	0,18	0,32	-0,20	0,26	0,17	0,35	SUMO-specific isopeptidase
AN8253	-0,87	0,00	0,00	1,00	-0,70	0,00	0,11	0,67	-0,42	0,04	-0,05	0,87	Ortholog(s) have cytosol, nucleus localization
AN8258	0,63	0,02	0,32	0,34	0,42	0,13	0,45	0,11	0,64	0,02	0,55	0,05	Putative ubiquitin-conjugating enzyme; ortholog of <i>S. cerevisiae</i> Ubc7p
AN8445	0,75	0,10	0,39	0,52	1,15	0,01	0,60	0,23	0,13	0,84	1,13	0,02	Putative aminopeptidase Y; transcript is induced by nitrate
AN8468	-0,08	0,90	-1,72	0,00	0,62	0,18	-0,83	0,08	0,67	0,18	-1,46	0,00	Ortholog of <i>A. nidulans</i> FGSC A4 : AN2021, <i>A. fumigatus</i> Af293 : Afu7g00550 and <i>A. niger</i> CBS 513.88 : An15g05630, An11g03460, An11g07530, An04g03850, An09g00640
AN8585	0,91	0,12	-0,93	0,14	2,81	0,00	0,08	0,92	1,96	0,00	-1,25	0,03	Has domain(s) with predicted oxidoreductase activity and role in metabolic process
AN8603	-0,31	0,15	0,12	0,71	0,14	0,52	0,41	0,06	-0,12	0,64	0,80	0,00	Has domain(s) with predicted oxidoreductase activity and role in metabolic process
AN8702	0,02	0,91	-0,10	0,66	0,00	0,99	-0,14	0,45	-0,22	0,22	-0,13	0,49	Ortholog(s) have protein homodimerization activity, ubiquitin-protein transferase activity and role in UV-damage excision repair, free ubiquitin chain polymerization, postreplication repair, protein K63-linked ubiquitination
AN8780	-0,29	0,17	-0,08	0,78	-0,46	0,02	-0,16	0,51	0,38	0,08	0,54	0,01	Ortholog(s) have serine-type endopeptidase activity, role in glycoprotein metabolic process and mitochondrion localization
AN8783	0,14	0,20	-0,34	0,00	0,38	0,00	-0,55	0,00	0,00	0,98	-0,43	0,00	Protein required for progression through mitosis
AN8844	0,14	0,37	0,05	0,83	0,15	0,35	0,00	1,00	0,01	0,97	0,18	0,28	Putative E3 ubiquitin-protein ligase; NeddH-associated protein

AN8967	-0,28	0,21	-0,26	0,33	0,17	0,47	0,10	0,72	-0,18	0,50	-0,20	0,44	Has domain(s) with predicted UDP-N-acetylmuramate dehydrogenase activity, flavin adenine dinucleotide binding, oxidoreductase activity, acting on CH-OH group of donors activity and role in oxidation-reduction process
AN9059	-0,02	0,86	-0,24	0,03	-0,08	0,51	-0,19	0,07	0,00	0,98	-0,15	0,17	Putative F-box protein
AN9372	-1,31	0,01	0,72	0,30	-0,21	0,73	0,89	0,15	0,45	0,47	0,81	0,20	Has domain(s) with predicted serine-type peptidase activity and role in proteolysis
AN9421	0,08	0,56	0,24	0,06	0,02	0,89	0,20	0,11	0,16	0,24	0,28	0,02	Has domain(s) with predicted zinc ion binding activity
AN9434	-0,07	0,72	0,09	0,72	-0,14	0,43	0,00	1,00	-0,66	0,00	-0,21	0,28	Ortholog(s) have cytosol, nucleus localization
AN10008	0,35	0,01	0,52	0,00	0,22	0,13	0,39	0,01	-0,04	0,84	0,02	0,93	Predicted ubiquitin protein ligase; role in ubiquitin-dependent protein catabolism and cullin-RING ubiquitin ligase complex localization; NeddH-associated protein
AN10020	0,22	0,03	-0,05	0,71	0,16	0,11	-0,03	0,84	0,02	0,91	-0,14	0,19	Ortholog(s) have role in proteasome-mediated ubiquitin-dependent protein catabolic process and cytosol, nucleus localization
AN10030	0,41	0,01	0,01	0,96	0,26	0,10	-0,04	0,86	-0,04	0,87	-0,14	0,47	Putative alkaline serine protease; predicted glycosylphosphatidylinositol (GPI)-anchored protein
AN10182	-0,57	0,00	0,07	0,77	-0,28	0,08	0,17	0,35	-0,59	0,00	-0,02	0,94	Putative translation initiation factor 3, subunit f (eIF-3f); expression reduced after exposure to farnesol
AN10184	-0,36	0,01	-0,23	0,13	-0,31	0,02	-0,31	0,02	-0,15	0,31	-0,24	0,09	Protein predicted to have a role in pheromone precursor processing
AN10191	-0,54	0,00	0,16	0,31	-0,41	0,00	0,08	0,60	-0,08	0,64	0,13	0,43	Ortholog(s) have chromatin binding, histone binding activity
AN10198	0,04	0,86	-0,04	0,89	0,05	0,84	-0,11	0,64	-0,51	0,01	-0,16	0,50	Ortholog(s) have cytosol, nucleus localization
AN10213	0,21	0,34	0,36	0,11	0,36	0,07	0,20	0,39	0,65	0,00	0,30	0,18	Ortholog(s) have role in CVT pathway, cellular response to nitrogen starvation, late endosome to vacuole transport, macroautophagy, peroxisome degradation and phosphatidylinositol biosynthetic process, more
AN10251	0,59	0,00	0,42	0,06	0,57	0,00	0,87	0,00	0,56	0,01	0,59	0,00	Ortholog(s) have nuclear localization sequence binding, ubiquitin binding activity, role in response to ethanol and cytosol localization
AN10258	0,02	0,95	-0,29	0,26	-0,07	0,78	-0,34	0,13	-0,25	0,30	-0,22	0,38	Ortholog(s) have anaphase-promoting complex, cytosol localization
AN10266	0,40	0,00	0,06	0,75	0,48	0,00	0,08	0,59	-0,01	0,95	0,03	0,89	Putative ubiquitin-activating enzyme; ortholog of <i>S. cerevisiae</i> Uba1p; transcript upregulated in response to camptothecin; protein induced by farnesol
AN10324	0,72	0,00	0,05	0,88	0,39	0,04	0,14	0,53	-0,10	0,68	-0,11	0,65	Putative neddylation machinery protein; constitutively expressed during all stages of the fungal life cycle
AN10337	0,21	0,14	-0,02	0,95	0,09	0,59	-0,01	0,97	0,19	0,24	0,14	0,40	Has domain(s) with predicted enzyme regulator activity, role in regulation of protein catabolic process and proteasome complex localization
AN10351	-0,10	0,57	-0,12	0,60	-0,03	0,90	-0,30	0,08	-0,45	0,01	-0,42	0,01	Ortholog(s) have aminopeptidase activity, role in cellular response to drug, chaperone-mediated protein folding, proteolysis and cytosol, fungal-type vacuole lumen, ribosome localization
AN10365	0,90	0,00	0,36	0,12	0,60	0,00	0,00	1,00	-0,80	0,00	-0,28	0,21	Ortholog(s) have role in hyphal growth
AN10394	0,42	0,10	-0,01	0,99	-0,01	0,97	-0,25	0,39	-0,41	0,16	-0,28	0,34	Ortholog(s) have ubiquitin-protein transferase activity, role in anaphase-promoting complex-dependent proteasomal ubiquitin-dependent protein catabolic process, protein ubiquitination and anaphase-promoting complex localization
AN10397	-0,56	0,11	-0,27	0,57	-0,16	0,70	-0,88	0,02	0,46	0,25	0,26	0,53	Protein of unknown function
AN10456	-0,10	0,55	0,23	0,17	-0,06	0,74	0,32	0,03	-0,27	0,08	0,04	0,84	NEDD8-specific protease; required for light-dependent development

AN10494	-0,38	0,58	-0,81	0,28	1,05	0,09	1,17	0,07	-0,31	0,71	-1,02	0,13	Has domain(s) with predicted oxidoreductase activity and role in metabolic process
AN10513	-1,30	0,00	-1,09	0,00	-1,01	0,00	-0,62	0,11	0,99	0,01	-0,91	0,01	Has domain(s) with predicted calcium-dependent cysteine-type endopeptidase activity, role in proteolysis and intracellular localization
AN10514	0,81	0,00	-0,01	0,98	0,28	0,36	-0,38	0,17	0,65	0,03	0,05	0,87	Has domain(s) with predicted oxidoreductase activity and role in metabolic process
AN10516	-0,19	0,19	-0,02	0,93	-0,07	0,68	0,33	0,02	0,38	0,01	0,43	0,00	Putative F-box protein with a role in meiosis; NeddH-associated protein; required for ascospore development; transcript is highly expressed during sexual development
AN10519	0,23	0,05	-0,18	0,19	0,26	0,03	-0,09	0,49	0,06	0,73	-0,19	0,15	Ortholog(s) have cytosol, nucleus localization
AN10540	0,62	0,00	0,38	0,11	0,78	0,00	0,34	0,13	-0,60	0,01	0,18	0,48	Ortholog(s) have dipeptidyl-peptidase activity and cytoplasm, nucleus localization
AN10556	0,40	0,02	0,20	0,36	0,40	0,02	0,34	0,06	0,14	0,54	0,24	0,23	Ortholog(s) have cytoplasm, nucleus localization
AN10609	-0,29	0,02	-0,26	0,06	-0,22	0,08	-0,49	0,00	0,53	0,00	0,27	0,04	Ortholog(s) have role in mitochondrial respiratory chain complex III assembly and integral component of mitochondrial inner membrane localization
AN10673	-0,51	0,00	0,01	0,98	-0,64	0,00	-0,09	0,57	0,35	0,01	0,14	0,37	Ortholog(s) have serine-type peptidase activity, role in apoptotic process, cellular lipid metabolic process, cellular response to heat, protein catabolic process and nucleus localization
AN10708	0,33	0,01	-0,20	0,20	0,25	0,06	-0,17	0,26	-0,27	0,06	-0,47	0,00	Ortholog(s) have role in proteasomal ubiquitin-independent protein catabolic process, proteasome assembly, proteasome-mediated ubiquitin-dependent protein catabolic process
AN10722	-0,05	0,66	0,13	0,31	-0,20	0,07	0,09	0,50	-0,02	0,88	-0,01	0,96	Ortholog(s) have ubiquitin-specific protease activity, role in protein deubiquitination, ubiquitin-dependent protein catabolic process via the multivesicular body sorting pathway and cytosol localization
AN10778	0,51	0,03	0,22	0,49	0,52	0,03	0,30	0,27	0,88	0,00	0,60	0,02	Ortholog(s) have mitochondrion localization
AN10788	0,17	0,37	0,16	0,49	0,22	0,23	0,24	0,20	-0,14	0,53	0,32	0,08	Ortholog(s) have ubiquitin-specific protease activity
AN10815	-0,29	0,67	-1,30	0,04	0,34	0,62	-0,65	0,32	0,36	0,63	-1,15	0,06	Has domain(s) with predicted oxidoreductase activity and role in metabolic process
AN10822	-0,48	0,00	-0,03	0,90	-0,55	0,00	-0,07	0,67	-0,01	0,98	-0,01	0,94	SumO conjugation (E2) enzyme
AN10849	-0,12	0,22	0,07	0,58	-0,12	0,26	0,11	0,34	-0,03	0,85	0,17	0,11	Protein with similarity to <i>Saccharomyces cerevisiae</i> Vam6p/Vps39p; plays a role in vacuolar morphogenesis
AN10874	-0,42	0,00	-0,15	0,25	-0,29	0,01	-0,24	0,04	0,03	0,85	-0,14	0,28	Ortholog(s) have ubiquitin-protein transferase activity, role in ER-associated ubiquitin-dependent protein catabolic process and endoplasmic reticulum membrane localization
AN10877	0,27	0,39	0,23	0,57	0,43	0,16	0,51	0,10	0,36	0,30	0,29	0,41	Has domain(s) with predicted role in ubiquitin-dependent protein catabolic process
AN10900	0,00	0,99	0,67	0,28	0,90	0,06	1,78	0,00	0,60	0,27	1,05	0,05	Has domain(s) with predicted serine-type peptidase activity and role in proteolysis
AN10986	0,42	0,52	0,08	0,93	0,01	0,99	-0,36	0,62	-0,45	0,55	-0,41	0,57	Ortholog(s) have carboxypeptidase activity, role in nitrogen compound metabolic process, proteolysis involved in cellular protein catabolic process and fungal-type vacuole lumen localization
AN10994	0,27	0,17	0,17	0,48	-0,01	0,97	0,02	0,93	-0,41	0,04	-0,09	0,71	Ortholog(s) have ubiquitin-protein transferase activity, role in protein autoubiquitination, protein import into peroxisome matrix, receptor recycling, protein monoubiquitination and cytosol, nucleus, peroxisome localization
AN11004	0,33	0,03	0,42	0,01	0,28	0,06	0,64	0,00	-0,07	0,72	0,31	0,04	Ortholog(s) have Atg8 ligase activity, role in C-terminal protein lipidation, CVT pathway, autophagic vacuole assembly, mitochondrion degradation, piecemeal microautophagy of nucleus and cytosol localization
AN11005	0,01	0,97	-0,24	0,09	-0,05	0,73	-0,34	0,01	-0,27	0,04	-0,44	0,00	Ortholog(s) have cytosol, nucleus localization

AN11010	0,13	0,41	-0,03	0,89	-0,08	0,61	-0,31	0,04	-0,11	0,53	-0,25	0,11	Ortholog(s) have Rab GTPase activator activity, role in intracellular protein transport and cell division site, cytosol localization
AN11028	1,32	0,03	-2,08	0,00	1,75	0,00	-0,77	0,23	1,65	0,01	-2,05	0,00	Predicted nucleotide binding protein with oxidoreductase activity and a role in oxidation-reduction; predicted secondary metabolism gene cluster member
AN11055	0,00	0,99	-0,18	0,19	-0,10	0,46	-0,36	0,00	0,01	0,94	-0,16	0,24	Ortholog(s) have protein phosphatase type 1 regulator activity, ubiquitin binding activity
AN11070	0,17	0,42	0,14	0,61	0,14	0,52	0,08	0,75	-0,11	0,68	0,09	0,73	Ortholog(s) have metalloaminopeptidase activity and fungal-type vacuole localization
AN11071	0,82	0,00	0,19	0,63	0,61	0,04	0,04	0,92	0,37	0,26	0,19	0,61	Ortholog(s) have chaperone binding activity
AN11102	0,33	0,00	-0,12	0,43	0,28	0,02	-0,04	0,77	-0,06	0,68	-0,33	0,00	Ortholog(s) have ubiquitin-specific protease activity, role in protein deubiquitination and nucleoplasm, proteasome complex localization
AN11105	0,12	0,87	-1,23	0,04	0,77	0,17	-0,03	0,96	0,82	0,18	-0,58	0,35	Has domain(s) with predicted oxidoreductase activity and role in metabolic process
AN11163	-0,01	0,94	0,03	0,85	-0,07	0,53	-0,18	0,09	-0,24	0,02	-0,22	0,04	Has domain(s) with predicted calcium ion binding, mannosyl-oligosaccharide 1,2-alpha-mannosidase activity and membrane localization
AN11164	0,23	0,14	0,39	0,01	0,06	0,74	0,28	0,08	0,02	0,94	0,11	0,55	Ortholog of <i>A. fumigatus</i> Af293 : Afu7g02110, <i>A. oryzae</i> RIB40 : AO090038000589, <i>Neosartorya fischeri</i> NRRL 181 : NFIA_114840 and <i>Aspergillus wentii</i> : Aspwe1_0579892
AN11218	-1,16	0,04	-0,60	0,41	-0,62	0,28	-0,16	0,84	0,23	0,74	-0,33	0,65	Has domain(s) with predicted ubiquitin-specific protease activity, role in ubiquitin-dependent protein catabolic process and intracellular, membrane localization
AN11218	-1,16	0,04	-0,60	0,41	-0,62	0,28	-0,16	0,84	0,23	0,74	-0,33	0,65	Has domain(s) with predicted ubiquitin-specific protease activity, role in ubiquitin-dependent protein catabolic process and intracellular, membrane localization

**Table S4.** 38 differentially expressed genes in the functional subcategory “14.13 Protein/peptide degradation”.

AspGD	Strain	Regulation	Response	Name	Description in AspGD	Orthologs and best hit in <i>S. cerevisiae</i>	Description Saccharomyces Genome Database
AN0444	1542 2h	down	early (1542)	hulB	HECT Ubiquitin Ligase	HUL4	Protein with similarity to hect domain E3 ubiquitin-protein ligases; not essential for viability; found in association with Trf4 in TRAMP complex
AN0482	1542 2h and AbfA 2h	up	early (1542 and AbfA)		Putative ubiquitin-conjugating enzyme; transcript repressed by nitrate		
AN0709	1542 2h	down	early (1542)	silG	Putative zinc-finger protein; expression upregulated after exposure to farnesol	RPN4	Transcription factor that stimulates expression of proteasome genes; Rpn4p levels are in turn regulated by the 26S proteasome in a negative feedback control mechanism; RPN4 is transcriptionally regulated by various stress responses; relative distribution to the nucleus increases upon DNA replication stress
AN0858	all	up	early (1542 and BglC); continuous (AbfA)	hsp104	Putative chaperone	HSP104	Disaggregase; heat shock protein that cooperates with Ydj1p (Hsp40) and Ssa1p (Hsp70) to refold and reactivate previously denatured, aggregated proteins; responsive to stresses including: heat, ethanol, and sodium arsenite; involved in [PSI+] propagation; protein becomes more abundant and forms cytoplasmic foci in response to DNA replication stress; potentiated Hsp104p variants decrease TDP-43 proteotoxicity by eliminating its cytoplasmic aggregation
AN0927	1542 8h	down	late (1542)		Ortholog(s) have ubiquitin-specific protease activity, role in cellular response to drug, protein deubiquitination and nuclear periphery localization		
AN10513	1542 2h and 8h and AbfA 2h	down	early (abfA) ; continuous (1542)		Has domain(s) with predicted calcium-dependent cysteine-type endopeptidase activity, role in proteolysis and intracellular localization		
AN10900	AbfA	up	late (AbfA)		Has domain(s) with predicted serine-type peptidase activity and role in proteolysis		
AN11028	all	both	early (AbfA);continuous (BglC); late (1542)		Predicted nucleotide binding protein with oxidoreductase activity and a role in oxidation-reduction; predicted secondary metabolism gene cluster member		

<b>AN1163</b>	all	up	early (1542 and AbfA); continuous (BglC)		Putative chaperone; ortholog of <i>S. cerevisiae</i> Hsp78p; expression upregulated after exposure to farnesol	HSP78	Oligomeric mitochondrial matrix chaperone; cooperates with Ssc1p in mitochondrial thermotolerance after heat shock; able to prevent the aggregation of misfolded proteins as well as resolubilize protein aggregates
<b>AN1426</b>	1542 8h and AbfA 8h	down	late (1542 and AbfA)		Ortholog(s) have serine-type carboxypeptidase activity	YBR139W	Putative serine type carboxypeptidase; role in phytochelatin synthesis; green fluorescent protein (GFP)-fusion protein localizes to the vacuole; expression induced by nitrogen limitation in a GLN3, GAT1-independent manner
<b>AN1857</b>	1542 2h and AbfA 2 and 8h	up	early (1542); continuous (AbfA)		Putative kynureninase with a predicted role in aromatic amino acid biosynthesis	BNA5	Kynureninase; required for the de novo biosynthesis of NAD from tryptophan via kynurenine; expression regulated by Hst1p
<b>AN1982</b>	1542 2h and AbfA 2h	up	early (1542 and AbfA)		Ortholog of <i>A. nidulans</i> FGSC A4 : AN0814/cdc20, <i>A. fumigatus</i> Af293 : Afu1g14730, Afu4g10570, <i>A. niger</i> CBS 513.88 : An04g06100, An01g12750 and <i>A. oryzae</i> RIB40 : AO090003001154, AO090003000500	AMA1	Activator of meiotic anaphase promoting complex (APC/C); Cdc20p family member; required for initiation of spore wall assembly; required for Clb1p degradation during meiosis; prevents premature assembly of the meiosis I spindle, required for DSB induced prophase I arrest
<b>AN2000</b>	AbfA 2h	up	early (AbfA)	ubi4	Polyubiquitin, contains four head to tail repeats of ubiquitin; transcript upregulated in response to camptothecin	UBI4	Ubiquitin; becomes conjugated to proteins, marking them for selective degradation via the ubiquitin-26S proteasome system; essential for the cellular stress response; encoded as a polyubiquitin precursor comprised of 5 head-to-tail repeats; protein abundance increases in response to DNA replication stress
<b>AN2045</b>	1542 8h	down	late (1542)		Has domain(s) with predicted calcium ion binding, mannosyl-oligosaccharide 1,2-alpha-mannosidase activity and membrane localization	MNS1	Alpha-1,2-mannosidase; involved in ER-associated protein degradation (ERAD); catalyzes the removal of one mannose residue from a glycosylated protein, converting the modification from Man9GlcNAc to Man8GlcNAc; catalyzes the last step in glycoprotein maturation in the ER and is critical for ER protein degradation
<b>AN2366</b>	1542 8h and AbfA 8h	down	late (1542 and AbfA)		Putative trypsin-like protease with a role in the proteolytic cleavage of NmrA		
<b>AN2555</b>	1542 2h and BglC 2h	up	early (1542 and BglC)		Ortholog(s) have serine-type carboxypeptidase activity	KEX1	Cell death protease essential for hypochlorite-induced apoptosis; involved in the processing of killer toxin and alpha factor precursor; cleaves Lys and Arg residues from the C-terminus of peptides and proteins
<b>AN2861</b>	AbfA 2h	down	early (AbfA)		Putative F-box protein	MET30	F-box protein containing five copies of the WD40 motif; controls cell cycle function, sulfur metabolism, and methionine biosynthesis as part of the ubiquitin ligase complex; interacts with and regulates Met4p, localizes within the nucleus; dissociation of Met30p from SCF complex in response to cadmium stress is regulated by Cdc48p

<b>AN3226</b>	all	up	early (1542 and BglC); continuous (AbfA)	pkfC	Has domain protein; aspernidine A secondary metabolism gene cluster member; protein levels decrease in response to farnesol	ENV9	Protein proposed to be involved in vacuolar functions; mutant shows defect in CPY processing and defects in vacuolar morphology; has similarity to oxidoreductases, found in lipid particles; required for replication of Brome mosaic virus in <i>S. cerevisiae</i> , a model system for studying replication of positive-strand RNA viruses in their natural hosts
<b>AN3305</b>	AbfA and BglC 8h	up	late (BglC and AbfA)		Has domain(s) with predicted oxidoreductase activity and role in metabolic process	ENV9	Protein proposed to be involved in vacuolar functions; mutant shows defect in CPY processing and defects in vacuolar morphology; has similarity to oxidoreductases, found in lipid particles; required for replication of Brome mosaic virus in <i>S. cerevisiae</i> , a model system for studying replication of positive-strand RNA viruses in their natural hosts
<b>AN3321</b>	BglC 2h	up	early (BglC)		Has domain(s) with predicted aspartic-type endopeptidase activity and role in proteolysis		
<b>AN3393</b>	BglC 8h	up	late (BglC)	pepI	Protein with similarity to neutral metalloprotease II		
<b>AN3493</b>	all	up 2h, down 8h	continuous (all)		Predicted threonine-type endopeptidase; inp secondary metabolite gene cluster member	PRE7	Beta 6 subunit of the 20S proteasome
<b>AN3787</b>	1542 2h and AbfA 2h	down	early (1542 and AbfA)		Ortholog(s) have glycoprotein binding, metal ion binding, misfolded protein binding, peptide-N4-(N-acetyl-beta-glucosaminyl)asparagine amidase activity, structural constituent of cell wall activity	PNG1	Conserved peptide N-glycanase; deglycosylating enzyme that cleaves N-glycans that are attached to misfolded ERAD substrate glycoproteins prior to proteasome-dependent degradation; localizes to the cytoplasm and nucleus; activity is enhanced by interaction with Rad23p; human ortholog NGLY1 is associated with a syndrome characterized by developmental delays, epilepsy, absence of tears and liver disease
<b>AN5055</b>	BglC 8h	up	late (BglC)		Has domain(s) with predicted aminopeptidase activity, metalloexopeptidase activity and role in cellular process, proteolysis	MAPI	Methionine aminopeptidase; catalyzes the cotranslational removal of N-terminal methionine from nascent polypeptides; function is partially redundant with that of Map2p
<b>AN5558</b>	all	both	early (1542 and AbfA); late (BglC)	prtA	Broad specificity thermostable alkaline protease; extracellular; regulated by nitrogen, carbon and sulfur metabolite repression; transcript repressed by light in developmentally competent mycelia	PRB1	Vacuolar proteinase B (yscB) with H3 N-terminal endopeptidase activity; serine protease of the subtilisin family; involved in protein degradation in the vacuole and required for full protein degradation during sporulation; activity inhibited by Pbi2p; protein abundance increases in response to DNA replication stress; PRB1 has a paralog, YSP3, that arose from the whole genome duplication
<b>AN5619</b>	1542 2h	down	early (1542)		Ortholog(s) have metallopeptidase activity, role in ascospore wall assembly and ascospore wall, endoplasmic reticulum membrane localization		
<b>AN5810</b>	1542 2h	up	early (1542)	pepP	Prolidase specific for cleavage of X-Pro dipeptides	YFR006W	Putative X-Pro aminopeptidase; green fluorescent protein (GFP)-fusion protein localizes to the cytoplasm; YFR006W is not an essential gene



<b>AN6064</b>	1542 2h	up	early (1542)		Ortholog(s) have hydrolase activity, acting on ester bonds activity	IAH1	Isoamyl acetate-hydrolyzing esterase; required in balance with alcohol acetyltransferase to maintain optimal amounts of isoamyl acetate, which is particularly important in sake brewing
<b>AN6399</b>	AbfA 2h	up	early (AbfA)		Putative bleomycin hydrolase	LAP3	Cysteine aminopeptidase with homocysteine-thiolactonase activity; protects cells against homocysteine toxicity; has bleomycin hydrolase activity in vitro; transcription is regulated by galactose via Gal4p; orthologous to human BLMH
<b>AN6426</b>	1542 8h and BglC 2h	both	early (BglC); late (1542)		Has domain(s) with predicted metallopeptidase activity		
<b>AN6931</b>	all	down	late (all)		Has domain(s) with predicted oxidoreductase activity and role in metabolic process	ENV9	Protein proposed to be involved in vacuolar functions; mutant shows defect in CPY processing and defects in vacuolar morphology; has similarity to oxidoreductases, found in lipid particles; required for replication of Brome mosaic virus in <i>S. cerevisiae</i> , a model system for studying replication of positive-strand RNA viruses in their natural hosts
<b>AN7201</b>	AbfA 8h	up	late (AbfA)		Ortholog(s) have role in proteolysis		
<b>AN7491</b>	AbfA 2h	up	early (AbfA)		Putative ubiquitin C-terminal hydrolase; ortholog of <i>S. cerevisiae</i> Yuh1p which has role in protein deubiquitination; expression upregulated after exposure to farnesol	YUH1	Ubiquitin C-terminal hydrolase; cleaves ubiquitin-protein fusions to generate monomeric ubiquitin; hydrolyzes the peptide bond at the C-terminus of ubiquitin; also the major processing enzyme for the ubiquitin-like protein Rub1p
<b>AN7577</b>	1542 and BglC 8h	down	late (1542 and BglC)		Has domain(s) with predicted acid-amino acid ligase activity	UBC7	Ubiquitin conjugating enzyme; involved in the ER-associated protein degradation (ERAD) pathway and in the inner nuclear membrane-associated degradation (INMAD) pathway; requires Cue1p for recruitment to the ER membrane; proposed to be involved in chromatin assembly
<b>AN7962</b>	all	both	early (1542); continuous (AbfA); late (BglC)	pepJ	Extracellular deuterolysin-type metallo-proteinase		
<b>AN8074</b>	AbfA 2h	up	early (AbfA)		Has domain(s) with predicted ubiquitinyl hydrolase activity, zinc ion binding activity and role in protein deubiquitination, ubiquitin-dependent protein catabolic process	UBP15	Ubiquitin-specific protease involved in protein deubiquitination; forms a complex with AAA peroxins Pex1p and Pex6p; deubiquitinates mono- and polyubiquitinated forms of Pex5p; deubiquitinates Clb5p, counteracting APC activity, and facilitating both Clb5p accumulation and S phase entry; physically interacts with anaphase-promoting complex/cyclosome (APC/C) activator, Cdh1p; catalytic activity regulated by an N-terminal TRAF-like domain and and C-terminal sequences

<b>AN8468</b>	1542 and BglC 8h	both	late (1542 and BglC)		Ortholog of <i>A. nidulans</i> FGSC A4 : AN2021, <i>A. fumigatus</i> Af293 : Afu7g00550 and <i>A. niger</i> CBS 513.88 : An15g05630, An11g03460, An11g07530, An04g03850, An09g00640	RSA4	WD-repeat protein involved in ribosome biogenesis; may interact with ribosomes; required for maturation and efficient intra-nuclear transport or pre-60S ribosomal subunits, localizes to the nucleolus
<b>AN8585</b>	AbfA and BglC 2h	up	early (AbfA and BglC)		Has domain(s) with predicted oxidoreductase activity and role in metabolic process	ENV9	Protein proposed to be involved in vacuolar functions; mutant shows defect in CPY processing and defects in vacuolar morphology; has similarity to oxidoreductases, found in lipid particles; required for replication of Brome mosaic virus in <i>S. cerevisiae</i> , a model system for studying replication of positive-strand RNA viruses in their natural hosts

**Table S5.** 43 genes related to the functional subcategory “14.07.02.02 N-directed glycosylation, deglycosylation”.

Gene	1542 2h FC	padj	1542 8h FC	padj	AbfA 2h FC	padj	AbfA 8h FC	padj	BglC 2h FC	padj	BglC 8h FC	padj	Description
AN0086	-0,63	0,00	0,02	0,91	-0,73	0,00	-0,08	0,58	0,03	0,87	0,14	0,30	Ortholog(s) have role in fungal-type cell wall organization and cytosol, nucleus localization
AN0104	-0,03	0,88	0,10	0,65	0,01	0,98	-0,24	0,18	-0,33	0,06	0,19	0,27	Ortholog(s) have endoplasmic reticulum localization
AN0551	0,02	0,95	0,71	0,01	-0,17	0,56	0,01	0,97	-0,54	0,05	0,41	0,15	Putative mannosyl-oligosaccharide 1,2-alpha-mannosidase with a predicted role in mannose polymer metabolism
AN10118	-0,59	0,00	0,28	0,22	-0,47	0,01	0,20	0,38	-0,16	0,49	0,36	0,09	Ortholog(s) have endoplasmic reticulum localization
AN10265	-0,48	0,00	0,17	0,40	-0,72	0,00	0,05	0,80	-0,18	0,33	0,06	0,78	Ortholog(s) have alpha-1,6-mannosyltransferase activity, role in protein N-linked glycosylation and Golgi trans cisterna, alpha-1,6-mannosyltransferase complex, endoplasmic reticulum localization
AN1048	0,00	0,99	0,07	0,81	-0,31	0,09	-0,13	0,55	-0,39	0,05	-0,24	0,26	Ortholog of <i>A. fumigatus</i> Af293 : Afu1g12630, <i>A. niger</i> CBS 513.88 : An08g05380, <i>A. oryzae</i> RIB40 : AO090113000130, <i>Aspergillus wentii</i> : Aspwe1_0111448 and <i>Aspergillus terreus</i> NIH2624 : ATET_00454
AN10496	-0,63	0,01	-0,18	0,58	-0,48	0,05	-0,18	0,52	0,52	0,04	0,22	0,45	Putative regulator of mannosylphosphorylation
AN10702	0,07	0,71	0,17	0,40	0,04	0,83	0,05	0,82	-0,27	0,12	-0,07	0,76	Ortholog(s) have alpha-1,4-glucosidase activity, role in polysaccharide biosynthetic process, protein N-linked glycosylation and endoplasmic reticulum lumen, glucosidase II complex localization
AN10710	-0,28	0,13	0,06	0,84	-0,30	0,11	-0,06	0,81	-0,65	0,00	-0,13	0,56	Ortholog(s) have phosphomannomutase activity, role in ER to Golgi vesicle-mediated transport, establishment or maintenance of cell polarity, nuclear envelope organization, protein targeting to ER and cytosol, nucleus localization
AN11141	-0,21	0,08	-0,06	0,75	-0,46	0,00	-0,28	0,03	-0,33	0,01	-0,11	0,47	Ortholog(s) have acetylglucosaminyltransferase activity, role in protein N-linked glycosylation and Golgi medial cisterna localization
AN1455	-0,67	0,00	0,00	1,00	-0,26	0,05	0,00	0,98	-0,09	0,58	0,20	0,17	Ortholog(s) have dolichyl-diphosphooligosaccharide-protein glycotransferase activity, role in protein N-linked glycosylation and oligosaccharyltransferase complex, plasma membrane localization
AN1620	-0,24	0,50	-1,55	0,00	0,08	0,85	-1,26	0,00	0,74	0,03	-0,12	0,78	Ortholog of <i>A. nidulans</i> FGSC A4 : AN2626, <i>A. fumigatus</i> Af293 : Afu8g02040/och3, <i>A. niger</i> CBS 513.88 : An03g01090/hocA, An05g02320 and <i>A. oryzae</i> RIB40 : AO090010000615
AN1683	-0,47	0,00	0,18	0,35	-0,63	0,00	-0,42	0,01	-0,02	0,94	0,17	0,35	Putative oligosaccharyltransferase delta subunit; ortholog of <i>S. cerevisiae</i> Swp1p
AN1969	-0,13	0,75	0,30	0,50	0,05	0,90	0,60	0,10	-0,21	0,63	-0,13	0,79	Ortholog(s) have alpha-1,6-mannosyltransferase activity, role in protein glycosylation and alpha-1,6-mannosyltransferase complex, endoplasmic reticulum localization

AN2626	-0,10	0,70	0,10	0,76	0,08	0,77	0,23	0,38	0,25	0,35	0,23	0,39	Ortholog of <i>A. nidulans</i> FGSC A4 : AN1620, <i>A. fumigatus</i> Af293 : Afu8g02040/och3, <i>A. niger</i> CBS 513.88 : An03g01090/hocA, An05g02320 and <i>A. oryzae</i> RIB40 : AO090010000615
AN2752	-0,33	0,04	-0,35	0,04	-0,20	0,24	-0,28	0,09	-0,03	0,90	-0,35	0,03	Ortholog(s) have alpha-1,2-mannosyltransferase activity
AN3588	0,04	0,83	-0,16	0,28	-0,16	0,24	-0,38	0,00	0,13	0,39	-0,08	0,62	Ortholog(s) have alpha-1,6-mannosyltransferase activity, role in dolichol-linked oligosaccharide biosynthetic process, protein glycosylation and endoplasmic reticulum localization
AN4031	0,22	0,15	0,03	0,89	0,17	0,29	-0,17	0,30	-0,17	0,34	0,10	0,57	Putative oligosaccharyltransferase epsilon subunit; ortholog of <i>S. cerevisiae</i> Ost2p
AN4395	-0,37	0,00	0,09	0,51	-0,70	0,00	-0,29	0,01	-0,05	0,71	0,05	0,71	Ortholog of <i>A. fumigatus</i> Af293 : Afu4g06870, <i>A. niger</i> CBS 513.88 : An04g01260, <i>A. oryzae</i> RIB40 : AO090023000901, <i>Aspergillus wentii</i> : Aspwe1_0023285 and <i>Aspergillus sydowii</i> : Aspsy1_0545881
AN4683	-0,47	0,00	-0,12	0,55	-0,25	0,11	-0,34	0,03	-0,17	0,35	0,16	0,37	Putative oligosaccharyltransferase beta subunit; ortholog of <i>S. cerevisiae</i> Wbp1p
AN4716	-0,32	0,10	-0,61	0,00	-0,36	0,06	-0,47	0,02	0,14	0,56	-0,03	0,90	Ortholog(s) have alpha-1,6-mannosyltransferase activity
AN4864	-0,52	0,00	-0,03	0,92	-0,45	0,01	-0,16	0,45	-0,11	0,62	0,00	0,99	Putative glucosyltransferase; locus contains the conserved upstream open reading frame (uORF) AN4864-uORF
AN4947	-0,58	0,00	-0,10	0,66	-0,45	0,00	-0,39	0,02	0,27	0,12	0,12	0,54	Ortholog(s) have endoplasmic reticulum, plasma membrane localization
AN5346	-0,12	0,52	0,13	0,56	-0,19	0,29	0,03	0,91	0,15	0,47	0,32	0,07	Ortholog(s) have role in establishment or maintenance of cell polarity and endoplasmic reticulum localization
AN5748	-0,34	0,02	-0,10	0,63	-0,46	0,00	-0,42	0,01	-0,08	0,70	-0,08	0,69	Putative mannosyl-oligosaccharide 1,2-alpha-mannosidase with a predicted role in mannose polymer metabolism
AN5788	0,03	0,84	0,04	0,83	-0,14	0,31	0,28	0,04	-0,04	0,81	0,04	0,85	Ortholog(s) have COPII adaptor activity and role in ER to Golgi vesicle-mediated transport, fungal-type cell wall organization, protein glycosylation, protein retention in Golgi apparatus
AN5888	-0,36	0,08	-0,10	0,73	-0,08	0,75	-0,21	0,41	-0,18	0,47	-0,07	0,82	Ortholog(s) have UDP-N-acetylglucosamine-dolichyl-phosphate N-acetylglucosaminophosphotransferase activity and role in N-glycan processing, aerobic respiration, cellular response to drug, dolichyl diphosphate biosynthetic process
AN5902	-0,06	0,81	-0,03	0,93	-0,31	0,12	-0,35	0,09	-0,13	0,61	-0,11	0,65	Ortholog(s) have dolichyl-phosphate-glucose-glycolipid alpha-glucosyltransferase activity, role in protein N-linked glycosylation and endoplasmic reticulum membrane localization
AN6170	-0,04	0,81	0,02	0,94	0,12	0,37	-0,06	0,68	-0,16	0,25	-0,02	0,90	Ortholog(s) have chaperone binding activity, role in ER-associated ubiquitin-dependent protein catabolic process, protein folding in endoplasmic reticulum, response to unfolded protein and endoplasmic reticulum lumen localization
AN6606	-0,20	0,18	-0,04	0,86	-0,34	0,02	-0,40	0,01	0,09	0,64	0,08	0,68	Ortholog(s) have role in N-glycan processing, post-translational protein modification and endoplasmic reticulum localization
AN6610	0,98	0,00	0,24	0,16	0,63	0,00	0,27	0,08	-0,19	0,30	0,11	0,55	Putative phosphatidylglycerol phosphate phosphatase with a predicted role in phospholipid metabolism
AN6874	0,08	0,68	-0,10	0,64	-0,06	0,73	-0,14	0,45	0,15	0,45	0,21	0,24	Putative mannosyltransferase; transcript levels increase during the unfolded-protein response (UPR); <i>S. cerevisiae</i> ortholog Alg2p has glycolipid 6-alpha-mannosyltransferase activity

AN7301	-0,30	0,12	-0,13	0,63	-0,41	0,03	-0,34	0,09	-0,34	0,10	-0,36	0,07	Putative glucosyltransferase; ortholog of <i>S. cerevisiae</i> Alg8p; expression reduced after exposure to farnesol
AN7425	-0,31	0,09	-0,20	0,38	-0,36	0,05	-0,36	0,06	0,20	0,34	-0,31	0,12	Has domain(s) with predicted lipid transporter activity, role in lipid transport and integral component of membrane localization
AN7472	-0,15	0,39	0,01	0,97	-0,03	0,87	-0,18	0,35	-0,28	0,13	-0,06	0,80	Ortholog(s) have dolichyl-diphosphooligosaccharide-protein glycotransferase activity, role in protein N-linked glycosylation via asparagine and oligosaccharyltransferase complex, plasma membrane localization
AN7534	-1,39	0,00	-0,28	0,25	-1,13	0,00	-0,14	0,55	0,12	0,65	0,04	0,88	Ortholog of <i>A. fumigatus</i> Af293 : Afu1g01380/och4, <i>A. niger</i> CBS 513.88 : An14g07140, An12g07020, <i>Aspergillus versicolor</i> : Aspve1_0085820 and <i>Aspergillus clavatus</i> NRRL 1 : ACLA_033030
AN7562	0,01	0,98	0,47	0,04	0,08	0,75	0,56	0,01	-0,11	0,68	0,52	0,01	Ortholog(s) have alpha-1,6-mannosyltransferase activity, role in ascospore formation, barrier septum assembly and alpha-1,6-mannosyltransferase complex localization
AN7672	-0,84	0,00	-0,11	0,69	-0,66	0,00	-0,29	0,17	0,17	0,47	0,27	0,23	Ortholog(s) have alpha-1,6-mannosyltransferase activity, mannosyltransferase activity
AN7715	0,17	0,37	-0,07	0,78	0,30	0,10	0,03	0,91	-0,01	0,98	-0,06	0,81	Ortholog(s) have dolichyl-phosphate beta-glucosyltransferase activity and endoplasmic reticulum membrane localization
AN8119	-0,53	0,00	-0,09	0,68	-0,61	0,00	-0,37	0,02	0,05	0,81	-0,10	0,62	Ortholog(s) have mannosylphosphate transferase activity, mannosyltransferase activity
AN8848	-0,72	0,00	-0,11	0,70	-0,78	0,00	-0,43	0,03	-0,08	0,75	-0,15	0,54	Putative GDP-mannose transporter
AN8986	0,56	0,25	-1,15	0,01	0,39	0,45	-0,30	0,57	0,76	0,14	-1,41	0,00	Ortholog of <i>A. oryzae</i> RIB40 : AO090005001017, <i>Aspergillus versicolor</i> : Aspve1_0047420, <i>Aspergillus clavatus</i> NRRL 1 : ACLA_018770 and <i>Aspergillus sydowii</i> : Aspsy1_0051004
AN9298	-0,90	0,00	-0,78	0,00	-0,70	0,00	-0,60	0,00	-0,11	0,61	-0,25	0,24	Putative GDP-mannose transporter

**Table S6.** 3 differentially expressed genes in the functional subcategory “14.07.02.02 N-directed glycosylation, deglycosylation”.

AspGD	Strain	Regulation	Response	Name	Description in AspGD	Orthologs and best hit in <i>S. cerevisiae</i>	Description Saccharomyces Genome Database
AN8986	BglC 8h	down	late (BglC)		Ortholog of <i>A. oryzae</i> RIB40 : AO090005001017, <i>Aspergillus versicolor</i> : Aspve1_0047420, <i>Aspergillus clavatus</i> NRRL 1 : ACLA_018770 and <i>Aspergillus sydowii</i> : Aspsy1_0051004	OCH1	Mannosyltransferase of the cis-Golgi apparatus; initiates the polymannose outer chain elongation of N-linked oligosaccharides of glycoproteins
AN7534	1542 and AbfA 2h	down	early (1542 and AbfA)		Ortholog of <i>A. fumigatus</i> Af293 : Afu1g01380/och4, <i>A. niger</i> CBS 513.88 : An14g07140, An12g07020, <i>Aspergillus versicolor</i> : Aspve1_0085820 and <i>Aspergillus clavatus</i> NRRL 1 : ACLA_033030	HOC1	Alpha-1,6-mannosyltransferase; involved in cell wall mannan biosynthesis; subunit of a Golgi-localized complex that also contains Anp1p, Mnn9p, Mnn11p, and Mnn10p; identified as a suppressor of a cell lysis sensitive <i>pkc1-371</i> allele
AN1620	1542 and AbfA 8h	down	late (1542 and AbfA)		Ortholog of <i>A. nidulans</i> FGSC A4 : AN2626, <i>A. fumigatus</i> Af293 : Afu8g02040/och3, <i>A. niger</i> CBS 513.88 : An03g01090/hocA, An05g02320 and <i>A. oryzae</i> RIB40 : AO090010000615	HOC1	Alpha-1,6-mannosyltransferase; involved in cell wall mannan biosynthesis; subunit of a Golgi-localized complex that also contains Anp1p, Mnn9p, Mnn11p, and Mnn10p; identified as a suppressor of a cell lysis sensitive <i>pkc1-371</i> allele

**Additional file 2: Secretory pathway analysis of the differentially expressed genes obtained from the RNA-seq data.** Liu et al. (2014) defined a list of genes of protein secretion pathway of *A. oryzae* using the secretory model of *S. cerevisiae* as a scaffold. Based on this list it were found the *A. nidulans* homologous genes by using the AspGD data. **Table S7. 374 genes related to the *A. nidulans* secretory pathway and the transcriptional response to heterologous protein secretion.** This table contains Fold Change (FC) values of all three *A. nidulans* heterologous protein (1542, AbfA and BglC) secretor strains with 2 and 8 hours of induction. For each FC value there is a statistic p-value (padj) from t test. **Tables S8. 17 differentially expressed genes related to secretory pathway and its transcriptional response characterization.** This table contains the differentially expressed genes and its transcriptional responses characterization. Differentially expressed genes were obtained using the FC filters  $(\log_2) \leq -1.0$  or  $\geq 1.0$  and p-value  $\leq 0.01$ .

**Table S7.** 374 genes related to the *A. nidulans* secretory pathway and the transcriptional response to heterologous protein secretion.

Genes	1542 2h FC	padj	1542 8h FC	padj	AbfA 2h FC	padj	AbfA 8h FC	padj	BglC 2h FC	padj	BglC 8h FC	padj	AspGD Description
AN0049	-0,07	0,76	-0,15	0,55	-0,29	0,15	-0,27	0,20	0,25	0,26	0,23	0,28	Ortholog(s) have endoplasmic reticulum localization
AN0068	0,18	0,30	-0,39	0,02	0,13	0,46	-0,59	0,00	-0,53	0,00	-0,67	0,00	Has domain(s) with predicted 7S RNA binding activity, role in SRP-dependent cotranslational protein targeting to membrane, negative regulation of translational elongation and signal recognition particle localization
AN0075	-0,40	0,00	-0,08	0,63	-0,21	0,09	-0,19	0,17	-0,07	0,64	0,03	0,86	Putative protein disulfide isomerase
AN0086	-0,63	0,00	0,02	0,91	-0,73	0,00	-0,08	0,58	0,03	0,87	0,14	0,30	Ortholog(s) have role in fungal-type cell wall organization and cytosol, nucleus localization
AN0089	0,25	0,16	0,07	0,81	0,29	0,10	0,18	0,36	0,08	0,73	0,11	0,64	Putative small GTPase involved in endosomal maturation and vacuolar biogenesis
AN0104	-0,03	0,88	0,10	0,65	0,01	0,98	-0,24	0,18	-0,33	0,06	0,19	0,27	Ortholog(s) have endoplasmic reticulum localization
AN0112	-0,30	0,03	-0,12	0,51	-0,24	0,08	-0,26	0,07	-0,27	0,07	-0,21	0,17	Putative guanine nucleotide exchange factor for ADP ribosylation factors (ARFs)
AN0140	0,23	0,08	-0,13	0,44	-0,01	0,97	-0,40	0,00	-0,40	0,00	-0,38	0,00	Protein with a predicted role in actin assembly; similar to <i>Saccharomyces cerevisiae</i> Arp3p
AN0165	0,05	0,79	0,06	0,75	0,11	0,49	0,10	0,55	-0,01	0,97	0,13	0,41	Ortholog(s) have role in Golgi to vacuole transport, protein targeting to vacuole and AP-3 adaptor complex, cytosol, nucleus localization
AN0170	0,23	0,38	0,09	0,80	0,16	0,55	0,02	0,95	0,08	0,81	0,04	0,91	Thioredoxin; predicted role in cell redox homeostasis; required for conidiation; expression upregulated after exposure to farnesol
AN0182	-0,46	0,00	0,10	0,57	-0,62	0,00	-0,23	0,10	0,08	0,63	0,22	0,14	Small monomeric GTPase of the Ras superfamily involved in regulation of development; involved in conidiophore formation and conidial germination
AN0235	-0,02	0,93	0,29	0,12	0,06	0,75	0,17	0,36	-0,09	0,67	0,24	0,20	Putative serine-threonine kinase with a predicted role in the endoplasmic reticulum (ER) unfolded protein response (UPR); ortholog of <i>S. cerevisiae</i> Ire1p; mutants are inviable and produce swollen hyphae
AN0248	-0,54	0,00	-0,25	0,27	-0,06	0,78	0,05	0,85	-0,28	0,19	-0,01	0,98	Putative protein disulfide isomerase; pdiB mRNA levels increase in the presence of farnesol
AN0261	-0,25	0,01	-0,01	0,93	-0,25	0,01	-0,21	0,05	-0,30	0,00	-0,04	0,76	COPII coat component; considered a prototypic marker of transitional ER (endoplasmic reticulum); localizes to a cytosolic haze and to numerous small foci that predominate near the hyphal tips
AN0295	-0,22	0,10	-0,40	0,00	0,10	0,49	-0,26	0,06	0,28	0,05	-0,06	0,75	Ortholog(s) have role in ER-associated misfolded protein catabolic process and cytoplasm-associated proteasomal ubiquitin-dependent protein catabolic process, more
AN0306	0,28	0,01	-0,28	0,01	0,28	0,01	-0,14	0,23	-0,26	0,02	-0,36	0,00	Ortholog(s) have role in Arp2/3 complex-mediated actin nucleation and Arp2/3 protein complex, actin cortical patch, cell division site, cell tip, cytosol, nucleus localization
AN0316	-0,40	0,00	0,13	0,46	-0,21	0,14	-0,09	0,60	-0,39	0,01	0,17	0,28	Alpha-tubulin, forms a heterodimer with beta-tubulin that promotes microtubule assembly
AN0329	-0,02	0,89	-0,22	0,15	0,26	0,05	-0,07	0,69	0,11	0,49	0,01	0,96	Ortholog(s) have polyubiquitin binding activity



AN0347	-0,30	0,03	-0,10	0,63	-0,39	0,01	-0,32	0,03	-0,15	0,38	-0,11	0,54	Putative GTPase with a predicted role in intra-Golgi transport; transcript levels increase during the unfolded-protein response (UPR)
AN0411	-0,01	0,93	-0,05	0,71	-0,09	0,38	-0,16	0,11	-0,02	0,89	-0,08	0,51	Putative GTPase with a predicted role in ER to Golgi transport
AN0417	-0,51	0,00	0,29	0,14	-0,41	0,01	0,06	0,79	0,07	0,74	0,53	0,00	Putative protein translocation complex subunit; expression reduced after exposure to farnesol
AN0462	-0,24	0,02	-0,03	0,85	-0,16	0,14	-0,04	0,77	-0,12	0,35	-0,08	0,54	Predicted exocyst complex component with similarity to <i>Saccharomyces cerevisiae</i> Sec3p; SecC-GFP localizes to the apex of the hyphal tip
AN0560	0,37	0,00	0,09	0,54	0,40	0,00	0,06	0,67	-0,32	0,01	0,04	0,81	Ortholog(s) have role in Golgi to plasma membrane transport, exocyst assembly, exocyst localization, spliceosomal complex assembly
AN0571	0,26	0,08	-0,05	0,82	0,11	0,51	0,02	0,92	0,28	0,08	0,19	0,25	Ortholog(s) have cell septum, fungal-type vacuole, late endosome, plasma membrane localization
AN0591	0,36	0,22	0,37	0,29	0,34	0,26	0,35	0,28	0,32	0,34	0,41	0,20	Ortholog(s) have cytosol, nucleus localization
AN0634	0,23	0,06	-0,01	0,96	0,18	0,16	0,06	0,68	0,00	0,99	-0,01	0,95	Predicted ADP ribosylation factor GTPase
AN0636	-0,04	0,84	-0,06	0,78	-0,08	0,64	-0,28	0,07	-0,02	0,92	-0,05	0,80	Ortholog(s) have acetylglucosaminyltransferase activity and role in GPI anchor biosynthetic process, conidium formation, establishment or maintenance of cell polarity, fungal-type cell wall biogenesis, regulation of growth rate
AN0651	-0,47	0,01	-0,18	0,45	-0,65	0,00	-0,47	0,01	-0,22	0,31	-0,26	0,21	Alpha subunit of a heterotrimeric G protein composed of FadA, SfaD, GpgA and involved in regulation of proliferation and conidiophore development; mutant produces increased amounts of extracellular proteinase during carbon starvation
AN0665	-0,36	0,00	0,05	0,76	-0,33	0,00	0,04	0,80	-0,18	0,14	0,11	0,42	Coatomer subunit epsilon involved in vesicle transport; mutants are defective in cleistothecium formation
AN0673	0,14	0,37	-0,20	0,27	-0,07	0,70	-0,34	0,02	-0,36	0,02	-0,34	0,03	Protein with a predicted role in actin assembly; similar to <i>Saccharomyces cerevisiae</i> Arp2p
AN0706	-0,39	0,00	0,09	0,52	-0,32	0,00	0,00	0,99	-0,19	0,09	0,11	0,38	Ortholog(s) have role in ER to Golgi vesicle-mediated transport, Golgi vesicle docking, SNARE complex assembly and ER to Golgi transport vesicle membrane, Golgi membrane localization
AN0770	0,29	0,01	-0,41	0,00	0,11	0,39	-0,51	0,00	-0,01	0,94	-0,33	0,00	Ortholog(s) have Dsc E3 ubiquitin ligase complex, endoplasmic reticulum localization
AN0810	-0,02	0,86	0,12	0,20	-0,01	0,95	-0,12	0,19	-0,12	0,20	0,08	0,36	Protein with a predicted role in ER-associated protein degradation
AN0819	0,33	0,03	-0,23	0,22	0,47	0,00	-0,17	0,34	0,08	0,70	0,06	0,78	Ortholog(s) have endoplasmic reticulum, plasma membrane localization
AN0827	-0,13	0,33	-0,09	0,58	-0,21	0,09	-0,28	0,03	-0,11	0,46	0,00	0,98	Ortholog(s) have glucosaminyl-phosphatidylinositol O-acyltransferase activity and role in GPI anchor biosynthetic process, cellular response to drug
AN0834	-0,61	0,00	0,25	0,13	-0,17	0,24	0,35	0,01	-0,43	0,00	0,27	0,07	Putative ER protein-translocation complex subunit; transcript levels increase during the unfolded-protein response (UPR); ortholog of <i>S. cerevisiae</i> Sec63p
AN0847	-0,25	0,03	0,08	0,61	-0,01	0,93	0,10	0,47	-0,39	0,00	-0,11	0,43	Putative chaperone of the endoplasmic reticulum (ER) lumen
AN0861	-0,33	0,00	-0,27	0,04	-0,26	0,03	-0,20	0,13	0,16	0,25	0,06	0,73	Ortholog of <i>A. fumigatus</i> Af293 : Afu1g15250, <i>A. oryzae</i> RIB40 : AO090005001206, <i>Aspergillus wentii</i> : Aspwe1_0051149, <i>Aspergillus sydowii</i> : Aspsy1_0122516 and <i>Aspergillus terreus</i> NIH2624 : ATET_00827

AN0871	0,22	0,29	-0,28	0,22	0,31	0,11	-0,08	0,76	-0,30	0,16	-0,18	0,46	Ortholog(s) have GPI-anchor transamidase activity, role in attachment of GPI anchor to protein and GPI-anchor transamidase complex localization
AN0922	-0,35	0,00	-0,05	0,78	-0,32	0,00	-0,14	0,23	-0,11	0,42	0,05	0,74	Ortholog(s) have role in ER to Golgi vesicle-mediated transport, Golgi inheritance, Golgi localization, retrograde vesicle-mediated transport, Golgi to ER and COPI vesicle coat localization
AN0930	-0,44	0,03	0,03	0,92	-0,28	0,19	0,27	0,22	0,61	0,00	0,73	0,00	Ortholog(s) have endoplasmic reticulum localization
AN1002	0,00	0,98	-0,25	0,04	-0,26	0,02	-0,24	0,04	-0,11	0,41	-0,01	0,95	Ortholog(s) have role in Golgi to plasma membrane transport, endoplasmic reticulum inheritance, establishment or maintenance of cell polarity, exocyst assembly
AN10020	0,22	0,03	-0,05	0,71	0,16	0,11	-0,03	0,84	0,02	0,91	-0,14	0,19	Ortholog(s) have role in proteasome-mediated ubiquitin-dependent protein catabolic process and cytosol, nucleus localization
AN10118	-0,59	0,00	0,28	0,22	-0,47	0,01	0,20	0,38	-0,16	0,49	0,36	0,09	Ortholog(s) have endoplasmic reticulum localization
AN10170	0,13	0,31	0,08	0,63	0,01	0,97	-0,08	0,60	-0,70	0,00	-0,03	0,87	Ortholog(s) have ATPase activity, role in negative regulation of G2/M transition of mitotic cell cycle and cytosol, nucleus localization
AN10184	-0,36	0,01	-0,23	0,13	-0,31	0,02	-0,31	0,02	-0,15	0,31	-0,24	0,09	Protein predicted to have a role in pheromone precursor processing
AN10186	0,25	0,02	0,14	0,30	0,12	0,33	-0,01	0,94	0,32	0,01	0,17	0,18	Ortholog(s) have role in ER to Golgi vesicle-mediated transport, cellular response to cadmium ion, detoxification of cadmium ion
AN1023	0,17	0,19	-0,19	0,17	0,06	0,67	-0,40	0,00	0,00	1,00	-0,23	0,07	Protein that plays a role in sensitivity to DNA-damaging agents
AN10265	-0,48	0,00	0,17	0,40	-0,72	0,00	0,05	0,80	-0,18	0,33	0,06	0,78	Ortholog(s) have alpha-1,6-mannosyltransferase activity, role in protein N-linked glycosylation and Golgi trans cisterna, alpha-1,6-mannosyltransferase complex, endoplasmic reticulum localization
AN10266	0,40	0,00	0,06	0,75	0,48	0,00	0,08	0,59	-0,01	0,95	0,03	0,89	Putative ubiquitin-activating enzyme; ortholog of <i>S. cerevisiae</i> Uba1p; transcript upregulated in response to camptothecin; protein induced by farnesol
AN10324	0,72	0,00	0,05	0,88	0,39	0,04	0,14	0,53	-0,10	0,68	-0,11	0,65	Putative neddylation machinery protein; constitutively expressed during all stages of the fungal life cycle
AN10337	0,21	0,14	-0,02	0,95	0,09	0,59	-0,01	0,97	0,19	0,24	0,14	0,40	Has domain(s) with predicted enzyme regulator activity, role in regulation of protein catabolic process and proteasome complex localization
AN10354	0,20	0,26	-0,11	0,65	0,20	0,25	-0,05	0,84	-0,36	0,05	-0,14	0,49	Putative signal sequence processing protein with a predicted role in targeting proteins to the endoplasmic reticulum
AN10367	-0,75	0,00	0,03	0,90	-0,62	0,00	-0,08	0,65	-0,21	0,23	0,00	1,00	Putative P-type ATPase
AN10439	0,02	0,89	0,10	0,53	-0,19	0,13	-0,29	0,02	0,02	0,93	0,08	0,61	Ortholog(s) have role in attachment of GPI anchor to protein and GPI-anchor transamidase complex localization
AN10446	0,11	0,44	0,01	0,97	0,04	0,79	0,08	0,65	-0,03	0,86	-0,13	0,43	Ortholog(s) have phosphoprotein phosphatase activity, role in endoplasmic reticulum unfolded protein response, protein dephosphorylation, traversing start control point of mitotic cell cycle and endoplasmic reticulum localization
AN1047	0,60	0,03	0,44	0,18	0,87	0,00	0,67	0,02	0,78	0,01	0,63	0,03	Putative heat shock protein

AN10489	-0,51	0,01	-0,14	0,63	-0,24	0,27	-0,19	0,42	-0,17	0,50	-0,03	0,93	FKBP-type peptidyl-prolyl cis-trans isomerase; expression reduced after exposure to farnesol
AN10504	0,13	0,59	0,01	0,97	0,29	0,17	0,14	0,58	-0,33	0,16	-0,26	0,26	Ortholog(s) have role in conidiophore development, hyphal growth, sporocarp development involved in sexual reproduction, syncytium formation by plasma membrane fusion
AN10519	0,23	0,05	-0,18	0,19	0,26	0,03	-0,09	0,49	0,06	0,73	-0,19	0,15	Ortholog(s) have cytosol, nucleus localization
AN10556	0,40	0,02	0,20	0,36	0,40	0,02	0,34	0,06	0,14	0,54	0,24	0,23	Ortholog(s) have cytoplasm, nucleus localization
AN10611	-0,07	0,69	-0,01	0,97	-0,29	0,06	-0,43	0,01	-0,47	0,00	-0,20	0,24	Ortholog(s) have role in GPI anchor biosynthetic process, mitotic cytokinesis and endoplasmic reticulum localization
AN10637	-0,32	0,01	-0,38	0,00	-0,17	0,19	-0,41	0,00	0,19	0,18	0,03	0,85	Ortholog(s) have role in microautophagy, polyphosphate metabolic process, protein localization, vacuolar transport, vacuole fusion, non-autophagic
AN10639	-0,03	0,89	-0,06	0,84	-0,10	0,64	-0,41	0,03	-0,02	0,95	0,00	1,00	Ortholog(s) have GPI-anchor transamidase activity, role in attachment of GPI anchor to protein and GPI-anchor transamidase complex, endoplasmic reticulum, integral component of membrane localization
AN10702	0,07	0,71	0,17	0,40	0,04	0,83	0,05	0,82	-0,27	0,12	-0,07	0,76	Ortholog(s) have alpha-1,4-glucosidase activity, role in polysaccharide biosynthetic process, protein N-linked glycosylation and endoplasmic reticulum lumen, glucosidase II complex localization
AN10708	0,33	0,01	-0,20	0,20	0,25	0,06	-0,17	0,26	-0,27	0,06	-0,47	0,00	Ortholog(s) have role in proteasomal ubiquitin-independent protein catabolic process, proteasome assembly, proteasome-mediated ubiquitin-dependent protein catabolic process
AN10709	-0,79	0,00	-0,47	0,02	-0,92	0,00	-0,54	0,01	0,61	0,00	-0,22	0,33	Putative glutamine-fructose-6-phosphate transaminase
AN10724	-0,60	0,00	-0,37	0,02	-0,50	0,00	-0,45	0,00	-0,29	0,06	-0,30	0,05	Ortholog(s) have role in ER to Golgi vesicle-mediated transport and ER to Golgi transport vesicle, Golgi apparatus, endoplasmic reticulum localization
AN10791	-0,93	0,00	-0,43	0,01	-0,80	0,00	-0,33	0,06	0,09	0,69	-0,01	0,98	Putative 1-phosphatidylinositol 4-kinase; mutants have a strong growth defect
AN1082	-0,75	0,00	-0,13	0,60	-0,68	0,00	-0,21	0,27	-0,22	0,26	0,00	0,99	Putative nucleoside phosphatase; ortholog of <i>S. cerevisiae</i> Gda1p; expression reduced after exposure to farnesol; this locus is reported to contain an upstream open reading frame (uORF)
AN10826	-0,36	0,00	0,00	0,99	-0,35	0,00	-0,09	0,56	-0,16	0,27	0,02	0,93	Component of the TRAPII complex that mediates Rab guanyl-nucleotide exchange factor activity, involved in Golgi vesicle-mediated transport
AN1085	-0,30	0,17	0,02	0,95	-0,46	0,03	-0,05	0,85	0,13	0,62	0,38	0,10	Ortholog(s) have GTPase activity, role in cellular response to drug, endoplasmic reticulum inheritance, endoplasmic reticulum membrane fusion, hexose transport, pathogenesis and cortical endoplasmic reticulum, cytosol localization
AN10918	0,13	0,36	0,11	0,54	-0,08	0,58	-0,09	0,57	0,04	0,84	0,11	0,48	Has domain(s) with predicted calcium ion binding, phosphatidylinositol binding activity and role in cell communication
AN10975	-0,86	0,00	-0,65	0,00	-0,63	0,00	-0,52	0,01	0,55	0,01	-0,13	0,63	Ortholog of <i>A. fumigatus</i> Af293 : Afu5g06970, <i>A. niger</i> CBS 513.88 : An17g00170, <i>A. oryzae</i> RIB40 : AO090701000290, <i>Aspergillus versicolor</i> : Aspve1_0135244 and <i>Aspergillus clavatus</i> NRRL 1 : ACLA_010110
AN10987	-0,49	0,00	-0,03	0,92	-0,40	0,02	-0,18	0,36	-0,15	0,50	-0,11	0,63	Ortholog(s) have cytosol, nucleus localization

AN10994	0,27	0,17	0,17	0,48	-0,01	0,97	0,02	0,93	-0,41	0,04	-0,09	0,71	Ortholog(s) have ubiquitin-protein transferase activity, role in protein autoubiquitination, protein import into peroxisome matrix, receptor recycling, protein monoubiquitination and cytosol, nucleus, peroxisome localization
AN11007	-0,24	0,04	-0,05	0,77	-0,12	0,33	-0,05	0,75	-0,04	0,80	0,14	0,28	Ortholog(s) have role in Golgi inheritance, Golgi to plasma membrane transport, cytokinetic cell separation, endocytosis, endoplasmic reticulum inheritance, exocytosis
AN11054	0,05	0,77	0,32	0,04	-0,08	0,62	0,00	1,00	-0,46	0,00	0,00	0,99	Putative alpha-1,4-glucosidase
AN11141	-0,21	0,08	-0,06	0,75	-0,46	0,00	-0,28	0,03	-0,33	0,01	-0,11	0,47	Ortholog(s) have acetylglucosaminyltransferase activity, role in protein N-linked glycosylation and Golgi medial cisterna localization
AN11163	-0,01	0,94	0,03	0,85	-0,07	0,53	-0,18	0,09	-0,24	0,02	-0,22	0,04	Has domain(s) with predicted calcium ion binding, mannosyl-oligosaccharide 1,2-alpha-mannosidase activity and membrane localization
AN1117	-0,47	0,00	0,05	0,78	-0,24	0,06	0,10	0,48	-0,43	0,00	0,05	0,76	Ortholog(s) have role in ER to Golgi vesicle-mediated transport and ER to Golgi transport vesicle, Golgi apparatus, endoplasmic reticulum, plasma membrane localization
AN11226	-0,60	0,00	-0,38	0,14	-0,42	0,06	-0,44	0,05	0,01	0,97	-0,01	0,98	Ortholog(s) have HDEL sequence binding activity, role in ER to Golgi vesicle-mediated transport, protein retention in ER lumen and Golgi apparatus, integral component of endoplasmic reticulum membrane localization
AN11232	-0,43	0,03	0,33	0,13	-0,42	0,03	0,18	0,42	-0,41	0,05	-0,08	0,78	Ortholog(s) have endoplasmic reticulum localization
AN1126	-0,13	0,15	0,18	0,06	-0,03	0,78	0,23	0,01	0,13	0,18	0,30	0,00	Putative ADP ribosylation factor involved in hyphal growth and secretion; essential gene; ArfA-GFP localizes to presumed Golgi compartments
AN11500	0,04	0,84	0,12	0,64	0,20	0,28	0,36	0,05	-0,31	0,12	-0,02	0,93	Component of the TRAPII complex that mediates Rab guanyl-nucleotide exchange factor activity, involved in Golgi vesicle-mediated transport
AN1154	-0,33	0,03	0,03	0,91	-0,13	0,47	-0,06	0,75	-0,27	0,12	0,18	0,30	Ortholog(s) have role in ER to Golgi vesicle-mediated transport, protein retention in ER lumen, vesicle organization and ER to Golgi transport vesicle, endoplasmic reticulum, plasma membrane localization
AN11694	0,02	0,92	-0,19	0,28	0,13	0,42	-0,19	0,25	0,21	0,22	0,17	0,31	Ortholog(s) have role in cellular response to drug, fungal-type cell wall organization, retrograde vesicle-mediated transport, Golgi to ER and endoplasmic reticulum, integral component of membrane localization
AN1177	-0,65	0,00	-0,06	0,72	-0,38	0,00	-0,20	0,13	-0,37	0,00	-0,16	0,25	Ortholog(s) have cytosol, plasma membrane localization
AN11802	0,40	0,01	0,05	0,85	0,35	0,02	0,15	0,43	-0,30	0,09	-0,32	0,05	Ortholog(s) have N-acetylglucosaminyl-diphosphodolichol N-acetylglucosaminyltransferase activity and role in dolichol-linked oligosaccharide biosynthetic process
AN1182	-0,29	0,05	0,10	0,61	-0,45	0,00	-0,48	0,00	-0,22	0,19	0,13	0,46	Beta-tubulin, highly conserved component of microtubules; <i>A. nidulans</i> has two beta-tubulin genes, <i>benA</i> and <i>tubC</i> ; temperature sensitive mutants are blocked in mitosis and in nuclear division
AN11900	0,00	0,99	0,15	0,65	-0,14	0,61	-0,10	0,73	-0,13	0,65	0,14	0,64	Ortholog(s) have Golgi apparatus localization
AN11913	0,81	0,00	-0,39	0,00	0,40	0,00	-0,52	0,00	0,14	0,39	-0,40	0,00	Ortholog(s) have role in meiotic nuclear division and fungal-type vacuole localization
AN11956	-0,52	0,00	-0,35	0,04	-0,51	0,00	-0,30	0,06	-0,01	0,98	-0,16	0,38	Ortholog(s) have role in cellular copper ion homeostasis, endosomal transport, invasive growth in response to glucose limitation, pseudohyphal growth, vacuolar transport

AN11995	0,17	0,45	-0,07	0,81	0,01	0,98	-0,40	0,05	0,01	0,97	-0,07	0,80	Ortholog(s) have role in GPI anchor biosynthetic process, conidium formation, regulation of growth rate
AN12017	-0,40	0,00	-0,27	0,04	-0,42	0,00	-0,42	0,00	0,27	0,04	0,23	0,09	Ortholog(s) have polyphosphate kinase activity and role in microautophagy, polyphosphate metabolic process, vacuolar transport, vacuole fusion, non-autophagic
AN12122	-0,19	0,24	-0,13	0,53	-0,13	0,44	-0,16	0,39	-0,14	0,44	0,01	0,98	Ortholog(s) have role in ER-associated misfolded protein catabolic process, hyphal growth, regulation of transcription from RNA polymerase II promoter, secretion by cell and endoplasmic reticulum localization
AN12171	-0,27	0,08	-0,10	0,65	-0,18	0,27	0,17	0,31	0,31	0,06	0,17	0,34	Ortholog(s) have SNAP receptor activity, role in endocytosis, vesicle fusion and Golgi apparatus, SNARE complex, cell septum, endoplasmic reticulum, endosome, trans-Golgi network localization
AN1229	-0,56	0,00	-0,40	0,00	-0,38	0,00	-0,25	0,07	0,09	0,61	-0,17	0,25	Ortholog(s) have SNAP receptor activity, role in Golgi vesicle transport, vesicle fusion and Golgi medial cisterna, SNARE complex localization
AN12408	-0,23	0,03	0,01	0,97	-0,25	0,02	-0,04	0,81	0,01	0,95	0,06	0,65	Ortholog(s) have role in cellular response to biotic stimulus, filamentous growth of a population of unicellular organisms in response to biotic stimulus, hyphal growth, vacuole inheritance
AN12427	-0,43	0,00	0,06	0,79	-0,09	0,55	0,14	0,41	-0,07	0,71	0,20	0,21	Protein of unknown function
AN12452	0,24	0,07	0,29	0,05	-0,14	0,35	0,13	0,38	0,19	0,23	-0,03	0,89	Has domain(s) with predicted phosphotransferase activity, for other substituted phosphate groups activity, role in phospholipid biosynthetic process and membrane localization
AN12473	-0,94	0,00	0,03	0,91	-0,77	0,00	-0,11	0,61	-0,47	0,01	0,08	0,72	Putative heat shock protein
AN12492	0,35	0,61	0,44	0,59	0,58	0,37	0,38	0,59	0,61	0,39	0,84	0,21	Has domain(s) with predicted GTP binding, GTPase activity
AN1282	-0,25	0,01	-0,21	0,04	0,01	0,96	-0,09	0,43	0,05	0,70	-0,07	0,55	Ortholog(s) have protein complex scaffold activity, role in posttranslational protein targeting to membrane, response to heat and TRC complex, nucleus localization
AN1296	0,09	0,75	-0,20	0,52	0,53	0,02	0,89	0,00	0,42	0,11	1,54	0,00	Ortholog(s) have 2',3'-cyclic-nucleotide 3'-phosphodiesterase activity, GTP-dependent polyribonucleotide 5'-hydroxyl-kinase activity, RNA ligase (ATP) activity
AN1309	-0,56	NA	0,46	NA	-0,02	NA	0,46	NA	0,49	NA	-0,19	NA	Has domain(s) with predicted GTP binding, GTPase activity
AN1341	-0,13	0,50	-0,30	0,14	-0,24	0,19	-0,26	0,19	-0,42	0,02	-0,59	0,00	Membrane coat complex Retromer subunit; locus contains the conserved upstream open reading frame (uORF) AN1341-uORF
AN1358	0,03	0,79	0,28	0,01	-0,01	0,93	0,18	0,09	-0,36	0,00	0,18	0,11	Ortholog(s) have protein serine/threonine phosphatase activity and role in cellular response to osmotic stress, inactivation of MAPK activity involved in osmosensory signaling pathway, protein dephosphorylation
AN1394	-0,57	0,00	-0,02	0,94	-0,55	0,00	-0,39	0,00	-0,08	0,66	0,11	0,52	Putative septin
AN1442	-0,34	0,00	0,08	0,62	-0,25	0,03	0,03	0,84	-0,15	0,23	0,09	0,53	Ortholog(s) have role in filamentous growth, posttranslational protein targeting to membrane, translocation and Sec62/Sec63 complex localization
AN1455	-0,67	0,00	0,00	1,00	-0,26	0,05	0,00	0,98	-0,09	0,58	0,20	0,17	Ortholog(s) have dolichyl-diphosphooligosaccharide-protein glycotransferase activity, role in protein N-linked glycosylation and oligosaccharyltransferase complex, plasma membrane localization

AN1459	-0,26	0,02	0,00	0,99	-0,26	0,02	-0,14	0,28	-0,05	0,74	0,20	0,11	Subfamily 4 protein O-mannosyltransferase; involved in hyphal growth and conidia formation
AN1461	0,05	0,82	0,05	0,85	0,08	0,68	-0,22	0,23	0,04	0,88	-0,05	0,82	Ortholog of <i>A. fumigatus</i> Af293 : Afu8g04530, <i>A. niger</i> CBS 513.88 : An16g08470, <i>A. oryzae</i> RIB40 : AO090023000334, <i>Aspergillus wentii</i> : Aspwe1_0043883 and <i>Aspergillus sydowii</i> : Aspsy1_0145261
AN1481	0,29	0,10	-0,50	0,00	0,12	0,53	-0,54	0,00	0,36	0,04	-0,27	0,12	Has domain(s) with predicted role in transmembrane transport and integral component of membrane localization
AN1488	0,03	0,79	0,19	0,05	-0,13	0,15	-0,04	0,71	-0,17	0,09	0,01	0,96	Putative zinc-finger protein with a predicted role in ER unfolded protein degradation
AN1510	0,55	0,06	0,08	0,86	0,46	0,13	0,12	0,76	0,36	0,29	0,06	0,88	Ortholog(s) have protein disulfide isomerase activity, protein disulfide oxidoreductase activity, thiol oxidase activity, role in oxidation-reduction process, protein folding and endoplasmic reticulum membrane localization
AN1525	-0,05	0,78	0,16	0,40	0,07	0,68	0,16	0,34	-0,32	0,04	0,18	0,28	Ortholog(s) have peptidase activity, role in protein targeting to ER, signal peptide processing and plasma membrane, signal peptidase complex localization
AN1620	-0,24	0,50	-1,55	0,00	0,08	0,85	-1,26	0,00	0,74	0,03	-0,12	0,78	Ortholog of <i>A. nidulans</i> FGSC A4 : AN2626, <i>A. fumigatus</i> Af293 : Afu8g02040/och3, <i>A. niger</i> CBS 513.88 : An03g01090/hocA, An05g02320 and <i>A. oryzae</i> RIB40 : AO090010000615
AN1683	-0,47	0,00	0,18	0,35	-0,63	0,00	-0,42	0,01	-0,02	0,94	0,17	0,35	Putative oligosaccharyltransferase delta subunit; ortholog of <i>S. cerevisiae</i> Swp1p
AN1700	-0,08	0,28	0,00	1,00	-0,05	0,49	-0,14	0,05	0,06	0,51	0,03	0,74	Putative 26S proteasome regulatory subunit; transcript upregulated in response to camptothecin
AN1757	0,15	0,33	-0,26	0,13	0,07	0,69	-0,36	0,02	-0,08	0,69	-0,29	0,07	Predicted alpha 3 subunit of the 20S core proteasome; involved in N-myristoylation and cell morphogenesis
AN1775	-0,14	0,50	-0,10	0,71	-0,16	0,44	-0,17	0,41	-0,02	0,95	-0,18	0,40	Ortholog(s) have GPI-anchor transamidase activity and role in attachment of GPI anchor to protein, conidium formation, fungal-type cell wall organization, fungal-type cell wall polysaccharide biosynthetic process, regulation of growth rate
AN1811	-0,24	0,01	0,19	0,06	-0,22	0,02	0,01	0,92	-0,07	0,52	0,36	0,00	Ortholog(s) have dolichyl-phosphate-mannose-glycolipid alpha-mannosyltransferase activity, glutathione binding activity, role in GPI anchor biosynthetic process and endoplasmic reticulum localization
AN1835	-0,12	NA	0,29	NA	0,14	NA	0,33	NA	0,35	NA	0,10	NA	Ortholog of <i>A. fumigatus</i> Af293 : Afu6g11880, <i>A. oryzae</i> RIB40 : AO090701000551, <i>Neosartorya fischeri</i> NRRL 181 : NFIA_057460, <i>Aspergillus wentii</i> : Aspwe1_0120396 and <i>Aspergillus versicolor</i> : Aspve1_0122785
AN1845	0,22	0,15	0,05	0,84	-0,02	0,93	-0,13	0,45	-0,34	0,03	-0,12	0,49	Endoplasmic reticulum packaging chaperone, required for incorporation of amino acid permeases (aspartate and proline transporters) into COPII coated vesicles for transport to the cell surface
AN1904	-0,51	0,00	-0,24	0,16	-0,36	0,01	-0,28	0,07	-0,42	0,01	-0,30	0,05	Ortholog(s) have chaperonin-containing T-complex localization
AN1933	-1,17	0,00	-0,08	0,78	-1,20	0,00	-0,18	0,44	0,16	0,52	0,21	0,36	Has domain(s) with predicted endoplasmic reticulum membrane, integral component of membrane localization

AN1969	-0,13	0,75	0,30	0,50	0,05	0,90	0,60	0,10	-0,21	0,63	-0,13	0,79	Ortholog(s) have alpha-1,6-mannosyltransferase activity, role in protein glycosylation and alpha-1,6-mannosyltransferase complex, endoplasmic reticulum localization
AN1973	-0,08	0,52	-0,06	0,71	-0,16	0,15	0,02	0,92	-0,17	0,15	0,13	0,28	Ortholog(s) have SNAP receptor activity and role in Golgi to vacuole transport, intra-Golgi vesicle-mediated transport, vacuole fusion, non-autophagic, vesicle fusion
AN1981	0,11	0,45	-0,48	0,00	0,07	0,65	-0,64	0,00	0,14	0,41	-0,52	0,00	Ortholog(s) have Rab geranylgeranyltransferase activity and role in ER to Golgi vesicle-mediated transport, protein geranylgeranylation, protein targeting to membrane
AN1988	0,06	0,76	0,00	1,00	-0,06	0,78	-0,27	0,14	0,04	0,89	-0,14	0,51	Ortholog(s) have role in cytokinetic cell separation and cell cortex of cell tip, cell division site, exocyst, mitotic spindle pole body, nucleus localization
AN2014	0,04	0,79	0,00	1,00	-0,10	0,48	-0,18	0,21	-0,14	0,37	0,03	0,87	Ortholog(s) have cytosol, nucleus localization
AN2045	-0,41	0,04	-1,06	0,00	-0,40	0,05	-0,93	0,00	-0,03	0,93	-0,61	0,00	Has domain(s) with predicted calcium ion binding, mannosyl-oligosaccharide 1,2-alpha-mannosidase activity and membrane localization
AN2047	0,35	0,01	-0,20	0,26	0,32	0,03	-0,27	0,07	-0,47	0,00	-0,37	0,01	Calmodulin; EF-hands containing calcium binding protein; required for normal progression through the cell-cycle; localizes to hyphal tips and transiently to sites of septation; transcript upregulated in response to camptothecin
AN2048	0,21	0,13	0,04	0,85	-0,10	0,51	-0,18	0,25	-0,15	0,34	-0,11	0,50	Protein similar to <i>S. cerevisiae</i> Tlg2p; localizes to endosomes
AN2050	-0,33	0,01	-0,19	0,21	-0,33	0,01	-0,44	0,00	0,00	0,99	-0,28	0,04	Ortholog(s) have Golgi apparatus, cytoplasmic vesicle localization
AN2062	-0,88	0,00	0,18	0,56	-0,40	0,08	0,38	0,11	-0,08	0,78	0,64	0,00	Putative ER-resident chaperone of the HSP70 family; unfolded-protein response (UPR) target gene; transcript levels increase during the UPR
AN2072	-0,08	0,65	-0,10	0,66	-0,21	0,20	-0,23	0,18	-0,05	0,84	-0,17	0,34	Putative ubiquitin-specific protease; ortholog of <i>S. cerevisiae</i> Doa4p
AN2085	0,31	0,02	-0,20	0,19	0,29	0,03	-0,25	0,07	-0,17	0,29	-0,33	0,01	Ortholog(s) have endopeptidase activity and role in proteasomal ubiquitin-independent protein catabolic process, proteasome-mediated ubiquitin-dependent protein catabolic process
AN2169	0,16	0,16	0,11	0,45	-0,02	0,89	0,21	0,08	0,00	0,99	-0,07	0,62	Ortholog(s) have role in Golgi to vacuole transport and Golgi trans cisterna, endoplasmic reticulum, late endosome localization
AN2224	0,26	0,02	-0,02	0,92	0,14	0,26	-0,05	0,74	0,22	0,08	0,08	0,56	Putative vacuolar protein-sorting protein with homology to <i>Saccharomyces cerevisiae</i> Vps17p; identified as a suppressor of xprG
AN2240	0,10	0,69	-0,22	0,41	0,20	0,39	-0,33	0,14	-0,27	0,28	-0,06	0,85	Ortholog(s) have mannosyltransferase activity, role in ER-associated ubiquitin-dependent protein catabolic process, GPI anchor biosynthetic process, protein processing and endoplasmic reticulum localization
AN2303	-0,74	0,00	-0,03	0,93	-0,80	0,00	0,07	0,79	0,03	0,92	0,63	0,00	Ortholog(s) have alpha-1,2-mannosyltransferase activity, dolichyl-phosphate-mannose-glycolipid alpha-mannosyltransferase activity and role in GPI anchor biosynthetic process, fungal-type cell wall biogenesis, plasmid maintenance
AN2304	0,39	0,01	0,03	0,91	0,46	0,00	-0,02	0,95	-0,28	0,11	0,03	0,90	Ortholog(s) have ubiquitin binding activity, role in negative regulation of protein catabolic process, nucleotide-excision repair, protein ubiquitination and cytosol, nuclear envelope localization
AN2317	0,20	0,14	-0,12	0,48	0,21	0,11	-0,13	0,39	-0,15	0,32	-0,08	0,62	Predicted actin depolymerizing protein with similarity to <i>Saccharomyces cerevisiae</i> Cof1p

AN2406	0,34	0,03	-0,03	0,92	0,16	0,38	-0,41	0,01	0,11	0,61	-0,21	0,26	Ortholog(s) have intracellular localization
AN2418	0,11	0,43	0,06	0,74	0,06	0,68	0,01	0,97	0,35	0,01	-0,12	0,44	Putative protein with a predicted role in vacuolar sorting
AN2480	-0,08	0,63	-0,10	0,60	-0,01	0,96	-0,15	0,32	-0,23	0,14	-0,20	0,20	Ortholog(s) have role in Golgi to plasma membrane protein transport and Golgi apparatus, cytosol localization
AN2518	-0,39	0,00	0,01	0,95	-0,39	0,00	-0,19	0,14	-0,05	0,74	-0,01	0,95	Ortholog(s) have cytosol localization
AN2626	-0,10	0,70	0,10	0,76	0,08	0,77	0,23	0,38	0,25	0,35	0,23	0,39	Ortholog of <i>A. nidulans</i> FGSC A4 : AN1620, <i>A. fumigatus</i> Af293 : Afu8g02040/och3, <i>A. niger</i> CBS 513.88 : An03g01090/hocA, An05g02320 and <i>A. oryzae</i> RIB40 : AO090010000615
AN2731	0,45	0,18	0,37	0,37	0,51	0,13	0,34	0,36	1,04	0,00	0,58	0,10	Ortholog(s) have ATPase activator activity, unfolded protein binding activity
AN2738	-0,63	0,00	-0,10	0,75	-0,16	0,51	-0,02	0,94	-0,30	0,22	-0,40	0,08	Ortholog(s) have endoplasmic reticulum localization
AN2752	-0,33	0,04	-0,35	0,04	-0,20	0,24	-0,28	0,09	-0,03	0,90	-0,35	0,03	Ortholog(s) have alpha-1,2-mannosyltransferase activity
AN2756	-0,01	0,95	0,03	0,86	-0,12	0,22	-0,20	0,05	0,02	0,89	-0,02	0,89	Predicted actin binding protein with similarity to <i>Saccharomyces cerevisiae</i> Sla2p; essential for conidial germination
AN2862	-0,26	0,15	-0,28	0,17	-0,26	0,15	-0,64	0,00	-0,41	0,03	-0,33	0,08	Predicted CAP-Gly domain protein with similarity to <i>Saccharomyces cerevisiae</i> Bim1p
AN2877	-0,64	0,00	-0,54	0,00	-0,12	0,54	-0,10	0,64	0,28	0,14	0,21	0,28	Ortholog(s) have oxysterol binding, phosphatidic acid binding, phosphatidylinositol-4,5-bisphosphate binding, phosphatidylinositol-4-phosphate binding, sterol transporter activity
AN2904	0,19	0,02	-0,22	0,02	0,09	0,35	-0,25	0,00	0,06	0,57	-0,27	0,00	Putative 26S proteasome regulatory subunit; ortholog of <i>S. cerevisiae</i> Rpt3p
AN2909	-0,26	0,08	0,04	0,86	-0,16	0,32	-0,08	0,68	0,26	0,11	0,24	0,14	Ortholog(s) have cytosol, nucleus localization
AN2918	-0,14	0,34	-0,22	0,16	-0,19	0,20	-0,30	0,04	-0,37	0,01	-0,42	0,00	Putative chaperonin complex component, TCP-1 delta subunit; ortholog of <i>S. cerevisiae</i> Cct4p; expression reduced after exposure to farnesol
AN2936	0,56	0,00	0,02	0,93	0,54	0,00	0,08	0,72	0,05	0,82	0,17	0,38	Putative Class 2C alpha-mannosidase with a predicted role in mannose polymer metabolism
AN2946	0,18	0,21	-0,03	0,89	0,11	0,49	0,20	0,20	0,01	0,97	-0,21	0,18	Protein predicted to have a role in pheromone precursor processing
AN3019	0,29	0,00	-0,10	0,36	0,11	0,27	-0,16	0,10	0,21	0,03	-0,15	0,14	Ortholog(s) have role in ubiquitin-dependent protein catabolic process and nucleus, proteasome regulatory particle, lid subcomplex, proteasome storage granule localization
AN3026	-0,68	0,00	0,06	0,70	-0,33	0,00	-0,03	0,84	-0,24	0,04	0,11	0,40	Alpha-COP coatamer-related protein involved in the establishment and maintenance of polarized growth; temperature sensitive mutants defective in nuclear division at the restrictive temperature
AN3029	-0,26	0,03	0,14	0,36	-0,31	0,01	-0,16	0,21	-0,11	0,44	0,09	0,55	Ortholog(s) have role in cellular response to drug
AN3061	0,09	0,58	0,11	0,55	0,22	0,13	0,10	0,57	-0,25	0,12	0,08	0,67	Ortholog(s) have ATP binding, ATPase activity, protein homodimerization activity
AN3062	-0,37	0,00	-0,60	0,00	0,05	0,75	-0,59	0,00	0,01	0,95	-0,32	0,02	Putative pericentrin-related protein involved in microtubule organization and hyphal polarity
AN3080	-0,32	0,01	0,04	0,83	-0,35	0,01	-0,21	0,13	-0,41	0,00	-0,06	0,72	Ortholog(s) have cytosol localization
AN3098	-0,12	0,23	-0,06	0,66	-0,02	0,83	0,08	0,49	-0,06	0,59	-0,03	0,83	Putative secretory component; ortholog of <i>S. cerevisiae</i> Sec18p



AN3122	-0,43	0,00	-0,04	0,79	-0,44	0,00	-0,28	0,02	-0,04	0,77	0,02	0,88	Transcript levels increase during the unfolded-protein response (UPR); <i>S. cerevisiae</i> ortholog of Bch1p
AN3370	-0,06	0,80	-0,15	0,54	-0,03	0,89	-0,37	0,06	-0,12	0,61	-0,31	0,11	Ortholog(s) have role in GPI anchor biosynthetic process, fungal-type cell wall organization
AN3416	-0,85	0,00	-0,50	0,00	-0,87	0,00	-0,66	0,00	0,56	0,00	-0,06	0,79	Similar to syntaxin proteins; SsoA-GFP localizes to the plasma membrane and to the hyphal tip
AN3463	-0,39	0,00	0,08	0,57	-0,33	0,00	0,03	0,85	-0,09	0,48	0,17	0,12	Ortholog(s) have chaperone binding, sequence-specific DNA binding, unfolded protein binding activity
AN3579	-0,14	0,31	0,16	0,34	-0,30	0,03	-0,07	0,66	-0,13	0,41	0,05	0,77	Ortholog(s) have role in mitotic spindle elongation, vesicle-mediated transport and integral component of Golgi membrane localization
AN3583	-0,38	0,01	0,05	0,85	-0,30	0,06	0,14	0,45	0,18	0,32	0,31	0,06	Protein with homology to subtilisin serine proteases; enhanced specificity for cleavage of dibasic peptide sequences
AN3588	0,04	0,83	-0,16	0,28	-0,16	0,24	-0,38	0,00	0,13	0,39	-0,08	0,62	Ortholog(s) have alpha-1,6-mannosyltransferase activity, role in dolichol-linked oligosaccharide biosynthetic process, protein glycosylation and endoplasmic reticulum localization
AN3592	-0,44	0,03	0,58	0,01	-0,24	0,29	0,28	0,22	-0,11	0,68	0,65	0,00	Putative calnexin with a predicted role in protein folding and protein quality control on the endoplasmic reticulum (ER) membrane
AN3594	0,35	0,04	-0,07	0,77	0,14	0,49	-0,34	0,06	-0,22	0,28	-0,22	0,27	Putative vacuolar protein-sorting protein with homology to <i>Saccharomyces cerevisiae</i> Vps5p; identified as a suppressor of xprG
AN3598	0,51	0,00	0,58	0,00	0,75	0,00	0,52	0,01	-0,82	0,00	0,13	0,57	Putative peptidyl-prolyl cis-trans isomerase; FKBP12 homolog; mutant displays reduced growth on 2-pyrrolidone and enhanced growth on threonine
AN3642	0,38	0,01	-0,10	0,62	0,62	0,00	-0,04	0,85	0,05	0,79	0,05	0,80	Ortholog(s) have role in ascospore formation, cellular response to biotic stimulus and cellular response to starvation, more
AN3675	-0,42	0,00	-0,53	0,00	-0,40	0,00	-0,55	0,00	-0,35	0,00	-0,48	0,00	Transcription factor of the Gcn4p c-Jun-like transcriptional activator family; involved in cross-pathway control of amino acid biosynthesis in response to amino acid starvation; role in sexual development; contains two 5' uORFs
AN3716	0,20	0,05	-0,15	0,20	0,28	0,01	-0,21	0,04	-0,03	0,85	-0,11	0,33	Ortholog of <i>A. fumigatus</i> Af293 : Afu6g12770, <i>A. niger</i> CBS 513.88 : An08g10710, <i>A. oryzae</i> RIB40 : AO090003000397, <i>Aspergillus wentii</i> : Aspwe1_0102826 and <i>Aspergillus sydowii</i> : Aspsy1_0032599
AN3720	-0,04	0,77	0,14	0,30	-0,25	0,03	-0,18	0,14	-0,21	0,10	-0,10	0,49	Ortholog(s) have cytosol, endoplasmic reticulum exit site localization
AN3733	-0,44	0,00	0,40	0,01	-0,32	0,03	0,60	0,00	-0,52	0,00	0,38	0,02	Putative alpha-1,2 mannosidase with a predicted role in mannose polymer metabolism
AN3756	0,39	0,01	-0,29	0,10	0,23	0,17	-0,33	0,04	-0,29	0,09	-0,63	0,00	Ortholog(s) have endopeptidase activity and role in proteasomal ubiquitin-independent protein catabolic process, proteasome-mediated ubiquitin-dependent protein catabolic process
AN3757	-0,17	0,40	0,02	0,95	-0,38	0,04	-0,31	0,12	-0,24	0,26	-0,01	0,96	Ortholog(s) have role in establishment of cell polarity, mycelium development, spore germination and endoplasmic reticulum, hyphal tip, plasma membrane localization

AN3759	0,06	0,75	-0,02	0,94	-0,34	0,05	-0,33	0,06	-0,17	0,41	0,06	0,81	Ortholog(s) have protein disulfide isomerase activity, thiol oxidase activity, role in oxidation-reduction process and integral component of endoplasmic reticulum membrane localization
AN3787	-1,10	0,00	-0,47	0,12	-1,33	0,00	-0,44	0,12	0,07	0,85	-0,03	0,93	Ortholog(s) have glycoprotein binding, metal ion binding, misfolded protein binding, peptide-N4-(N-acetyl-beta-glucosaminy)asparagine amidase activity, structural constituent of cell wall activity
AN3814	0,55	0,00	0,25	0,07	0,38	0,00	-0,01	0,95	-0,28	0,04	0,17	0,24	Putative peptidyl-prolyl cis-trans isomerase (PPIase); cyclophilin
AN3817	-0,91	0,00	0,08	0,62	-0,59	0,00	0,20	0,10	-0,18	0,16	0,13	0,32	Putative 3-hydroxy-3-methylglutaryl-coenzyme A (HMG-CoA) reductase isozyme with a predicted role in sterol metabolism
AN3821	-0,08	0,33	0,00	0,98	-0,26	0,00	-0,15	0,07	-0,06	0,58	-0,06	0,53	Ortholog of <i>A. fumigatus</i> Af293 : Afu2g03650, <i>A. niger</i> CBS 513.88 : An07g08220, <i>A. oryzae</i> RIB40 : AO090120000220, <i>Aspergillus wentii</i> : Aspwe1_0172303 and <i>Aspergillus sydowii</i> : Aspsy1_0030705
AN3826	-0,25	0,03	0,18	0,20	-0,41	0,00	-0,12	0,42	-0,01	0,95	-0,11	0,45	Ortholog(s) have role in attachment of GPI anchor to protein, conidium formation, hyphal growth, sporocarp development involved in sexual reproduction and GPI-anchor transamidase complex localization
AN3839	-0,11	0,28	-0,10	0,41	-0,01	0,94	-0,09	0,41	-0,50	0,00	-0,22	0,03	Putative glycolpeptide N-tetradecanoyltransferase involved in control of polar growth; predicted role in protein, peptide, and amino acid metabolism
AN3842	-0,16	0,13	-0,13	0,30	-0,08	0,49	0,00	0,99	0,22	0,05	0,19	0,09	Putative GTPase required for early endosome trafficking; recruits prototypical Rab5 effectors Vps19, Vps45 and Vps34 and plays the major role in endocytic degradation; involved in vacuolar biogenesis; synthetically lethal with srgG/rabA
AN3906	0,07	0,65	0,10	0,59	-0,11	0,46	-0,07	0,70	-0,19	0,23	0,09	0,62	Ortholog of <i>A. nidulans</i> FGSC A4 : AN3062/pcpA, AN2480, <i>A. fumigatus</i> Af293 : Afu3g09370, Afu4g02990, Afu6g08660 and <i>A. niger</i> CBS 513.88 : An11g05730, An14g03040, An16g03020
AN3932	0,27	0,00	-0,27	0,00	0,06	0,55	-0,45	0,00	0,04	0,75	-0,21	0,03	Putative proteasome beta-5 subunit
AN4014	-0,33	0,02	0,04	0,88	-0,56	0,00	-0,25	0,11	-0,22	0,18	-0,13	0,44	Putative vacuolar sorting protein; ortholog of <i>S. cerevisiae</i> Vps52p; expression reduced after exposure to farnesol
AN4016	-0,27	0,03	0,34	0,01	-0,23	0,07	0,11	0,44	-0,38	0,00	0,22	0,11	Possible pseudogene, similar to 60S ribosomal protein L40
AN4018	0,46	0,00	-0,07	0,67	0,37	0,00	-0,11	0,42	-0,20	0,15	-0,28	0,02	Ortholog(s) have role in protein targeting to vacuole
AN4043	-0,02	0,92	0,13	0,46	-0,38	0,00	-0,22	0,13	-0,13	0,45	-0,09	0,62	Ortholog(s) have signal sequence binding activity, role in protein targeting to ER and cytosol, nuclear periphery, signal recognition particle, endoplasmic reticulum targeting localization
AN4068	-0,73	0,00	0,30	0,24	-0,25	0,25	0,56	0,01	-0,17	0,52	0,30	0,21	Ortholog(s) have UDP-galactose transmembrane transporter activity, role in UDP-galactose transmembrane transport, UDP-glucose transport, regulation of protein folding in endoplasmic reticulum and endoplasmic reticulum localization
AN4095	-0,48	0,00	0,05	0,81	-0,52	0,00	0,09	0,57	-0,12	0,45	0,10	0,55	Ortholog(s) have Golgi apparatus localization
AN4207	-0,14	0,12	-0,02	0,89	-0,13	0,15	-0,05	0,61	-0,30	0,00	-0,15	0,13	Ortholog(s) have role in endosomal transport, vesicle-mediated transport and AP-1 adaptor complex, endosome localization

AN4234	-0,63	0,01	-0,41	0,13	-0,54	0,02	-0,34	0,20	0,28	0,31	0,07	0,83	Putative phosphoacetylglucosamine mutase with a predicted role in chitin biosynthesis
AN4236	0,21	0,01	-0,15	0,14	0,25	0,00	-0,12	0,20	0,14	0,14	-0,10	0,31	Probable 26S proteasome subunit and member of the CDC48/PAS1/SEC18 family of ATPases; transcript upregulated in response to camptothecin
AN4281	-0,27	0,01	-0,17	0,18	-0,22	0,04	-0,08	0,51	0,09	0,50	-0,01	0,94	Putative GTPase with a predicted role in transport between cis and medial Golgi compartments
AN4317	-0,52	0,00	-0,18	0,16	-0,42	0,00	-0,21	0,07	-0,28	0,02	-0,07	0,63	Putative nuclear pore complex protein with homology to <i>Saccharomyces cerevisiae</i> Sec13p
AN4342	-0,02	0,94	0,00	0,99	-0,14	0,47	-0,09	0,67	0,05	0,82	0,27	0,13	Ortholog(s) have endoplasmic reticulum localization
AN4395	-0,37	0,00	0,09	0,51	-0,70	0,00	-0,29	0,01	-0,05	0,71	0,05	0,71	Ortholog of <i>A. fumigatus</i> Af293 : Afu4g06870, <i>A. niger</i> CBS 513.88 : An04g01260, <i>A. oryzae</i> RIB40 : AO090023000901, <i>Aspergillus wentii</i> : Aspwe1_0023285 and <i>Aspergillus sydowii</i> : Aspsy1_0545881
AN4416	0,32	0,01	-0,05	0,78	0,17	0,23	0,00	0,98	0,42	0,00	0,09	0,57	Syntaxin; ortholog(s) have SNAP receptor activity, role in Golgi to vacuole transport, vacuole inheritance and Golgi apparatus, endosome localization
AN4441	0,18	0,05	-0,03	0,84	0,15	0,12	0,07	0,55	-0,15	0,14	-0,16	0,11	Ortholog(s) have endoplasmic reticulum localization
AN4446	-0,26	0,05	0,11	0,53	-0,07	0,67	0,16	0,30	-0,17	0,26	0,08	0,65	Ortholog(s) have role in ER to Golgi vesicle-mediated transport and ER to Golgi transport vesicle, Golgi apparatus, endoplasmic reticulum, mitochondrion localization
AN4449	0,29	0,03	-0,20	0,20	0,25	0,06	-0,31	0,02	0,03	0,90	-0,37	0,01	Ortholog(s) have endopeptidase activator activity and role in proteasomal ubiquitin-independent protein catabolic process, proteasome-mediated ubiquitin-dependent protein catabolic process
AN4457	0,13	0,45	-0,29	0,09	0,15	0,37	-0,31	0,05	-0,26	0,12	-0,40	0,01	Ortholog(s) have endopeptidase activator activity and role in proteasomal ubiquitin-independent protein catabolic process, proteasome-mediated ubiquitin-dependent protein catabolic process
AN4463	-0,31	0,00	0,00	0,99	-0,32	0,00	-0,32	0,00	-0,01	0,93	0,10	0,42	Ortholog(s) have cytoplasm localization
AN4467	-0,26	0,15	0,29	0,16	0,00	1,00	0,39	0,04	-0,43	0,02	0,20	0,34	Cyclophilin B, with a possible role in growth at high temperature; predicted N-terminal ER signal sequence; protein levels decrease in response to farnesol
AN4495	-0,06	0,75	-0,15	0,46	-0,19	0,26	-0,49	0,00	0,18	0,36	0,05	0,82	Ortholog(s) have role in ER to Golgi vesicle-mediated transport and endoplasmic reticulum localization
AN4501	0,07	0,54	-0,04	0,79	0,24	0,02	0,02	0,87	-0,12	0,34	0,01	0,94	Putative 14-3-3 protein; induced by carbon starvation-induced autophagy
AN4528	-0,51	0,00	-0,26	0,08	-0,39	0,00	-0,24	0,09	-0,10	0,53	-0,08	0,64	Has domain(s) with predicted ER retention sequence binding activity, role in protein retention in ER lumen and integral component of membrane localization
AN4547	-0,38	0,00	-0,03	0,89	-0,44	0,00	-0,25	0,07	-0,21	0,15	0,05	0,80	Ortholog(s) have role in establishment or maintenance of cell polarity and cytosol localization
AN4563	0,02	0,91	0,25	0,15	0,38	0,01	0,50	0,00	0,38	0,02	0,47	0,00	Casein kinase I; required for delivery of amino acid transporters to the plasma membrane; mutants arrest as short germlings
AN4580	-0,10	0,64	-0,09	0,74	-0,22	0,30	-0,16	0,49	-0,62	0,00	-0,45	0,02	Has domain(s) with predicted 7S RNA binding, endoplasmic reticulum signal peptide binding activity and role in SRP-dependent cotranslational protein targeting to membrane

AN4583	0,87	0,01	0,42	0,29	1,11	0,00	0,54	0,12	0,92	0,01	0,71	0,04	Putative peptidyl-prolyl cis-trans isomerase D (PPIase); cyclophilin family member; protein abundance decreased by menadione stress; transcript levels increase during the unfolded-protein response (UPR) and in response to camptothecin
AN4616 (ssz1)	#N/D	#N/D	#N/D	#N/D	#N/D	#N/D	#N/D	#N/D	#N/D	#N/D	#N/D	#N/D	#N/D
AN4623	-0,37	0,00	0,16	0,27	-0,23	0,06	-0,07	0,64	-0,21	0,12	0,09	0,56	Ortholog(s) have UDP-glucose:glycoprotein glucosyltransferase activity, calcium ion binding, mannose binding, misfolded protein binding activity
AN4667	-0,38	0,00	0,11	0,40	-0,31	0,00	-0,22	0,04	-0,03	0,86	0,27	0,01	Septin, involved in development; prevents formation of inappropriate germ tubes and branches; required for formation of normal conidiophores; protein induced by farnesol
AN4683	-0,47	0,00	-0,12	0,55	-0,25	0,11	-0,34	0,03	-0,17	0,35	0,16	0,37	Putative oligosaccharyltransferase beta subunit; ortholog of <i>S. cerevisiae</i> Wbp1p
AN4695	0,03	0,87	-0,05	0,80	-0,11	0,41	-0,56	0,00	0,28	0,04	0,19	0,17	Putative Woronin body protein; HapX-regulated gene; protein induced by farnesol
AN4716	-0,32	0,10	-0,61	0,00	-0,36	0,06	-0,47	0,02	0,14	0,56	-0,03	0,90	Ortholog(s) have alpha-1,6-mannosyltransferase activity
AN4724	0,28	0,04	0,13	0,45	-0,19	0,20	-0,22	0,15	-0,02	0,94	-0,11	0,51	Ortholog(s) have cell division site, cell tip, cytosol, nucleus localization
AN4727	-0,07	0,85	-0,15	0,70	-0,68	0,01	-0,56	0,05	0,00	0,99	-0,55	0,06	UDP-glucose 4-epimerase, involved in galactose metabolism; converts UDP-galactose to UDP-glucose; intracellular; protein abundance decreased by menadione stress
AN4761	-0,44	0,00	-0,11	0,50	-0,32	0,01	-0,36	0,00	-0,29	0,02	-0,02	0,92	Subfamily 1 protein O-mannosyltransferase; required for normal hyphal growth and conidiophore development
AN4775	0,34	0,00	-0,19	0,16	0,31	0,01	-0,20	0,11	-0,08	0,61	-0,22	0,08	Ortholog(s) have role in cullin deneddylation, positive regulation of mitotic metaphase/anaphase transition, proteasome assembly, proteasome localization, proteasome-mediated ubiquitin-dependent protein catabolic process
AN4864	-0,52	0,00	-0,03	0,92	-0,45	0,01	-0,16	0,45	-0,11	0,62	0,00	0,99	Putative glucosyltransferase; locus contains the conserved upstream open reading frame (uORF) AN4864-uORF
AN4869	0,18	0,08	-0,38	0,00	0,17	0,10	-0,40	0,00	-0,02	0,90	-0,46	0,00	Putative 20S proteasome component; protein expressed at decreased levels in a hapX mutant versus wild-type; transcript upregulated in response to camptothecin
AN4872	0,01	0,97	0,39	0,09	0,18	0,43	0,45	0,04	-0,56	0,01	0,34	0,13	Fusion protein consisting of N-terminal ubiquitin and C-terminal extension protein (CEP) of the small ribosomal subunit; transcript upregulated in response to camptothecin
AN4876	-0,14	0,20	0,01	0,95	0,06	0,65	0,28	0,01	0,33	0,00	0,42	0,00	Ortholog(s) have role in cellular response to biotic stimulus, cellular response to starvation and filamentous growth of a population of unicellular organisms in response to biotic stimulus, more
AN4915	0,10	0,27	-0,17	0,07	-0,02	0,89	-0,23	0,01	0,11	0,26	-0,32	0,00	Putative RAB family GTPase; co-localizes with early endosomes; mutants have atypically small vacuoles
AN4925	-0,48	0,00	-0,13	0,48	-0,38	0,00	-0,14	0,39	0,01	0,98	-0,09	0,60	Ortholog(s) have endoplasmic reticulum localization
AN4947	-0,58	0,00	-0,10	0,66	-0,45	0,00	-0,39	0,02	0,27	0,12	0,12	0,54	Ortholog(s) have endoplasmic reticulum, plasma membrane localization

AN4951	-0,23	0,02	-0,07	0,61	-0,25	0,02	-0,22	0,04	0,04	0,77	0,04	0,75	Ortholog(s) have protein transporter activity and role in ascospore formation, intracellular protein transport, protein retention in Golgi apparatus, retrograde transport, endosome to Golgi
AN4997	-0,09	0,51	-0,19	0,20	-0,01	0,97	-0,08	0,61	-0,12	0,44	-0,09	0,58	Ortholog(s) have phosphatidylcholine transporter activity, phosphatidylinositol transporter activity
AN5011	0,02	0,93	0,26	0,12	-0,29	0,05	-0,14	0,40	-0,16	0,37	0,10	0,58	Ortholog(s) have role in GPI anchor biosynthetic process, fungal-type cell wall organization and cellular bud neck, cellular bud tip, endoplasmic reticulum, integral component of plasma membrane localization
AN5100	-0,44	0,01	-0,17	0,43	-0,43	0,01	0,06	0,78	0,39	0,03	0,20	0,31	Ortholog(s) have phospholipid-translocating ATPase activity and role in actin cortical patch localization, endocytosis, intracellular protein transport, phospholipid translocation
AN5105	-1,19	0,00	-0,17	0,51	-1,19	0,00	-0,14	0,53	0,07	0,80	0,21	0,36	Pmt 2 subfamily protein O-mannosyltransferase; required for normal germination, hyphal growth and conidiophore development; mutants are sensitive to growth at high temperature and to cell wall perturbing agents
AN5121	0,22	0,06	-0,29	0,02	0,19	0,10	-0,43	0,00	0,17	0,20	-0,22	0,07	Protein similar to proteasome regulatory subunit 8; menadione stress-induced protein
AN5127	-0,19	0,15	0,04	0,84	-0,06	0,71	0,21	0,14	-0,29	0,03	0,16	0,28	Ortholog(s) have SNAP receptor activity and role in ER to Golgi vesicle-mediated transport, retrograde vesicle-mediated transport, Golgi to ER, vesicle fusion
AN5129	0,79	0,01	0,64	0,05	1,24	0,00	0,88	0,00	1,29	0,00	1,04	0,00	70 kilodalton heat shock protein; protein abundance decreased by menadione stress; physically associates with importin-alpha, KapA; palA-dependent expression independent of pH; protein induced by farnesol
AN5327	-0,19	0,53	-0,13	0,74	-0,22	0,46	-0,46	0,11	0,58	0,05	-0,33	0,29	Has domain(s) with predicted GTP binding, GTPase activity
AN5346	-0,12	0,52	0,13	0,56	-0,19	0,29	0,03	0,91	0,15	0,47	0,32	0,07	Ortholog(s) have role in establishment or maintenance of cell polarity and endoplasmic reticulum localization
AN5351	0,38	0,06	0,38	0,09	0,14	0,54	0,45	0,03	0,37	0,10	0,49	0,02	Putative ubiquitin-conjugating enzyme
AN5451	0,43	0,00	0,03	0,91	0,26	0,07	-0,02	0,94	0,35	0,02	0,08	0,68	Ortholog(s) have polyubiquitin binding activity, role in negative regulation of protein catabolic process and cytosol, nucleus localization
AN5519	-0,22	0,35	-0,31	0,25	-0,06	0,83	0,02	0,94	-0,23	0,38	-0,28	0,27	Ortholog(s) have role in Golgi to vacuole transport, pathogenesis, protein targeting to vacuole and AP-3 adaptor complex, cytosol, nucleus localization
AN5521	-0,25	0,03	-0,07	0,64	-0,16	0,18	-0,02	0,90	-0,04	0,81	-0,07	0,63	Microtubule stabilizing, plus end-binding protein; Dis1/XMAP215 family, group 3; mutation causes polarity defects, hyphal curving, Spitzenkorper mislocalization, misplaced germ tube emergence, fewer and less dynamic cytoplasmic microtubules
AN5586	-0,50	0,00	-0,01	0,98	-0,78	0,00	-0,26	0,16	0,37	0,04	0,50	0,00	Putative mannose-1-phosphate guanylyltransferase with a predicted role in mannose/mannitol, fructose, and sorbose/sorbitol metabolism
AN5600	-0,49	0,00	-0,58	0,00	-0,66	0,00	-0,55	0,00	-0,05	0,82	-0,37	0,03	Has domain(s) with predicted transferase activity, transferring alkyl or aryl (other than methyl) groups activity
AN5602	0,71	0,03	0,30	0,49	0,81	0,01	0,54	0,12	0,96	0,00	0,50	0,17	Ortholog(s) have ATPase activator activity, chaperone binding activity, role in protein folding, response to stress and cytosol localization

AN5607	-0,23	0,07	0,05	0,80	-0,05	0,76	0,33	0,01	0,25	0,06	0,26	0,05	Ortholog(s) have peptidase activator activity, proteasome binding activity, role in proteasome assembly, regulation of proteasomal protein catabolic process and nucleus, proteasome core complex localization
AN5641	0,01	0,94	0,07	0,64	0,03	0,81	0,10	0,42	-0,08	0,57	0,14	0,23	Ortholog(s) have cell division site, cell tip, mitotic spindle pole body localization
AN5666	0,61	0,00	0,42	0,01	0,27	0,10	-0,14	0,47	-0,09	0,68	0,06	0,80	Putative mitogen-activated protein kinase (MAP kinase) involved in conidial germination and polarized growth; mutants arrest as branched germlings, phenotype is remediated by sucrose and NaCl; reduced growth on AVICEL medium
AN5674	0,06	0,77	0,08	0,75	0,41	0,01	0,00	0,99	-0,62	0,00	-0,03	0,92	MAP kinase, kinase, kinase, kinase (MAPK K K K K); mutants undergo premature but incomplete sexual development
AN5710	-0,07	0,69	-0,17	0,37	-0,24	0,13	-0,50	0,00	-0,32	0,06	-0,28	0,08	Ortholog(s) have phosphatidylinositol-4-phosphate binding, ubiquitin binding activity
AN5713	0,03	0,82	0,06	0,75	0,09	0,49	0,10	0,46	-0,44	0,00	-0,06	0,72	Putative chaperonin complex component, TCP-1 eta subunit; ortholog of <i>S. cerevisiae</i> Cct7p; expression reduced after exposure to farnesol
AN5725	0,33	0,11	0,05	0,89	-0,06	0,82	-0,30	0,17	0,09	0,73	-0,17	0,49	Protein with a predicted role in asparagine-linked glycosylation; <i>S. cerevisiae</i> ortholog Alg11p has alpha-1,2-mannosyltransferase activity
AN5740	-0,65	0,00	0,07	0,68	-0,41	0,00	0,07	0,65	-0,02	0,93	0,11	0,45	Protein with similarity to <i>Saccharomyces cerevisiae</i> Rho family GTPase Rho1p; involved in polar growth, hyphal branching, and cell wall synthesis
AN5744	0,15	0,18	0,25	0,03	0,20	0,07	0,18	0,11	-0,30	0,01	0,04	0,82	Putative 14-3-3-like protein; transcript upregulated in response to camptothecin
AN5747	0,06	0,67	-0,05	0,78	0,07	0,61	0,04	0,78	-0,32	0,01	-0,21	0,10	Ortholog(s) have protein domain specific binding activity
AN5748	-0,34	0,02	-0,10	0,63	-0,46	0,00	-0,42	0,01	-0,08	0,70	-0,08	0,69	Putative mannosyl-oligosaccharide 1,2-alpha-mannosidase with a predicted role in mannose polymer metabolism
AN5757	-0,33	0,01	0,17	0,28	-0,64	0,00	-0,07	0,68	0,09	0,59	0,26	0,06	Putative casein kinase-type protein kinase; ortholog of <i>S. cerevisiae</i> Yck2p; expression reduced after exposure to farnesol; mutant has a strong growth defect
AN5770	-0,47	0,01	-0,05	0,88	-0,44	0,02	-0,46	0,02	-0,40	0,05	-0,35	0,08	Ortholog(s) have endoplasmic reticulum localization
AN5784	0,16	0,22	0,01	0,97	0,15	0,26	0,01	0,97	-0,31	0,02	-0,10	0,54	Ortholog(s) have role in proteasomal ubiquitin-independent protein catabolic process, proteasome-mediated ubiquitin-dependent protein catabolic process and cytosol, nucleus, proteasome core complex, beta-subunit complex localization
AN5793	0,32	0,00	-0,11	0,45	0,37	0,00	-0,04	0,77	-0,19	0,14	-0,19	0,13	Putative 20S proteasome beta-type subunit; transcript upregulated in response to camptothecin
AN5819	0,28	0,03	-0,01	0,97	-0,13	0,34	-0,09	0,58	-0,01	0,94	-0,46	0,00	Ortholog(s) have GTP binding, signal recognition particle binding activity, role in protein targeting to ER and integral component of endoplasmic reticulum membrane, plasma membrane localization
AN5824	0,00	0,99	-0,38	0,00	-0,16	0,15	-0,33	0,00	-0,42	0,00	-0,59	0,00	Ortholog(s) have palmitoyltransferase activity and role in protein palmitoylation, protein targeting to membrane, regulation of endocytosis, regulation of pheromone-dependent signal transduction involved in conjugation with cellular fusion
AN5872	0,16	0,21	-0,35	0,01	0,30	0,01	-0,32	0,01	-0,13	0,39	-0,34	0,01	Ortholog(s) have role in proteasomal ubiquitin-independent protein catabolic process, proteasome-mediated ubiquitin-dependent protein catabolic process

AN5888	-0,36	0,08	-0,10	0,73	-0,08	0,75	-0,21	0,41	-0,18	0,47	-0,07	0,82	Ortholog(s) have UDP-N-acetylglucosamine-dolichyl-phosphate N-acetylglucosaminophosphotransferase activity and role in N-glycan processing, aerobic respiration, cellular response to drug, dolichyl diphosphate biosynthetic process
AN5895	0,32	0,02	0,49	0,00	0,29	0,03	0,37	0,01	-0,51	0,00	0,21	0,18	Putative Rab GDP-dissociation inhibitor; ortholog of <i>S. cerevisiae</i> Gdi1p
AN5902	-0,06	0,81	-0,03	0,93	-0,31	0,12	-0,35	0,09	-0,13	0,61	-0,11	0,65	Ortholog(s) have dolichyl-phosphate-glucose-glycolipid alpha-glucosyltransferase activity, role in protein N-linked glycosylation and endoplasmic reticulum membrane localization
AN5915	-0,41	0,00	-0,20	0,24	-0,41	0,00	-0,17	0,30	-0,07	0,69	-0,22	0,17	Integral membrane protein; retrieval receptor for ER resident proteins; early Golgi marker in studies of cisternal maturation
AN5970	-0,17	0,06	0,18	0,09	-0,22	0,02	-0,14	0,17	-0,35	0,00	0,01	0,92	Ortholog(s) have Golgi apparatus localization
AN5972	-0,54	0,00	-0,04	0,79	-0,43	0,00	-0,12	0,32	-0,36	0,00	-0,04	0,80	Ortholog(s) have ubiquitin binding activity
AN6010	-0,02	0,92	0,05	0,88	0,03	0,91	-0,07	0,80	1,01	0,00	0,79	0,00	Hsp70-family protein; required for conidial germination; protein expressed at increased levels during osmoadaptation
AN6047	0,00	0,99	0,12	0,45	-0,03	0,86	0,07	0,65	-0,15	0,32	0,01	0,96	Ortholog of <i>A. fumigatus</i> Af293 : Afu2g09670, <i>A. oryzae</i> RIB40 : AO090011000678/ufe1, <i>Neosartorya fischeri</i> NRRL 181 : NFIA_085140 and <i>Aspergillus wentii</i> : Aspwe1_0054391
AN6059	-0,04	0,78	0,04	0,83	0,04	0,75	0,03	0,86	-0,34	0,00	0,02	0,89	Ortholog of <i>A. fumigatus</i> Af293 : Afu2g09470, <i>A. niger</i> CBS 513.88 : An16g06820, <i>A. oryzae</i> RIB40 : AO090011000717, <i>Aspergillus wentii</i> : Aspwe1_0054380 and <i>Aspergillus sydowii</i> : Aspsy1_0045140
AN6080	-0,38	0,00	-0,06	0,74	-0,10	0,43	-0,14	0,30	-0,08	0,59	-0,05	0,74	Ortholog(s) have role in retrograde vesicle-mediated transport, Golgi to ER and COPI vesicle coat, cytosol, nucleus localization
AN6089	0,58	0,03	0,31	0,37	0,56	0,04	0,36	0,24	1,41	0,00	1,06	0,00	Putative 60 kilodalton heat shock protein
AN6112	-0,49	0,00	-0,08	0,67	-0,40	0,00	-0,09	0,54	0,19	0,17	0,11	0,49	Ortholog(s) have phospholipid-translocating ATPase activity
AN6139	-0,71	0,00	-0,20	0,38	-0,53	0,00	-0,17	0,43	-0,03	0,90	-0,30	0,13	Putative 1-acylglycerol-3-phosphate acyltransferase with a predicted role in phospholipid metabolism
AN6145	0,96	0,00	-0,01	0,98	1,01	0,00	0,21	0,30	-0,67	0,00	-0,45	0,01	Essential phospho-Ser/Thr-directed peptidyl prolyl-isomerase involved in cell cycle progression; regulates NimA function
AN6170	-0,04	0,81	0,02	0,94	0,12	0,37	-0,06	0,68	-0,16	0,25	-0,02	0,90	Ortholog(s) have chaperone binding activity, role in ER-associated ubiquitin-dependent protein catabolic process, protein folding in endoplasmic reticulum, response to unfolded protein and endoplasmic reticulum lumen localization
AN6210	0,10	0,47	-0,10	0,51	0,02	0,91	-0,18	0,19	0,03	0,84	-0,05	0,74	Ortholog(s) have GTP-Rho binding, phosphatidylinositol-4,5-bisphosphate binding activity and role in Golgi to plasma membrane transport, Rho protein signal transduction, exocyst assembly, exocyst localization
AN6257	-0,36	0,00	0,24	0,03	-0,24	0,02	0,19	0,07	-0,30	0,00	0,29	0,00	Ortholog(s) have role in ER to Golgi vesicle-mediated transport, intracellular protein transport, nuclear envelope organization and cytosol localization
AN6267	0,11	0,49	-0,05	0,80	0,12	0,43	-0,06	0,74	-0,06	0,74	-0,07	0,70	Ortholog(s) have role in cellular response to nitrogen starvation, negative regulation of G0 to G1 transition

AN6269	-0,15	0,17	-0,07	0,67	-0,39	0,00	-0,13	0,30	-0,15	0,23	-0,13	0,29	Putative ER protein-translocation complex subunit; ortholog of <i>S. cerevisiae</i> Sec62p
AN6307	-0,33	0,02	0,15	0,42	0,03	0,87	0,16	0,35	-0,29	0,07	0,19	0,25	Ortholog(s) have Golgi apparatus, endoplasmic reticulum, fungal-type vacuole membrane localization
AN6351	0,07	0,65	-0,05	0,83	0,01	0,96	-0,10	0,54	-0,28	0,05	-0,14	0,39	Ortholog(s) have phosphatidylinositol-3-phosphate binding activity and role in CVT pathway, early endosome to Golgi transport, macroautophagy, mitochondrion degradation
AN6493	0,10	0,57	0,00	1,00	-0,23	0,13	-0,20	0,23	-0,22	0,20	-0,19	0,28	Has domain(s) with predicted role in vesicle docking involved in exocytosis and exocyst localization
AN6531	-0,07	0,70	0,06	0,80	-0,21	0,17	-0,11	0,52	-0,37	0,02	-0,10	0,58	Putative Sec1p-like protein with a predicted role in vacuolar protein sorting
AN6533	-0,04	0,85	-0,58	0,00	-0,02	0,94	-0,58	0,00	-0,08	0,75	-0,53	0,00	Component of the TRAPII complex; required for normal morphology; mutants are defective in polarity maintenance and secretion; ortholog of <i>S. cerevisiae</i> Trs120p, involved in targeting and fusion of ER-Golgi vesicles
AN6542	-0,04	0,68	-0,28	0,00	0,08	0,39	-0,30	0,00	0,01	0,97	-0,06	0,59	Gamma-actin
AN6547	0,44	0,00	-0,18	0,19	0,30	0,01	-0,05	0,74	-0,18	0,20	-0,38	0,00	Ortholog(s) have role in proteasomal ubiquitin-independent protein catabolic process, proteasome-mediated ubiquitin-dependent protein catabolic process
AN6589	-0,22	0,24	0,00	1,00	-0,18	0,34	-0,09	0,69	-0,30	0,13	0,07	0,77	Ortholog(s) have mannose-ethanolamine phosphotransferase activity
AN6606	-0,20	0,18	-0,04	0,86	-0,34	0,02	-0,40	0,01	0,09	0,64	0,08	0,68	Ortholog(s) have role in N-glycan processing, post-translational protein modification and endoplasmic reticulum localization
AN6614	0,10	0,40	0,08	0,60	0,15	0,16	0,23	0,04	-0,02	0,88	-0,01	0,97	Ortholog(s) have role in endocytosis, retrograde vesicle-mediated transport, Golgi to ER, vacuole organization and COPI-coated vesicle, Golgi membrane, endosome localization
AN6615	-0,21	0,04	0,06	0,69	-0,12	0,28	0,25	0,02	0,42	0,00	0,47	0,00	Has domain(s) with predicted role in COPII vesicle coating
AN6627	-0,12	0,18	0,07	0,52	-0,25	0,00	0,16	0,08	-0,08	0,43	0,10	0,33	Ortholog(s) have GTP binding, signal recognition particle binding activity, role in protein targeting to ER and cytosol, endoplasmic reticulum membrane, nucleus localization
AN6628	-0,12	0,37	0,06	0,75	-0,38	0,00	0,01	0,94	0,04	0,84	0,20	0,15	Ortholog(s) have role in cellular response to nitrogen starvation, establishment or maintenance of cell polarity, negative regulation of G0 to G1 transition
AN6702	-0,48	0,00	-0,13	0,59	-0,58	0,00	-0,32	0,08	0,02	0,94	-0,08	0,73	Ortholog(s) have Golgi apparatus, endoplasmic reticulum localization
AN6709	-0,39	0,00	-0,09	0,55	-0,34	0,00	-0,27	0,02	-0,11	0,43	-0,14	0,28	Putative ADP ribosylation factor guanine nucleotide exchange factor; Sec7-domain protein; role in hyphal morphogenesis; mutants display abnormal hyphae, hyphal tip cell death and excessive septum formation
AN6726	0,08	0,46	-0,34	0,00	-0,04	0,78	-0,45	0,00	-0,23	0,04	-0,39	0,00	Ortholog(s) have role in proteasomal ubiquitin-independent protein catabolic process, proteasome-mediated ubiquitin-dependent protein catabolic process
AN6741	0,66	0,00	-0,30	0,05	0,36	0,01	-0,28	0,05	0,17	0,30	-0,29	0,05	Ortholog(s) have polyubiquitin binding activity
AN6825	0,42	0,00	0,07	0,65	0,35	0,00	-0,18	0,17	-0,06	0,69	-0,27	0,02	Component of the TRAPII complex that mediates Rab guanyl-nucleotide exchange factor activity, involved in Golgi vesicle-mediated transport
AN6838	-0,16	0,31	0,68	0,00	-0,47	0,00	0,36	0,02	-0,44	0,00	0,19	0,28	Beta-tubulin, highly conserved component of microtubules; <i>A. nidulans</i> has two beta-tubulin genes, tubC and benA; expression of tubC increases during conidiation



AN6874	0,08	0,68	-0,10	0,64	-0,06	0,73	-0,14	0,45	0,15	0,45	0,21	0,24	Putative mannosyltransferase; transcript levels increase during the unfolded-protein response (UPR); <i>S. cerevisiae</i> ortholog Alg2p has glycolipid 6-alpha-mannosyltransferase activity
AN6911	-0,13	0,35	0,12	0,44	-0,14	0,31	0,12	0,42	-0,11	0,46	0,07	0,67	Ortholog(s) have cytosol, nucleus localization
AN6974	-0,28	0,02	0,03	0,86	-0,30	0,01	-0,01	0,97	0,02	0,93	0,24	0,07	Putative Rab-like GTPase
AN6988	-0,02	0,88	-0,07	0,61	0,07	0,53	-0,06	0,61	-0,08	0,53	0,02	0,91	Ortholog(s) have protein domain specific binding activity
AN7016	-0,28	0,01	-0,01	0,97	-0,25	0,03	-0,22	0,06	0,00	0,99	-0,02	0,88	Has domain(s) with predicted role in intracellular protein transport, vesicle-mediated transport and clathrin adaptor complex, membrane coat localization
AN7049	-0,61	0,00	0,03	0,90	-0,63	0,00	-0,30	0,10	-0,20	0,33	0,13	0,55	Ortholog(s) have mannose-ethanolamine phosphotransferase activity and role in ATP transport, GPI anchor biosynthetic process, conidium formation, fungal-type cell wall organization or biogenesis, regulation of growth rate
AN7143	-0,56	0,01	-0,27	0,30	-0,20	0,39	-0,06	0,82	-0,27	0,27	-0,34	0,15	Ortholog(s) have cytosol localization
AN7254	0,32	0,02	0,20	0,23	0,55	0,00	0,43	0,00	0,47	0,00	0,35	0,02	Protein with a conserved CDC48, cell division protein N-terminal domain and two ATPase domains of the AAA-superfamily; protein expressed at increased levels during osmoadaptation; protein induced by farnesol
AN7301	-0,30	0,12	-0,13	0,63	-0,41	0,03	-0,34	0,09	-0,34	0,10	-0,36	0,07	Putative glucosyltransferase; ortholog of <i>S. cerevisiae</i> Alg8p; expression reduced after exposure to farnesol
AN7302	-0,47	0,00	0,04	0,86	-0,30	0,07	-0,16	0,41	-0,15	0,45	0,24	0,19	Ortholog(s) have role in ER to Golgi vesicle-mediated transport and ER to Golgi transport vesicle, fungal-type vacuole membrane, integral component of Golgi membrane, integral component of endoplasmic reticulum membrane localization
AN7311	0,00	0,99	0,21	0,23	0,40	0,01	0,90	0,00	0,06	0,75	0,58	0,00	Ortholog(s) have cytosol localization
AN7425	-0,31	0,09	-0,20	0,38	-0,36	0,05	-0,36	0,06	0,20	0,34	-0,31	0,12	Has domain(s) with predicted lipid transporter activity, role in lipid transport and integral component of membrane localization
AN7426	-0,60	0,00	0,06	0,81	-0,40	0,01	-0,11	0,57	-0,27	0,13	0,09	0,67	Ortholog(s) have dolichyl-diphosphooligosaccharide-protein glycotransferase activity and role in protein N-linked glycosylation, protein O-linked mannosylation, protein complex assembly
AN7436	-0,74	0,00	0,24	0,14	-0,56	0,00	0,06	0,76	-0,09	0,61	0,34	0,02	Putative protein disulfide isomerase; pdiA mRNA expression increased in the presence of farnesol
AN7464	-0,38	0,01	-0,01	0,96	-0,43	0,00	-0,38	0,01	-0,36	0,02	-0,26	0,11	Putative calcium-transporting ATPase with a predicted role in energy metabolism; putative secretory pathway component; up-regulated under osmotic stress conditions
AN7472	-0,15	0,39	0,01	0,97	-0,03	0,87	-0,18	0,35	-0,28	0,13	-0,06	0,80	Ortholog(s) have dolichyl-diphosphooligosaccharide-protein glycotransferase activity, role in protein N-linked glycosylation via asparagine and oligosaccharyltransferase complex, plasma membrane localization
AN7534	-1,39	0,00	-0,28	0,25	-1,13	0,00	-0,14	0,55	0,12	0,65	0,04	0,88	Ortholog of <i>A. fumigatus</i> Af293 : Afu1g01380/och4, <i>A. niger</i> CBS 513.88 : An14g07140, An12g07020, <i>Aspergillus versicolor</i> : Aspve1_0085820 and <i>Aspergillus clavatus</i> NRRL 1 : ACLA_033030

AN7562	0,01	0,98	0,47	0,04	0,08	0,75	0,56	0,01	-0,11	0,68	0,52	0,01	Ortholog(s) have alpha-1,6-mannosyltransferase activity, role in ascospore formation, barrier septum assembly and alpha-1,6-mannosyltransferase complex localization
AN7602	-0,15	0,34	-0,08	0,70	-0,37	0,01	-0,38	0,01	0,07	0,71	0,00	0,99	Putative GTPase with a role in retrograde traffic from endosomes to the Golgi; partially localizes to the late Golgi and to the Spitzenkorper; mutants display an increase in abundance of early endosomes
AN7625	0,65	0,00	0,30	0,24	0,31	0,16	-0,13	0,60	-0,75	0,00	0,01	0,98	Putative myo-inositol-1-phosphate synthase with a predicted role in phospholipid metabolism; intracellular, menadione stress-induced protein; palA-dependent expression independent of pH
AN7672	-0,84	0,00	-0,11	0,69	-0,66	0,00	-0,29	0,17	0,17	0,47	0,27	0,23	Ortholog(s) have alpha-1,6-mannosyltransferase activity, mannosyltransferase activity
AN7679	-0,58	0,00	0,15	0,54	-0,34	0,05	-0,08	0,74	-0,26	0,21	0,00	1,00	Ortholog(s) have role in ER to Golgi vesicle-mediated transport and ER to Golgi transport vesicle, integral component of Golgi membrane, integral component of endoplasmic reticulum membrane localization
AN7683	-0,21	0,34	-0,27	0,28	-0,63	0,00	-0,19	0,41	0,13	0,63	-0,02	0,95	Protein associated with the nonclassical protein export pathway; ortholog of <i>S. cerevisiae</i> Nce102p
AN7715	0,17	0,37	-0,07	0,78	0,30	0,10	0,03	0,91	-0,01	0,98	-0,06	0,81	Ortholog(s) have dolichyl-phosphate beta-glucosyltransferase activity and endoplasmic reticulum membrane localization
AN7721	-0,39	0,00	0,26	0,07	-0,40	0,00	-0,03	0,87	-0,21	0,14	0,22	0,12	Putative translocon, alpha subunit; ortholog of <i>S. cerevisiae</i> Sec61p
AN8023	0,16	0,37	0,23	0,23	0,16	0,39	0,55	0,00	0,53	0,00	0,43	0,01	Protein required for vacuole biogenesis
AN8054	0,29	0,03	-0,20	0,23	0,26	0,07	-0,21	0,15	-0,03	0,89	-0,32	0,03	Predicted alpha 4 subunit of the 20S core proteasome; involved in N-myristoylation and cell morphogenesis; menadione stress-induced protein
AN8065	0,22	0,07	-0,18	0,20	0,40	0,00	-0,15	0,28	-0,32	0,01	-0,31	0,01	Ortholog(s) have role in Arp2/3 complex-mediated actin nucleation, actin cortical patch localization, cellular response to drug, endocytosis and establishment of mitochondrion localization, more
AN8119	-0,53	0,00	-0,09	0,68	-0,61	0,00	-0,37	0,02	0,05	0,81	-0,10	0,62	Ortholog(s) have mannosylphosphate transferase activity, mannosyltransferase activity
AN8153	-0,33	0,13	-2,07	0,00	1,75	0,00	-0,43	0,06	0,95	0,46	-1,63	0,00	Has domain(s) with predicted ATP binding, nucleoside-triphosphatase activity, nucleotide binding activity
AN8182	-0,27	0,02	-0,04	0,85	-0,39	0,00	-0,48	0,00	-0,03	0,88	0,01	0,96	Septin, involved in development; prevents formation of inappropriate germ tubes and branches; required for formation of normal conidiophores
AN8194	-0,43	0,00	-0,01	0,95	-0,34	0,01	-0,21	0,13	-0,06	0,71	0,15	0,33	Ortholog(s) have Golgi apparatus, endoplasmic reticulum localization
AN8246	-0,16	0,08	-0,17	0,08	-0,38	0,00	-0,18	0,05	0,12	0,24	-0,24	0,01	Putative signal recognition particle protein
AN8258	0,63	0,02	0,32	0,34	0,42	0,13	0,45	0,11	0,64	0,02	0,55	0,05	Putative ubiquitin-conjugating enzyme; ortholog of <i>S. cerevisiae</i> Ubc7p
AN8268	-0,22	0,14	-0,20	0,23	-0,20	0,19	-0,45	0,00	-0,20	0,21	-0,29	0,05	Putative RasGAP SH3 binding protein, contains NTF2 and RRM domains; expression reduced after exposure to farnesol
AN8269	0,66	0,03	0,71	0,03	0,96	0,00	0,68	0,03	1,14	0,00	0,95	0,00	90 kilodalton heat shock protein; physically associates with importin-alpha, KapA; palA-dependent expression independent of pH

AN8291	0,11	0,39	0,16	0,28	0,16	0,19	0,02	0,91	-0,05	0,78	0,18	0,18	Ortholog(s) have nucleus localization
AN8343	-0,02	0,92	0,05	0,82	0,16	0,34	0,17	0,33	-0,44	0,01	-0,12	0,54	Protein with similarity to FK506 binding proteins (FKBPs); putative N-terminal signal sequence, predicted ER localization; protein levels decrease in response to farnesol
AN8488	0,12	0,48	0,07	0,76	0,07	0,68	0,05	0,79	-0,09	0,65	-0,01	0,97	Ortholog(s) have SNAP receptor activity, palmitoyltransferase activity
AN8488	0,12	0,48	0,07	0,76	0,07	0,68	0,05	0,79	-0,09	0,65	-0,01	0,97	Ortholog(s) have SNAP receptor activity, palmitoyltransferase activity
AN8605	0,60	0,01	-0,02	0,95	0,76	0,00	-0,14	0,65	-0,62	0,01	-0,60	0,02	Putative peptidyl-prolyl cis-trans isomerase (PPIase); cyclophilin
AN8631	-0,15	0,49	-0,38	0,07	-0,15	0,49	-0,37	0,07	-0,03	0,92	-0,13	0,58	Protein with similarity to FK506 binding proteins (FKBPs)
AN8769	-0,12	0,34	-0,20	0,16	-0,17	0,17	0,08	0,56	0,48	0,00	0,23	0,08	Putative synaptobrevin homolog; secretory v-SNARE; GFP-SynA localizes to the plasma membrane at the tips of hyphae
AN8795	-0,33	0,00	-0,08	0,61	-0,36	0,00	-0,22	0,06	-0,19	0,12	-0,02	0,89	Ortholog(s) have role in endosomal transport, regulation of cytokinesis, regulation of fungal-type cell wall organization, regulation of vacuole fusion, non-autophagic, vesicle-mediated transport
AN8798	-0,33	0,00	0,12	0,37	-0,50	0,00	0,11	0,37	0,10	0,46	0,19	0,10	Ortholog(s) have Golgi apparatus localization
AN8828	-0,18	0,26	0,23	0,19	-0,38	0,01	0,05	0,82	-0,15	0,40	0,03	0,90	Component of the TRAPII complex that mediates Rab guanyl-nucleotide exchange factor activity, involved in Golgi vesicle-mediated transport
AN8831	-0,39	0,01	-0,14	0,52	-0,27	0,10	-0,01	0,97	0,06	0,81	-0,30	0,09	Ortholog(s) have GTPase activator activity and role in actin filament organization, actomyosin contractile ring assembly, hyphal growth, small GTPase mediated signal transduction, syncytium formation by plasma membrane fusion
AN8848	-0,72	0,00	-0,11	0,70	-0,78	0,00	-0,43	0,03	-0,08	0,75	-0,15	0,54	Putative GDP-mannose transporter
AN8862	-0,53	0,00	-0,07	0,74	-0,36	0,01	-0,03	0,85	0,15	0,36	0,25	0,09	Myosin V; involved in the movement of vesicles to the hyphal tip; essential for polarized growth in the absence of microtubules
AN8864	-0,43	0,00	0,11	0,48	-0,51	0,00	-0,10	0,48	0,07	0,64	0,19	0,16	Ortholog(s) have endoplasmic reticulum localization
AN8874	-0,35	0,00	-0,11	0,40	-0,39	0,00	-0,28	0,01	-0,10	0,41	-0,14	0,24	Ortholog(s) have GTPase activity, protein homodimerization activity
AN8879	0,04	0,81	0,08	0,69	-0,41	0,00	-0,21	0,13	0,18	0,23	-0,02	0,93	Ortholog(s) have role in Golgi to plasma membrane transport, cytokinetic cell separation, exocytosis and cell cortex of cell tip, cell division site, cytosol, excyst, mating projection tip, mitotic spindle pole body, nucleus localization
AN8880	-0,30	0,01	0,01	0,98	-0,25	0,02	-0,20	0,09	-0,26	0,03	-0,03	0,83	Putative vacuolar hydrolase sorting receptor
AN9086	0,05	0,85	0,15	0,56	0,12	0,59	0,15	0,51	-0,58	0,00	-0,09	0,73	Component of the TRAPII complex that mediates Rab guanyl-nucleotide exchange factor activity, involved in Golgi vesicle-mediated transport
AN9101	0,04	0,80	-0,12	0,39	-0,18	0,15	-0,10	0,45	-0,02	0,89	-0,04	0,81	Ortholog of <i>A. fumigatus</i> Af293 : Afu7g02090, <i>A. niger</i> CBS 513.88 : An12g00580, <i>A. oryzae</i> RIB40 : AO090038000586, <i>Aspergillus wentii</i> : Aspwe1_0158097 and <i>Aspergillus sydowii</i> : Aspsy1_0061410
AN9124	0,85	0,00	0,42	0,24	0,84	0,00	0,46	0,16	1,06	0,00	0,74	0,02	Ortholog(s) have ATPase inhibitor activity, Hsp70 protein binding, Hsp90 protein binding, mRNA binding activity, role in protein folding and cytosol, nucleus localization

AN9148	-0,58	0,00	-0,40	0,02	-0,26	0,11	-0,22	0,19	0,13	0,50	0,24	0,18	Putative UTP-glucose-1-phosphate uridylyltransferase with a predicted role in galactose and galactitol metabolism; protein expressed at decreased levels in a hapX mutant versus wild-type
AN9149	-0,37	0,02	0,15	0,47	-0,50	0,00	-0,05	0,81	-0,24	0,18	0,14	0,48	Ortholog(s) have Golgi apparatus, cell tip, cytoplasmic vesicle, endoplasmic reticulum, plasma membrane localization
AN9397	-1,45	0,00	-0,46	0,18	-1,37	0,00	0,00	1,00	0,70	0,02	0,09	0,83	Putative basic leucine zipper (bZIP) transcription factor that regulates the unfolded protein response; hacA mRNA expression increased in the presence of farnesol
AN9420	-0,02	0,91	-0,03	0,91	-0,10	0,52	-0,12	0,48	-0,49	0,00	-0,25	0,10	Putative peptidyl-prolyl cis-trans isomerase H (PPIase)
AN9460	-0,04	0,83	0,17	0,32	0,19	0,19	0,11	0,51	-0,36	0,01	-0,06	0,74	Ortholog(s) have peptidase activity, role in protein targeting to ER, signal peptide processing and signal peptidase complex localization
AN9526	-0,48	0,00	-0,25	0,06	-0,17	0,17	-0,07	0,66	0,09	0,54	-0,04	0,81	t-SNARE; role in vesicular transport between the ER and the Golgi complex; involved in polarity establishment and secretion

---

**Table S8.** 17 differentially expressed genes related to secretory pathway and its transcriptional response characterization.

AspGD	Regulation	Strain	Name	Description in AspGD	Orthologs and best hit in <i>S. cerevisiae</i>	Description Saccharomyces Genome Database
AN1296	up	BglC 8h	-	Ortholog(s) have 2',3'-cyclic-nucleotide 3'-phosphodiesterase activity, GTP-dependent polyribonucleotide 5'-hydroxyl-kinase activity, RNA ligase (ATP) activity	TRL1	tRNA ligase; required for tRNA splicing and for both splicing and translation of HAC1 mRNA in the UPR; has phosphodiesterase, polynucleotide kinase, and ligase activities; localized at the inner nuclear envelope and partially to polysomes
AN1620	down	1542 8h , AbfA 8h	-	Ortholog of <i>A. nidulans</i> FGSC A4 : AN2626, <i>A. fumigatus</i> Af293 : Afu8g02040/och3, <i>A. niger</i> CBS 513.88 : An03g01090/hocA, An05g02320 and <i>A. oryzae</i> RIB40 : AO090010000615	HOC1	Alpha-1,6-mannosyltransferase; involved in cell wall mannan biosynthesis; subunit of a Golgi-localized complex that also contains Anp1p, Mnn9p, Mnn11p, and Mnn10p; identified as a suppressor of a cell lysis sensitive <i>pkc1-371</i> allele
AN1933	down	1542 2h , AbfA 2h	-	Has domain(s) with predicted endoplasmic reticulum membrane, integral component of membrane localization	ORM1	Protein that mediates sphingolipid homeostasis; evolutionarily conserved, required for resistance to agents that induce unfolded protein response; Orm1p and Orm2p together control membrane biogenesis by coordinating lipid homeostasis with protein quality control; ORM1 has a paralog, ORM2, that arose from the whole genome duplication
AN2045	down	1542 8h	-	Has domain(s) with predicted calcium ion binding, mannosyl-oligosaccharide 1,2-alpha-mannosidase activity and membrane localization	MNS1	Alpha-1,2-mannosidase; involved in ER-associated protein degradation (ERAD); catalyzes the removal of one mannose residue from a glycosylated protein, converting the modification from Man9GlcNAc to Man8GlcNAc; catalyzes the last step in glycoprotein maturation in the ER and is critical for ER protein degradation
AN2731	up	BglC 2h	-	Ortholog(s) have ATPase activator activity, unfolded protein binding activity	YDJ1	Type I HSP40 co-chaperone; involved in regulation of HSP90 and HSP70 functions; acts as an adaptor that helps Rsp5p recognize cytosolic misfolded proteins for ubiquitylation after heat shock; critical for determining cell size at Start as a function of growth rate; involved in protein translocation across membranes; member of the DnaJ family
AN3787	down	1542 2h , AbfA 2h	-	Ortholog(s) have glycoprotein binding, metal ion binding, misfolded protein binding, peptide-N4-(N-acetyl-beta-glucosaminyl)asparagine amidase activity, structural constituent of cell wall activity	PNG1	Conserved peptide N-glycanase; required for deglycosylation of misfolded glycoproteins during proteasome-dependent degradation; localizes to the cytoplasm and nucleus; activity is enhanced by interaction with Rad23p
AN4583	up	AbfA 2h	cyp7	Putative peptidyl-prolyl cis-trans isomerase D (PPIase); cyclophilin family member; protein abundance decreased by menadione stress; transcript levels increase during the unfolded-protein response (UPR) and in response to camptothecin	CPR6	Peptidyl-prolyl cis-trans isomerase (cyclophilin); catalyzes the cis-trans isomerization of peptide bonds N-terminal to proline residues; plays a role in determining prion variants; binds to Hsp82p and contributes to chaperone activity; protein abundance increases in response to DNA replication stress

<b>AN5105</b>	down	1542 2h , AbfA 2h	pmtA	Pmt 2 subfamily protein O-mannosyltransferase; required for normal germination, hyphal growth and conidiophore development; mutants are sensitive to growth at high temperature and to cell wall perturbing agents	PMT2	Protein O-mannosyltransferase of the ER membrane; transfers mannose residues from dolichyl phosphate-D-mannose to protein serine/threonine residues; involved in ER quality control; acts in a complex with Pmt1p, can instead interact with Pmt5p; antifungal drug target; PMT2 has a paralog, PMT3, that arose from the whole genome duplication
<b>AN5129</b>	up	AbfA 2h , BglC 2h , BglC 8h	hsp70	70 kilodalton heat shock protein; protein abundance decreased by menadione stress; physically associates with importin-alpha, KapA; palA-dependent expression independent of pH; protein induced by farnesol	SSA1	ATPase involved in protein folding and NLS-directed nuclear transport; member of HSP70 family; forms chaperone complex with Ydj1p; localized to nucleus, cytoplasm, and cell wall; 98% identical with paralog Ssa2p, but subtle differences between the two proteins provide functional specificity with respect to propagation of yeast [URE3] prions and vacuolar-mediated degradations of gluconeogenesis enzymes; general targeting factor of Hsp104p to prion fibrils
<b>AN6010</b>	up	BglC 2h	sgdE	Hsp70-family protein; required for conidial germination; protein expressed at increased levels during osmoadaptation	SSC1	Hsp70 family ATPase; constituent of the import motor component of the Translocase of the Inner Mitochondrial membrane (TIM23 complex); involved in protein translocation and folding; subunit of Scel endonuclease; SSC1 has a paralog, ECM10, that arose from the whole genome duplication
<b>AN6089</b>	up	BglC 2h , BglC 8h	-	Putative 60 kilodalton heat shock protein	HSP60	Tetradecameric mitochondrial chaperonin; required for ATP-dependent folding of precursor polypeptides and complex assembly; prevents aggregation and mediates protein refolding after heat shock; role in mtDNA transmission; phosphorylated
<b>AN6145</b>	up	AbfA 2h	pinA	Essential phospho-Ser/Thr-directed peptidyl prolyl-isomerase involved in cell cycle progression; regulates NimA function	ESS1	Peptidylprolyl-cis/trans-isomerase (PPIase); specific for phosphorylated Ser and Thr residues N-terminal to proline; regulates phosphorylation of RNAPII large subunit (Rpo21p) C-terminal domain (CTD) at Ser7; associates with phospho-Ser5 form of RNAPII in vivo; present along entire coding length of genes; represses initiation of CUTs; required for efficient termination of mRNA transcription, trimethylation of histone H3; human homolog PIN1 can complement yeast null mutant
<b>AN7534</b>	down	1542 2h , AbfA 2h	-	Ortholog of <i>A. fumigatus</i> Af293 : Afu1g01380/och4, <i>A. niger</i> CBS 513.88 : An14g07140, An12g07020, <i>Aspergillus versicolor</i> : Aspve1_0085820 and <i>Aspergillus clavatus</i> NRRL 1 : ACLA_033030	HOC1	Alpha-1,6-mannosyltransferase; involved in cell wall mannan biosynthesis; subunit of a Golgi-localized complex that also contains Anp1p, Mnn9p, Mnn11p, and Mnn10p; identified as a suppressor of a cell lysis sensitive <i>pkc1-371</i> allele
<b>AN8153</b>	down	1542 8h	-	Has domain(s) with predicted ATP binding, nucleoside-triphosphatase activity, nucleotide binding activity	CDC48	ATPase; subunit of polyubiquitin-selective segregase complex involved in ERAD, cell wall integrity during heat stress, mitotic spindle disassembly; role in mobilizing membrane bound transcription factors by regulated ubiquitin/proteasome-dependent processing in macroautophagy, PMN, RAD, ribophagy, homotypic ER membrane fusion, disassembly of Met30p from SCF complex, telomerase regulation via Est1p degradation; human ortholog VCP can complement yeast <i>cdc48</i> mutant

<b>AN8269</b>	up	BglC 2h	hsp90	90 kilodalton heat shock protein; physically associates with importin-alpha, KapA; palA-dependent expression independent of pH	HSC82	Cytoplasmic chaperone of the Hsp90 family; plays a role in determining prion variants; redundant in function and nearly identical with Hsp82p, and together they are essential; expressed constitutively at 10-fold higher basal levels than HSP82 and induced 2-3 fold by heat shock; contains two acid-rich unstructured regions that promote the solubility of chaperone-substrate complexes; HSC82 has a paralog, HSP82, that arose from the whole genome duplication
<b>AN9124</b>	up	BglC 2h	-	Ortholog(s) have ATPase inhibitor activity, Hsp70 protein binding, Hsp90 protein binding, mRNA binding activity, role in protein folding and cytosol, nucleus localization	STI1	Hsp90 cochaperone; regulates spatial organization of amyloid-like proteins in the cytosol, thereby buffering the proteotoxicity caused by amyloid-like proteins; interacts with the Ssa group of the cytosolic Hsp70 chaperones and activates Ssa1p ATPase activity; interacts with Hsp90 chaperones and inhibits their ATPase activity; homolog of mammalian Hop
<b>AN9397</b>	down	1542 2h , AbfA 2h	hacA	Putative basic leucine zipper (bZIP) transcription factor that regulates the unfolded protein response; hacA mRNA expression increased in the presence of farnesol	HAC1	Basic leucine zipper (bZIP) transcription factor (ATF/CREB1 homolog); regulates the unfolded protein response, via UPRE binding, and membrane biogenesis; ER stress-induced splicing pathway facilitates efficient Hac1p synthesis; two functional forms of Hac1p are produced; translation initiation is repressed under non-stress conditions; protein abundance increases in response to DNA replication stress

**Additional file 3. Table S9: Summary of RNA-seq data. Raw reads, percentage of ribosomal RNA reads and concordant pairs alignment rate obtained.** Approximately 148 million 100 bp paired-end reads were obtained for *A. nidulans* A773, AbfA and BglC producer strains, and 130 million reads were obtained for 1542 strain, representing 115 GB.



**Table S9:** Summary of RNA-seq data. Raw reads, percentage of ribosomal RNA reads and concordant pairs alignment rate obtained.

Sample	Input Reads	Both Surviving	Forward Only Surviving	Reverse Only Surviving	Dropped	% ribosomal RNA	Input Reads for pairs alignment	% concordant pairs alignment
1542_2h1	22874083	18282816 (79.93%)	3369838 (14.73%)	524628 (2.29%)	696801 (3.05%)	3.86%	17582893	92.0%
1542_2h2	18218018	14912590 (81.86%)	2362258 (12.97%)	426374 (2.34%)	516796 (2.84%)	9.65%	13481070	92.5%
1542_2h3	20114219	16053304 (79.81%)	2954969 (14.69%)	484891 (2.41%)	621055 (3.09%)	16.31%	13443578	91.9%
1542_8h1	27682916	23416305 (84.59%)	2758961 (9.97%)	785950 (2.84%)	721700 (2.61%)	2.36%	22866360	92.9%
1542_8h2	20948279	17711140 (84.55%)	2014004 (9.61%)	651855 (3.11%)	571280 (2.73%)	12.30%	15536878	92.9%
1542_8h3	20524525	17566992 (85.59%)	1851926 (9.02%)	596877 (2.91%)	508730 (2.48%)	2.95%	17051627	92.6%
A773_2h1	19441621	15684057 (80.67%)	2716223 (13.97%)	467093 (2.40%)	574248 (2.95%)	2.17%	15349125	92.3%
A773_2h2	20807956	16919783 (81.31%)	2845704 (13.68%)	471119 (2.26%)	571350 (2.75%)	3.04%	16408973	92.5%
A773_2h3	27038293	21541530 (79.67%)	4003978 (14.81%)	645509 (2.39%)	847276 (3.13%)	12.99%	18755075	92.3%
A773_8h1	25274439	21705462 (85.88%)	2282268 (9.03%)	681032 (2.69%)	605677 (2.40%)	2.47%	21173358	92.9%
A773_8h2	33426421	27999516 (83.76%)	3602172 (10.78%)	917886 (2.75%)	906847 (2.71%)	2.14%	27409221	89.8%
A773_8h3	22771558	19120384 (83.97%)	2409399 (10.58%)	632048 (2.78%)	609727 (2.68%)	2.63%	18620600	92.8%
AbfA_2h1	44277145	36983415 (83.53%)	5019601 (11.34%)	1090890 (2.46%)	1183239 (2.67%)	2.45%	36091826	91.0%
AbfA_2h2	19531134	15905586 (81.44%)	2621570 (13.42%)	444097 (2.27%)	559881 (2.87%)	2.00%	15593498	91.2%
AbfA_2h3	25798647	21495834 (83.32%)	2972811 (11.52%)	644072 (2.50%)	685930 (2.66%)	3.04%	20851713	84.5%
AbfA_8h1	20581245	17517010 (85.11%)	1872377 (9.10%)	656064 (3.19%)	535794 (2.60%)	3.12%	16975140	91.6%
AbfA_8h2	20278973	16486377 (81.30%)	2525387 (12.45%)	659529 (3.25%)	607680 (3.00%)	51.70%	7975840	91.4%
AbfA_8h3	17990035	15432859 (85.79%)	1616352 (8.98%)	508315 (2.83%)	432509 (2.40%)	2.33%	15077306	91.2%
BglC_2h1	24335833	19657066 (80.77%)	3386939 (13.92%)	551933 (2.27%)	739895 (3.04%)	1.53%	19362725	91.1%
BglC_2h2	24809743	20213169 (81.47%)	3275913 (13.20%)	596209 (2.40%)	724452 (2.92%)	1.65%	19885353	90.8%
BglC_2h3	22632342	18611102 (82.23%)	2857654 (12.63%)	526099 (2.32%)	637487 (2.82%)	1.41%	18353227	90.9%
BglC_8h1	25403670	21822034 (85.90%)	2184696 (8.60%)	764367 (3.01%)	632573 (2.49%)	1.61%	21475373	90.9%
BglC_8h2	27433696	23691216 (86.36%)	2242054 (8.17%)	822152 (3.00%)	678274 (2.47%)	2.74%	23046556	90.5%
BglC_8h3	23326256	19960333 (85.57%)	2126655 (9.12%)	661906 (2.84%)	577362 (2.48%)	2.40%	19486055	90.9%

**Additional file 4. Table S10. Sequences of primers used for qPCR analysis for the different genes studied.** F - Primer Forward; R - Primer Reverse. *tubC* was used as an endogenous control in the qPCR analysis.

**Table S10.** Sequences of primers used for qPCR analysis for the different genes studied.

Template DNA	Sequence of the primer (5' to 3')
<i>tubC</i>	F: ACTGCTCTGTGCTCTATG R: TGTGAACTGGTTGGAGAC
<i>abfA</i>	F: TTCTGGGTGCCGAAAGAAAC R: TGAGCATGGGTGCGTAGGT
<i>sell</i>	F: CTCGCTGCGTCGTAATAAAA R: AGCCATAAGCATCGGGATAAAA
<i>hacAi</i>	F: TGACCGACTACTCCCCAACT R: GCGGAAGTCATCGTCAGA
<i>bipA</i>	F: GTAACAGCCTGGAGAATA R: TTGTCGTCCTCATCAATCT
<i>bglC</i>	F: TCACCGTTAGTGTGGATGTCA R: CCTGGATGTACACCTGCACAA
<i>1542</i>	F: AACCTGGCAGGCAGAATTTG R: TTCAACTGCAACGCACCATT
<i>sec63</i>	F: AACACTACAAGCGTCTCT R: TTGCGAACTTCTTCATCAG

## CAPÍTULO 3

### 4. CONSIDERAÇÕES FINAIS

Os resultados apresentados nesta dissertação de mestrado mostraram a análise comparativa dos mecanismos de secreção de proteínas heterólogas de *A. nidulans*. Nesta análise foi possível observar a adaptação transcriptômica deste fungo filamentososo ao secretar diferentes proteínas provenientes de *A. fumigatus* e da bactéria hipertermofílica *T. petrophila*. Estas proteínas possuem níveis crescentes de secreção heteróloga por *A. nidulans*, o que permitiu a realização de uma ampla análise comparativa.

Dentre os principais resultados obtidos, foram identificados 17 genes da via de secreção de *A. nidulans* diferencialmente expressos no momento de secreção das três proteínas heterólogas. Com isso foi possível determinar um perfil transcriptômico da via de secreção deste organismo, destacando diferentes processos e vias celulares alteradas de formas específicas para cada proteína heteróloga produzida. Este é um resultado interessante por comprovar que não há uma resposta única realizada por *A. nidulans* ao produzir e secretar diferentes tipos de proteínas, mas sim respostas específicas e diferentes para cada proteína em questão.

Além disso, com este trabalho foi possível observar perfis da resposta transcriptômica das linhagens recombinantes *A. nidulans* ao analisar vias clássicas descritas por influenciar a produção de proteínas heterólogas, como UPR, ERAD e glicosilação. Também foi identificado splicing alternativo de *hacA* com 2h de indução proteica, indicando níveis de estresse celular e UPR, o que é normalizado no tempo 8h. Com a obtenção destes perfis de vias clássicas foi possível observar algumas particularidades da linhagem melhor secretora de proteínas, com mais processos celulares regulados em relação a produção e obtenção de energia, necessária para processamento correto de grande carga proteica. As linhagens com níveis menores de secreção de proteínas alvo apresentaram mais processos celulares relacionados a defesa celular. Este processo já foi relatado na literatura por dificultar nos fungos a produção de genes não nativos, sendo uma das justificativas de baixos níveis proteicos heterólogos em linhagens recombinantes [1].

Os fungos filamentosos são organismos espetaculares no que diz respeito a produção natural de enzimas lignocelulolíticas [2]. Por sua capacidade em secretar altos níveis proteicos, diversas espécies de *Aspergillus* são atualmente muito exploradas pela indústria [3]. Embora diversas estratégias já realizadas aumentaram os níveis de produção de proteínas heterólogas em *Aspergillus*, seus níveis de produção em relação as proteínas homólogas ainda são muito

baixos [4]. Diante disto, estudos que visam a compreensão dos mecanismos de *Aspergillus* na superexpressão de proteínas heterólogas são de grande importância por seu apelo industrial [5]. Como forma de esclarecer tais mecanismos, diversas pesquisas focam seus estudos na via de secreção, observando sua resposta a níveis de proteômica, genômica ou transcriptômica [6–10].

Atualmente estudos voltados a transcriptômica estão revolucionando a biologia. A evolução da bioinformática, iniciada com análises de sequenciamento, oferece grandes avanços nas ciências “ômicas”, principalmente nas anotações dos transcriptomas, permitindo a inter-relação entre o genoma funcional e a informação codificada [11]. Diversos estudos de transcriptômica utilizando a técnica de RNA-seq já foram realizados com *A. nidulans*, permitindo a identificação de novas regiões promotoras, o melhor entendimento de seu desenvolvimento sexual e novas interações com a lignocelulose [12–14]. Entretanto nenhum estudo ainda utilizou esta técnica na compreensão de mecanismo de secreção de *A. nidulans*, especificamente na produção de proteínas heterólogas.

Muitos pesquisadores apostam na maquinaria de secreção como elemento chave no melhoramento da produção de enzimas pelos fungos filamentosos [15,16]. Com esta finalidade, diversos gargalos encontrados na indústria precisam ser superados. Um deles é a grande dificuldade de promover a desconstrução da biomassa lignocelulósica, um grande obstáculo enfrentado atualmente na perspectiva das biorrefinarias e na produção do etanol de segunda geração no Brasil [17]. Por sua elevada recalcitrância, há necessidade de grandes quantidades de enzimas ao realizar hidrólise enzimática da biomassa vegetal, o que torna um processo caro pelo alto custo de produção de enzimas [18]. Os fungos filamentosos e sua excelente maquinaria de secreção de enzimas lignocelulolíticas representam uma estratégia importante podendo superar desafios enfrentados pela indústria.

De forma geral, os objetivos deste trabalho foram atingidos ao contribuir com a identificação de genes regulados no momento da secreção de proteínas heterólogas em *A. nidulans*. Além disso, a resposta transcriptômica observada permitiu a determinação do perfil da via de secreção nas linhagens recombinantes desta espécie. Este foi o primeiro trabalho a realizar a análise comparativa dos mecanismos de secreção de proteínas heterólogas em *A. nidulans*, com o diferencial de observar linhagens com níveis de secreção crescentes.

Nossos resultados fornecem novos conhecimentos de como *A. nidulans* se adapta a superprodução e secreção de proteínas heterólogas, disponibilizando novos alvos para manipulação genética com possíveis chances de melhorias na maquinaria de secreção proteica. Estudos futuros com este organismo podem desvendar ainda mais os mecanismos utilizados

pelos fungos filamentosos ao secretar proteínas, e contribuir para superação dos desafios enfrentados atualmente pela indústria que utiliza sua complexa maquinaria para produção de enzimas comerciais.

#### 4.1 Referências Bibliográficas

1. Su X, Schmitz G, Zhang M, Mackie RI, Cann IKO. Heterologous Gene Expression in Filamentous Fungi. *Adv. Appl. Microbiol.* Elsevier; 2012;81:1-61.
2. Zhao Z, Liu H, Wang C, Xu J. Comparative analysis of fungal genomes reveals different plant cell wall degrading capacity in fungi. *BMC Genomics.* BMC Genomics; 2014;15:6.
3. Fleißner A, Dersch P. Expression and export: recombinant protein production systems for *Aspergillus*. *Appl. Microbiol. Biotechnol.* 2010;87:1255–70.
4. Jin F-J, Katayama T, Maruyama J, Kitamoto K. Comparative genomic analysis identified a mutation related to enhanced heterologous protein production in the filamentous fungus *Aspergillus oryzae*. *Appl. Microbiol. Biotechnol. Applied Microbiology and Biotechnology*; 2016;100:9163–74.
5. Ward OP. Production of recombinant proteins by filamentous fungi. *Biotechnol. Adv. Elsevier B.V.*; 2012;30:1119–39.
6. Nevalainen KMH, Te'o VSJ, Bergquist PL. Heterologous protein expression in filamentous fungi. *Trends Biotechnol.* 2005;23:468–74.
7. Guillemette T, van Peij NN, Goosen T, Lanthaler K, Robson GD, van den Hondel CA, et al. Genomic analysis of the secretion stress response in the enzyme-producing cell factory *Aspergillus niger*. *BMC Genomics.* 2007;8:158.
8. Kwon MJ, Jørgensen TR, Nitsche BM, Arentshorst M, Park J, Ram AF, et al. The transcriptomic fingerprint of glucoamylase over-expression in *Aspergillus niger*. *BMC Genomics.* 2012;13:701.
9. Sims AH, Gent ME, Lanthaler K, Dunn-Coleman NS, Oliver SG, Robson GD. Transcriptome Analysis of Recombinant Protein Secretion by *Aspergillus nidulans* and the Unfolded-Protein Response In Vivo. *Appl. Environ. Microbiol.* 2005;71:2737–47.
10. Liu L, Feizi A, Österlund T, Hjort C, Nielsen J. Genome-scale analysis of the high-efficient protein secretion system of *Aspergillus oryzae*. *BMC Syst. Biol.* 2014;8:73.
11. Espindola FS, Calábria LK, Rezende AAA de, Pereira BB, Santana FA, Amaral IMR, et al. Recursos de bioinformática aplicados às ciências ômicas como genômica, transcriptômica, proteômica, interatômica e metabolômica. *Biosci. J.* 2010;26:463–77.
12. Coradetti ST, Xiong Y, Glass NL. Analysis of a conserved cellulase transcriptional regulator reveals inducer-independent production of cellulolytic enzymes in *Neurospora crassa*. *Microbiologyopen.* 2013;2:595–609.
13. Sibthorp C, Wu H, Cowley G, Wong PWH, Palaima P, Morozov IY, et al. Transcriptome analysis of the filamentous fungus *Aspergillus nidulans* directed to the global identification of promoters. *BMC Genomics.* 2013;14:847.

14. Brown NA, Ries LNA, Reis TF, Rajendran R, Corrêa dos Santos RA, Ramage G, et al. RNAseq reveals hydrophobins that are involved in the adaptation of *Aspergillus nidulans* to lignocellulose. *Biotechnol. Biofuels*. 2016;9:145.
15. Schalén M, Anyaogu DC, Hoof JB, Workman M. Effect of secretory pathway gene overexpression on secretion of a fluorescent reporter protein in *Aspergillus nidulans*. *Fungal Biol. Biotechnol. BioMed Central*; 2016;3:3.
16. Gouka RJ, Punt PJ, van den Hondel CAMJJ. Efficient production of secreted proteins by *Aspergillus* : progress, limitations and prospects. *Appl. Microbiol. Biotechnol*. 1997;47:1–11.
17. Bastos VD. Etanol, álcoolquímica e biorrefinarias. *Banco Nac. Desenvolv. Econômico e Soc*. 2007;1:1–35.
18. Klein-Marcuschamer D, Oleskiewicz-Popiel P, Simmons BA, Blanch HW. The challenge of enzyme cost in the production of lignocellulosic biofuels. *Biotechnol. Bioeng*. 2012;109:1083–7.

## 5. ANEXOS

## 5.1. Artigos Publicados

## ARTICLE

BIOTECHNOLOGY  
and  
BIOENGINEERING**Molecular Basis of Substrate Recognition and Specificity Revealed in Family 12 Glycoside Hydrolases**Felipe Calzado,<sup>1,2</sup> Erica T. Prates,<sup>3</sup> Thiago A. Gonçalves,<sup>1,2</sup> Marcelo V. Rubio,<sup>1,2</sup> Mariane P. Zubieta,<sup>1,2</sup> Fabio M. Squina,<sup>1</sup> Munir S. Skaf,<sup>3</sup> André R.L. Damásio<sup>1,2</sup><sup>1</sup>Laboratório Nacional de Ciência e Tecnologia do Bioetanol (CTBE), Centro Nacional de Pesquisa em Energia e Materiais (CNPEM), Campinas-SP, Brazil<sup>2</sup>Department of Biochemistry and Tissue Biology, Institute of Biology, University of Campinas (UNICAMP), Campinas-SP 13083862, Brazil; telephone: +551935211437; e-mail: adamasio@unicamp.br<sup>3</sup>Institute of Chemistry, University of Campinas (UNICAMP), Campinas-SP, Brazil

**ABSTRACT:** Fungal GH12 enzymes are classified as xyloglucanases when they specifically target xyloglucans, or promiscuous endoglucanases when they exhibit catalytic activity against xyloglucan and  $\beta$ -glucan chains. Several structural and functional studies involving GH12 enzymes tried to explain the main patterns of xyloglucan activity, but what really determines xyloglucanase specificity remains elusive. Here, three fungal GH12 enzymes from *Aspergillus clavatus* (AclaXegA), *A. zonatus* (AspzoGH12), and *A. terreus* (AtEglD) were studied to unveil the molecular basis for substrate specificity. Using functional assays, site-directed mutagenesis, and molecular dynamics simulations, we demonstrated that three main regions are responsible for substrate selectivity: (i) the YSG group in loop 1; (ii) the SST group in loop 2; and (iii) loop A3-B3 and neighboring residues. Functional assays and sequence alignment showed that while AclaXegA is specific to xyloglucan, AtEglD cleaves  $\beta$ -glucan, and xyloglucan. However, AspzoGH12 was also shown to be promiscuous contrarily to a sequence alignment-based prediction. We find that residues Y111 and R93 in AtEglD harbor the substrate in an adequate orientation for hydrolysis in the catalytic cleft entrance and that residues Y19 in AclaXegA and Y30 in AspzoGH12 partially compensate the absence of the YSG segment, typically found in promiscuous enzymes. The results point out the multiple structural factors underlying the substrate specificity of GH12 enzymes.

Biotechnol. Bioeng. 2016;113: 2577–2586.

© 2016 Wiley Periodicals, Inc.

**KEYWORDS:** fungal glucanases; GH12; xyloglucanases; xyloglucan specific; *Aspergillus***Introduction**

Cellulose, hemicellulose, and lignin are the major components of plant cell walls. Xyloglucan (XyG) is the most abundant hemicellulose in primary walls of spermatophytes except for grasses (Scheller and Ulvskov, 2010) and can also occur as a storage amyloid in seeds (Schultink et al., 2014). XyG is also widely used in the food industry and pharmaceutical applications (Mishra and Malhotra, 2009).

Xyloglucan consists of a linear (1  $\rightarrow$  4)  $\beta$ -D-glucan chain, as well as cellulose, with numerous  $\alpha$ -D-xylose units linked at regular sites of glucose O-6 position (Carpita and McCann, 2000). Some of xylosyl units are further substituted with  $\alpha$ -L-Arabinose or  $\beta$ -D-Galactose, depending on the plant species, and sometimes galactose is further substituted with  $\alpha$ -L-fucose (Carpita and McCann, 2000). The major structural features of XyGs are well described, as well as various glycosyl transferases responsible for their biosynthesis and transglycosylases and glycoside hydrolases (GHs) involved in XyG remodeling and fragmentation (Eckardt, 2008).

The GHs specifically responsible for the hydrolysis of xyloglucan backbone are named xyloglucan endo- $\beta$ -1,4-glucanases or xyloglucanases (XEGs; EC 3.2.1.151) and oligoxyloglucan reducing end-specific cellobiohydrolase (EC 3.2.1.150). Xyloglucanases cover many different enzyme sequences, structures, and hydrolytic mechanisms, with either inversion or retention of the anomeric carbon (Segato et al., 2014). According to carbohydrate-active enzymes (CAZy) database (Henrissat and Bairoch, 1996; Henrissat and Davies, 1997), members of the GH5, GH12, GH16, and GH44 families operate through a double-displacement mechanism of glycosyl transfer, which results in a net retention of the anomeric configuration. Enzymes belonging to families GH9 and GH74

Felipe Calzado and Erica T. Prates contributed equally to this work.

Correspondence to: A.R.L. Damásio

Contract grant sponsor: FAPESP (São Paulo Research Foundation)

Contract grant numbers: 2012/20549-4; 2014/06923-6; 2013/08293-7; 2014/23051-2; 2014/15403-6; 2013/24988-5

Contract grant sponsor: National Council for Scientific and Technological Development (CNPq)

Contract grant numbers: 140796/2013-4; 441912/2014-1; 310186/2014-5; 442333/2014-5

Received 18 March 2016; Revision received 29 May 2016; Accepted 5 June 2016

Accepted manuscript online 18 June 2016;

Article first published online 30 June 2016 in Wiley Online Library

(http://onlinelibrary.wiley.com/doi/10.1002/bit.26036/abstract).

DOI 10.1002/bit.26036



RESEARCH

Open Access



# Mapping N-linked glycosylation of carbohydrate-active enzymes in the secretome of *Aspergillus nidulans* grown on lignocellulose

Marcelo Ventura Rubio<sup>1,2</sup>, Mariane Paludetti Zubieta<sup>1,2</sup>, João Paulo Lourenço Franco Cairo<sup>1,2</sup>, Felipe Calzado<sup>1,2</sup>, Adriana Franco Paes Leme<sup>3</sup>, Fabio Marcio Squina<sup>4</sup>, Rolf Alexander Prade<sup>4</sup> and André Ricardo de Lima Damásio<sup>1,2\*</sup>

## Abstract

**Background:** The genus *Aspergillus* includes microorganisms that naturally degrade lignocellulosic biomass, secreting large amounts of carbohydrate-active enzymes (CAZymes) that characterize their saprophyte lifestyle. *Aspergillus* has the capacity to perform post-translational modifications (PTM), which provides an additional advantage for the use of these organisms as a host for the production of heterologous proteins. In this study, the N-linked glycosylation of CAZymes identified in the secretome of *Aspergillus nidulans* grown on lignocellulose was mapped.

**Results:** *Aspergillus nidulans* was grown in glucose, xylan and pretreated sugarcane bagasse (SCB) for 96 h, after which glycoproteomics and glycomics were carried out on the extracellular proteins (secretome). A total of 265 proteins were identified, with 153, 210 and 182 proteins in the glucose, xylan and SCB substrates, respectively. CAZymes corresponded to more than 50 % of the total secretome in xylan and SCB. A total of 182 N-glycosylation sites were identified, of which 121 were detected in 67 CAZymes. A prevalence of the N-glyc sequon N-X-T (72.2 %) was observed in N-glyc sites compared with N-X-S (27.8 %). The amino acids flanking the validated N-glyc sites were mainly composed of hydrophobic and polar uncharged amino acids. Selected proteins were evaluated for conservation of the N-glyc sites in *Aspergilli* homologous proteins, but a pattern of conservation was not observed. A global analysis of N-glycans released from the proteins secreted by *A. nidulans* was also performed. While the proportion of N-glycans with Hex<sub>5</sub> to Hex<sub>3</sub> was similar in the xylan condition, a prevalence of Hex<sub>5</sub> was observed in the SCB and glucose conditions.

**Conclusions:** The most common and frequent N-glycosylated motifs, an overview of the N-glycosylation of the CAZymes and the number of mannoses found in N-glycans were analyzed. There are many bottlenecks in protein production by filamentous fungi, such as folding, transport by vesicles and secretion, but N-glycosylation in the correct context is a fundamental event for defining the high levels of secretion of target proteins. A comprehensive analysis of the protein glycosylation processes in *A. nidulans* will assist with a better understanding of glycoprotein structures, profiles, activities and functions. This knowledge can help in the optimization of heterologous expression and protein secretion in the fungal host.

\*Correspondence: adamasio@unicamp.br

<sup>2</sup> Department of Biochemistry and Tissue Biology, Institute of Biology, University of Campinas (UNICAMP), Rua Monteiro Lobato, 255, Cidade Universitária Zeferino Vaz, Campinas, SP 13083-862, Brazil  
 Full list of author information is available at the end of the article



©2016 The Author(s). This article is distributed under the terms of the Creative Commons Attribution 4.0 International License (<http://creativecommons.org/licenses/by/4.0/>), which permits unrestricted use, distribution, and reproduction in any medium, provided you give appropriate credit to the original author(s) and the source, provide a link to the Creative Commons license, and indicate if changes were made. The Creative Commons Public Domain Dedication waiver (<http://creativecommons.org/publicdomain/zero/1.0/>) applies to the data made available in this article, unless otherwise stated.

## 5.2. Capítulos de livros Publicados

## Chapter 18

# Agro-Industrial Residues and Microbial Enzymes: An Overview on the Eco-Friendly Bioconversion into High Value-Added Products

Jose Valdo Madeira Jr<sup>1</sup>, Fabiano Jares Contesini<sup>2</sup>, Felipe Calzado<sup>2</sup>, Marcelo Ventura Rubio<sup>2</sup>, Mariane Paludetti Zubieta<sup>2</sup>, Danielle Branta Lopes<sup>1</sup> and Ricardo Rodrigues de Melo<sup>1</sup>

<sup>1</sup>Faculty of Food Engineering, University of Campinas, Campinas, São Paulo, Brazil <sup>2</sup>Laboratório Nacional de Ciência e Tecnologia do Bioetanol (CTBE), Centro Nacional de Pesquisa em Energia e Materiais (CNPEM), Campinas, São Paulo, Brazil

## 18.1 INTRODUCTION

Biotechnology has passed through a maturation phase, in which research and development have discovered new applications for biocatalysts in chemical, pharmaceutical, and food industries. The advances in biotechnology, particularly in genetics, protein engineering, and direct evolution, have contributed a new era for enzymes, and the use of enzymes has increased so far in research laboratories as well as at the industrial scale due to their ability to carry out a variety of reactions under varied environmental conditions. Moreover, the capacity to replace harmful chemical reaction conditions and the trend for developing cleaner technologies have enhanced the importance of enzymes for the green chemistry and the bio-based economy society towards the creation of new processes and product innovation in the market. The use of enzymes results in many benefits, such as higher product quality, lower manufacturing costs, less waste, and lower energy consumption (Binod, 2013).

Enzymes have been applied in biotechnology since the earliest of times for the manufacturing of foods, chemicals, and biofuels. For their empirical usages,

Biotechnology of Microbial Enzymes. DOI: <http://dx.doi.org/10.1016/B978-0-12-803725-6.00018-2>  
© 2017 Elsevier Inc. All rights reserved.

475

## ***Aspergillus* Lipases: Biotechnological and Industrial Application**

Fabiano Jares Contesini, Felipe Calzado, Jose Valdo Madeira Jr, Marcelo Ventura Rubio, Mariane Paludetti Zubieta, Ricardo Rodrigues de Melo, and Thiago Augusto Gonçalves

### **Contents**

1	Introduction .....	3
2	<i>Aspergillus</i> as a Biotechnological Tool .....	4
3	Obtainment and Properties of Lipases from <i>Aspergillus</i> .....	5
4	Immobilization of Lipases Obtained from the Genus <i>Aspergillus</i> .....	11
5	Industrial and Biotechnological Applications of Lipases .....	15
	5.1 Food Industry .....	15
	5.2 Pharmaceutical Industry .....	18
	5.3 Chemical Industry .....	19
	5.4 Detergent Industry .....	21
	5.5 Biofuel Industry .....	21
6	Conclusions .....	22
	References .....	23

### **Abstract**

Lipases are enzymes with remarkable properties and catalytic versatility. These proteins are capable of catalyzing hydrolytic and synthetic reactions, allowing the

F.J. Contesini (✉)

Laboratório Nacional de Ciência e Tecnologia do Bioetanol (CTBE), Centro Nacional de Pesquisa em Energia e Materiais (CNPEM), Campinas, Brazil  
e-mail: [fabiano.contesini@gmail.com](mailto:fabiano.contesini@gmail.com)

F. Calzado • M.V. Rubio • M.P. Zubieta • T.A. Gonçalves

Laboratório Nacional de Ciência e Tecnologia do Bioetanol (CTBE), Centro Nacional de Pesquisa em Energia e Materiais (CNPEM), Campinas, Brazil

Institute of Biology, University of Campinas, Campinas, Brazil

e-mail: [fecalzado@gmail.com](mailto:fecalzado@gmail.com); [marcelov.rubio@gmail.com](mailto:marcelov.rubio@gmail.com); [marianezubieta@gmail.com](mailto:marianezubieta@gmail.com); [thiago.bioetanol@gmail.com](mailto:thiago.bioetanol@gmail.com)

J.V. Madeira Jr • R.R. de Melo

Faculty of Food Engineering, University of Campinas, Campinas, Brazil  
e-mail: [madeira\\_jr@hotmail.com](mailto:madeira_jr@hotmail.com); [ricardomelo@yahoo.com.br](mailto:ricardomelo@yahoo.com.br)

© Springer International Publishing Switzerland 2016  
J.-M. Mérillon, K.G. Ramawat (eds.), *Fungal Metabolites*,  
DOI 10.1007/978-3-319-19456-1\_17-1

1



### 5.3. Aprovação do projeto na CIBio

Uso exclusivo da CIBio:

Número de projeto / processo: 2015-29

**Formulário de encaminhamento de projetos de pesquisa para análise pela CIBio - Comissão Interna de Biossegurança do CNPEM – Centro Nacional de Pesquisa em Energia e Materiais**

**Título do projeto:** Análise comparativa do mecanismo de secreção de proteínas heterólogas em *Aspergillus nidulans*.

**Pesquisador responsável:** André Ricardo de Lima Damásio

**Experimentador:** Felipe Calzado

**Classe de risco do OGM:** [ x ] Risco I [ ] Risco II

Nível do treinamento do experimentador: [ ]-Iniciação científica, [ X ]-mestrado, [ ]-doutorado, [ ]-doutorado direto, [ ]-pós-doutorado, [ ]-nível técnico, [ ]-outro, especifique: \_\_\_\_\_

**Resumo do projeto:**

Como forma de diminuir o uso de energias de origem fóssil e aumentar do uso de energias renováveis, o etanol de segunda geração obtido a partir da conversão de biomassa vegetal lignocelulósica em açúcares fermentáveis tem sido foco de muitas pesquisas atualmente a fim de viabilizar seu uso. Os fungos filamentosos se destacam na produção e secreção de enzimas lignocelulolíticas de forma homóloga e heteróloga, entretanto pouco se sabe sobre os mecanismos de secreção de proteínas utilizados por estes microrganismos. Pensado nisso, a utilização do organismo modelo de fungos filamentosos *Aspergillus nidulans* se torna um importante recurso de estudos por ser geneticamente bem caracterizado. O objetivo deste projeto de mestrado é realizar a análise comparativa dos mecanismos de secreção de diferentes proteínas heterólogas em *A. nidulans* gerando dados de transcriptoma a partir da técnica de RNA-seq (*Next Generation RNA sequencing*) e analisá-los com auxílio de ferramentas de bioinformática. Para monitorar o processo de secreção, adotaremos 4 genes alvo: arabinase GH43 (AbnA), celobiohidrolase GH7 (Cbhl), beta-glucosidase GH3 (BglC) e mananase GH5 termofílica (1542.1). Estes genes foram previamente transformados em *A. nidulans*, sendo que para AbnA e Cbhl atingiu-se altos níveis de secreção, diferente de BglC e 1542.1, onde os níveis de secreção foram mínimos. Com os resultados obtidos, nosso objetivo central é de pelo menos demonstrar como a cepa se adapta a expressão heteróloga de diferentes genes alvo, incluindo um gene de característica termofílica.

A CIBio analisou este projeto em reunião realizada no dia: 01/06/2015.

**Parecer final:** [ X ]-projeto aprovado, [ ]-projeto recusado, [ ]-projeto com deficiências, comentários anexo:

Marcio C.F.  
Presidente da CIBio – CNPEM-LNBio  
Marcio Chaim Bajgelman

Uso Benedetti  
Membro da CIBio – CNPEM -LNBio  
Celso Eduardo Benedetti

Carolina  
Membro da CIBio – CNPEM -LNBio  
Carolina Borsoi Moraes H. Freitas

Fabio Márcio Squina  
Membro da CIBio da CNPEM -CTBE  
Fabio Márcio Squina

Sindélia F. Azzoni  
Membro da CIBio da CNPEM -CTBE  
Sindélia Freitas Azzoni

Roberto Ruller  
Membro da CIBio da CNPEM -CTBE  
Roberto Ruller

#### 5.4. Declaração de direitos autorais

##### Declaração

As cópias de artigos de minha autoria ou de minha co-autoria, já publicados ou submetidos para publicação em revistas científicas ou anais de congressos sujeitos a arbitragem, que constam da minha Dissertação/Tese de Mestrado/Doutorado, intitulada **Análise comparativa do mecanismo de secreção de proteínas heterólogas em *Aspergillus nidulans***, não infringem os dispositivos da Lei n.º 9.610/98, nem o direito autoral de qualquer editora.

Campinas, 13 de março de 2017

Assinatura : *Felipe Calzado*  
Nome do(a) autor(a): **Felipe calzado**  
RG n.º 496098925

Assinatura : *André R.L. Damásio*  
Nome do(a) orientador(a): **André Ricardo de Lima Damásio**  
RG n.º 595124227